frontiers | Research Topics

Emerging human viruses with pandemic potential: Diagnostics, pathogenesis, and therapeutics

Edited by
Edmarcia Elisa De Souza, Edison Luiz Durigon and Viviane Fongaro Botosso

Published in
Frontiers in Cellular and Infection Microbiology

ISSN 1664-8714
ISBN 978-2-8325-2113-7
DOI 10.3389/978-2-8325-2113-7

About Frontiers

Frontiers is more than just an open access publisher of scholarly articles: it is a pioneering approach to the world of academia, radically improving the way scholarly research is managed. The grand vision of Frontiers is a world where all people have an equal opportunity to seek, share and generate knowledge. Frontiers provides immediate and permanent online open access to all its publications, but this alone is not enough to realize our grand goals.

Frontiers journal series

The Frontiers journal series is a multi-tier and interdisciplinary set of open-access, online journals, promising a paradigm shift from the current review, selection and dissemination processes in academic publishing. All Frontiers journals are driven by researchers for researchers; therefore, they constitute a service to the scholarly community. At the same time, the *Frontiers journal series* operates on a revolutionary invention, the tiered publishing system, initially addressing specific communities of scholars, and gradually climbing up to broader public understanding, thus serving the interests of the lay society, too.

Dedication to quality

Each Frontiers article is a landmark of the highest quality, thanks to genuinely collaborative interactions between authors and review editors, who include some of the world's best academicians. Research must be certified by peers before entering a stream of knowledge that may eventually reach the public - and shape society; therefore, Frontiers only applies the most rigorous and unbiased reviews. Frontiers revolutionizes research publishing by freely delivering the most outstanding research, evaluated with no bias from both the academic and social point of view. By applying the most advanced information technologies, Frontiers is catapulting scholarly publishing into a new generation.

What are Frontiers Research Topics?

Frontiers Research Topics are very popular trademarks of the *Frontiers journals series*: they are collections of at least ten articles, all centered on a particular subject. With their unique mix of varied contributions from Original Research to Review Articles, Frontiers Research Topics unify the most influential researchers, the latest key findings and historical advances in a hot research area.

Find out more on how to host your own Frontiers Research Topic or contribute to one as an author by contacting the Frontiers editorial office: frontiersin.org/about/contact

Emerging human viruses with pandemic potential: Diagnostics, pathogenesis, and therapeutics

Topic editors

Edmarcia Elisa De Souza — University of São Paulo, Brazil

Edison Luiz Durigon — University of São Paulo, Brazil

Viviane Fongaro Botosso — Butantan Institute, Brazil

Citation

De Souza, E. E., Durigon, E. L., Botosso, V. F., eds. (2023). *Emerging human viruses with pandemic potential: Diagnostics, pathogenesis, and therapeutics*. Lausanne: Frontiers Media SA. doi: 10.3389/978-2-8325-2113-7

Table of contents

frontiers | Frontiers in Cellular and Infection Microbiology

TYPE Editorial
PUBLISHED 23 March 2023
DOI 10.3389/fcimb.2023.1182522

OPEN ACCESS

EDITED AND REVIEWED BY
Nahed Ismail,
University of Illinois at Chicago,
United States

*CORRESPONDENCE
Viviane Fongaro Botosso
viviane.botosso@butantan.gov.br
Edison Luiz Durigon
eldurigo@usp.br
Edmarcia Elisa de Souza
edmarciaelisa@usp.br

SPECIALTY SECTION
This article was submitted to Clinical Microbiology, a section of the journal Frontiers in Cellular and Infection Microbiology

RECEIVED 08 March 2023
ACCEPTED 13 March 2023
PUBLISHED 23 March 2023

CITATION
Botosso VF, Durigon EL and de Souza EE (2023) Editorial: Emerging human viruses with pandemic potential: Diagnostics, pathogenesis, and therapeutics. *Front. Cell. Infect. Microbiol.* 13:1182522. doi: 10.3389/fcimb.2023.1182522

Editorial: Emerging human viruses with pandemic potential: Diagnostics, pathogenesis, and therapeutics

Viviane Fongaro Botosso[1]*, Edison Luiz Durigon[2,3]* and Edmarcia Elisa de Souza[4]*

[1]Virology Laboratory, Butantan Institute, São Paulo, Brazil, [2]Scientific Platform Pasteur-University of São Paulo, São Paulo, Brazil, [3]Department of Microbiology, Institute of Biomedical Sciences, University of São Paulo, São Paulo, Brazil, [4]Unit for Drug Discovery, Department of Parasitology, Institute of Biomedical Sciences, University of São Paulo, São Paulo, Brazil

KEYWORDS

emerging viruses, diagnostics, pathogenesis, therapeutics, epidemiology

Editorial on the Research Topic
Emerging human viruses with pandemic potential: Diagnostics, pathogenesis, and therapeutics

The emergence of viral pathogens and their subsequent spreading have caused an extremely significant impact on human health and the global economy. Most notably, the COVID-19 pandemic posed an enormous threat to public health worldwide, both because of its pathological characteristics in addition to high transmissibility and rapid evolution of SARS-CoV-2. Considering this, studies focused on biology, pathogenesis, epidemiology, diagnosis and prevention of viral pathogens are fundamental to control future emerging infectious diseases. In this Research Topic, we received 19 manuscripts, of which 9 were accepted for publication after rigorous peer review processes. We thank all the authors and reviewers for their valuable contributions, and we expect that this article collection will be helpful for the scientific community seeking knowledge about emerging viruses.

Andrade et al., present a comprehensive review highlighting the homeostatic alterations caused by SARS-CoV-2 infections. In general, hypercoagulation, endothelial dysfunction and dysregulation of the renin-angiotensin system are important determinants for pulmonary thrombus formation and impairment of respiratory functions observed in patients with severe COVID-19. Chen et al., report that ferroptosis, a cell death mechanism characterized by iron overload and lipid peroxidation, may participate in SARS-CoV-2 infection associated liver injury, a common feature in COVID-19. Potential links between ferroptosis and COVID-19 are associated with higher frequencies of hepatic steatosis, Kupffer cell activation, vascular thrombosis, and inflammatory infiltration. However, it is still unclear how ferroptosis drives these pathological processes contributing to liver injury caused by SARS-CoV-2. Additionally, Yang et al., emphasis the roles of non-coding RNAs (ncRNAs) in neurological complications induced by Enterovirus 71 (EV71). In this respect, host ncRNAs target EV71 genome to promote invasion and modulate its replication; this event may damage key signaling pathways of central nervous system, resulting in acute immune and inflammatory responses. Essentially, these reports provide a basis for the mechanisms that contribute to pathological features of COVID-19 or EV71-associated diseases.

Understanding risk factors and serological markers that can influence the progression of the disease are crucial for treatment and prevention measures. Under these premises, Queiroz et al., evaluate the main risk factors correlated with the severity and progression of COVID-19. In this study, the assessment of clinical manifestations of patients infected with SARS-CoV-2 demonstrated that elevated cytokine levels among individuals with severe acute COVID-19 is associated to sex, advanced age, and presence of comorbidities such as diabetes mellitus, hypertension, chronic kidney disease, obesity, and immunosuppression. In addition, it was possible to identify cytokine markers that are characteristic for disease progression to long COVID-19. Similarly, Torres et al., provide a detailed study of risk factors associated to SARS-CoV-2 seroprevalence at first wave in comparison with the second wave of COVID-19 in the city of Beleím, state of Paraí, northern Brazil. According to this study, behavioral profiles including the frequency of travel, low frequency of protective mask use, hygiene habits, lack of social isolation, and contact with infected people, in addition to socioeconomic discrepancies as low education level, are considered risk factors for SARS-CoV-2 infection. In addition, Chen et al., present an interesting research manuscript regarding the predictability of mortality of COVID-19 patients. The prognostic model demonstrated that age and high levels of UREA and lactate dehydrogenase (LDH) were associated with mortality of 80-days COVID-19 patients, suggesting a robust tool for predicting mortality and assist clinicians in the early screening of patients with COVID-19 poor prognoses.

Hu et al., and Yang et al., highlight the need to the development of tools that can be applicable to early diagnosis of COVID-19 and HIV infection, respectively. Hu et al., report a RNA fluorescence *in situ* hybridization (FISH) method that detects SARS-CoV-2 spike (S) and envelope (E) proteins and their mRNAs, with enhanced signal of fluorescence generated within a hybridization reaction inside HEK 293T cells. Yang et al., evaluate the performance of Elecsys® HIV Duo assay for diagnostic of HIV/AIDS from clinical patient samples in southwest China. This study demonstrated the detection of the earliest immune markers HIV-1 p24 antigen and HIV-1/2 antibody simultaneously, which greatly enhanced the performance of test results. These approaches might improve the detection sensitivity and specificity and support the early diagnosis of SARS-CoV-2 and HIV, respectively.

While several emerging viruses have caused outbreaks, detailed knowledge of their behavior and habitats are essential to predict potential outbreaks and spillovers of zoonotic diseases (Harvey and Holmes, 2022). Regarding to that, Loh et al., present a study of viral diversity in bat host species in deforested versus forested areas of the Atlantic Forest of Brazil. Overall, the study demonstrated the prevalence of high viral richness in active deforestation sites, which may result in increased risk to human exposure with zoonotic infections and disease reservoirs.

Author contributions

VB, ED and ES wrote and edited the manuscript. All authors contributed to the article and approved the Editorial.

Funding

We thank for the financial support of CAPES (Coordination for Improvement of Higher Education Personnel), FINEP (Funding Authority for Studies and Projects), CNPq (National Council for Scientific and Technological Development) and Rede Virus from the Ministry of Science, Technology and Innovation, (Finep 01.20.0010 and 01.20.0005.00; CNPq 403514/2020-7). We also thank Fundação de Amparo à Pesquisa do Estado de São Paulo (FAPESP) for financial support (grants 2015/26722-8, 2020/12277-0 and 2021/11946-9).

Conflict of interest

The authors declare that the research was conducted in the absence of any commercial or financial relationships that could be construed as a potential conflict of interest.

Publisher's note

Reference

Harvey, E., and Holmes, E. C. (2022). Diversity and evolution of the animal virome. *Nat. Rev. Microbiol.* 20, 321–334. doi: 10.1038/s41579-021-00665-x

frontiers | Frontiers in Cellular and Infection Microbiology

REVIEW
published: 25 April 2022
doi: 10.3389/fcimb.2022.873304

Role of Non-Coding RNA in Neurological Complications Associated With Enterovirus 71

Feixiang Yang[1,2,3,4†], Ning Zhang[1,5†], Yuxin Chen[1,6†], Jiancai Yin[5], Muchen Xu[1,6], Xiang Cheng[5], Ruyi Ma[1], Jialin Meng[2,3,4] and Yinan Du[1*]*

[1] School of Basic Medical Sciences, Anhui Medical University, Hefei, China, [2] Department of Urology, The First Affiliated Hospital of Anhui Medical University, Hefei, China, [3] Institute of Urology, Anhui Medical University, Hefei, China, [4] Anhui Province Key Laboratory of Genitourinary Diseases, Anhui Medical University, Hefei, China, [5] First School of Clinical Medicine, Anhui Medical University, Hefei, China, [6] School of Public Health, Anhui Medical University, Hefei, China

OPEN ACCESS

Edited by:
Edison Luiz Durigon,
University of São Paulo, Brazil

Reviewed by:
Kuo-Feng Weng,
Stanford University, United States
Dawei Cui,
Zhejiang University School of Medicine, China

***Correspondence:**
Yinan Du
duyinannan@126.com
Jialin Meng
mengjialin@ahmu.edu.cn

†These authors have contributed equally to this work

Specialty section:
This article was submitted to Virus and Host, a section of the journal Frontiers in Cellular and Infection Microbiology

Received: 10 February 2022
Accepted: 30 March 2022
Published: 25 April 2022

Citation:
Yang F, Zhang N, Chen Y, Yin J, Xu M, Cheng X, Ma R, Meng J and Du Y (2022) Role of Non-Coding RNA in Neurological Complications Associated With Enterovirus 71. Front. Cell. Infect. Microbiol. 12:873304. doi: 10.3389/fcimb.2022.873304

Enterovirus 71 (EV71) is the main pathogenic virus that causes hand, foot, and mouth disease (HFMD). Studies have reported that EV71-induced infections including aseptic meningitis, acute flaccid paralysis, and even neurogenic pulmonary edema, can progress to severe neurological complications in infants, young children, and the immunosuppressed population. However, the mechanisms through which EV71 causes neurological diseases have not been fully explored. Non-coding RNAs (ncRNAs), are RNAs that do not code for proteins, play a key role in biological processes and disease development associated with EV71. In this review, we summarized recent advances concerning the impacts of ncRNAs on neurological diseases caused by interaction between EV71 and host, revealing the potential role of ncRNAs in pathogenesis, diagnosis and treatment of EV71-induced neurological complications.

Keywords: virus-host interaction, enterovirus 71, hand, foot, and mouse disease, microRNA, long non-coding RNA, non-coding RNA

1 INTRODUCTION

Enteroviruses (EVs) are a genus of the Picornaviridae family characterized by small, single-stranded, positive-sense RNA (Solomon et al., 2010; Baggen et al., 2018). There are 13 species in this family, of which 7 species, including four species of enteroviruses (enteroviruses A, B, C, and D) and three species of rhinoviruses (rhinoviruses A, B, and C) are pathogenic to humans (Nikonov et al., 2017). Enterovirus 71 (EV71) is a member of species group A and has an icosahedral structure that is characteristic of all EVs. The viral capsid comprises 60 repeating units referred to as protomers. Each protomer consists of four structural viral proteins (surface proteins (VP1-VP3) and the internal protein (VP4)) (Solomon et al., 2010; Plevka et al., 2012; Baggen et al., 2018). The P1 coding region of the virus genome codes for structural proteins, whereas other seven non-structural proteins (proteins 2A-2C and 3A-3D) are encoded by the P2 and P3 regions (Solomon et al., 2010). Structure proteins of EV71 play important roles in viral pathogenicity, virulence and host resistance, as well as serve as regulatory targets for biological factors (Zheng et al., 2011; Wang B. et al., 2013).

EV71 is the main etiological agent that causes brief, generally mild, self-limiting HFMD, which is characterized by red spots or herpes on the hands, feet, and mouth and which resolves in 3-7 days without treatment (Solomon et al., 2010; Cox and Levent, 2018). Since EV71 was first isolated from the human central nervous system in 1974 (Schmidt et al., 1974). The EV71-associated neurological diseases, such as aseptic meningitis, acute flaccid paralysis, neurogenic cardiopulmonary failure and fatal encephalitis, have been widely reported in China, America, Brazil, Vietnam and other countries (Xing et al., 2014; Huang et al., 2015; Liu et al., 2015; Hasbun et al., 2017; B'Krong et al., 2018; Ramalho et al., 2019). A large epidemiological study conducted from 2008 to 2012 in China reported 7,200,092 probable cases among which 80% laboratory-confirmed severe cases (patients with neurological or cardiopulmonary complications) and 93% fatal cases were attributed to EV71 infection (Xing et al., 2014). Currently, there are no specific therapeutic options for EV71-induced neurological diseases, and the mechanisms of severe nervous system diseases have not been fully elucidated (Ooi et al., 2010; Solomon et al., 2010; Chen et al., 2020). Expanding evidence reveals that ncRNAs play essential roles in normal physiological and pathological processes (Beermann et al., 2016). Researchers found that ncRNAs were closely related to development of HFMD and pathogenicity of EV71, which may provide basis for pathogenesis, diagnosis and treatment of EV71-associated diseases.

2 OVERVIEW OF NON-CODING RNAS

ncRNAs are RNAs without the potential for encoding biological proteins. Based on the number of nucleotides (nt), they are divided into two subclasses, small or short non-coding RNAs (less than 200 nt) and long non-coding RNAs (lncRNAs) (more than 200 nt) (Kapranov et al., 2007; Esteller, 2011; Beermann et al., 2016; Engreitz et al., 2016). Small non-coding RNAs are further classified into three main categories: microRNAs (miRNAs), short interfering RNAs (siRNAs), and piwi-interacting RNAs (piRNAs). Small non-coding RNAs act as disincentives to gene expression and regulation by combining with members of the Argonaute protein (Ago protein) superfamily (Carthew and Sontheimer, 2009). miRNAs, which mediate post-transcriptional gene suppression by binding mRNAs or viral genomes, are one of the most important and widely studied classes of ncRNAs (He and Hannon, 2004). In the nucleus, lncRNAs modulate expressions of neighboring genes through chromatin remodeling, and transcriptional and post-transcriptional regulation, thereby regulating biological processes (Mercer et al., 2009; Engreitz et al., 2016).

The synthesis of miRNAs is dependent on two pivotal enzymes, Drosha and Dicer, which belong to the ribonuclease-III (RNase III) family (Hutvágner et al., 2001; Lee et al., 2003). Primary miRNA (pri-miRNA) is transcribed from endogenous miRNA genes by RNA polymerase II (Pol II) to generate pre-miRNA after processing by Drosha inside the nucleus (Lee et al., 2003). Exportin-5 is involved in extranuclear transportation of pre-miRNA, which is subsequently cleaved by Dicer into an imperfect dsRNA duplex (miRNA: miRNA duplex) (Hutvágner et al., 2001; Carthew and Sontheimer, 2009). One miRNA strand: miRNA duplex is assembled into an RNA-induced silencing complex (RISC), namely miRISC. miRISC mediates post-transcriptional gene inhibition by translational repression or mRNA cleavage (He and Hannon, 2004; Rana, 2007; Carthew and Sontheimer, 2009). In various aspects, such as the same type of transcriptase, Pol II, lncRNAs are similar to mRNAs. However, compared to mRNAs, lncRNAs exhibit a lower transcription number and are evolutionarily conserved (Quinn and Chang, 2016). lncRNAs modulate genes expressions by interacting with chromatin and proteins through secondary structures such as hairpin and stem ring structures (Quinn and Chang, 2016; Statello et al., 2021), and this function plays an important role in the body against external infection.

ncRNAs have ability to cope with environmental changes and defend against external threats through the corresponding machinery. Dysregulated ncRNAs may damage various physiological processes and promote pathological conditions. For instance, dysregulated miR-143/145 cluster, which is extensively recognized as a tumor suppressor, promotes tumor growth by inducing angiogenesis in the tumor microenvironment (Dimitrova et al., 2016). The focus of this review is ncRNAs, particularly miRNAs and lncRNAs, with an emphasis on the effect of miRNAs on development of EV71-induced CNS complications and the potential of lncRNAs and miRNAs as biomarkers for clinical diagnosis and therapeutic targets.

3 ROLE OF MIRNAS IN EV71-INDUCED CNS INFECTION

3.1 miRNAs and Neurotropism of EV71

Several studies on polioviruses (PVs), the one important species of enterovirus, have widely explored enterovirus tropism. Although viral tropism is determined by cellular receptors (Holland, 1961), internal ribosomal entry sites (IRESs) (Gromeier et al., 1996), and interference responses (especially α/β IFN) (Ida-Hosonuma et al., 2005), the cellular receptors play the most important role in cell and tissue tropism of PV. Previous studies have shown that non-susceptible mouse cells became susceptible after introducing human PVR gene into the mouse genome, and ultimately presented with CNS diseases similar to those in infected humans (Ren et al., 1990; Koike et al., 1991).

Relative to PVR, EV71 receptors are more complicated. Scavenger receptor class B, member 2 (SCARB2, also known as LGP85), which belongs to the CD36 family, is a type III transmembrane protein involved in membrane transport. SCARB2 is a major receptor for EV71 and plays a crucial role in attachment, internalization, and viral conformational changes for uncoating, which determines the cell and tissue tropism of EV71 (Yamayoshi et al., 2009; Dang et al., 2014). SCARB2 is highly expressed in several cells and tissues, including CNS

neurons, pneumocytes, hepatocytes, splenocytes, renal tubular epithelia, and intestinal epithelia (Fujii et al., 2013). Fujii et al. (2013) and Yang et al. (2019) demonstrated that expression of only SCARB2was sufficient to allow transgenic mice to develop EV71-associated CNS diseases that resemble those in infected humans. Moreover, SCARB2 expression profiles in mice were comparable to those in humans, which may explain neurotropism and cell tropism of EV71. Although SCARB2 is of great significance in EV71 infection and tropism, it is not the only receptor that is implicated in EV71 infection. During EV71 infection process, other molecules can support attachment but not uncoating. These molecules are known as "attachment receptors" and they include P-selectin glycoprotein ligand-1 (PSGL-1) (Nishimura et al., 2009), annexin A2 (Anx2) (Yang et al., 2011), vimentin (Du et al., 2014), sialylated glycan (Yang et al., 2009), heparan sulfate glycosaminoglycan (Tan et al., 2013), nucleolin (Su et al., 2015), fibronectin (He et al., 2018) and prohibitin (Too et al., 2018). Attachment receptors lack the uncoating function, thus SCARB2 has a stronger correlation with EV71 infection processes compared to attachment receptors and is the decisive receptor that mediates EV71 cell and tissue tropism (He et al., 2014; Kobayashi and Koike, 2020).

miRNAs regulate EV71 tropism mainly by modulating the expression of SCARB2. Directly, miR-127-5p targets the SCARB2 mRNA 3' untranslated region (UTR) and suppresses expression of SCARB2 in Gaucher fibroblasts (Siebert et al., 2014). Through further experiments, Feng et al. confirmed that miR-127-5p expression was upregulated after EV71 infection and that upregulation of miR-127-5p downregulated SCARB2 levels on cell surfaces through specific target binding, which principally affected the susceptibility of uninfected cells to EV71 infection and cell tropism of EV71 (Feng C. et al., 2017). Jin et al. found that downregulation of hsa-miR-3605-5p might advance tSCARB2 expression in human embryonic kidney 293T cells infected with coxsackievirus A16 (CVA16), thereby increasing susceptibility to EV71/CVA16 (Jin et al., 2017). Moreover, miR-202-3p (Li et al., 2020), miR-19a-5p (Siebert et al., 2014), and miR-1262 (Siebert et al., 2014) attenuated expression of SCARB2 mRNAs and proteins in non-EV71-indected cells, providing a basis for further research on EV71 infection and proliferation.

3.2 Effects of miRNAs on CNS Invasion of EV71

As a classic species of neurotropic enteroviruses transmitted by the fecal-oral route, EV71 proliferates in the digestive tract and invades the brain and other tissues and organs, resulting in encephalitis and other diseases (Ooi et al., 2010). After initial infection in the gastrointestinal tract neurotropic enteroviruses cross the blood-brain barrier (BBB) into the CNS through multiple routes. Intensive studies on CNS invasion routes of PVs have reported presence of three fundamental pathways through which enteroviruses gain access to the CNS (Huang and Shih, 2015; Chen et al., 2020). First, upon reaching the BBB by hematogenous transport, enteroviruses directly infect brain microvascular endothelial cells (BMECs) that constitute and maintain the integrity as well as permeability of the BBB. For instance, activation of the protein tyrosine phosphatase SHP-2 by PVR (Coyne et al., 2007) and attachment of PVs by mouse transferrin receptor 1 (Mizutani et al., 2016) facilitate PV CNS invasion by damaging BMECs. Second, enteroviruses hijack retrograde axonal transport [transport of vesicles or substances from the terminals along microtubules to the nerve cell body (Millecamps and Julien, 2013)] and spread into spinal motoneurons in the CNS through neuromuscular junctions. For instance, PV gains entry into the CNS through receptor-dependent and receptor-independent endocytosis at neuromuscular junctions (Ohka et al., 2004; Ohka et al., 2012). Third, peripheral circulating immune cells can serve as transport vehicles that carry intracellular enteroviruses and pass the CNS through the so-called "Trojan Horse" pathway. Previous studies present that Coxsackieviruses (CVs) migrate to the CNS and traverse the BBB by CV-infected myeloid cells (Tabor-Godwin et al., 2010). Neurotoxic PV can also infect monocytes and exhibits a stronger proliferation ability in these cells (Freistadt and Eberle, 1996). Consequently, a hypothesis has been proposed that monocytes carry PV across CNS (Squires, 1997), although more studies should verify this hypothesis.

EV71 crosses the BBB and invades the CNS in similar ways as PV, in which miRNAs are involved in regulation of several pathways (**Figure 1**). With regards to the first route, Zhu et al. (Zhu et al., 2019) and Wang et al. (Wang W. et al., 2020) observed that EV71 infected BMECs with the capsid protein, VP1, which reduced claudin-5, the junction protein of endothelial cells, leading to increased BBB permeability and upregulation of the EV71 receptor vimentin to facilitate attachment. miR-2911 and miR-23b mediate neural invasion of EV71 by directly targeting the VP1-coding sequence that regulates VP1 translation (Wen et al., 2013; Li X. et al., 2018). For the second route, Chen et al. (Chen et al., 2007) reported that EV71 infected and entered the CNS through retrograde axonal transport at spinal motor nerves. Lim et al. (Lim et al., 2021) further showed that surface-expressed peripherin in motor neurons provides anchor points for EV71 and contributes to viral transmission, whereas intracellular peripherin modulates EV71 genome replication, resulting in CNS infection. In amyotrophic lateral sclerosis (ALS) patients, miR-105 and miR-9 mainly dominate peripherin expression in motor neurons by targeting the 3'UTR of peripheral mRNA (Hawley et al., 2019); however, their effects on EV71 have not been explored. In EV71-infected mouse neurons, miR-3473a plays a role in axon guidance and Wnt signaling pathways, which control axon growth and guidance (Van Battum et al., 2015) and mediate neuronal positioning as well as axon development (Salinas and Zou, 2008), respectively. Downregulation of miR-3473a activates these two pathways and promotes retrograde axonal transport of EV71 (Yang et al., 2017). For the third route, EV71 was demonstrated to infect human CD14+ cells (Wang J. et al., 2013), leukocytes (Nishimura et al., 2009), dendritic cells (Lin et al., 2009), and other peripheral immune cells, increasing the ability of EV71 to invade the CNS through the Trojan horse pathway. miR-3473a was considered to modulate leukocyte trans-endothelial migration and induce EV71-associated BBB

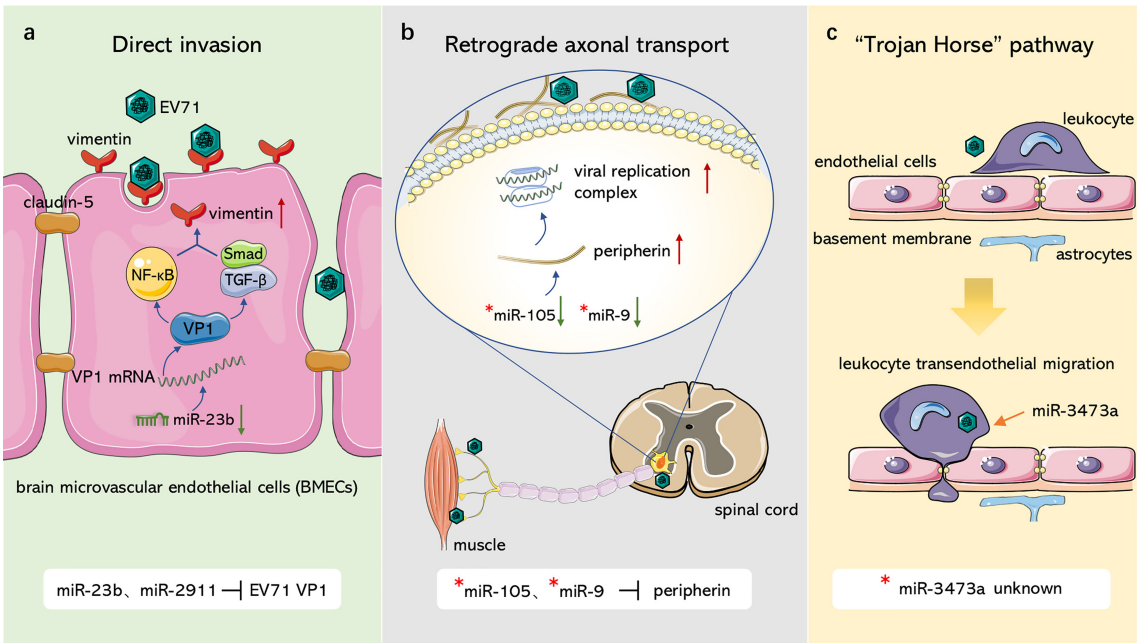

FIGURE 1 | Role of ncRNAs in EV71 invasion through blood-brain barrier. **(A)** Direct invasion. miR-23b and miR-2911 downregulate junction protein claudin-5 and upregulate EV71 receptor vimentin, resulting in damage to blood-brain barrier and the attachment of EV71 through modulating VP1 expression. **(B)** Retrograde axonal transport. miR-105 and miR-9 can target peripherin, which facilitates EV71 attachment and replication, to modulate viral retrograde axonal transport. **(C)** "Trojan Horse" pathway. EV71 can hijack immune cells to intrude CNS, miR-3473a may mediate leukocyte trans-endothelial migration and induce BBB disruption associated with EV71. "*": non-EV71-infected disease model.

disruption (Yang et al., 2017), however, studies should verify this hypothesis.

4 NCRNAS AND NERVOUS SYSTEM INJURY OF EV71

Although multiple complications have been reported, brainstem encephalitis with associated neurological pulmonary edema is a characteristic presentation of EV71 CNS infection (Wong et al., 2000; Nolan et al., 2003; Ooi et al., 2010). Affected children develop rapidly progressing cardiopulmonary failure that causes death, which is attributed to respiratory failure and severe pulmonary edema without intensive care. Autopsy and MRI reports indicate that EV71 lesions are mainly located in the ventral, medial, and lateral medulla oblongata (Zimmerman, 1999; Kao et al., 2004). In addition, EV71 has been detected in other nerve tissues, such as the spinal cord, which may explain generation of acute flaccid paralysis.

The pathogenesis of EV71-induced neurological complications is caused by host-virus interaction including direct damage by the virus and indirect injury mediated by immune and inflammatory responses (**Figure 2**). Apoptosis is a pivotal process for removing damaged cells and virus-infected cells to resist EV71 infection. Viruses are cytotropic microorganisms that completely rely on the host to survive, and they regulate host cells survival and complete their life cycle by mediating cell apoptosis to facilitate viral translation, replication, assembly, and release. The balance between viral replication and host apoptosis is t key for viral infection and determines direct damage of the virus to the host. On the other hand, the host counters against EV71 infection through innate immune and acquired immune cells, while EV71 escapes immune defense through several pathways, such as intracellular parasitism and immune cell destruction. Inflammatory cells infiltrate brain tissues mediated by virus particles stimulation and immune response, which further releases several inflammatory factors, such as IL-1, IL-6, IL-12, as well as TNF-α; and aggravates nervous system injury.

4.1 Direct Damage of EV71 to the Nervous System

4.1.1 Effect of ncRNAs on EV71 Replication

ncRNAs play a crucial regulatory role in various interactions between viruses and their hosts (Esteller, 2011; Beermann et al., 2016). EV71 hijacks host ncRNAs targeting proliferation-related genes of the host or even the virus itself to constitute a microenvironment that promotes EV71 replication. Mechanisms of directly targeting EV71 genome sequence by ncRNAs or modulating key host processes and signaling pathways to inhibit or promote viral replication are presented in this section (**Table 1**).

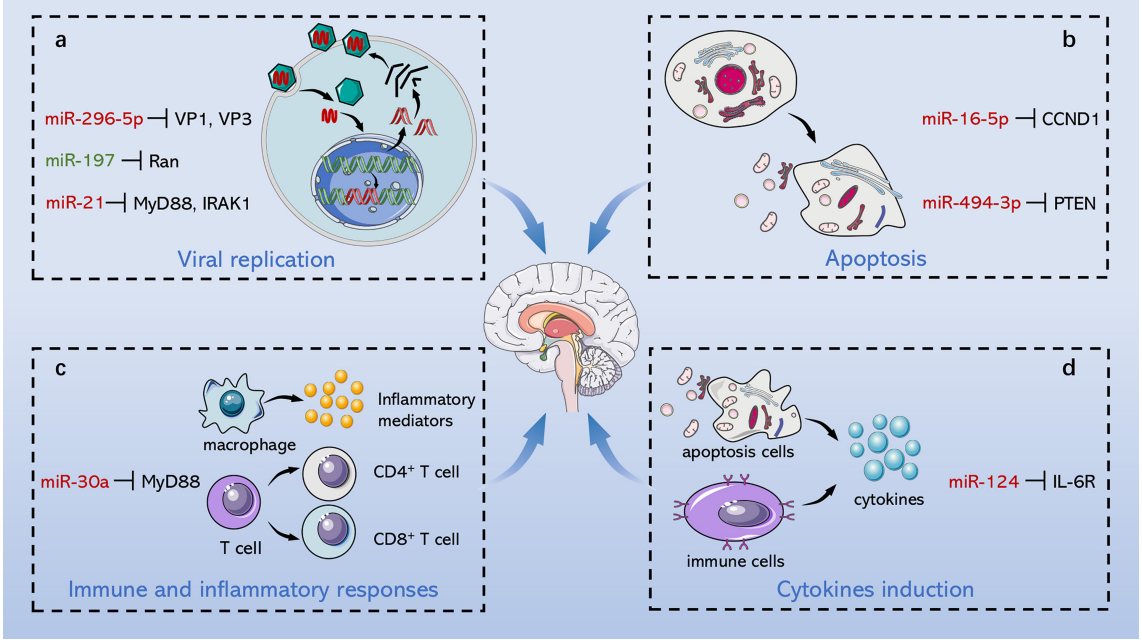

FIGURE 2 | Role of ncRNAs in central nervous system injury of EV71. EV71 injures CNS through direct damage by the virus and indirect injury mediated by immune and inflammatory responses. On the one hand, ncRNAs mediate direct injury of EV71 by modulating viral replication and host apoptosis. **(A)** miR-296-5p, miR-197 and miR-21 separately target viral genome, key host proteins and NF-κB pathway to involve in regulation of viral replication. **(B)** miR-16-5p and miR-494-3p respectively modulate cyclin expression and PI3K/Akt pathway to involve in regulation of host apoptosis. On the other hand, ncRNAs indirectly damage CNS through immunological concomitant inflammatory response and cytokines induction. **(C)** miR-30a promotes CNS damage by regulating immune and inflammatory responses, and **(D)** miR-124 upregulates the key pro-inflammatory cytokine, IL-6, aggravating damage induced by EV71. Red words indicate "upregulation"; green words indicate "downregulation".

The host suppresses EV71 replication through RNA interference of the combination of miRNAs and the viral genome, whereas EV71 downregulates the corresponding miRNAs to circumvent its suppression. miR-296-5p targets EV71 VP1 and VP3 coding sequences (2115 to 2135 nt and 2896 to 2920 nt) and is upregulated in the infected cells. miR-296-5p is a key factor in resisting EV71 infection by preventing synthesis of EV71 VP1/VP3 (Zheng et al., 2013). Several miRNAs, including miR-2911 (Li X. et al., 2018), miR-23b (Wen et al., 2013), and members of the miR-17-92 family (Fu et al., 2019) can also modulate VP1 gene expression of EV71. EV71 downregulates expression of miR-23b, miR-17-5p, and miR-19a/b to strengthen virus invasion and host injury, whereas miR-2911 expression is upregulated by initiation of the antiviral damage system. Yang et al. explored the relationship between miR-373 and miR-542-5p and EV71 replication, and revealed that miR-373 and miR-542-5p directly target the 5'UTR of the viral genome to inhibit EV71 replication (Yang and Tien, 2014). Short hairpin RNAs (shRNAs) have been found to act as therapeutic targets by antagonizing EV71 replication, whereas 29-mer shRNA effectively inhibits EV71 replication by targeting EV71 3D(pol) (Tan et al., 2007). Additionally, ncRNAs target the viral genome to modulate replication of EV71, as well as target receptor-related genes. Further, the EV71 receptor, SCARB2 induces viral infection of cells to directly mediate viral replication and cell tropism (Yamayoshi et al., 2009). miR-127-5p attenuates expression of SCARB2 mRNA and protein (Feng et al.), thus restraining viral internalization and ultimately abrogating virus immune escape. Furthermore, Liu et al. and Sim et al. transfected rhabdomyosarcoma (RD) cells with siRNAs targeting 2Apro (Liu et al., 2016), 3'UTR, 2C, 3C, and 3D (Sim et al., 2005) region of EV71 genome separately, significantly decreasing cytopathic effects of EV71 through RNA interference. These findings indicate that ncRNAs are potential therapeutic targets for preventing viral infection and alleviating body injury.

ncRNAs are involved in key processes and signaling pathways to modulate viral biosynthesis. The nuclear protein Ran affects several significant cellular processes, including the regulation and control of cell cycle progression by mediating mitosis, and nucleocytoplasmic transport associated with Ran GTPase (Dasso, 2001; Clarke and Zhang, 2008). EV71-induced miR-197 (Tang et al., 2016) and miR-134 (Orr-Burks et al., 2017) target Ran gene, which assists nuclear transportation of viral proteins 3D/3C and replication-associated proteins, ultimately dampening EV71 replication. The life cycle of viruses is dependent on the host translation machinery, whereby cap-dependent protein translation is beneficial to the host whereas cap-independent translation is beneficial to the virus. Notably, it is evident that degradation of eukaryotic initiation factor 4E (eIF4E) determines the progress of the switch between the two translation processes (Richter and Sonenberg, 2005; Sukarieh et al., 2010). Elsewhere, Ho et al. found that the eIF4E gene is

TABLE 1 | ncRNAs involved in EV71 replication.

ncRNAs	Expression	Target	Description	Process	Disease model	Reference
miR-296-5p	up	EV71 VP1 and VP3	miR-296-5p decreases EV71 replication by interacting with viral VP1vand VP3 genes	EV71 replication	*in vitro*: EV71 infected RD and SK-N-SH cells	(Zheng et al., 2013)
miR-373, miR-542-5p	unknown	5'UTR of EV71 genome	miR-373 and miR-542-5p inhibit EV71 replication by targeting 5'-UTR of viral genome	EV71 replication	*in vitro*: EV71 infected RD cells	(Yang and Tien, 2014)
miR-2911	up	EV71 VP1	miR-2911 reduces EV71 replication by directly targeting the VP1-coding sequence	EV71 replication	*in vitro*: EV71(Fuyang-0805 and Lianyungang2015) infected Vero cells	(Li X. et al., 2018)
miR-23b	down	EV71 VP1	downregulated miR-23b advances EV71 replication by targeting the VP1 gene 3'UTR	EV71 replication	*in vitro*: EV71 (Fuyang No. EU703812) infected RD cells	(Wen et al., 2013)
miR-17-5p, miR-19a/b	down	EV71 VP1	downregulated miR-17-5p and miR-19a/b enhance EV71 replication by targeting EV71 gene VP1	EV71 replication	*in vitro*: EV71 (strain FY0805) infected Vero cells	(Fu et al., 2019)
miR-18a, miR-452	up	EV71 VP3	miR-18a and miR-452 decrease EV71 replication by expression inhibition of VP3	EV71 replication	*in vitro*: EV71 (Hubei-09 strain GU434678.1) infected RD cells	(Yang et al., 2021)
29-mer shRNA	:	EV71 3D (pol)	29-mer shRNA most effectively inhibits EV71 replication by targeting EV71 3D(pol)	EV71 replication	*in vitro*: EV71 infected RD cells	(Tan et al., 2007)
miR-127-5p	up	SCARB2	miR-127-5p downregulates the expression of SCARB2 by target SCARB2-coding gene 3' UTR	EV71 replication	*in vitro*: EV71 (Fuyang0805 strain) infected HeLa and HepG2 cells	(Feng C. et al., 2017)
miR-197	down	Ran	downregulated miR-197 facilitates EV71 replication by suppressing Ran to assist transportation of viral 3D/3C and replication protein	EV71 replication	*in vitro*: EV71 (2231 TW strain) infected HEK 293T and RD cells	(Tang et al., 2016)
miR-134	unknown	Ran	miR-134 represses EV71 replication by decreasing Ran expressions	EV71 replication	*in vitro*: EV71 infected Hep2 and RD cells	(Orr-Burks et al., 2017)
miR-141	up	eIF4E	miR-141 promotes EV71 replication by targeting eIF4E for shutoff of host protein synthesis	EV71 replication	*in vitro*: EV71 infected RD cells	(Ho et al., 2011)
miR-876-5p	up	CREB5	miR-876-5p accelerates EV71 replication by targeting host CREB5	EV71 replication	*in vitro*: EV71 (2231 Taiwan strain) infected RD and SK-N-SH cells	(Xu et al., 2020)
miR-155	up	PICALM	miR-155 inhibits EV71 replication by targeting PICALM	EV71 replication	*in vitro*: EV71 infected RD and SK-N-SH cells	(Wu et al., 2019)
miR-30a	down	Beclin-1	downregulated miR-30a advances EV71 replication by targeting 3' UTR of Beclin-1 transcripts to inhibit autophagy	EV71 replication	*in vitro*: EV71 infected Hep2 and Vero cells	(Fu et al., 2015)
miR-30a	up	MyD88	miR-30a facilitates EV71 replication by targeting MyD88 and subsequently inhibits IFN-1 production	EV71 replication	*in vitro*: EV71 infected OE cells	(Wang Y. et al., 2020)
miR-548	down	IFN-λ1	downregulated miR-548 decrease EV71 replication by enhancing IFN-λ1 expression	EV71 replication	*in vitro*: EV71 (C4 subtype) infected RD cells	(Li et al., 2013)
miR-155-5p	up	FOXO3, IRF7	miR-155-5p facilitates EV71 replication by negatively regulating FOXO3/IRF7 axis to inhibit IFN-1 response	EV71 replication	*in vitro*: EV71 (BrCr strain) infected RD cells; *in vivo*: EV71 (BrCr strain) infected C57BL/6 mice	(Yang et al., 2020)
lncRNA-AK097647	up	unknown	lncRNA AK097647 facilitates EV71 replication by decreasing IFN-λ1 lncRNA AK097647 induces the phosphorylation of NF-κB	EV71 replication	*in vitro*: EV71 (BrCr strain) infected RD cells	(Chu et al., 2021)
miR-526a	down	CYLD	downregulated miR-526a promotes EV71 replication by targeting CYLD to promote the RIG-I-dependent NF-κB pathway	EV71 replication	*in vitro*: EV71 (GDV-103 strain) infected RD cells	(Xu et al., 2014)
miR-9-5p	down	NF-κB	downregulated miR-9-5p promotes EV71 replication by targeting NF-κB and improving its expression	EV71 replication	*in vitro*: EV71 (Shenzhen strain AF30299.1) infected HEK 293T, Vero, RD, HT-29, HeLa, and THP-1 cells; *in vivo*: EV71 (Shenzhen strain AF30299.1) infected ICR mice	(Li and Zheng, 2018)
miR-146a	up	TRAF6, IRAK1	miR-146a accelerates EV71 replication by targeting TRAF6 and IRAK1 TRAF6 activates the NF-κB pathway	EV71 replication	*in vivo*: EV71 infected RD cells	(Ho et al., 2014; Fu et al., 2017)
miR-545	up	TRAF6	miR-545 advances EV71 replication by attenuating TRAF6 expression	EV71 replication	*in vitro*: EV71 infected HEK 293T and RD cells	(Sun et al., 2019)

(Continued)

TABLE 1 | Continued

ncRNAs	Expression	Target	Description	Process	Disease model	Reference
miR-628-5p	Up	TRAF3	miR-628-5p promotes EV71 replication by inhibiting TRAF3 expression	EV71 replication	*in vitro*: EV71 infected RD cells	(Li et al., 2021)
miR-21	up	MyD88, IRAK1	miR-21 promotes EV71 replication by targeting MyD88 and IRAK1 MyD88 and IRAK1 activate the NF-κB pathway	EV71 replication	*in vitro*: EV71 infected HCoEpiC and Human NCM460 cells	(Feng N. et al., 2017)
miR-124	up	IL-6R, STAT3	miR-124 promotes EV71 replication by restraining the expression of IL-6R and STAT3	EV71 replication	*in vitro*: EV71 infected RD and HeLa cells	(Chang et al., 2017)
miR-302	down	KPNA2	downregulated miR-302 promotes EV71 replication by targeting KPNA2 to regulate the JNK pathway	EV71 replication	*in vitro*: EV71 (Xiangyang strain JN230523.1) infected HEK293T and RD cells	(Peng et al., 2018)
let-7c-5p	up	MAP4K4	MAP4K4 is a key inhibitory factor of the JNK pathway let-7c-5p remotes EV71 replication by inhibiting MAP4K4 expression	EV71 replication	*in vitro*: EV71 infected RD cells	(Zhou et al., 2017)
miR-103, miR-107	down	SOCS3	downregulated miR-103 and miR-107 increase EV71 replication and suppress production of IFN-1 by regulating SOCS3/STAT3 pathway	EV71 replication	*in vitro*: EV71 (BrCr strain) infected Vero and RD cells	(Huang et al., 2021)

combined and cleaved by upregulated miR-141 resulting in shutoff of the host protein synthesis and generation of viral proteins (Ho et al., 2011).

In addition, it has been found that ncRNAs are associated with dysregulated signaling pathways (**Figure 3**). The nuclear factor-kappa B (NF-κB) pathway regulates several genes related to cell proliferation, differentiation, innate immune response, and inflammatory cytokine production (Perkins, 2012). NF-κB pathway plays an essential role in EV71 pathogenicity, which is represented by the viral 2C protein, which suppresses NF-κB pathway activation to promote viral replication (Tung et al., 2010; Du H. et al., 2015). Myeloid differentiation factor 88 (MyD88) and IL-1 receptor-associated kinase-1 (IRAK1) modulate initiation of the Toll-like receptor-dependent NF-κB pathway (Hayden et al., 2006). According to Feng N. et al. (2017), it is demonstrated that miR-21 promotes EV71 replication by suppressing the NF-κB pathway mediated by MyD88 and IRAK1. Moreover, other studies including Ho et al. (2014) and Fu et al. (2017) confirmed that miR-146a downregulates expression of TNF receptor-associated factor 6

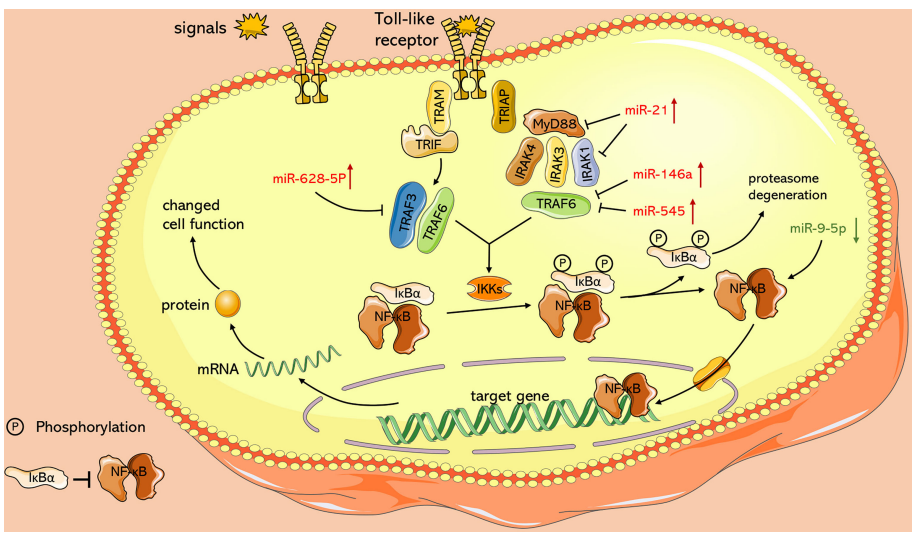

FIGURE 3 | Role of ncRNAs in activation of NF-κB pathway with TLR signaling as an example. Toll-like receptors activate and recruit TIR-containing adaptor molecules, MyD88 and TRIF, which prime downstream effectors respectively, under the stimulation of signals such as LPS. Both of upstream signal paths finally transfer signals to IKKs, the protein kinase of IκB, and relieve inhibition of NF-κB. miR-628-5p, miR-21, miR-146a, miR-545 and miR-9-5p play an essential role in this process.

(TRAF6), which regulates activation of NF-κB pathway (Xia et al., 2011), and hence facilitates viral biosynthesis. However, downregulated miR-526a (Xu et al., 2014) and miR-9-5p (Li and Zheng, 2018) induced by EV71 infection facilitate EV71 replication by activating the NF-κB pathway. These conflicting results may be ascribed to multiple functions of NF-κB in different cases. Under physiological conditions, NF-κB mediates immune response to resist external invasion, whereas aberrant regulation of NF-κB is implicated in cancer development and EV71 pathogenicity (Baud and Karin, 2009; Tung et al., 2010; Jin et al., 2018). In addition, Chu et al. reported that lncRNA-AK097647 has been found significantly upregulated during EV71 infection, which facilitates EV71 replication through blocking interferon-λ1 secretion and inducing the phosphorylation of NF-κB (Chu et al., 2021).

In conclusion, these findings indicate that ncRNAs regulate viral replication by targeting key virus and host genes. In the future, we can target these ncRNAs to inhibit EV71 replication and reduce body injury.

4.1.2 ncRNAs and Host Apoptosis Induced by EV71

Host injury affected by viruses is influenced by apoptosis. Viruses regulate the host apoptosis to complete their replication cycle, whereas virus-infected host cells initiate apoptotic pathways to resist viral infection and reduce virus damage on the body (Benedict et al., 2002; Orzalli and Kagan, 2017). The endogenous mitochondrial cytochrome C pathway and exogenous death receptor Fas/FasL pathway are the key pathways in controlling cell apoptosis. The cascade of caspase protease family activation, which is the mutually terminal process of the two pathways, contributes to decomposition of potentially harmful cells (Sen, 1992; Riedl and Shi, 2004; Green and Llambi, 2015). ncRNAs control EV71-related cell apoptosis by regulating protein expression and signal transduction of the caspase pathway (**Table 2**).

Cyclin D1 (CCND1) and cyclin E1 (CCNE1) are the main regulators of G1 phase progression (Blomen and Boonstra, 2007). Notably, miR-16-5p (Zheng et al., 2017), and miR-let-7b (Du X. et al., 2015) abrogate EV71 replication through inhibition of CCND1 synthesis and initiation of caspase-dependent apoptosis. Furthermore, endogenous miR-let-7b released from injured neurons can induce neuronal cell death through Toll-like receptor (TLR) 7 signaling (Lehmann et al., 2012). Son of sevenless homolog 1 (SOS1) is a critical anti-apoptotic protein associated with TNFα-induced apoptosis (Kurada et al., 2009; Hao et al., 2018), Growth arrest and DNA damage-inducible protein 45β (GADD45β) promotes apoptosis by upregulating expression of the apoptosis-related factors, caspase-3 and p53 (Ou et al., 2010; Yu et al., 2013). Elsewhere, Chang et al. (Chang et al., 2015) reported that induction of miR-146a and degradation of miR-370 together trigger apoptosis of the EV71-infected cells by targeting SOS1 and GADD45β, respectively. Moreover, the long non-coding RNA, lnc-IRAK3-3 was found to capture miR-891b upregulate GADD45β expression and eventually promote host apoptosis (Liao et al., 2019). Moreover, Lu et al. filtered differentially expressed ncRNAs associated with EV71 infection, including 6 lncRNAs, 28 miRNAs, and 349 mRNAs. Their further studies reported that MALAT1/miR-194-5p/DUSP1 axis, a lncRNA-miRNA-mRNA-associated competing endogenous RNA regulatory network, involved in host apoptosis induced by EV71 infection (Lu et al., 2021).

Phosphatidylinositide 3-kinase (PI3K)/Akt is an important signaling pathway that mediates cell survival, growth, and metabolism (Osaki et al., 2004; Soulard and Hall, 2007; Ediriweera et al., 2019), This pathway attenuates cell apoptosis by inhibiting phosphorylation of caspase-9 and Bad protein (members of the B-cell lymphoma-2 family) (She et al., 2005; Hohenester et al., 2010). Phosphatase and tensin homologue (PTEN) facilitates dephosphorylation of Akt and hence prevents the events of downstream signaling that are regulated by Akt, and thus it is a negative regulator of the PI3K/Akt pathway (Song et al., 2012). The function of PTEN in inhibiting cell apoptosis has been shown in multiple cell types, including kidney cancer cells, mouse mammary epithelia and B lymphocytes (Dupont et al., 2002; Lin et al., 2007; Cheng et al., 2009). Notably, miR-494-3p expression is significantly upregulated following EV71 infection, repressing host apoptosis and promoting EV71 replication through degeneration of PTEN. Overexpression of miR-494-3p mimics antagonizes this process by restoring miR-494-3p levels of expression and activating the PI3K/Akt pathway (Zhao et al., 2018). miR-545 separately targets PTEN and TRAF6 and activates PI3K/Akt and NF-κB pathways to modulate EV71 replication and host apoptosis (Sun et al., 2019). Epidermal growth factor receptor (EGFR) is an activator of the PI3K/Akt pathway (Guo et al., 2015), and is upregulated by EV71-induced downregulation of miR-27a and eventually inhibits nerve cell apoptosis (Zhang et al., 2014).

These findings indicate that hosts and viruses fight for damage and anti-damage around viral replication and host apoptosis, which are regulated by ncRNAs. These ncRNAs can serve as therapeutic targets to inhibit viral life cycle and alleviate host injury in EV71 treatment.

4.2 Indirect Injury Mediated by Immune and Inflammatory Responses

Although inflammation is a protective response to minimize pathogen spread and promote the recovery of damaged tissue, a dysregulated inflammatory response results in various inflammatory injuries (Nathan and Ding, 2010). Immunological concomitant inflammatory injury is the major damage mode of EV71 to hosts with severe nervous system diseases such as neurogenic pulmonary edema (Lin et al., 2003; Huang et al., 2011; Griffiths et al., 2012; Yu et al., 2019). A complex immune defense mechanism is triggered when EV71 infects the body, which is accompanied by resistance mediated by the innate immune response to exogenous pathogens and activation of acquired immune response mediated by antigen-presenting cells (Edsall, 1949). Subsequently, the activated immune-related cells (innate immune cells and specific immune cells) release cytokines and inflammatory factors, which may cause immune-mediated inflammatory injury in pathological conditions. Effects of ncRNAs on immune and

TABLE 2 | ncRNAs involved in host apoptosis.

ncRNAs	Expression	Target	Description	Process	Disease model	Reference
miR-16-5p	up	CCND1, CCNE1	miR-16-5p promotes host apoptosis by targeting CCNE1 and CCDN1	Apoptosis	*in vitro*: EV71 (GZ-CII strain) infected RD, CCF-STTG1 and SK-N-SH cells; *in vivo*: KM and ICR mice	(Zheng et al., 2017)
miR-let-7b	up	CCND1	miR-let-7b promotes host apoptosis by inhibiting CCND1 expression	Apoptosis	*in vitro*: EV71 infected SH-SY5Y cells	(Du X. et al., 2015)
miR-146a	up	SOS1	miR-146a promotes EV71-induced host apoptosis by targeting 3'UTR of SOS1 gene SOS1 accelerates cell apoptosis	Apoptosis	*in vitro*: EV71 infected RD cells	(Chang et al., 2015)
miR-370	down	GADD45β	downregulated miR-370 advances EV71-induced apoptosis by targeting GADD45β	Apoptosis	*in vitro*: EV71 infected RD cells	(Chang et al., 2015)
lnc-IRAK3-3	up	miR-891b	lnc-IRAK3-3 restrain the expression of miR-891b to promote host apoptosis	Apoptosis	*in vitro*: EV71 infected RD cells	(Liao et al., 2019)
miR-891b	down	GADD45β	miR-891b is inhibited by lnc-IRAK3-3 downregulated miR-891b increases host apoptosis by raising GADD45β generation	Apoptosis	*in vitro*: EV71 infected RD cells	(Liao et al., 2019)
miR-874	down	GZMB	downregulated miR-874 facilitates host apoptosis by reducing GZMB expression	Apoptosis	*in vitro*: EV71 infected Jurkat cells	(Zhang M. et al., 2020)
miR-27a	down	EGFR	downregulated miR-27a inhibits host apoptosis by enhancing EGFR expression and initiating PI3K/AKT pathway The activation of the PI3K/AKT pathway suppresses host apoptosis	Apoptosis	*in vitro*: EV71 infected RD and SK-N-SH cells	(Zhang et al., 2014)
miR-494-3p	up	PTEN	miR-494-3p inhibits host apoptosis by targeting PTEN and initiating PI3K/Akt signaling pathway PTEN is an inhibitor of the PI3K/AKT pathway	Apoptosis	*in vitro*: EV71 infected RD and HEK 293T cells	(Zhao et al., 2018)
miR-545	up	TRAF6, PTEN	miR-545 inhibits host apoptosis by attenuating PTEN expression	Apoptosis	*in vitro*: EV71 infected RD and HEK 293T cells	(Sun et al., 2019)
lncRNA-MALAT1	up	miR-194-5p	lncRNA- MALAT1 induces host apoptosis by MALAT1/miR-194-5p/DUSP1 ceRNA regulatory axis	Apoptosis	*in vitro*: EV71 (87-2008 Xi'an Shaanxi strain) infected RD cells	(Lu et al., 2021)

inflammatory responses as well as cytokine expression are discussed in the subsequent section (**Table 3**).

4.2.1 Role of ncRNAs in Immune and Inflammatory Responses During EV71 Infection

Innate immune system serves as the first line of defense against exogenous pathogens and internal apoptosis, aberrant cells, and other "nonself" components. Chemokines and cytokines are released and inflammatory response is initiated after rapid activation of innate immune cells through recognition of foreign or harmful substances. Recognition of viruses is primarily initiated by pattern recognition receptors (PRRs), including Toll-like receptors (TLRs), retinoic acid inducible-gene I (RIG-I)-like receptors, NOD-like receptors (NLRs), and C-type lectin receptors (Takeuchi and Akira, 2010; Fitzgerald and Kagan, 2020). Serving as a key target of viruses against body immunity, MyD88 is an essential adaptor molecule for TLR signaling cascades (Takeda and Akira, 2004). Research conducted by Wang et al., illustrated that overexpression of miR-30a upon EV71 infection inhibited innate immunity by repressing type I interferon production, and the direct target of miR-30a, MyD88, played a key role in this process (Wang Y. et al., 2020). Analogously, miR-21 targets MyD88 and IRAK1 to reduce the level of type I interferon through the TLR pathway (Feng N. et al., 2017). In addition, Xu et al. reported that RIG-I activity is mediated by miR-526a through inhibition of CYLD expression, which negatively regulates generation of type I interferon (Xu et al., 2014). Overexpression of miR-9-5p which is induced by EV71 also inhibits RIG-I-dependent innate immune response by targeting NF-κB (Li and Zheng, 2018). These ncRNAs control occurrence of inflammatory response by mediating innate immunity, while the recognition receptors of innate immune cells, PRRs, are involved in transcriptional regulation of inflammatory mediators (Takeuchi and Akira, 2010; Luo et al., 2019). For instance, overexpression of pro-inflammatory cytokines (TNF-α, IL-6, and IL-1) induced by EV71 is restored through modulation of RIG-associated miR-9-5p (Li and Zheng, 2018). In innate immune response, macrophages play an important role in the initiation, maintenance and dissipation of inflammation, and Early Growth Response 1 (EGR1) inhibits expression of pro-inflammatory genes in macrophages (Trizzino et al., 2021). Hu et al. evaluated the relationship of circRNA/miRNA/mRNA associated with EV71 infection, and eventually screened hsa_circ_0017115/hsa-miR-150-5p/EGR1 axis (Hu et al., 2021), which might regulate inflammatory response through interaction between EGR1 and macrophages.

Acquired immune cells are activated by stimulation of antigen signals and play an essential role in resisting infections (Edsall, 1949). Chang et al. (2006) and Yang et al. (2001) found that

TABLE 3 | ncRNAs involved in immune and inflammatory responses.

ncRNAs	Expression	Target	Description	Process	Disease model	Reference
miR-21	up	MyD88, IRAK1	miR-21 reduces the production of IFN-1 by targeting MyD88 and IRAK1	pro-inflammatory factor	*in vitro*: EV71 infected HCoEpiC and Human NCM460 cells	(Feng N. et al., 2017)
miR-30a	up	MyD88	miR-30a reduces the production of IFN-1 by targeting MyD88 and IRAK2	pro-inflammatory factor	*in vitro*: EV71 infected OE cells	(Wang Y. et al., 2020)
miR-526a	down	CYLD	miR-526a rises the level of IFN-1 through the RIG-I-dependent pathway	anti-inflammatory factor	*in vitro*: EV71 (GDV-103 strain) infected RD cells	(Xu et al., 2014)
miR-9-5p	down	NFκB	miR-9-5p inhibits excessive production of IL-6, IL-1β, and TNF-α induced by EV71 miR-9-5p increases production of IFN-1 by targeting NFκB	anti-inflammatory factor	*in vitro*: EV71 (Shenzhen strain AF30299.1) infected HEK 293T, Vero, RD, HT-29, HeLa, and THP-1 cells; *in vivo*: EV71 (Shenzhen strain AF30299.1) infected ICR mice	(Li and Zheng, 2018)
miR-146a	up	IRAK1, TRAF6	miR-146a reduces the expression of IFN-β by targeting IRAK1 and TRAF6	pro-inflammatory factor	*in vivo*: EV71 infected RD cells	(Ho et al., 2014; Fu et al., 2017)
miR-155-5p	up	FOXO3, IRF7	miR-155-5p inhibits IFN-1 response by negatively regulating the FOXO3/IRF7 axis	pro-inflammatory factor	*in vitro*: EV71 (BrCr strain) infected RD cells; *in vivo*: EV71 (BrCr strain) infected C57BL/6 mice	(Yang et al., 2020)
miR-545	up	PTEN, TRAF6	miR-545 inhibits IFN-1 generation by attenuating TRAF6 and PTEN expression	pro-inflammatory factor	*in vitro*: EV71 infected HEK 293T and RD cells	(Sun et al., 2019)
miR-628-5p	up	TRAF3	miR-628-5p inhibits IFN-β expression by targeting TRAF3	pro-inflammatory factor	*in vitro*: EV71 infected RD cells	(Li et al., 2021)
miR-103, miR-107	down	SOCS3, STAT3	miR-103 and miR-107 advance the level of IFN-1 by targeting SOCS3	anti-inflammatory factor	*in vitro*: EV71 (BrCr strain) infected Vero and RD cells	(Huang et al., 2021)
miR-124	up	IL-6R, STAT3	miR-124 enhances the level of IL-6 by targeting IL-6R	pro-inflammatory factor	*in vitro*: EV71 infected RD and HeLa cells	(Chang et al., 2017)
miR-302	down	KPNA2	KPNA2 overexpression promotes EV71-induced production of the IL-6 and TNF-α miR-302 inhibits the expression of KPNA2 mRNA and protein	anti-inflammatory factor	*in vitro*: EV71 (Xiangyang strain JN230523.1) infected HEK 293T and RD cells	(Peng et al., 2018)
let-7c-5p	up	MAP4K4	MAP4K4 is a key inhibitory factor of the JNK pathway let-7c-5p promotes IL-6 and TNF-α by inhibiting MAP4K4 expression	pro-inflammatory factor	*in vitro*: EV71 infected RD cells	(Zhou et al., 2017)

cellular rather than humoral immunity is associated with host acquired immune response against EV71 infection. Dicer serves as an RNase III enzyme and modulates production of mature miRNAs (Burger and Gullerova, 2015). Knockout of Dicer during the early stage of lymphocyte development shows that miRNAs play a key role in T-cell proliferation as indicated by a 90% reduction in T cells in circulation (Cobb et al., 2005). Moreover, miRNAs are implicated in production of CD4+ Treg cells and Th2 cells late T cell differentiation (Muljo et al., 2005). Previous studies conducted by Thai et al. (2007) and Rodriguez et al. (2007) discovered that miR-155 knockout mice were unable to mount an effective acquired immune response and showed a selective tendency towards Th2 phenotype. Subsequent studies established that miR-155 was conducive to Treg development by targeting suppressor of cytokine signaling 1 (SOCS1) (Lu et al., 2009). Furthermore, Liu et al. (2008) showed that miR-181a induces CD4+ and CD8+ double-positive (DP) T cell development. Th1 cells mainly produce IFN-γ, which has been proven to be a pro-inflammatory factor (Farrar and Schreiber, 1993). Moreover, Th2 and Treg cells mainly produce IL-10, which serves as an anti-inflammatory factor and prevents excessive tissue disruptions caused by inflammation (Ouyang et al., 2011). These results indicate that ncRNAs contribute to inflammation by releasing inflammatory factors through regulation of T cell differentiation and initiating T lymphocytes. However, studies have not explored the effects of ncRNAs on T-cell development and differentiation in EV71-induced disease models.

4.2.2 Role of ncRNAs in Expression of EV71-Induced Cytokines

Abundant cytokines and chemokines are released from activated immune and apoptotic cells induced by EV71, including IFNs, IL-6, IL-13, IL-1β, and TNF-α among other inflammatory mediators (Huang et al., 2011; Ouyang et al., 2011; Griffiths et al., 2012; Luo et al., 2019; Yu et al., 2019). Pro-inflammatory cytokines (such as IL-6, IL-12, IL-1β, TNF-α, and IFN-γ) play a significant role in EV71-mediated CNS inflammatory injury (Lin et al., 2003). The key pro-inflammatory mediator, IL-6, is the main pathogenic factor for pulmonary edema-associated

encephalitis (Lin et al., 2002; Luo et al., 2019). Further, the ncRNAs modulate expression of inflammatory cytokines during EV71 infection. A separate study conducted by Chang et al. (Chang et al., 2017) found that miR-124 decreased the level of IL-6 by directly targeting IL-6R and hence promoted EV71 pathogenesis. Moreover, let-7c-5p, which also acts as a pro-inflammatory factor, increases production of IL-6 and TNF-α through the MAP4K4-mediated c-Jun N-terminal kinase (JNK) pathway (Zhou et al., 2017). Analogously, miR-302 has exhibited an anti-inflammatory function by inhibiting EV71-induced generation of IL-6 and TNF-α to alleviate body damage through the miR-302/karyopherin α2 (KPNA2) axis associated with the JNK pathway (Peng et al., 2018). An investigation conducted by Li et al. reported that excessive production of IL-6, IL-1β, and TNF-α was transferred to physiological levels by anti-inflammatory factor miR-9-5p through modulation of the RIG-I-dependent NF-κB pathway (Li and Zheng, 2018). In addition, several ncRNAs, such as miR-103, miR-107 (Huang et al., 2021), miR-146a (Ho et al., 2014; Fu et al., 2017), miR-155-5p (Yang et al., 2020), miR-545 (Sun et al., 2019), and miR-628-5p (Li et al., 2021) negatively or positively affect inflammatory response by modulating expression of interferons. Accordingly, EV71 facilitates inflammatory injury by upregulating pro-inflammatory factors such as miR-124 and downregulating inflammatory factors such as miR-302. Many researchers have reported the role of lncRNAs in secretion of enteroviruses-mediated inflammatory factors. In Coxsackievirus B3 infection, Cao et al. found that lncRNA HIF1A-AS1 activated NF-κB pathway by targeting miR-138, and presented a role of pro-apoptosis and pro-inflammation (Cao et al., 2020). However, EV71-associated lnRNAs in immune and inflammatory responses have not been clarified, more attention should be paid to lncRNAs because of their important potential.

5 POTENTIAL CLINICAL APPLICATION OF NCRNAS IN HFMD

5.1 ncRNAs and HFMD Diagnosis

Additional laboratory tests are generally deemed unnecessary for mild cases of HFMD because it is a self-limiting disease (Cox and Levent, 2018). However, classification of pathogenic enterovirus and definitive therapy is crucial in the presence of severe or fatal neurological complications associated with HFMD. For instance, the early clinical symptoms of EV71 and CVA16 (the two main pathogens of HFMD) are similar, but few patients with EV71 infection may progress into serious CNS complications; nevertheless, most patients with CVA16 infection show good prognosis (Liu et al., 2015). The golden criterion for diagnosis of enterovirus infection is isolation of viruses from clinical samples, which is time-consuming and laborious (Ooi et al., 2010). Quantitative real-time PCR (qRT–PCR) is a fast method which is developed to circumvent the limitations of conventional diagnostic methods. However, the method is associated with a high number of false-positive and false-negative results owing to the high rate of gene mutation in enterovirus (Perera et al., 2004; Chen et al., 2006). Furthermore, the ncRNAs have highly stable physical and chemical properties during circulation; and thus they can rapidly and conveniently provide an alternative diagnosis strategy for HFMD (Grasedieck et al., 2012; Zhang et al., 2019).

Accumulating studies indicate that ncRNAs can serves as potential candidate biomarkers for the diagnosis of HFMD. A miRNA-based prediction model of HFMD was established by Min et al. (Min et al., 2018), results of the study showed that circulating salivary hsa-miR-221 was continuously and significantly downregulated in all HFMD cohorts. The detection of circulating salivary hsa-miR-221 could be used as a convenient diagnostic method for HFMD. Li Y. et al. (2018) analyzed lncRNA and mRNA expression profiles associated with EV71 infection, and 23 lncRNAs and 372 mRNAs with remarkable differential expression were found between infected and uninfected RD cells. Subsequent studies discovered that these lncRNA were involved in EV71 infection-induced pathogenesis. Additionally, ncRNA can be used to differentiate HFMD caused by EV71 and CVA16, providing a basis for clinical treatment. Cui et al. (2011) reported that miR-545, miR-324-3p, and miR-143 can be used to effectively distinguish EV71 and CVA16 infections in patients with HFMD. Moreover, an investigation conducted by Liu et al. (2020) indicated that patients with EV71-induced HFMD presented significantly higher levels of serum miR-494 as compared with the level in healthy people or those with CVA16-induced HFMD, showing its potential diagnostic value. In addition, ncRNAs play an important role in prediction of disease severity. Meng et al. analyzed the dynamic differential expression profile of lncRNAs and filtered out 10 lncRNAs that were differentially expressed in patients with HFMD presenting with different severities (Meng et al., 2017). Similarly, the comparison of miRNA expression profiles between patients with mild and severe HFMD shows that miR-671-5p, miR-16-5p, and miR-150-3p are potential diagnostic markers for differentiating severity of HFMD (Jia et al., 2014). Furthermore, the level of miR-876-5p is 9.5-fold higher in severe cases than level in cases with mild EV71 symptoms, and the clinical symptoms were alleviated after knockdown of miR-876-5p (Wang et al., 2016). In addition, there are ncRNAs serving as biomarkers for HFMD caused by other non-EV71 and non-CVA16 enteroviruses. Coxsackievirus B5 (CVB5) is a major pathogen of HFMD, which has an increasing incidence in recent years. Teng et al. analyzed the lncRNA profile of CVB5 infected RD and SH–SY5Y cells through RNA sequencing, and revealed the potential of lncRNA-IL12A as a biomarker (Teng et al., 2022). These studies indicate that ncRNAs have significant potential for application in clinical diagnosis of HFMD.

5.2 ncRNAs and Treatment of EV71-Induced HFMD

Several studies have explored the potential of ncRNAs as therapeutic targets for treatment of the disease. Studies on miRNAs have achieved positive results and miRNAs are applied in clinical practice (Lee et al., 2020). Novel antiviral drugs have been developed by mainly modulating the function of miRNAs to enhance their roles through mimics and downregulate their roles

through inhibition using antisense oligonucleotides (ASOs) (Beermann et al., 2016). As mentioned above, ncRNAs modulate progression of EV71-induced HFMD by regulating the viral life cycle and host immune and inflammatory responses; therefore, these processes can serve as potential therapeutic targets. The miRNAs such as miR-296-5p, miR-197, miR-16-5p, and miR-27a inhibit EV71 proliferation and reduce host injury by modulating viral replication and host apoptosis, respectively. The miRNA analogues can be designed for treatment of EV71-induced HFMD. In addition, inhibitors of proinflammatory factors such as miR-21, miR-146a, and miR-124 can modulate immune response and hence relieve inflammatory injury caused by EV71. Clinical trials of miRNAs based on therapy in cancers are underway implying that miRNA-based therapy for HFMD may be realized in the future (Janssen et al., 2013; van Zandwijk et al., 2017).

However, some limitations were noted in the current study, several of which should be solved before miRNAs can be applied in clinical practice. First, some miRNAs, such as the miR-143/145 cluster (Dimitrova et al.) mentioned above, exhibit opposite effects under different conditions, and thus unified standards of the disease model should be determined. Second, it has been noted that one miRNA can target several genes, whereas one gene can be targeted by several miRNAs. Studies should explore strategies to ensure that miRNAs act on desired targets and to minimize side effects. Third, miRNAs function in multiple organs of the whole body, and the blood-brain barrier blocks entry of most pathogens and drugs. Methods for facilitating miRNA-targeted transport to the brain and across the blood-brain barrier should be explored. Finally, stability of mRNAs should be improved and rapid degeneration of miRNAs should also be minimized. Therefore, further studies should be conducted to explore the role and mechanism of miRNAs in HFMD induced by EV71.

6 CONCLUSIONS AND PERSPECTIVE

As the main pathogen of HFMD with severe neurological complications, EV71 significantly does harm to patient health and results in a huge economic burden. Therefore, explore neuropathogenic mechanism of EV71 is necessary for reducing severe cases and for development of effective therapeutic ways. We illustrate recent advances concerning the role of ncRNAs in EV71-induced CNS infection and CNS injury by virus-host interaction. As the essential molecules of gene regulation, ncRNAs present broad clinical application prospects. Especially in diagnosis of HFMD, the different expression of ncRNAs have potential in prediction of disease severity and differentiation of HFMD. In conclusion, ncRNAs are closely related to EV71-induced infection progression and virus-host interaction, as well as represent a significant potential direction for therapeutic and diagnostic research. Among them, miRNAs were widely reported in regulation of EV71 life cycle and host immune response. However, although lncRNAs have been shown to participate in viral replication, host apoptosis, and immune and inflammatory responses in enteroviruses infection (Shi et al., 2016; Liu et al., 2019; Zhang Y. et al., 2020), current research on the role of lncRNAs in EV71 infection is limited. It has been shown that lncRNAs may be equally or even more important compared with miRNAs in terms of clinical benefits owing to their tissue specificity. Therefore, there is still need for further studies to explore role of lncRNAs in pathogenesis, diagnosis and treatment of EV71 is necessary.

AUTHOR CONTRIBUTIONS

Conceptualization, FY, NZ, YD, and JM; resources, YC; writing—original draft preparation, JY and XC; writing—review and editing, MX and RM. All authors have read and agreed to the published version of the manuscript.

FUNDING

This work was funded by the National Natural Science Foundation of China (No. 31701162) and the Key Research and Development Program of Anhui Province (No. 202104a07020031).

REFERENCES

B'Krong, N., Minh, N. N. Q., Qui, P. T., Chau, T. T. H., Nghia, H. D. T., Do, L. A. H., et al. (2018). Enterovirus Serotypes in Patients With Central Nervous System and Respiratory Infections in Viet Nam 1997-2010. *Virol. J.* 15 (1), 69. doi: 10.1186/s12985-018-0980-0

Baggen, J., Thibaut, H. J., Strating, J., and van Kuppeveld, F. J. M. (2018). The Life Cycle of non-Polio Enteroviruses and How to Target it. *Nat. Rev. Microbiol.* 16 (6), 368–381. doi: 10.1038/s41579-018-0005-4

Baud, V.r., and Karin, M. (2009). Is NF-kappaB a Good Target for Cancer Therapy? Hopes and Pitfalls. *Nat. Rev. Drug Discovery* 8 (1), 33–40. doi: 10.1038/nrd2781

Beermann, J., Piccoli, M. T., Viereck, J., and Thum, T. (2016). Non-Coding RNAs in Development and Disease: Background, Mechanisms, and Therapeutic Approaches. *Physiol. Rev.* 96 (4), 1297–1325. doi: 10.1152/physrev.00041.2015

Benedict, C. A., Norris, P. S., and Ware, C. F. (2002). To Kill or be Killed: Viral Evasion of Apoptosis. *Nat. Immunol.* 3 (11), 1013–1018. doi: 10.1038/ni1102-1013

Blomen, V. A., and Boonstra, J. (2007). Cell Fate Determination During G1 Phase Progression. *Cell. Mol. Life Sci. CMLS* 64 (23), 3084–3104. doi: 10.1007/s00018-007-7271-z

Burger, K., and Gullerova, M. (2015). Swiss Army Knives: non-Canonical Functions of Nuclear Drosha and Dicer. *Nat. Rev. Mol. Cell Biol.* 16 (7), 417–430. doi: 10.1038/nrm3994

Cao, H., Yang, B., Zhao, Y., Deng, X., and Shen, X. (2020). The Pro-Apoptosis and Pro-Inflammation Role of LncRNA HIF1A-AS1 in Coxsackievirus B3-Induced Myocarditis *via* Targeting miR-138. *Cardiovasc. Diagn. Ther.* 10 (5), 1245–1255. doi: 10.21037/cdt-20-545

Carthew, R. W., and Sontheimer, E. J. (2009). Origins and Mechanisms of miRNAs and siRNAs. *Cell* 136 (4), 642–655. doi: 10.1016/j.cell.2009.01.035

Chang, Y. L., Ho, B. C., Sher, S., Yu, S. L., and Yang, P. C. (2015). miR-146a and miR-370 Coordinate Enterovirus 71-Induced Cell Apoptosis Through Targeting SOS1 and GADD45beta. *Cell Microbiol.* 17 (6), 802–818. doi: 10.1111/cmi.12401

Chang, L.-Y., Hsiung, C. A., Lu, C.-Y., Lin, T.-Y., Huang, F.-Y., Lai, Y.-H., et al. (2006). Status of Cellular Rather Than Humoral Immunity is Correlated With Clinical Outcome of Enterovirus 71. *Pediatr. Res.* 60 (4), 466–471. doi: 10.1203/01.pdr.0000238247.86041.19

Chang, Z., Wang, Y., Bian, L., Liu, Q., and Long, J.-E. (2017). Enterovirus 71 Antagonizes the Antiviral Activity of Host STAT3 and IL-6R With Partial Dependence on Virus-Induced miR-124. *J. Gen. Virol.* 98 (12), 3008–3025. doi: 10.1099/jgv.0.000967

Chen, T.-C., Chen, G.-W., Hsiung, C. A., Yang, J.-Y., Shih, S.-R., Lai, Y.-K., et al. (2006). Combining Multiplex Reverse Transcription-PCR and a Diagnostic Microarray to Detect and Differentiate Enterovirus 71 and Coxsackievirus A16. *J. Clin. Microbiol.* 44 (6), 2212–2219. doi: 10.1128/JCM.02393-05

Cheng, S., Hsia, C. Y., Feng, B., Liou, M.-L., Fang, X., Pandolfi, P. P., et al. (2009). BCR-Mediated Apoptosis Associated With Negative Selection of Immature B Cells is Selectively Dependent on Pten. *Cell Res.* 19 (2), 196–207. doi: 10.1038/cr.2008.284

Chen, B. S., Lee, H. C., Lee, K. M., Gong, Y. N., and Shih, S. R. (2020). Enterovirus and Encephalitis. *Front. Microbiol.* 11. doi: 10.3389/fmicb.2020.00261

Chen, C.-S., Yao, Y.-C., Lin, S.-C., Lee, Y.-P., Wang, Y.-F., Wang, J.-R., et al. (2007). Retrograde Axonal Transport: A Major Transmission Route of Enterovirus 71 in Mice. *J. Virol.* 81 (17), 8996–9003. doi: 10.1128/JVI.00236-07

Chu, M., Zhou, B., Tu, H., Li, M., Huang, L., He, Y., et al. (2021). The Upregulation of a Novel Long Noncoding RNA AK097647 Promotes Enterovirus 71 Replication and Decreases IFN-Lambda1 Secretion. *Intervirology* 64 (3), 147–155. doi: 10.1159/000515903

Clarke, P. R., and Zhang, C. (2008). Spatial and Temporal Coordination of Mitosis by Ran GTPase. *Nat. Rev. Mol. Cell Biol.* 9 (6), 464–477. doi: 10.1038/nrm2410

Cobb, B. S., Nesterova, T. B., Thompson, E., Hertweck, A., O'Connor, E., Godwin, J., et al. (2005). T Cell Lineage Choice and Differentiation in the Absence of the RNase III Enzyme Dicer. *J. Exp. Med.* 201 (9), 1367–1373. doi: 10.1084/jem.20050572

Cox, B., and Levent, F. (2018). Hand, Foot, and Mouth Disease. *JAMA* 320 (23), 2492. doi: 10.1001/jama.2018.17288

Coyne, C. B., Kim, K. S., and Bergelson, J. M. (2007). Poliovirus Entry Into Human Brain Microvascular Cells Requires Receptor-Induced Activation of SHP-2. *EMBO J.* 26 (17), 4016–4028. doi: 10.1038/sj.emboj.7601831

Cui, L., Qi, Y., Li, H., Ge, Y., Zhao, K., Qi, X., et al. (2011). Serum microRNA Expression Profile Distinguishes Enterovirus 71 and Coxsackievirus 16 Infections in Patients With Hand-Foot-and-Mouth Disease. *PloS One* 6 (11), e27071. doi: 10.1371/journal.pone.0027071

Dang, M., Wang, X., Wang, Q., Wang, Y., Lin, J., Sun, Y., et al. (2014). Molecular Mechanism of SCARB2-Mediated Attachment and Uncoating of EV71. *Protein Cell* 5 (9), 692–703. doi: 10.1007/s13238-014-0087-3

Dasso, M. (2001). Running on Ran: Nuclear Transport and the Mitotic Spindle. *Cell* 104 (3), 321–324. doi: 10.1016/s0092-8674(01)00218-5

Dimitrova, N., Gocheva, V., Bhutkar, A., Resnick, R., Jong, R. M., Miller, K. M., et al. (2016). Stromal Expression of miR-143/145 Promotes Neoangiogenesis in Lung Cancer Development. *Cancer Discovery* 6 (2), 188–201. doi: 10.1158/2159-8290.CD-15-0854

Du, N., Cong, H., Tian, H., Zhang, H., Zhang, W., Song, L., et al. (2014). Cell Surface Vimentin is an Attachment Receptor for Enterovirus 71. *J. Virol.* 88 (10), 5816–5833. doi: 10.1128/JVI.03826-13

Dupont, J.l., Renou, J. P., Shani, M., Hennighausen, L., and LeRoith, D. (2002). PTEN Overexpression Suppresses Proliferation and Differentiation and Enhances Apoptosis of the Mouse Mammary Epithelium. *J. Clin. Invest.* 110 (6), 815–825. doi: 10.1172/JCI0213829

Du, X., Wang, H., Xu, F., Huang, Y., Liu, Z., and Liu, T. (2015). Enterovirus 71 Induces Apoptosis of SHSY5Y Human Neuroblastoma Cells Through Stimulation of Endogenous microRNA Let-7b Expression. *Mol. Med. Rep.* 12 (1), 953–959. doi: 10.3892/mmr.2015.3482

Du, H., Yin, P., Yang, X., Zhang, L., Jin, Q., and Zhu, G. (2015). Enterovirus 71 2c Protein Inhibits NF-κb Activation by Binding to RelA(P65). *Sci. Rep.* 5, 14302. doi: 10.1038/srep14302

Ediriweera, M. K., Tennekoon, K. H., and Samarakoon, S. R. (2019). Role of the PI3K/AKT/mTOR Signaling Pathway in Ovarian Cancer: Biological and Therapeutic Significance. *Semin. Cancer Biol.* 59, 147–160. doi: 10.1016/j.semcancer.2019.05.012

Edsall, G. (1949). Active Immunization. *New Engl. J. Med.* 241 (3), 99. doi: 10.1056/NEJM194907212410305

Engreitz, J. M., Ollikainen, N., and Guttman, M. (2016). Long non-Coding RNAs: Spatial Amplifiers That Control Nuclear Structure and Gene Expression. *Nat. Rev. Mol. Cell Biol.* 17 (12), 756–770. doi: 10.1038/nrm.2016.126

Esteller, M. (2011). Non-Coding RNAs in Human Disease. *Nat. Rev. Genet.* 12 (12), 861–874. doi: 10.1038/nrg3074

Farrar, M. A., and Schreiber, R. D. (1993). The Molecular Cell Biology of Interferon-Gamma and its Receptor. *Annu. Rev. Immunol.* 11, 571–611. doi: 10.1146/annurev.iy.11.040193.003035

Feng, C., Fu, Y., Chen, D., Wang, H., Su, A., Zhang, L., et al. (2017). miR-127-5p Negatively Regulates Enterovirus 71 Replication by Directly Targeting SCARB2. *FEBS Open Bio* 7 (6), 747–758. doi: 10.1002/2211-5463.12197

Feng, N., Zhou, Z., Li, Y., Zhao, L., Xue, Z., Lu, R., et al. (2017). Enterovirus 71-Induced has-miR-21 Contributes to Evasion of Host Immune System by Targeting MyD88 and IRAK1. *Virus Res.* 237, 27–36. doi: 10.1016/j.virusres.2017.05.008

Fitzgerald, K. A., and Kagan, J. C. (2020). Toll-Like Receptors and the Control of Immunity. *Cell* 180 (6), 1044–1066. doi: 10.1016/j.cell.2020.02.041

Freistadt, M. S., and Eberle, K. E. (1996). Correlation Between Poliovirus Type 1 Mahoney Replication in Blood Cells and Neurovirulence. *J. Virol.* 70 (9), 6486–6492. doi: 10.1128/jvi.70.9.6486-6492.1996

Fujii, K., Nagata, N., Sato, Y., Ong, K. C., Wong, K. T., Yamayoshi, S., et al. (2013). Transgenic Mouse Model for the Study of Enterovirus 71 Neuropathogenesis. *Proc. Natl. Acad. Sci. United States America* 110 (36), 14753–14758. doi: 10.1073/pnas.1217563110

Fu, Y., Xu, W., Chen, D., Feng, C., Zhang, L., Wang, X., et al. (2015). Enterovirus 71 Induces Autophagy by Regulating has-miR-30a Expression to Promote Viral Replication. *Antiviral Res.* 124, 43–53. doi: 10.1016/j.antiviral.2015.09.016

Fu, Y., Zhang, L., Zhang, F., Tang, T., Zhou, Q., Feng, C., et al. (2017). Exosome-Mediated miR-146a Transfer Suppresses Type I Interferon Response and Facilitates EV71 Infection. *PloS Pathog.* 13 (9), e1006611. doi: 10.1371/journal.ppat.1006611

Fu, Y., Zhang, L., Zhang, R., Xu, S., Wang, H., Jin, Y., et al. (2019). Enterovirus 71 Suppresses miR-17-92 Cluster Through Up-Regulating Methylation of the miRNA Promoter. *Front. Microbiol.* 10. doi: 10.3389/fmicb.2019.00625

Grasedieck, S., SchÃ¶ler, N., Bommer, M., Niess, J. H., Tumani, H., Rouhi, A., et al. (2012). Impact of Serum Storage Conditions on microRNA Stability. *Leukemia* 26 (11), 2414–2416. doi: 10.1038/leu.2012.106

Green, D. R., and Llambi, F. (2015). Cell Death Signaling. *Cold Spring Harbor Perspect. Biol.* 7 (12), a006080. doi: 10.1101/cshperspect.a006080

Griffiths, M. J., Ooi, M. H., Wong, S. C., Mohan, A., Podin, Y., Perera, D., et al. (2012). In Enterovirus 71 Encephalitis With Cardio-Respiratory Compromise, Elevated Interleukin 1β, Interleukin 1 Receptor Antagonist, and Granulocyte Colony-Stimulating Factor Levels are Markers of Poor Prognosis. *J. Infect. Dis.* 206 (6), 881–892. doi: 10.1093/infdis/jis446

Gromeier, M., Alexander, L., and Wimmer, E. (1996). Internal Ribosomal Entry Site Substitution Eliminates Neurovirulence in Intergeneric Poliovirus Recombinants. *Proc. Natl. Acad. Sci.* 93 (6), 2370. doi: 10.1073/pnas.93.6.2370

Guo, G., Gong, K., Wohlfeld, B., Hatanpaa, K. J., Zhao, D., and Habib, A. A. (2015). Ligand-Independent EGFR Signaling. *Cancer Res.* 75 (17), 3436–3441. doi: 10.1158/0008-5472.CAN-15-0989

Hao, P.-Q., Zhang, X.-Y., Guo, H., Yang, Y., An, S., Liu, Y., et al. (2018). Research Progress on Pathophysiological Function of SOS1 Protein. *Sheng Li Xue Bao [Acta Physiol. Sin.]* 70 (5), 565–570. doi: 10.13294/j.aps.2018.0063

Hasbun, R., Rosenthal, N., Balada-Llasat, J. M., Chung, J., Duff, S., Bozzette, S., et al. (2017). Epidemiology of Meningitis and Encephalitis in the United States 2011-2014. *Clin. Infect. Dis.* 65 (3), 359–363. doi: 10.1093/cid/cix319

Hawley, Z. C. E., Campos-Melo, D., and Strong, M. J. (2019). MiR-105 and miR-9 Regulate the mRNA Stability of Neuronal Intermediate Filaments. Implications for the Pathogenesis of Amyotrophic Lateral Sclerosis (ALS). *Brain Res.* 1706, 93–100. doi: 10.1016/j.brainres.2018.10.032

Hayden, M. S., West, A. P., and Ghosh, S. (2006). SnapShot: NF-kappaB Signaling Pathways. *Cell* 127 (6), 1286–1287. doi: 10.1016/j.cell.2006.12.005

He, L., and Hannon, G. J. (2004). MicroRNAs: Small RNAs With a Big Role in Gene Regulation. *Nat. Rev. Genet.* 5 (7), 522–531. doi: 10.1038/nrg1379

He, Y., Ong, K. C., Gao, Z., Zhao, X., Anderson, V. M., McNutt, M. A., et al. (2014). Tonsillar Crypt Epithelium is an Important Extra-Central Nervous System Site for Viral Replication in EV71 Encephalomyelitis. *Am. J. Pathol.* 184 (3), 714–720. doi: 10.1016/j.ajpath.2013.11.009

He, Q.-Q., Ren, S., Xia, Z.-C., Cheng, Z.-K., Peng, N.-F., and Zhu, Y. (2018). Fibronectin Facilitates Enterovirus 71 Infection by Mediating Viral Entry. *J. Virol.* 92 (9), e02251-17. doi: 10.1128/JVI.02251-17

Hohenester, S., Gates, A., Wimmer, R., Beuers, U., Anwer, M. S., Rust, C., et al. (2010). Phosphatidylinositol-3-Kinase P110î³ Contributes to Bile Salt-Induced Apoptosis in Primary Rat Hepatocytes and Human Hepatoma Cells. *J. Hepatol.* 53 (5), 918–926. doi: 10.1016/j.jhep.2010.05.015

Holland, J. J. (1961). Receptor Affinities as Major Determinants of Enterovirus Tissue Tropisms in Humans. *Virology* 15 (3), 312–326. doi: 10.1016/0042-6822(61)90363-4

Ho, B.-C., Yu, S.-L., Chen, J. J. W., Chang, S.-Y., Yan, B.-S., Hong, Q.-S., et al. (2011). Enterovirus-Induced miR-141 Contributes to Shutoff of Host Protein Translation by Targeting the Translation Initiation Factor Eif4e. *Cell Host Microbe* 9 (1), 58–69. doi: 10.1016/j.chom.2010.12.001

Ho, B.-C., Yu, I. S., Lu, L.-F., Rudensky, A., Chen, H.-Y., Tsai, C.-W., et al. (2014). Inhibition of miR-146a Prevents Enterovirus-Induced Death by Restoring the Production of Type I Interferon. *Nat. Commun.* 5, 3344. doi: 10.1038/ncomms4344

Huang, B., Chen, H., and Zheng, Y. (2021). MiR-103/miR-107 Inhibits Enterovirus 71 Replication and Facilitates Type I Interferon Response by Regulating SOCS3/STAT3 Pathway. *Biotechnol. Lett.* 43 (7), 1357–1369. doi: 10.1007/s10529-021-03115-z

Huang, S.-W., Lee, Y.-P., Hung, Y.-T., Lin, C.-H., Chuang, J.-I., Lei, H.-Y., et al. (2011). Exogenous Interleukin-6, Interleukin-13, and Interferon-γ Provoke Pulmonary Abnormality With Mild Edema in Enterovirus 71-Infected Mice. *Respir. Res.* 12, 147. doi: 10.1186/1465-9921-12-147

Huang, H. I., and Shih, S. R. (2015). Neurotropic Enterovirus Infections in the Central Nervous System. *Viruses* 7 (11), 6051–6066. doi: 10.3390/v7112920

Huang, Y., Zhou, Y., Lu, H., Yang, H., Feng, Q., Dai, Y., et al. (2015). Characterization of Severe Hand, Foot, and Mouth Disease in Shenzhen, China 2009-2013. *J. Med. Virol.* 87 (9), 1471–1479. doi: 10.1002/jmv.24200

Hutvágner, G., McLachlan, J., Pasquinelli, A. E., Bálint, E., Tuschl, T., and Zamore, P. D. (2001). A Cellular Function for the RNA-Interference Enzyme Dicer in the Maturation of the Let-7 Small Temporal RNA. *Sci. (New York N.Y.)* 293 (5531), 834–838. doi: 10.1126/science.1062961

Hu, Y., Xu, Y., Deng, X., Wang, R., Li, R., You, L., et al. (2021). Comprehensive Analysis of the circRNA Expression Profile and circRNA-miRNA-mRNA Network in the Pathogenesis of EV-A71 Infection. *Virus Res.* 303, 198502. doi: 10.1016/j.virusres.2021.198502

Ida-Hosonuma, M., Iwasaki, T., Yoshikawa, T., Nagata, N., Sato, Y., Sata, T., et al. (2005). The Alpha/Beta Interferon Response Controls Tissue Tropism and Pathogenicity of Poliovirus. *J. Virol.* 79 (7), 4460–4469. doi: 10.1128/JVI.79.7.4460-4469.2005

Janssen, H. L. A., Reesink, H. W., Lawitz, E. J., Zeuzem, S., Rodriguez-Torres, M., Patel, K., et al. (2013). Treatment of HCV Infection by Targeting microRNA. *New Engl. J. Med.* 368 (18), 1685–1694. doi: 10.1056/NEJMoa1209026

Jia, H.-L., He, C.-H., Wang, Z.-Y., Xu, Y.-F., Yin, G.-Q., Mao, L.-J., et al. (2014). MicroRNA Expression Profile in Exosome Discriminates Extremely Severe Infections From Mild Infections for Hand, Foot and Mouth Disease. *BMC Infect. Dis.* 14, 506. doi: 10.1186/1471-2334-14-506

Jin, J., Li, R., Jiang, C., Zhang, R., Ge, X., Liang, F., et al. (2017). Transcriptome Analysis Reveals Dynamic Changes in Coxsackievirus A16 Infected HEK 293T Cells. *BMC Genomics* 18 (Suppl 1), 933. doi: 10.1186/s12864-016-3253-6

Jin, Y., Zhang, R., Wu, W., and Duan, G. (2018). Antiviral and Inflammatory Cellular Signaling Associated With Enterovirus 71 Infection. *Viruses* 10 (4), 155. doi: 10.3390/v10040155

Kao, S. J., Yang, F. L., Hsu, Y. H., and Chen, H. I. (2004). Mechanism of Fulminant Pulmonary Edema Caused by Enterovirus 71. *Clin. Infect. Dis. Off. Publ. Infect. Dis. Soc. America* 38 (12), 1784–1788. doi: 10.1086/421021

Kapranov, P., Cheng, J., Dike, S., Nix, D. A., Duttagupta, R., Willingham, A. T., et al. (2007). RNA Maps Reveal New RNA Classes and a Possible Function for Pervasive Transcription. *Science* 316 (5830), 1484–1488. doi: 10.1126/science.1138341

Kobayashi, K., and Koike, S. (2020). Cellular Receptors for Enterovirus A71. *J. Biomed. Sci.* 27 (1), 23. doi: 10.1186/s12929-020-0615-9

Koike, S., Taya, C., Kurata, T., Abe, S., Ise, I., Yonekawa, H., et al. (1991). Transgenic Mice Susceptible to Poliovirus. Proc Natl. Acad. Sci. U. S. A., Vol. 88 (3), 951–955. doi 10.1073/pnas.88.3.951

Kurada, B.R.V.V.S.N., Li, L. C., Mulherkar, N., Subramanian, M., Prasad, K. V., and Prabhakar, B. S. (2009). MADD, a Splice Variant of IG20, is Indispensable for MAPK Activation and Protection Against Apoptosis Upon Tumor Necrosis Factor-Alpha Treatment. *J. Biol. Chem.* 284 (20), 13533–13541. doi: 10.1074/jbc.M808554200

Lee, Y., Ahn, C., Han, J., Choi, H., Kim, J., Yim, J., et al. (2003). The Nuclear RNase III Drosha Initiates microRNA Processing. *Nature* 425 (6956), 415–419. doi: 10.1038/nature01957

Lee, T. J., Yuan, X., Kerr, K., Yoo, J. Y., Kim, D. H., Kaur, B., et al. (2020). Strategies to Modulate MicroRNA Functions for the Treatment of Cancer or Organ Injury. *Pharmacol. Rev.* 72 (3), 639–667. doi: 10.1124/pr.119.019026

Lehmann, S. M., Kruger, C., Park, B., Derkow, K., Rosenberger, K., Baumgart, J., et al. (2012). An Unconventional Role for miRNA: Let-7 Activates Toll-Like Receptor 7 and Causes Neurodegeneration. *Nat. Neurosci.* 15 (6), 827–835. doi: 10.1038/nn.3113

Liao, Y. W., Ho, B. C., Chen, M. H., and Yu, S. L. (2019). Host Relieves lnc-IRAK3-3-Sequestered miR-891b to Attenuate Apoptosis in Enterovirus 71 Infection. *Cell Microbiol.* 21 (9), e13043. doi: 10.1111/cmi.13043

Li, B., and Zheng, J. (2018). MicroR-9-5p Suppresses EV71 Replication Through Targeting Nfκb of the RIG-I-Mediated Innate Immune Response. *FEBS Open Bio* 8 (9), 1457–1470. doi: 10.1002/2211-5463.12490

Li, D., Chen, S., Zhang, W., Zhang, C., Sun, T., Du, Y., et al. (2021). MicroRNA-628-5p Facilitates Enterovirus 71 Infection by Suppressing TRAF3 Signaling. *Cell. Mol. Immunol.* 18 (5), 1320–1322. doi: 10.1038/s41423-020-0453-4

Li, L., Wu, F., Xie, Y., Xu, W., Xiong, G., Xu, Y., et al. (2020). MiR-202-3p Inhibits Foam Cell Formation and is Associated With Coronary Heart Disease Risk in a Chinese Population. *Int. Heart J.* 61 (1), 153–159. doi: 10.1536/ihj.19-033

Li, Y., Xie, J., Xu, X., Wang, J., Ao, F., Wan, Y., et al. (2013). MicroRNA-548 Down-Regulates Host Antiviral Response *via* Direct Targeting of IFN-λ1. *Protein Cell* 4 (2), 130–141. doi: 10.1007/s13238-012-2081-y

Li, Y., Zhang, C., Qin, L., Li, D., Zhou, G., Dang, D., et al. (2018). Characterization of Critical Functions of Long Non-Coding RNAs and mRNAs in Rhabdomyosarcoma Cells and Mouse Skeletal Muscle Infected by 71 Using RNA-Seq. *Viruses* 10 (10). doi: 10.3390/v10100556

Li, X., Huang, Y., Sun, M., Ji, H., Dou, H., Hu, J., et al. (2018). Honeysuckle-Encoded Microrna2911 Inhibits Enterovirus 71 Replication *via* Targeting VP1 Gene. *Antiviral Res.* 152, 117–123. doi: 10.1016/j.antiviral.2018.02.015

Lim, Z. Q., Ng, Q. Y., Oo, Y., Chu, J. J. H., Ng, S. Y., Sze, S. K., et al. (2021). Enterovirus-A71 Exploits Peripherin and Rac1 to Invade the Central Nervous System. *EMBO Rep.* 22 (6), e51777. doi: 10.15252/embr.202051777

Lin, T. Y., Chang, L. Y., Huang, Y. C., Hsu, K. H., Chiu, C. H., and Yang, K. D. (2002). Different Proinflammatory Reactions in Fatal and non-Fatal Enterovirus 71 Infections: Implications for Early Recognition and Therapy. *Acta Paediatr. (Oslo Norway 1992)* 91 (6), 632–635. doi: 10.1111/j.1651-2227.2002.tb03292.x

Lin, P.-Y., Fosmire, S. P., Park, S.-H., Park, J.-Y., Baksh, S., Modiano, J. F., et al. (2007). Attenuation of PTEN Increases P21 Stability and Cytosolic Localization in Kidney Cancer Cells: A Potential Mechanism of Apoptosis Resistance. *Mol. Cancer* 6, 16. doi: 10.1186/1476-4598-6-16

Lin, T.-Y., Hsia, S.-H., Huang, Y.-C., Wu, C.-T., and Chang, L.-Y. (2003). Proinflammatory Cytokine Reactions in Enterovirus 71 Infections of the Central Nervous System. *Clin. Infect. Dis. Off. Publ. Infect. Dis. Soc. America* 36 (3), 269–274. doi: 10.1086/345905

Lin, Y.-W., Wang, S.-W., Tung, Y.-Y., and Chen, S.-H. (2009). Enterovirus 71 Infection of Human Dendritic Cells. *Exp. Biol. Med. (Maywood N.J.)* 234 (10), 1166–1173. doi: 10.3181/0903-RM-116

Liu, Q., Kong, Y., Han, B., Jiang, D., Jia, H., and Zhang, L. (2019). Long Non-Coding RNA Expression Profile and Functional Analysis in Children With Acute Fulminant Myocarditis. *Front. Pediatr.* 7. doi: 10.3389/fped.2019.00283

Liu, J., Lu, X. C., and Zhou, W. D. (2020). Elevated Circulating miR-494 in Plasma of Children With Enterovirus 71 Induced Hand, Foot, and Mouth Disease and its Potential Diagnostic Value. *Acta Virol.* 64 (3), 338–343. doi: 10.4149/av_2020_311

Liu, G., Min, H., Yue, S., and Chen, C.-Z. (2008). Pre-miRNA Loop Nucleotides Control the Distinct Activities of Mir-181a-1 and Mir-181c in Early T Cell Development. *PloS One* 3 (10), e3592. doi: 10.1371/journal.pone.0003592

Liu, S. L., Pan, H., Liu, P., Amer, S., Chan, T. C., Zhan, J., et al. (2015). Comparative Epidemiology and Virology of Fatal and Nonfatal Cases of Hand, Foot and Mouth Disease in Mainland China From 2008 to 2014. *Rev. Med. Virol.* 25 (2), 115–128. doi: 10.1002/rmv.1827

Liu, H., Qin, Y., Kong, Z., Shao, Q., Su, Z., Wang, S., et al. (2016). siRNA Targeting the 2Apro Genomic Region Prevents Enterovirus 71 Replication *In Vitro*. *PloS One* 11 (2), e0149470. doi: 10.1371/journal.pone.0149470

Lu, Y., Gao, Z., Liu, C., Long, M., Yang, L., Li, R., et al. (2021). Integrative Analysis of lncRNA-miRNA-mRNA-Associated Competing Endogenous RNA Regulatory Network Involved in EV71 Infection. *Am. J. Trans. Res.* 13 (7), 7440–7457.

Lu, L.-F., Thai, T.-H., Calado, D. P., Chaudhry, A., Kubo, M., Tanaka, K., et al. (2009). Foxp3-Dependent Microrna155 Confers Competitive Fitness to Regulatory T Cells by Targeting SOCS1 Protein. *Immunity* 30 (1), 80–91. doi: 10.1016/j.immuni.2008.11.010

Luo, Z., Su, R., Wang, W., Liang, Y., Zeng, X., Shereen, M. A., et al. (2019). EV71 Infection Induces Neurodegeneration *via* Activating TLR7 Signaling and IL-6 Production. *PloS Pathog.* 15 (11), e1008142. doi: 10.1371/journal.ppat.1008142

Meng, J., Yao, Z., He, Y., Zhang, R., Yang, H., Yao, X., et al. (2017). Long non-Coding RNA Expression Profiles in Different Severity EV71-Infected Hand Foot and Mouth Disease Patients. *Biochem. Biophys. Res. Commun.* 493 (4), 1594–1600. doi: 10.1016/j.bbrc.2017.09.141

Mercer, T. R., Dinger, M. E., and Mattick, J. S. (2009). Long non-Coding RNAs: Insights Into Functions. *Nat. Rev. Genet.* 10 (3), 155–159. doi: 10.1038/nrg2521

Millecamps, S., and Julien, J.-P. (2013). Axonal Transport Deficits and Neurodegenerative Diseases. *Nat. Rev. Neurosci.* 14 (3), 161–176. doi: 10.1038/nrn3380

Min, N., Sakthi Vale, P. D., Wong, A. A., Tan, N. W. H., Chong, C. Y., Chen, C.-J., et al. (2018). Circulating Salivary miRNA hsa-miR-221 as Clinically Validated Diagnostic Marker for Hand, Foot, and Mouth Disease in Pediatric Patients. *EBioMedicine* 31, 299–306. doi: 10.1016/j.ebiom.2018.05.006

Mizutani, T., Ishizaka, A., and Nihei, C.-I. (2016). Transferrin Receptor 1 Facilitates Poliovirus Permeation of Mouse Brain Capillary Endothelial Cells. *J. Biol. Chem.* 291 (6), 2829–2836. doi: 10.1074/jbc.M115.690941

Muljo, S. A., Ansel, K. M., Kanellopoulou, C., Livingston, D. M., Rao, A., and Rajewsky, K. (2005). Aberrant T Cell Differentiation in the Absence of Dicer. *J. Exp. Med.* 202 (2), 261–269. doi: 10.1084/jem.20050678

Nathan, C., and Ding, A. (2010). Nonresolving Inflammation. *Cell* 140 (6), 871–882. doi: 10.1016/j.cell.2010.02.029

Nikonov, O. S., Chernykh, E. S., Garber, M. B., and Nikonova, E. Y. (2017). Enteroviruses: Classification, Diseases They Cause, and Approaches to Development of Antiviral Drugs. *Biochem. (Mosc)* 82 (13), 1615–1631. doi: 10.1134/S0006297917130041

Nishimura, Y., Shimojima, M., Tano, Y., Miyamura, T., Wakita, T., and Shimizu, H. (2009). Human P-Selectin Glycoprotein Ligand-1 is a Functional Receptor for Enterovirus 71. *Nat. Med.* 15 (7), 794–797. doi: 10.1038/nm.1961

Nolan, M. A., Craig, M. E., Lahra, M. M., Rawlinson, W. D., Prager, P. C., Williams, G. D., et al. (2003). Survival After Pulmonary Edema Due to Enterovirus 71 Encephalitis. *Neurology* 60 (10), 1651–1656. doi: 10.1212/01.WNL.0000066810.62490.FF

Ohka, S., Matsuda, N., Tohyama, K., Oda, T., Morikawa, M., Kuge, S., et al. (2004). Receptor (CD155)-Dependent Endocytosis of Poliovirus and Retrograde Axonal Transport of the Endosome. *J. Virol.* 78 (13), 7186–7198. doi: 10.1128/JVI.78.13.7186-7198.2004

Ohka, S., Nihei, C.-I., Yamazaki, M., and Nomoto, A. (2012). Poliovirus Trafficking Toward Central Nervous System *via* Human Poliovirus Receptor-Dependent and -Independent Pathway. *Front. Microbiol.* 3. doi: 10.3389/fmicb.2012.00147

Ooi, M. H., Wong, S. C., Lewthwaite, P., Cardosa, M. J., and Solomon, T. (2010). Clinical Features, Diagnosis, and Management of Enterovirus 71. *Lancet Neurol.* 9 (11), 1097–1105. doi: 10.1016/s1474-4422(10)70209-x

Orr-Burks, N. L., Shim, B.-S., Wu, W., Bakre, A. A., Karpilow, J., and Tripp, R. A. (2017). MicroRNA Screening Identifies miR-134 as a Regulator of Poliovirus and Enterovirus 71 Infection. *Sci. Data* 4, 170023. doi: 10.1038/sdata.2017.23

Orzalli, M. H., and Kagan, J. C. (2017). Apoptosis and Necroptosis as Host Defense Strategies to Prevent Viral Infection. *Trends Cell Biol.* 27 (11), 800–809. doi: 10.1016/j.tcb.2017.05.007

Osaki, M., Oshimura, M., and Ito, H. (2004). PI3K-Akt Pathway: Its Functions and Alterations in Human Cancer. *Apoptosis Int. J. Programmed Cell Death* 9 (6), 667–676. doi: 10.1023/B:APPT.0000045801.15585.dd

Ou, D.-L., Shen, Y.-C., Yu, S.-L., Chen, K.-F., Yeh, P.-Y., Fan, H.-H., et al. (2010). Induction of DNA Damage-Inducible Gene GADD45beta Contributes to Sorafenib-Induced Apoptosis in Hepatocellular Carcinoma Cells. *Cancer Res.* 70 (22), 9309–9318. doi: 10.1158/0008-5472.CAN-10-1033

Ouyang, W., Rutz, S., Crellin, N. K., Valdez, P. A., and Hymowitz, S. G. (2011). Regulation and Functions of the IL-10 Family of Cytokines in Inflammation and Disease. *Annu. Rev. Immunol.* 29, 71–109. doi: 10.1146/annurev-immunol-031210-101312

Peng, N., Yang, X., Zhu, C., Zhou, L., Yu, H., Li, M., et al. (2018). MicroRNA-302 Cluster Downregulates Enterovirus 71-Induced Innate Immune Response by Targeting Kpna2. *J. Immunol. (Baltimore Md. 1950)* 201 (1), 145–156. doi: 10.4049/jimmunol.1701692

Perera, D., Podin, Y., Akin, W., Tan, C.-S., and Cardosa, M. J. (2004). Incorrect Identification of Recent Asian Strains of Coxsackievirus A16 as Human Enterovirus 71: Improved Primers for the Specific Detection of Human Enterovirus 71 by RT PCR. *BMC Infect. Dis.* 4, 11. doi: 10.1186/1471-2334-4-11

Perkins, N. D. (2012). The Diverse and Complex Roles of NF-κb Subunits in Cancer. *Nat. Rev. Cancer* 12 (2), 121–132. doi: 10.1038/nrc3204

Plevka, P., Perera, R., Cardosa, J., Kuhn, R. J., and Rossmann, M. G. (2012). Crystal Structure of Human Enterovirus 71. *Science* 336 (6086), 1274. doi: 10.1126/science.1218713

Quinn, J. J., and Chang, H. Y. (2016). Unique Features of Long non-Coding RNA Biogenesis and Function. *Nat. Rev. Genet.* 17 (1), 47–62. doi: 10.1038/nrg.2015.10

Ramalho, E., Sousa, I. Jr., Burlandy, F., Costa, E., Dias, A., Serrano, R., et al. (2019). Identification and Phylogenetic Characterization of Human Enteroviruses Isolated From Cases of Aseptic Meningitis in Brazil 2013-2017. *Viruses* 11 (8), 690. doi: 10.3390/v11080690

Rana, T. M. (2007). Illuminating the Silence: Understanding the Structure and Function of Small RNAs. *Nat. Rev. Mol. Cell Biol.* 8 (1), 23–36. doi: 10.1038/nrm2085

Ren, R. B., Costantini, F., Gorgacz, E. J., Lee, J. J., and Racaniello, V. R. (1990). Transgenic Mice Expressing a Human Poliovirus Receptor: A New Model for Poliomyelitis. *Cell* 63 (2), 353–362. doi: 10.1016/0092-8674(90)90168-E

Richter, J. D., and Sonenberg, N. (2005). Regulation of Cap-Dependent Translation by Eif4e Inhibitory Proteins. *Nature* 433 (7025), 477–480. doi: 10.1038/nature03205

Riedl, S. J., and Shi, Y. (2004). Molecular Mechanisms of Caspase Regulation During Apoptosis. *Nat. Rev. Mol. Cell Biol.* 5 (11), 897–907. doi: 10.1038/nrm1496

Rodriguez, A., Vigorito, E., Clare, S., Warren, M. V., Couttet, P., Soond, D. R., et al. (2007). Requirement of Bic/microRNA-155 for Normal Immune Function. *Sci. (New York N.Y.)* 316 (5824), 608–611. doi: 10.1126/science.1139253

Salinas, P. C., and Zou, Y. (2008). Wnt Signaling in Neural Circuit Assembly. *Annu. Rev. Neurosci.* 31, 339–358. doi: 10.1146/annurev.neuro.31.060407.125649

Schmidt, N. J., Lennette, E. H., and Ho, H. H. (1974). An Apparently New Enterovirus Isolated From Patients With Disease of the Central Nervous System. *J. Infect. Dis.* 129 (3), 304–9. doi: 10.1093/infdis/129.3.304

Sen, S. (1992). Programmed Cell Death: Concept, Mechanism and Control. *Biol. Rev. Camb. Philos. Soc.* 67 (3), 287–319. doi: 10.1111/j.1469-185X.1992.tb00727.x

She, Q.-B., Solit, D. B., Ye, Q., O'Reilly, K. E., Lobo, J., and Rosen, N. (2005). The BAD Protein Integrates Survival Signaling by EGFR/MAPK and PI3K/Akt Kinase Pathways in PTEN-Deficient Tumor Cells. *Cancer Cell* 8 (4), 287–297. doi: 10.1016/j.ccr.2005.09.006

Shi, Y., Tu, H., Chen, X., Zhang, Y., Chen, L., Liu, Z., et al. (2016). The Long non-Coding RNA Expression Profile of Coxsackievirus A16 Infected RD Cells Identified by RNA-Seq. *Virol. Sin.* 31 (2), 131–141. doi: 10.1007/s12250-015-3693-1

Siebert, M., Westbroek, W., Chen, Y. C., Moaven, N., Li, Y., Velayati, A., et al. (2014). Identification of miRNAs That Modulate Glucocerebrosidase Activity in Gaucher Disease Cells. *RNA Biol.* 11 (10), 1291–1300. doi: 10.1080/15476286.2014.996085

Sim, A. C., Luhur, A., Tan, T. M., Chow, V. T., and Poh, C. L. (2005). RNA Interference Against Enterovirus 71 Infection. *Virology* 341 (1), 72–79. doi: 10.1016/j.virol.2005.06.047

Solomon, T., Lewthwaite, P., Perera, D., Cardosa, M. J., McMinn, P., and Ooi, M. H. (2010). Virology, Epidemiology, Pathogenesis, and Control of Enterovirus 71. *Lancet Infect. Dis.* 10 (11), 778–790. doi: 10.1016/s1473-3099(10)70194-8

Song, M. S., Salmena, L., and Pandolfi, P. P. (2012). The Functions and Regulation of the PTEN Tumour Suppressor. *Nat. Rev. Mol. Cell Biol.* 13 (5), 283–296. doi: 10.1038/nrm3330

Soulard, A., and Hall, M. N. (2007). SnapShot: mTOR Signaling. *Cell* 129 (2), 434. doi: 10.1016/j.cell.2007.04.010

Squires, R. F. (1997). How a Poliovirus Might Cause Schizophrenia: A Commentary on Eagles' Hypothesis. *Neurochem. Res.* 22 (5), 647–656. doi: 10.1023/A:1022486423238

Statello, L., Guo, C.-J., Chen, L.-L., and Huarte, M. (2021). Gene Regulation by Long non-Coding RNAs and its Biological Functions. *Nat. Rev. Mol. Cell Biol.* 22 (2), 96–118. doi: 10.1038/s41580-020-00315-9

Sukarieh, R., Sonenberg, N., and Pelletier, J. (2010). Nuclear Assortment of Eif4e Coincides With Shut-Off of Host Protein Synthesis Upon Poliovirus Infection. *J. Gen. Virol.* 91 (Pt 5), 1224–1228. doi: 10.1099/vir.0.018069-0

Sun, Y., Feng, L., Li, J., Xu, H., Mei, X., Feng, L., et al. (2019). miR-545 Promoted Enterovirus 71 Replication *via* Directly Targeting Phosphatase and Tensin Homolog and Tumor Necrosis Factor Receptor-Associated Factor 6. *J. Cell. Physiol* 234 (9), 15686–15697. doi: 10.1002/jcp.28222

Su, P.-Y., Wang, Y.-F., Huang, S.-W., Lo, Y.-C., Wang, Y.-H., Wu, S.-R., et al. (2015). Cell Surface Nucleolin Facilitates Enterovirus 71 Binding and Infection. *J. Virol.* 89 (8), 4527–4538. doi: 10.1128/JVI.03498-14

Tabor-Godwin, J. M., Ruller, C. M., Bagalso, N., An, N., Pagarigan, R. R., Harkins, S., et al. (2010). A Novel Population of Myeloid Cells Responding to Coxsackievirus Infection Assists in the Dissemination of Virus Within the Neonatal CNS. *J. Neurosci. Off. J. Soc. Neurosci.* 30 (25), 8676–8691. doi: 10.1523/JNEUROSCI.1860-10.2010

Takeda, K., and Akira, S. (2004). TLR Signaling Pathways. *Semin. Immunol.* 16 (1), 3–9. doi: 10.1016/j.smim.2003.10.003

Takeuchi, O., and Akira, S. (2010). Pattern Recognition Receptors and Inflammation. *Cell* 140 (6), 805–820. doi: 10.1016/j.cell.2010.01.022

Tang, W.-F., Huang, R.-T., Chien, K.-Y., Huang, J.-Y., Lau, K.-S., Jheng, J.-R., et al. (2016). Host MicroRNA miR-197 Plays a Negative Regulatory Role in the Enterovirus 71 Infectious Cycle by Targeting the RAN Protein. *J. Virol.* 90 (3), 1424–1438. doi: 10.1128/JVI.02143-15

Tan, C. W., Poh, C. L., Sam, I. C., and Chan, Y. F. (2013). Enterovirus 71 Uses Cell Surface Heparan Sulfate Glycosaminoglycan as an Attachment Receptor. *J. Virol.* 87 (1), 611–620. doi: 10.1128/JVI.02226-12

Tan, E. L., Tan, T. M. C., Chow, V. T. K., and Poh, C. L. (2007). Enhanced Potency and Efficacy of 29-Mer shRNAs in Inhibition of Enterovirus 71. *Antiviral Res.* 74 (1), 9–15. doi: 10.1016/j.antiviral.2007.01.004

Teng, P., Yang, H., Li, J., Yang, F., and Chen, W. (2022). Analysis of the Long Noncoding RNA Profiles of RD and SH-SY5Y Cells Infected With Coxsackievirus B5, Using RNA Sequencing. *Arch. Virol.* 167 (2), 367–376. doi: 10.1007/s00705-021-05313-6

Thai, T.-H., Calado, D. P., Casola, S., Ansel, K. M., Xiao, C., Xue, Y., et al. (2007). Regulation of the Germinal Center Response by microRNA-155. *Sci. (New York N.Y.)* 316 (5824), 604–608. doi: 10.1126/science.1141229

Too, I. H. K., Bonne, I., Tan, E. L., Chu, J. J. H., and Alonso, S. (2018). Prohibitin Plays a Critical Role in Enterovirus 71 Neuropathogenesis. *PloS Pathog.* 14 (1), e1006778. doi: 10.1371/journal.ppat.1006778

Trizzino, M., Zucco, A., Deliard, S., Wang, F., Barbieri, E., Veglia, F., et al. (2021). EGR1 is a Gatekeeper of Inflammatory Enhancers in Human Macrophages. *Sci. Adv.* 7 (3), eaaz8836. doi: 10.1126/sciadv.aaz8836

Tung, W.-H., Hsieh, H.-L., and Yang, C.-M. (2010). Enterovirus 71 Induces COX-2 Expression *via* MAPKs, NF-Kappab, and AP-1 in SK-N-SH Cells: Role of PGE(2) in Viral Replication. *Cell. Signal.* 22 (2), 234–246. doi: 10.1016/j.cellsig.2009.09.018

Van Battum, E. Y., Brignani, S., and Pasterkamp, R. J. (2015). Axon Guidance Proteins in Neurological Disorders. *Lancet. Neurol.* 14 (5), 532–546. doi: 10.1016/S1474-4422(14)70257-1

van Zandwijk, N., Pavlakis, N., Kao, S. C., Linton, A., Boyer, M. J., Clarke, S., et al. (2017). Safety and Activity of microRNA-Loaded Minicells in Patients With Recurrent Malignant Pleural Mesothelioma: A First-in-Man, Phase 1, Open-Label, Dose-Escalation Study. *Lancet Oncol.* 18 (10), 1386–1396. doi: 10.1016/S1470-2045(17)30621-6

Wang, J., Pu, J., Huang, H., Zhang, Y., Liu, L., Yang, E., et al. (2013). EV71-Infected CD14(+) Cells Modulate the Immune Activity of T Lymphocytes in Rhesus Monkeys. *Emerg. Microbes Infect.* 2 (7), e44. doi: 10.1038/emi.2013.44

Wang, W., Sun, J., Wang, N., Sun, Z., Ma, Q., Li, J., et al. (2020). Enterovirus A71 Capsid Protein VP1 Increases Blood-Brain Barrier Permeability and Virus Receptor Vimentin on the Brain Endothelial Cells. *J. Neurovirol.* 26 (1), 84–94. doi: 10.1007/s13365-019-00800-8

Wang, R. Y. L., Weng, K.-F., Huang, Y.-C., and Chen, C.-J. (2016). Elevated Expression of Circulating Mir876-5p is a Specific Response to Severe EV71 Infections. *Sci. Rep.* 6, 24149. doi: 10.1038/srep24149

Wang, B., Xi, X., Lei, X., Zhang, X., Cui, S., Wang, J., et al. (2013). Enterovirus 71 Protease 2Apro Targets MAVS to Inhibit Anti-Viral Type I Interferon Responses. *PloS Pathog.* 9 (3), e1003231. doi: 10.1371/journal.ppat.1003231

Wang, Y., Zhang, S., Song, W., Zhang, W., Li, J., Li, C., et al. (2020). Exosomes From EV71-Infected Oral Epithelial Cells can Transfer miR-30a to Promote EV71 Infection. *Oral. Dis.* 26 (4), 778–788. doi: 10.1111/odi.13283

Wen, B.-p., Dai, H.-j., Yang, Y.-h., Zhuang, Y., and Sheng, R. (2013). MicroRNA-23b Inhibits Enterovirus 71 Replication Through Downregulation of EV71 VPl Protein. *Intervirology* 56 (3), 195–200. doi: 10.1159/000348504

Wong, K. T., Lum, L. C., and Lam, S. K. (2000). Enterovirus 71 Infection and Neurologic Complications. *New Engl. J. Med.* 342 (5), 356–358. doi: 10.1056/NEJM200002033420514

Wu, J., Gu, J., Shen, L., Fang, D., Zou, X., Cao, Y., et al. (2019). Exosomal MicroRNA-155 Inhibits Enterovirus A71 Infection by Targeting PICALM. *Int. J. Biol. Sci.* 15 (13), 2925–2935. doi: 10.7150/ijbs.36388

Xia, X., Cui, J., Wang, H. Y., Zhu, L., Matsueda, S., Wang, Q., et al. (2011). NLRX1 Negatively Regulates TLR-Induced NF-κb Signaling by Targeting TRAF6 and IKK. *Immunity* 34 (6), 843–853. doi: 10.1016/j.immuni.2011.02.022

Xing, W., Liao, Q., Viboud, C., Zhang, J., Sun, J., Wu, J. T., et al. (2014). Hand, Foot, and Mouth Disease in China 2008–12: An Epidemiological Study. *Lancet Infect. Dis.* 14 (4), 308–318. doi: 10.1016/s1473-3099(13)70342-6

Xu, C., He, X., Zheng, Z., Zhang, Z., Wei, C., Guan, K., et al. (2014). Downregulation of microRNA miR-526a by Enterovirus Inhibits RIG-I-Dependent Innate Immune Response. *J. Virol.* 88 (19), 11356–11368. doi: 10.1128/JVI.01400-14

Xu, P., Xu, H., Cheng, H. S., Chan, H.-H., and Wang, R. Y. L. (2020). MicroRNA 876-5p Modulates EV-A71 Replication Through Downregulation of Host Antiviral Factors. *Virol. J.* 17 (1), 21. doi: 10.1186/s12985-020-1284-8

Yamayoshi, S., Yamashita, Y., Li, J., Hanagata, N., Minowa, T., Takemura, T., et al. (2009). Scavenger Receptor B2 is a Cellular Receptor for Enterovirus 71. *Nat. Med.* 15 (7), 798–801. doi: 10.1038/nm.1992

Yang, S.-L., Chou, Y.-T., Wu, C.-N., and Ho, M.-S. (2011). Annexin II Binds to Capsid Protein VP1 of Enterovirus 71 and Enhances Viral Infectivity. *J. Virol.* 85 (22), 11809–11820. doi: 10.1128/JVI.00297-11

Yang, B., Chuang, H., and Yang, K. D. (2009). Sialylated Glycans as Receptor and Inhibitor of Enterovirus 71 Infection to DLD-1 Intestinal Cells. *Virol. J.* 6, 141. doi: 10.1186/1743-422X-6-141

Yang, C.-H., Liang, C.-T., Jiang, S.-T., Chen, K.-H., Yang, C.-C., Cheng, M.-L., et al. (2019). A Novel Murine Model Expressing a Chimeric Mscarb2/Hscarb2 Receptor Is Highly Susceptible to Oral Infection With Clinical Isolates of Enterovirus 71. *J. Virol.* 93 (11), e00183-19. doi: 10.1128/JVI.00183-19

Yang, Z., and Tien, P. (2014). MiR373 and Mir542-5p Regulate the Replication of Enterovirus 71 in Rhabdomyosarcoma Cells. *Sheng Wu Gong Cheng Xue Bao = Chin. J. Biotechnol.* 30 (6), 943–953. doi: 10.13345/j.cjb.130555

Yang, D., Wang, X., Gao, H., Chen, B., Si, C., and Wang, S. (2020). Downregulation of miR-155-5p Facilitates Enterovirus 71 Replication Through Suppression of Type I IFN Response by Targeting FOXO3/IRF7 Pathway. *Cell Cycle (Georgetown Tex.)* 19 (2), 179–192. doi: 10.1080/15384101.2019.1704512

Yang, X., Xie, J., Jia, L., Liu, N., Liang, Y., Wu, F., et al. (2017). Analysis of miRNAs Involved in Mouse Brain Damage Upon Enterovirus 71 Infection. *Front. Cell Infect. Microbiol.* 7. doi: 10.3389/fcimb.2017.00133

Yang, K. D., Yang, M. Y., Li, C. C., Lin, S. F., Chong, M. C., Wang, C. L., et al. (2001). Altered Cellular But Not Humoral Reactions in Children With Complicated Enterovirus 71 Infections in Taiwan. *J. Infect. Dis.* 183 (6), 850–856. doi: 10.1086/319255

Yang, Z., Zhuo, Q., Qin, W., Wang, J., Wang, L., and Tien, P. (2021). MicroRNAs miR-18a and miR-452 Regulate the Replication of Enterovirus 71 by Targeting the Gene Encoding VP3. *Virus Genes* 57 (4), 318–326. doi: 10.1007/s11262-021-01842-z

Yu, L., He, J., Wang, L., and Yi, H. (2019). Inflammatory Profiles Revealed the Dysregulation of Cytokines in Adult Patients of HFMD. *Int. J. Infect. Dis. IJID Off. Publ. Int. Soc. Infect. Dis.* 79, 12–20. doi: 10.1016/j.ijid.2018.11.001

Yu, Y., Huang, H., Li, J., Zhang, J., Gao, J., Lu, B., et al. (2013). Gadd45β Mediates P53 Protein Degradation *via* Src/PP2A/MDM2 Pathway Upon Arsenite Treatment. *Cell Death Dis.* 4, e637. doi: 10.1038/cddis.2013.162

Zhang, M., Chen, Y., Cheng, X., Cai, Z., and Qiu, S. (2020). GATA1/SP1 and miR-874 Mediate Enterovirus-71-Induced Apoptosis in a Granzyme-B-Dependent Manner in Jurkat Cells. *Arch. Virol.* 165 (11), 2531–2540. doi: 10.1007/s00705-020-04783-4

Zhang, L., Chen, X., Shi, Y., Zhou, B., Du, C., Liu, Y., et al. (2014). miR-27a Suppresses EV71 Replication by Directly Targeting EGFR. *Virus Genes* 49 (3), 373–382. doi: 10.1007/s11262-014-1114-4

Zhang, X., Hong, R., Chen, W., Xu, M., and Wang, L. (2019). The Role of Long Noncoding RNA in Major Human Disease. *Bioorg. Chem.* 92, 103214. doi: 10.1016/j.bioorg.2019.103214

Zhang, Y., Li, X., Wang, C., Zhang, M., Yang, H., and Lv, K. (2020). lncRNA AK085865 Promotes Macrophage M2 Polarization in CVB3-Induced VM by Regulating ILF2-ILF3 Complex-Mediated miRNA-192 Biogenesis. *Mol. Ther. Nucleic Acids* 21, 441–451. doi: 10.1016/j.omtn.2020.06.017

Zhao, Q., Xiong, Y., Xu, J., Chen, S., Li, P., Huang, Y., et al. (2018). Host MicroRNA hsa-miR-494-3p Promotes EV71 Replication by Directly Targeting PTEN. *Front. Cell. Infect. Microbiol.* 8. doi: 10.3389/fcimb.2018.00278

Zheng, Z., Ke, X., Wang, M., He, S., Li, Q., Zheng, C., et al. (2013). Human microRNA hsa-miR-296-5p Suppresses Enterovirus 71 Replication by Targeting the Viral Genome. *J. Virol.* 87 (10), 5645–5656. doi: 10.1128/JVI.02655-12

Zheng, Z., Li, H., Zhang, Z., Meng, J., Mao, D., Bai, B., et al. (2011). Enterovirus 71 2C Protein Inhibits TNF-Î±-Mediated Activation of NF-Î°B by Suppressing IÎ° B Kinase Î² Phosphorylation. *J. Immunol. (Baltimore Md. 1950)* 187 (5), 2202–2212. doi: 10.4049/jimmunol.1100285

Zheng, C., Zheng, Z., Sun, J., Zhang, Y., Wei, C., Ke, X., et al. (2017). MiR-16-5p Mediates a Positive Feedback Loop in EV71-Induced Apoptosis and Suppresses Virus Replication. *Sci. Rep.* 7 (1), 16422. doi: 10.1038/s41598-017-16616-7

Zhou, B., Chu, M., Xu, S., Chen, X., Liu, Y., Wang, Z., et al. (2017). Hsa-Let-7c-5p Augments Enterovirus 71 Replication Through Viral Subversion of Cell Signaling in Rhabdomyosarcoma Cells. *Cell Biosci.* 7, 7. doi: 10.1186/s13578-017-0135-9

Zhu, H., Cao, Y., Su, W., Huang, S., Lu, W., Zhou, Y., et al. (2019). Enterovirus A71 VP1 Variation A289T Decreases the Central Nervous System Infectivity *via* Attenuation of Interactions Between VP1 and Vimentin *In Vitro* and *In Vivo*. *Viruses* 11 (5), 467. doi: 10.3390/v11050467

Zimmerman, R. D. (1999). MR Imaging Findings of Enteroviral Encephalomyelitis: An Outbreak in Taiwan. *AJNR. Am. J. Neuroradiol.* 20 (10), 1775–1776.

Conflict of Interest: The authors declare that the research was conducted in the absence of any commercial or financial relationships that could be construed as a potential conflict of interest.

Publisher's Note: All claims expressed in this article are solely those of the authors and do not necessarily represent those of their affiliated organizations, or those of the publisher, the editors and the reviewers. Any product that may be evaluated in this article, or claim that may be made by its manufacturer, is not guaranteed or endorsed by the publisher.

frontiers | Frontiers in Cellular and Infection Microbiology

ORIGINAL RESEARCH
published: 18 May 2022
doi: 10.3389/fcimb.2022.877643

Clinical Application Evaluation of Elecsys® HIV Duo Assay in Southwest China

Mei Yang, Wenjuan Yang, Wu Shi and Chuanmin Tao *

Department of Laboratory Medicine, West China Hospital, Sichuan University, Chengdu, China

Background: HIV/AIDS continues to be a serious health concern of morbidity and mortality globally, and novel HIV testing is still an important component of diagnosing HIV earlier and reducing the spread of HIV. The Elecsys® HIV Duo assay is a 4th generation assay that can detect both HIV-1 p24 antigen (Ag) and HIV-1/2 antibody (Ab) in parallel and show the subresults for the Ab and Ab units.

Objectives: To evaluate the clinical performance of the Elecsys® HIV Duo assay on the new cobas E 801 analyzer using a large number of clinical samples from a population in southwest China.

Methods: We collected testing results and information from all patients in a large general hospital. All eligible clinical specimens were first analyzed using the Elecsys® HIV Duo assay. The test results are given either as reactive or nonreactive as well as in the form of a cutoff index (COI). All initially reactive specimens were retested in duplicate with a 3rd-generation kit. Supplementary tests were divided into Ab confirmation tests and HIV-1 nucleic acid tests. GraphPad Prism and Python were used for plotting, and SPSS 21.0 software was used for statistical analysis.

Results: A total of 186391 specimens were received, and 436 patients were confirmed to be positive for HIV. Among the 86 cases with contact history available, there were more males than females, and heterosexual transmission was the most common route of HIV infection. The Elecsys® HIV Duo assay displayed 99.94%, 99.93% and 99.98% specificity for inpatient, outpatient and physical examination patients, respectively. The median COI ratios of the false-positive group were significantly lower than those of the true-positive group.

Conclusions: The Elecsys® HIV Duo test (Cobase801 analyzer) differentiates the detection of HIV-1 p24 Ag and HIV-1/2 Ab with high specificity and facilitates the diagnosis of patients with early HIV infection. Therefore, the Elecsys®HIV Duo test is used for differentiation of antigen and antibody reactivity, making it suitable for routine clinical diagnosis.

Keywords: diagnostic performance, southwest China, HIV duo assay, human immunodeficiency virus, cutoff index

OPEN ACCESS

Edited by:
Viviane Fongaro Botosso, Butantan Institute, Brazil

Reviewed by:
Michael A. Eller, National Institute of Allergy and Infectious Diseases (NIH), United States
Mark Stephen De Souza, Institute of HIV Research and Innovation (IHRI), Thailand

***Correspondence:**
Chuanmin Tao
taocm@scu.edu.cn

Specialty section:
This article was submitted to Virus and Host, a section of the journal Frontiers in Cellular and Infection Microbiology

Received: *17 February 2022*
Accepted: *19 April 2022*
Published: *18 May 2022*

Citation:
Yang M, Yang W, Shi W and Tao C (2022) Clinical Application Evaluation of Elecsys® HIV Duo Assay in Southwest China. Front. Cell. Infect. Microbiol. 12:877643. doi: 10.3389/fcimb.2022.877643

INTRODUCTION

HIV/AIDS continues to be a serious health concern of morbidity and mortality globally. Since 2010, the number of new HIV infections has fallen by 31%, from 2.1 million to 1.5 million in 2020. As a result, according to global data, much progress has been made in the prevention and treatment of AIDS. Morbidity, mortality and new HIV infections are declining year by year globally. Although the rate of HIV infection has decreased significantly compared with the early years, the current situation is still not optimistic. According to the World Health Organization, 37.7 million people were infected with HIV in 2020 worldwide; the number of deaths from AIDS topped the list of notifiable infectious diseases in China (Xu et al., 2020). A total of 1,045 million living HIV/AIDS patients were reported in China by October 31, 2020. The Joint United Nations Program on HIV/AIDS (UNAIDS) has launched the 90-90-90 targets, the first of which is that 90% of people living with HIV (PLHIV) know their infectious status and are the most challenging. However, as of 2019, the reality was that only approximately 81% of patients were aware of their HIV status (Lu et al., 2020). Additionally, an effective strategy for HIV testing forms risk assessment of transmission of blood-borne pathogens for hospital staff who are exposed to blood and body fluids (WHO Guidelines Approved by the Guidelines Review Committee, 2010). Thus, universal screening for HIV-infected individuals (both known and unknown), who may or may not be aware of their infection status, is recommended so that patients need to be linked to care, retained in care, take antiretroviral medications, adhere to the prescribed regimens, and receive prophylaxis against opportunistic infections (Chang et al., 2013).

The HIV-1 Ag is the core protein of HIV-1. It is a 24-25 kDa protein encoded by the gag gene, which plays an important role in the packaging and maturation of the virus. Similar to RNA, it can be detected before seroconversion, so it becomes a marker of early HIV infection (Rafferty et al., 2019). HIV-1 Ag typically appears around the first 2 weeks post-infection (Fiebig et al., 2003; Cohen et al., 2010), and the concentration reaches the peak in one to two months later. As the earliest detected immune marker in serum, accurate detection of HIV-1 p24 Ag is conducive to the early diagnosis of HIV and can effectively shorten the window period. Serum HIV antibodies (Ab) include IgM and IgG antibodies, which are appeared approximately 3 and 6 weeks post-HIV infection, respectively (Alexander, 2016). As HIV Ab reactions usually persist over the course of infection, the initial screening and diagnosis of HIV mainly rely on different methods to detect HIV Ab in China (Eshleman et al., 2019).

The CDC recommends a complex HIV detection algorithm. The basic principle of this algorithm is to perform preliminary screening based on Ag/Ab. Based on the screening results, if the initial test results are reactive, the differentiation analysis of HIV-1/2 Ab and nucleic acid testing (NAT) is performed. However, if the screening results are nonreactive, no additional testing is required, and the result is considered negative. Therefore, a highly sensitive test is a key factor in eliminating false negative results.

Newly approved 4th-generation HIV tests have entered the international market and are commercially available, and they are commonly used in many laboratories to screen for HIV infection based on new diagnostic algorithms (Miedouge et al., 2011; Liu et al., 2016; Chacón et al., 2017). 4th-generation HIV assays can detect different HIV type 1 (HIV-1) non-B subtypes (group O Abs), HIV-1 p24 Ag, HIV-1/2 IgM, and IgG Ab simultaneously with extremely high sensitivity and specificity (Alexander, 2016; Stone et al., 2018). Therefore, compared to other methods (Cohen et al., 2010), 4th-generation HIV assays decrease the "window period" to 11–14 days post-exposure and enable the testing of acute and early HIV infection (Alexander, 2016; Stone et al., 2018). However, some 4th-generation Ag and Ab combo assays only provide a single result and cannot distinguish between HIV Ag and Ab readings and therefore have interpretation difficulty (Alexander, 2016).

The Elecsys® HIV Duo assay (Roche Diagnostics) for use on the Cobas E 801 analyzer (Roche Diagnostics, Penzberg, Germany) is a new 4th-generation assay that can detect both HIV-1 p24 Ag and HIV-1/2 Ab of clinical patients samples in parallel by two different reactions with a rapid test time of 18 min. This new instrument allowing for continuous loading of reagents and consumables can not only quickly confirm whether a patient is in an acute stage but also facilitate doctor–patient communication and early treatment. Specifically, this instrument has high normal running time and requires less manual time. A previous study (Muhlbacher et al., 2019) suggested that the Elecsys® HIV Duo assay is highly sensitive for the early detection of HIV, which was assessed at five laboratories from four different countries and compared with other available 4th-generation assays. Another study (Zhang et al., 2020) also showed that the Elecsys® HIV Duo assay had excellent performance for 3039 serum samples from Chinese patients.

Our study is unique in that this is the first retrospective study to evaluate the clinical performance of the Elecsys® HIV Duo assay on the new cobas E 801 analyzer using a large number of clinical patients samples from a population in southwest China.

METHODS AND MATERIALS

Elecsys® HIV Duo

Elecsys® HIV Duo is an enzyme-linked assay using a sandwich principle that allows simultaneous detection of HIV-1 p24 Ag as well as HIV-1 (including group O) and HIV-2 Ab. Biotinylated and ruthenium-labeled anti-p24 monoclonal antibodies were used for the detection of p24 Ag. Biotinylated and ruthenium-labeled HIV-specific proteins and D-peptide-bound streptavidin are used for HIV Ab detection. The main results of Elecsys® HIV Duo are automatically calculated using the e-flow system unique to the Cobas E 801 platform. HIV Ag and antibodies can be used as an aid in the selection of the confirmation algorithm for reactive samples. The results were automatically calculated by Elecsys® software. COI values (sample signal value/critical value) by comparing the electrochemiluminescence signal of the sample with the critical value obtained in calibration. Elecsys® software automatically calculates HIV DUO primary

results based on secondary results. Calculation formula: HIV DUO[COI] = HIV DUO[COI] = $\sqrt{(\text{HIV Ag[COI]})^2 + (\text{HIV Ab[COI]})^2}$.

Study Design

This retrospective study was conducted in a large general hospital with a catchment population of approximately 16.33 million inhabitants in Sichuan, China. The hospital's laboratory has the HIV confirmation laboratory in China, which was certified as a laboratory by the College of American Pathologists (CAP) in 2006, and has also passed the competency verification of the Clinical Laboratory Center of the National Health Commission. We collected testing results and data from all patients who underwent initial screening for HIV discriminant Ag and Ab and HIV complementary testing (Ab confirmatory test or HIV-1 nucleic acid test) at this hospital between January 2021 and October 2021. In addition, by searching the electronic medical record management system of the hospital, we collected the patient's medical records, such as the reason for seeing a doctor, medical information, clinical symptoms, past medical history and disease course records.

The study was conducted in full compliance with the principles of the Helsinki Declaration and local regulations. The study protocol was approved by ethics committee of the West China Hospital of Sichuan University. Exemption for obtaining informed consents from subjects was granted as a retrospective analysis of routinely collected programmatic data, and there was no direct contact with patients and not interfere with the clinician's diagnosis and treatment.

Study Population and Specimens

HIV screening subjects: A total of 186,391 patients were inpatients, outpatients, emergency patients, and healthy physical examination participants who received an initial screening test for HIV differentiated Ag and Ab in the hospital from January 2021 to October 2021.

HIV confirmed subjects: A total of 578 patients tested reactive for HIV differentiated Ag and Ab during the initial screening period from January 2021 to October 2021.

All collected fresh clinical specimens were centrifuged at 3500 rpm/min for 10 min, and then serum or plasma was separated for detection. They are stored in the refrigerator at 4-8°C for up to 1 week and at -80°C for longer periods prior to testing.

Screening Procedures

All eligible clinical specimens were first analyzed using the Elecsys® HIV Duo assay, performed on the Cobas E 801 platform (Roche Diagnostics, Mannheim, Germany), following the manufacturer's instructions. The screening procedure and detection algorithm are shown in **Figure 1**. The test results were given either as reactive (COI≥1.0) or nonreactive (COI<1.0) as well as in the form of a cutoff index (COI). All initially reactive specimens were retested in duplicate with a 3rd-generation kit-colloidal gold method—anti-HIV (Livzon Diagnostics Inc.) according to technical specifications for national AIDS testing published by Chinese Center for Disease Control and Prevention. Specimens were considered repeatedly reactive [quality control line (C) and test line (T) appear simultaneously) and nonreactive (only one quality control line (C) does not appear detection line (T)].

Supplementary Test

Supplementary tests are divided into Ab confirmation tests and HIV-1 nucleic acid tests. The HIV-1 nucleic acid test includes qualitative and quantitative tests. Recommended confirmatory algorithms need to be confirmed for test results. Western Blot HIV blot 2.2 (MP Diagnostics, Singapore) was used as the HIV confirmatory test, which can detect IgG antibodies specific to viral Ag. On the basis of the manufacturer's specification, the results of WB were reported as HIV-1 positive [the presence of at least two bands, including two env bands (gpl60/gp41 and gpl20) or two gag bands (p17, p24, p55) or two pol bands (p31, p51, p66)]; HIV-1/2 positive (the presence of HIV-1 positive bands and clearly visible HIV-2 specific bands); negative (the absence of any of the specific bands or only p17 antibodies were detected); indeterminate (reactivity to any of the bands but not meeting the criteria for a positive indeterminate result); inconclusive but suggestive of HIV-2 positive infection (any specific band is present, but not sufficient to be positive, and the HIV-2-specific band is clearly visible).

When NAT is used as supplementary test: suspected HIV-infected patients who respond to the screening test but have uncertain or negative Ab confirmatory result should be judged based on NAT. A total of 123 patients were voluntarily tested for HIV-1 RNA.

Statistical Analysis

GraphPad Prism and Python were used for plotting, and SPSS 21.0 (SPSS Inc., Chicago, IL) software was used for statistical analysis. Quantitative data were confirmed and expressed as the median and interquartile range (IQR). Comparisons between continuous variables were made using the t test, depending on the normality of the distribution. A nonparametric test was used to analyze those that did not conform to a normal distribution. The chi-square test or Fisher's exact probability method was used for counting data. The test level is set as α=0.05. HIV screening positive rate = the number of HIV initial screening positive cases/the number of all tested cases; HIV confirmed positive rate = number of HIV confirmed positive cases/number of all tested cases; positive rate of HIV Ab retest = number of Ab retest positive cases/number of all tested cases; incidence of HIV uncertainty = number of HIV uncertainty/number of all tested cases; efficiency of HIV Ab retest = number of false positive cases of negative Ab retest/(number of positive cases screened - number of positive cases of Ab retest): this index can reflect the ability of retest to exclude false positive samples from screened positive samples; confirmation efficiency of HIV testing process = (number of HIV-positive confirmed cases + number of HIV-negative confirmed cases)/number of retested positive cases: this index reflects the ability of subsequent tests (WB or HIV-1 RNA detection) to remove false positives from retested positive samples after retesting; Positive

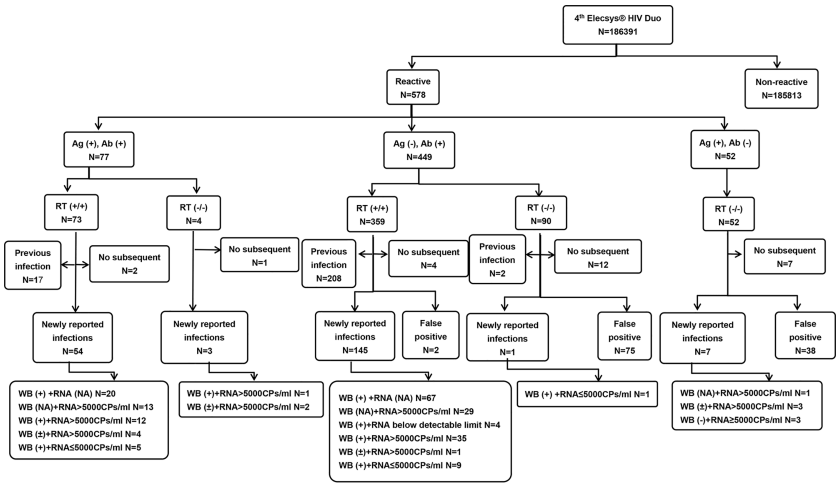

FIGURE 1 | The distributions of the results of the Elecsys® HIV Duo assay.

predictive value = true positive number/(true positive + false positive number).

RESULTS

The Testing Algorithm and Distributions of Specimens Tested in the Elecsys® HIV Duo Assay

As shown in **Figure 1**, a total of 186,391 specimens were received from January 1 to October 31. Of the 186,391 specimens tested, 185,813 (99.69%) were nonreactive. A total of 578 (0.31%) specimens were repeatedly reactive; Ag (+) and Ab (+), Ag (-) and Ab (+), Ag (+) and Ab (-) specimens were 77, 449, 52 cases, respectively. After excluding 26 samples that were lost to follow-up, 552 cases were confirmed to be reactive for screening. Then, the colloidal gold rapid detection method was used for subsequent repeated detection. After that, the patients were divided into previous HIV infection, newly reported HIV infection, false positive and no follow-up groups by means of case information query and telephone communication. In 210 (36.33%) patients with newly reported HIV infection, two complementary tests, WB and HIV RNA, were used for final determination. Finally, 436 patients were confirmed to be positive for HIV, and 116 cases were negative for supplementary tests.

Detailed Results for 186391 Samples Assayed and the Overall Specificity of Each Assay Calculated by Combining the Data

Table 1 showed HIV screening, HIV prevalence and performance evaluation of the Elecsys® HIV Duo method. Compared with inpatients and physical examination patients, outpatients had the largest number of HIV-positive screening patients, accounting for 0.46% of the positive screening patients. Similarly, the positive rate of HIV confirmed by supplementary testing in outpatients was the highest, reaching 0.37%. The overall specificity of the Elecsys® HIV Duo assay across all 186391 samples of inpatients, outpatients and physical examination patients in this study relative to the final HIV status was 99.94%, 99.93% and 99.98%, respectively.

Median (Quartile Range) Cutoff Index (COI) Ratios of All 522 WB or Subsequent Supplement Detections Confirmed Individuals

Table 2 showed that the differences in median COI ratios between true-positive and true-negative results of HIV Duo and HIV-1/2 Ab were large. As mentioned above, HIV infection status was determined by WB, follow-up, HIV-1 RNA, or HIV-1 p24 Ag. As seen in **Table 2**, the median COI value in true-positive group of HIV Duo, p24 Ag, and HIV-1/2 Ab were 522.00 (IQR:154.50,1397.50), 0.19 (IQR:0.16,0.31) and 522.00 (IQR:152.75,1388.75), respectively., while value in false-positive group was 2.02 (IQR:1.44,4.10), 0.19 (IQR:0.17,1.76) and 1.31 (IQR:0.10,2.03). Notably, there were significant differences in terms of true positive and false positive for HIV Duo (P=0.000) and HIV-1/2 Ab (P=0.000).

Predictive Value of the Stratified COI Value for HIV Infection

As shown in **Table 3**, for HIV Duo, the COI values of 43.30% of all tested specimens were less than 200. When the COI ranged from 1 to 4.99, 97.85% of the specimens were negative at the initial screening, while when the COI was between 5 and 14.99, 70% of the specimens were negative. In addition, the COI values

TABLE 1 | Detailed results for 186391 samples assayed and the overall specificity of each assay calculated by combining the data.

	Inpatient	Outpatient	Physical examination	Total
Screening non-reactive (n)	97864	68559	19390	185813
Screening reactive (n)	241	314	23	578
Screening reactive rate (%)	0.25	0.46	0.12	0.31
Total screening (n)	98105	68873	19413	186391
Confirmed negative (n)				
Confirmed positive (n)	174	252	10	436
Confirmed positive rate (%)	0.18	0.37	0.05	0.23
Total Confirmed (n)				
Specificity (%)	99.94	99.93	99.98	99.94

TABLE 2 | Median (quartile range) of cutoff index (COI) ratios of all 522 WB or subsequent supplement detections confirmed individuals.

Median (quartile range) of COI ratios	HIV Duo	P24 Ag	Ab	Total (n)
True positive	522.00 (154.50,1397.50)	0.19 (0.16,0.31)	522.00 (152.75,1388.75)	436
False positive	2.02 (1.44,4.10)	0.19 (0.17,1.76)	1.31 (0.10,2.03)	116
P	0.000	0.247	0.000	–

of negative specimens were mostly in the range of 1-49.99, and only 2 specimens had COI values ≥50.

For HIV-1/2 Ab, 43.48% of all tested specimens were less than 200. When the COI value was between 1 and 4.99, 97.06% of the specimens were negative in the initial screening, while the COI value was between 5 and 14.99, and the rate of negative specimens and true positive specimens was equal. Specifically, only the specimens with COI≥15 were truly positive. In fact, when the COI value was between 0 and 0.99, 7 true positive samples were missed. According to the progress of HIV viremia and immune response after primary infection, Ag and Ab were detected at different times. Ab could not be detected in the 7 patients with acute HIV infection, therefore, COI values is less than 1.0.

For HIV1-p24 Ag, the positive COI value accounted for 21.56% of all screened samples, and the COI were mainly distributed in the range of 1-49.99 (98.01%). Nearly, COI was between 1 and 4.99, and 44.26% of the specimens were negative, while when the COI value was ≥5, more than 75% of the specimens were true positive. In particular, negative values are still possible at high levels of COI≥100.

DISCUSSION

This research is the first attempt to evaluate the clinical diagnostic performance of the Elecsys® HIV Duo assay for HIV screening, to suggest the predictive value of COI for HIV infection and to confirm HIV infections in the context of a highly complex and multiethnic region of China. It is important to note that this study was carried out in southwest China, which has the highest number of HIV infection patients in the country, thus filling a gap in the lack of large-scale clinical evaluation of the Elecsys® HIV Duo assay in southwest China.

From all the conclusive results in this research, a total of 186391 specimens were entered into our analysis, and 552 patients were confirmed to be positive for screening. The Elecsys® HIV Duo assay, a 4th-generation assay, displayed 99.94%, 99.93% and 99.98% specificity of inpatient, outpatient and physical examination patients in detecting HIV patients from large and diverse clinical samples in China. Research subjects may be representative of a broad population, reflecting those who may present routinely testing in China. A study by Muehlbacher et al. (Muhlbacher et al., 2019) assessed the performance of the Elecsys® HIV Duo assay at five international laboratories, and the specificity of blood donor samples was 99.87% and 100% in 1000 diagnostic samples. Similarly, a study (Zhang et al., 2020) also reported 99.93% specificity of the Elecsys® HIV Duo assay. The high specificity of the Elecsys® HIV Duo assay, as demonstrated, could thus identify potentially HIV-infected patients and guide the precise use of antiviral treatment early as possible for clinicians. Another study (Krasowski et al., 2021) also looked at the clinical performance of the Elecsys. The overall specificity of the Elecsys assay was 99.84% [95% CI 99.73-99.91 (8129/8142)]. Furthermore, the high specificity is a crucial characteristic of the Elecsys® HIV Duo assay, which reduces the likelihood of false positives and not only meets the evaluation criteria set by the CDC but also reduces the number of additional Ab differential immunoassay confirmatory tests.

Previous studies (Kiely et al., 2010) showed that as the signal ratio of the negative control to the positive control, a high signal-to-cutoff (S/CO) ratio was predictive of confirmed HIV-positive results. Accordingly, this study also computed various overlap COIs between false positive and confirmed positive results, which suggests the predictive value of COI on HIV infection status. This study demonstrated that median COI ratios between true-positive and true-negative results of HIV Duo and HIV-1/2 Ab were large and false-positive group is significantly lower than that in the true-positive group. For HIV Duo, 99.49% (392/394) of individuals with COI ratios ≥50 were confirmed to be true-positive for HIV infection, and 97.85% of the specimens with COI ratios <15 were negative at the initial screening, verifying that high COI ratios were predictive of

TABLE 3 | Results of all 552 WB or subsequent supplementary test-confirmed individuals in relation to cutoff index (COI) ratios.

COI ratios	Positive n (%)			Negative n (%)		
	HIV DUO	HIV-1/2 Ab	HIV1-P24 Ag	HIV DUO	HIV-1/2 Ab	HIV1-P24 Ag
0-0.99	–	7 (15.22)	356 (82.22)	–	39 (84.78)	77 (17.78)
1-4.99	2 (2.11)	2 (2.94)	34 (55.74)	93 (97.89)	66 (97.06)	27 (44.26)
5-14.99	6 (30)	8 (42.11)	21 (80.77)	14 (70)	11 (57.89)	5 (19.23)
15-49.99	36 (83.72)	32 (100.00)	16 (76.19)	7 (16.28)	0	5 (23.81)
50-99.99	43 (97.73)	39 (100.00)	6 (85.71)	1 (2.27)	0	1 (14.29)
100-199.99	36 (97.30)	36 (100.00)	3 (75.00)	1 (2.70)	0	1 (25.00)
200-399.99	67 (100)	66 (100.00)	–	0	0	–
>399.99	246 (100%)	246 (100.00%)	–	0	0	–
Total n (%)	436 (78.99)	436 (100.00)	436 (78.99)	116 (21.01)	116 (21.01)	116 (21.01)

Ab, antibody; Ag, antigen.

confirmed positive results. 15.0 were false positive results, suggesting that no additional laboratory tests are needed to confirm the results, especially in weakly responsive samples. Reasons for false positivity include small sample size, sample handling and variation in fixation methods, such as sample contamination and mislabeling. However, it is worth noting that although the COI ratio has predictive value for HIV infection, it is only an auxiliary method and cannot be used as a diagnostic tool. When doctors communicate with patients, they need to avoid increasing the psychological burden of patients and causing unnecessary medical disputes. If the patient had an epidemiological history, especially if the single Ag is positive, the patient should receive additional testing to determine HIV infection status. It has been reported that NAT detection can be directly applied to serum with COI level less than 4.0 (Parker et al., 2019).

According to the HIV screening recommendation, once the initial screening result is positive, the patient must be retested and confirmed to determine the final HIV infection status. Most patients with high COI levels (e.g., COI > 200.0) can be diagnosed directly by the WB confirmatory test.

3th-generation tests have been the primary means of screening for HIV infection in most parts of China. However, compared to other 4th- or 3rd-generation tests, the Elecsys® HIV Duo assay has many advantages, such as excellent specificity, the ability to detect HIV-1 p24 Ag and HIV antibodies separately and a significantly shorter diagnostic window. Therefore, it can not only effectively and accurately diagnose early HIV infection but also distinguish between previously and newly reported infections. In the long term, widespread use of the method can help clinicians accurately identify and treat the disease, and early public health interventions can reduce the risk of transmission. In the area of diagnostic surveillance for the clinical management of HIV, the necessary cost savings can be achieved through the adoption of the Elecsys® HIV Duo assay, which uses advanced, well-coordinated modern technology to greatly improve the quality of test results. Diagnostic algorithms with superior performance deserve more support to avoid wasting limited medical resources and funds on expensive and/or untested methods (Petti et al., 2006; Brown, 2007). At the same time, laboratory workers should pay attention to and participate in more reasonable algorithm design and method evaluation, rather than overly ambitious laboratory testing work. We hope that more scientific and reasonable detection algorithms and methods can be widely used in resource-limited areas.

There are several limitations to our study. First, this is a large retrospective study; 26 patients did not go through a complete algorithm, some patients may have been infected with HIV, and others may have been confirmed. No follow-up reasons may include loss of follow-up, death and unwillingness to accept diagnosis, which may affect our final results. Therefore, it is necessary to store and retrieve the results based on computers for the laboratory of a large number of specimens and the study of large data. Then, one of the limitations of our study is that there is no independent gold standard for determining "true negative". A study conducted by Muhlbacher (Xu et al., 2020) et al. evaluated the performance of the Elecsys ® HIV Duo assay in five international centres and compared with other available 4th-generation tests. The evaluation by the 139 seroconversion panels indicated that the Elecsys ® HIV Duo test was highly sensitive. Therefore, we decided to just perform a specificity analysis. Finally, the original data come from a single hospital and are not fully representative or applicable to the entire local or even national population. We hope to expand the number and diversity of samples by collecting data in different regions.

CONCLUSION

The Elecsys® HIV Duo test (Cobase 801 analyzer) differentiates the detection of HIV Ag and anti-HIV antibodies with high specificity and facilitates the diagnosis of patients with early HIV infection. COI values are good predictors of HIV infection, with a high COI ratio predicting a confirmed positive result and 15.0 being a false positive result, indicating that no additional laboratory testing is required to confirm the result. Therefore, the Elecsys®HIV Duo test is an improvement of HIV Ag and Ab discrimination, making it suitable for routine clinical diagnosis.

DATA AVAILABILITY STATEMENT

The original contributions presented in the study are included in the article/supplementary material. Further inquiries can be directed to the corresponding author.

AUTHOR CONTRIBUTIONS

MY conceived and designed the study, and helped to draft and revise the manuscript for important intellectual content. CT and WY participated in study conception and design, collected data, performed statistical analysis and interpretation, and drafted and revised the manuscript. WS participated in study conception and design and helped to draft and revise the manuscript. MY prepared and collected data and helped to draft the manuscript. All authors made substantial contribution. All authors contributed to the article and approved the submitted version.

REFERENCES

Alexander, T. S. (2016). Human Immunodeficiency Virus Diagnostic Testing: 30 Years of Evolution. *Clin. Vaccine Immunol.* 23, 249–253. doi: 10.1128/CVI.00053-16

Brown, H. (2007). Global Health: Great Expectations. *BMJ (Clin. Res. Ed.)* 334, 874–876. doi: 10.1136/bmj.39183.534919.94

Chacón, L., Mateos, M. L., and Holguín, Á. (2017). Relevance of Cutoff on a 4th Generation ELISA Performance in the False Positive Rate During HIV Diagnostic in a Low HIV Prevalence Setting. *J. Clin. Virol.* 92, 11–13. doi: 10.1016/j.jcv.2017.04.014

Chang, L. W., Serwadda, D., Quinn, T. C., Wawer, M. J., Gray, R. H., and Reynolds, S. J. (2013). Combination Implementation for HIV Prevention: Moving From Clinical Trial Evidence to Population-Level Effects. *Lancet Infect. Dis.* 13, 65–76. doi: 10.1016/S1473-3099(12)70273-6

Cohen, M. S., Gay, C. L., Busch, M. P., and Hecht, F. M. (2010). The Detection of Acute HIV Infection. *J. Infect. Dis.* 202, S270–S277. doi: 10.1086/655651

Eshleman, S. H., Laeyendecker, O., Kammers, K., Chen, A., Sivay, M. V., Kottapalli, S., et al. (2019). Comprehensive Profiling of HIV Antibody Evolution. *Cell Rep.* 27, 1422–1433.e4. doi: 10.1016/j.celrep.2019.03.097

Fiebig, E. W., Wright, D. J., Rawal, B. D., Garrett, P. E., Schumacher, R. T., Peddada, L., et al. (2003). Dynamics of HIV Viremia and Antibody Seroconversion in Plasma Donors: Implications for Diagnosis and Staging of Primary HIV Infection. *Aids* 17, 1871–1879. doi: 10.1097/00002030-200309050-00005

Kiely, P., Walker, K., Parker, S., and Cheng, A. (2010). Analysis of Sample-To-Cutoff Ratios on Chemiluminescent Immunoassays Used for Blood Donor Screening Highlights the Need for Serologic Confirmatory Testing. *Transfusion* 50, 1344–1351. doi: 10.1111/j.1537-2995.2009.02572.x

Krasowski, M. D., Wier, D., Smith, S., Riedel, A., Lauseker-Hao, Y., Kelner, M., et al. (2021). Real-World Clinical Performance Evaluation of a Fourth-Generation HIV Antigen/Antibody Differentiation Test. *J. Appl. Lab. Med.* 6, 1417–1432. doi: 10.1093/jalm/jfab069

Liu, P., Jackson, P., Shaw, N., and Heysell, S. (2016). Spectrum of False Positivity for the Fourth Generation Human Immunodeficiency Virus Diagnostic Tests. *AIDS Res. Ther.* 13, 1. doi: 10.1186/s12981-015-0086-3

Lu, X., Sun, H., Li, H., Xia, W., Wu, H., Chen, D., et al. (2020). Validation of the BD FACSPresto System for the Measurement of CD4 T-Lymphocytes and Hemoglobin Concentration in HIV-Negative and HIV-Positive Subjects. *Sci. Rep.* 10, 19605–19605. doi: 10.1038/s41598-020-76549-6

Miedouge, M., Grèze, M., Bailly, A., and Izopet, J. (2011). Analytical Sensitivity of Four HIV Combined Antigen/Antibody Assays Using the P24 WHO Standard. *J. Clin. Virol.* 50, 57–60. doi: 10.1016/j.jcv.2010.09.003

Muhlbacher, A., Sauleda, S., Piron, M., Rietz, R., Permpikul, P., Klinkicht, M., et al. (2019). A Multicentre Evaluation of the Elecsys (R) HIV Duo Assay. *J. Clin. Virol.* 112, 45–50. doi: 10.1016/j.jcv.2018.11.005

Parker, J., Carrasco, A. F., and Chen, J. (2019). BioRad BioPlex (R) HIV Ag-Ab Assay: Incidence of False Positivity in a Low-Prevalence Population and its Effects on the Current HIV Testing Algorithm. *J. Clin. Virol.* 116, 1–3. doi: 10.1016/j.jcv.2019.04.002

Petti, C. A., Polage, C. R., Quinn, T. C., Ronald, A. R., and Sande, M. A. (2006). Laboratory Medicine in Africa: A Barrier to Effective Health Care. *Clin. Infect. Dis.* 42, 377–382. doi: 10.1086/499363

Rafferty, H., Chirro, O., Oduor, C., Wahome, E., Ngoi, C., van der Elst, E., et al. (2019). Pilot Testing of an Online Training Module About Screening for Acute HIV Infection in Adult Patients Seeking Urgent Healthcare. *Int. Health* 11, 93–100. doi: 10.1093/inthealth/ihy077

Stone, M., Bainbridge, J., Sanchez, A. M., Keating, S. M., Pappas, A., Rountree, W., et al. (2018). Comparison of Detection Limits of Fourth- and Fifth-Generation Combination HIV Antigen-Antibody, P24 Antigen, and Viral Load Assays on Diverse HIV Isolates. *J. Clin. Microbiol.* 56, e02045–17. doi: 10.1128/JCM.02045-17

WHO Guidelines Approved by the Guidelines Review Committee. (2010). *WHO Best Practices for Injections and Related Procedures Toolkit* (Geneva: World Health Organization Copyright © 2010, World Health Organization.).

Xu, F., Bu, K., Chen, F. F., Jin, S. S., Zhang, H. X., Zhang, D., et al. (2020). Structural Equation Modeling Test of the Pre-Intentional Phase of the Health Action Process Approach (HAPA) Model on Condom Use Intention Among Senior High School Students in Tianjin, China. *Medicine* 99, e22776. doi: 10.1097/MD.0000000000022776

Zhang, B. W., Ma, Q., Zhao, B., Wang, L., Pu, C. Y., and Han, X. X. (2020). Performance Evaluation of Elecsys HIV Duo on Cobas E 801 Using Clinical Samples in China. *J. Med. Virol.* 92, 3230–3236. doi: 10.1002/jmv.25845

Conflict of Interest: The authors declare that the research was conducted in the absence of any commercial or financial relationships that could be construed as a potential conflict of interest.

frontiers | Frontiers in Cellular and Infection Microbiology

REVIEW
published: 03 June 2022
doi: 10.3389/fcimb.2022.896972

Pathophysiology of COVID-19: Critical Role of Hemostasis

Sonia Aparecida de Andrade[1†], Daniel Alexandre de Souza[1†], Amarylis Lins Torres[1†], Cristiane Ferreira Graça de Lima[1†], Matteo Celano Ebram[1†], Rosa Maria Gaudioso Celano[2†], Mirta Schattner[3†] and Ana Marisa Chudzinski-Tavassi[4,5*†]*

[1] Biopharmaceuticals Laboratory, Instituto Butantan, São Paulo, Brazil, [2] University of Taubaté (UNITAU), Taubaté, Brazil, [3] Laboratory of Experimental Thrombosis. Instituto de Medicina Experimental – CONICET -Academia Nacional de Medicina, Buenos Aires, Argentina, [4] Center of Excellence in New Target Discovery (CENTD), Instituto Butantan, São Paulo, Brazil, [5] Innovation and Development Laboratory, Instituto Butantan, São Paulo, São Paulo, Brazil

The COVID-19 pandemic, caused by SARS-CoV-2, had its first cases identified in late 2019 and was considered a clinical pandemic in March 2020. In March 2022, more than 500 million people were infected and 6,2 million died as a result of this disease, increasingly associated with changes in human hemostasis, such as hypercoagulation. Numerous factors contribute to the hypercoagulable state, and endothelial dysfunction is the main one, since the activation of these cells can strongly activate platelets and the coagulation system. In addition, there is a dysregulation of the renin-angiotensin system due to the SARS-CoV-2 takeover of the angiotensin converting enzyme 2, resulting in a strong immune response that could further damage the endothelium. Thrombus formation in the pulmonary microvasculature structure in patients with COVID-19 is an important factor to determine the severity of the clinical picture and the outcome of this disease. This review describes the hemostatic changes that occur in SARS-CoV-2 infection, to further improve our understanding of pathogenic mechanisms and the interaction between endothelium dysfunction, kallikrein-kinins, renin angiotensin, and the Coagulation/fibrinolysis systems as underlying COVID-19 effectors. This knowledge is crucial for the development of new effective therapeutic approaches, attenuating the severity of SARS-CoV-2's infection and to reduce the deaths.

Keywords: COVID-19, SARS-CoV-2, hemostasis, coagulopathy, thrombus

OPEN ACCESS

Edited by:
Edmarcia Elisa De Souza, University of São Paulo, Brazil

Reviewed by:
Aikaterini Alexaki, Centre Hospitalier Universitaire Vaudois (CHUV), Switzerland
Jean-Luc Diehl, Université Paris Descartes, France
Ibrahim C. Haznedaroglu, Hacettepe University Hospital, Turkey

****Correspondence:***
Ana Marisa Chudzinski-Tavassi
ana.chudzinski@butantan.gov.br
Mirta Schattner
mschattner@hotmail.com

†ORCID:
Sonia Aparecida De Andrade
orcid.org/0000-0003-4862-8131
Daniel Alexandre De Souza
orcid.org/0000-0002-8972-662X
Amarylis Lins Torres
orcid.org/0000-0002-2925-3082
Matteo Celano Ebram
orcid.org/0000-0002-8245-9805
Rosa Maria Gaudioso Celano
orcid.org/0000-0001-5119-2856
Cristiane Ferreira Graça De Lima
orcid.org/0000-0001-9010-6279
Mirta Schattner
orcid.org/0000-0001-9439-2161
Ana Marisa Chudzinski-Tavassi
orcid.org/0000-0001-7717-7013

Specialty section:
This article was submitted to Clinical Microbiology, a section of the journal Frontiers in Cellular and Infection Microbiology

Received: *15 March 2022*
Accepted: *05 May 2022*
Published: *03 June 2022*

INTRODUCTION

COVID-19 is a disease caused by the severe acute respiratory syndrome coronavirus 2 (SARS-CoV-2), a virus of the Coronavidae family with an envelope and genome consisting of a single strand of positive-stranded RNA. COVID-19 had the first cases identified in Wuhan – China at the end of 2019, and was considered a pandemic by the World Health Organization (WHO) in March of 2020. To date, more than 500 million people have been infected, and over 6,2 million people have died

worldwide as a result of this disease (Dong et al., 2020; WHO Coronavirus (COVID-19) Dashboard, 2021).

It is known that some people infected with the new coronavirus remain asymptomatic, but these people can still carry and transmit the virus (Johansson et al., 2021). Normally, COVID-19 is a mild illness associated with, fever, fatigue, cough, muscle aches, sore throat, loss of smell or taste, and other symptoms; However, some patients infected with SARS-CoV-2, may suffer different clinical manifestations, as severe respiratory syndrome and even death (Wiersinga et al., 2020). Turk et al. described three critical clinicobiological phases of SARS-associated coronavirus infections in humans: "asymptomatic/pre-symptomatic phase", "respiratory phase with mild/moderate/severe symptoms" and "multi-systemic clinical syndrome with impaired/disproportionate and/or defective immunity" (Turk et al., 2020). Understanding the phases may be useful for clinical management and development of vaccines and/or specific drugs targeting the COVID-19 processes

The fatality rate of COVID-19 patients with diabetes was 7.3%, for patients with cardiovascular disease 10.5%, and for patients without any comorbidities 0.9% (Yang et al., 2020). Furthermore, when compared to according age groups, people with age 45 or higher are more likely to die from COVID-19 than the younger ones. Aging leads to structural and functional modifications of the vasculature, which may lead to endothelial dysfunction (Amraei and Rahimi, 2020). Endothelial cells play a major role in the pathogenesis of this disease, furthermore SARS-CoV-2 infection promotes changes in hemostasis; a recent study found that nearly 72% of non-survivors had evidence of hypercoagulability (Tang, 2020).

The major leading cause of mortality in patients with COVID-19 is respiratory failure from acute respiratory distress syndrome (ARDS) (Amraei and Rahimi, 2020). However, deaths resulting from COVID-19 are significantly associated with vascular injuries (Wu et al., 2021) and SARS-CoV-2 infection induces changes in the coagulation and fibrinolytic system (Leentjens et al., 2021). Such pathophysiological changes generate arterial and, mainly, venous thrombosis, especially in patients with severe symptoms. These thrombotic events occur more frequently in the lung, and both macro and microthrombi have been reported, the latter being usually not detectable by imaging, but only by post mortem autopsy (Asakura and Ogawa, 2021).

Post-mortem histopathological analysis of lung tissue from 38 patients with SARS-CoV-2 demonstrated, in most cases, the presence of fibrin- and platelet-rich thrombi in pulmonary arterioles, congested capillaries, and bleeding alveoli, often containing CD61+ megakaryocytes, and dense capillary foci, presumably resulting from angiogenesis (Carsana et al., 2020). In another post-mortem analysis in multiple tissues, there is a description of congestion and small vessel endotheliitis with accumulation of mononuclear/lymphocytic cells around the capillary endothelium in the heart, small intestine, kidney, liver and lung; in one case, caspase 3 immunostaining revealed the presence of apoptotic bodies in the endothelial cells lining the inner wall of inflamed blood vessels. As a consequence of this vascular disorder, after inflammation, congestion, thrombosis, hemorrhage, and endothelial cell death, the surrounding hypoxic tissues showed evidence of interstitial edema, destruction, inflammation, fibrosis, and vascular regeneration (Carsana et al., 2020; Varga et al., 2020). Deep vein thrombosis in the extremities was accompanied by evidence of recent thrombosis in the prostatic venous plexus in 6/7 cases by Wichmann and colleagues (Wichmann et al., 2020).

There are numerous factors that could contribute to the hypercoagulable state of COVID-19 patients, endothelial dysfunction being the main factor since endothelial cell activation can strongly activate platelets and the coagulation system (Yau et al., 2015). In addition, there is a dysregulation of the renin-angiotensin system due to SARS-CoV-2 takeover of the angiotensin converting enzyme 2 (ACE-2) resulting in a strong immune response that could further damage the endothelium (Amraei and Rahimi, 2020).

The pathophysiology of endothelial dysfunction and injury offers insights into COVID-19 associated mortality. Besides this, a process made up of three main steps which happen simultaneously in a fine orchestrated fashion – platelet aggregation, blood clotting and fibrinolysis. The integrity of the endothelium is also essential for the maintenance of hemostasis and any disturbances between any of these features can lead to hemorrhage or thrombosis (Maffei et al., 2015).

CHANGES ON THE ENDOTHELIUM

The infection and viral entry of SARS-CoV-2 into the cell is mediated by angiotensin ACE-2, transmembrane serine protease 2 (TMPRSS2) and cathepsin L, which cleaves the spike protein on the viral particle to allow engagement with ACE-2 (Jackson et al., 2021).

As it is known, some endothelial cells, especially in the lungs, highly express ACE-2 in its surface, making them a direct target for coronavirus infection (Hamming et al., 2004). ACE-2 is a type I transmembrane receptor with 3 domains, a single transmembrane domain, a cytoplasmic carboxyl domain, and a catalytic extracellular domain. The main physiological function of ACE-2 is in the regulation and metabolism of Renin-Angiotensin System peptides opposing the effects of angiotensin II, serving as a counter-regulatory mechanism to ACE. Usually, ACE-2 catalyzes polypeptides with preference for hydrolysis between proline and a hydrophobic aminoacid (Vickers et al., 2002).

ACE-2 generates Ang 1-9 peptide through cleavage of Ang I (1-10), while ACE converts Ang I into Ang II (Ang 1-8). ACE-2 also metabolizes Ang II (Ang 1-8) to generate Ang 1-7. The peptides generated by ACE-2 bind and activate the G-protein coupled receptor (GPCR). The receptor activation stimulates several major signaling pathways, including phospholipase A, which will further generate arachidonic acid (AA), phosphoinositide 3 kinase (PI3K)/AKT axis, which activates endothelial nitric oxide synthase (eNOS), and activation of phospholipase C, and an increase in intracellular calcium levels. These pathways regulate vasodilation, anti-fibrosis and anti-inflammatory responses in endothelial cells (Keidar et al., 2007; Heurich et al., 2014).

The internalization and shedding of ACE-2 could be mediated by the proteolytic activity of disintegrin and metalloprotease 17 (ADAM17) and transmembrane protease serine 2 (TMPRSS2) (Hoffmann et al., 2020). This serine competes with ADAM17 for ACE-2 processing and is found to promote SARS-CoV-2 entry by two mechanisms: ACE-2 cleavage, which promotes viral uptake and spike protein cleavage, which activates it for membrane fusion (Solinski et al., 2014).

SARS-CoV-2 spike protein can trigger downregulation of ACE-2 expression in lung tissue and in cell culture, allowing higher binding of Ang II to AT1 receptors and ultimately vasoconstriction, enhanced inflammation and thrombosis (**Figure 1**) (Verdecchia et al., 2020).

There is strong evidence for a complex association between viral infections, inflammatory processes, and endothelial cells. The endothelium is a monolayer of endothelial cells that internally coat the blood vessels; its importance on hemostasis goes beyond acting as a barrier against blood loss (Wu, 1992). In normal conditions of hemostasis, the endothelium maintains a balance between the procoagulant and fibrinolytic factors, producing molecules that inhibit platelet aggregation, like nitric oxide (NO), anti-clotting molecules, like thrombomodulin, and other important substances for the fibrinolytic system, such as tissue plasminogen activator (tPA) (Wu and Thiagarajan, 1996).

When endothelial cells encounter pathogen associated molecular patterns (PAMPs) such as lipopolysaccharide, proinflammatory cytokines, interleukin 1 (IL-1), tumor necrosis factor (TNF), (IL-6) or damage associated molecular patterns (DAMPs) derived from dead or dying cells, they become activated. Endothelial cells' activation can also occur as a direct cytopathic effect of viral infection (Libby and Lüscher, 2020). Although SARS-CoV-2 has been reported to directly infect vascular organoids (Monteil et al., 2020), and case studies reported endotheliitis in COVID-19 patients (Amraei and Rahimi, 2020), and endothelial infection in glomerular capillary loops and skin lesions it is still not clear whether vascular damage can be attributed to a systemic inflammatory response, or is a direct consequence of the viral infection and replication.

Endothelial activation is a key event that contributes to platelet activation, changes on hemostasis, and increase on vascular permeability, with decreased concentrations of anti-clotting molecules (Zhang et al., 2020). Once activated, the endothelium cells can express and exert tissue factor activity, amplifying the enzymatic activity of the coagulation cascade proteins and triggering thrombin generation and clot formation. These cells also release von Willebrand factor (vWF) from its Weibel-Palade bodies, stimulating platelet adhesion and aggregation (Lyons and Ginsburg, 1994). Associated with the prothrombotic effects of endothelial cells activation, there is also antifibrinolytic activity, mostly conformed by increased concentrations of plasminogen activator inhibitor–1 (PAI-1) (Wu and Thiagarajan, 1996).

SARS-CoV-2 infection of endothelium also triggers the secretion of the von Willebrand factor (vWF), PAI-1, soluble thrombomodulin, angiopoietin-2, an increase in endothelium-derived adhesion molecules (ICAM, VCAM-1 and P-selectin among others) expression, a decrease of endothelial progenitor cells circulation, as well as secretion of proinflammatory interleukins (IL-1, IL6) (Zhang et al., 2020). IL-1 can induce the production of more IL-1, IL-6 and other proinflammatory cytokines, and this overproduction is named a "cytokine storm". IL-1 stimulation also reduces VE-Cadherin, which maintains the integrity of the endothelium (Libby and Lüscher, 2020).

Neutrophils have also been shown to contribute to endothelial damage in COVID-19. Under the influence of the proinflammatory state, neutrophils in contact with endothelial cells can release enzymes such as myeloperoxidase (MPO),

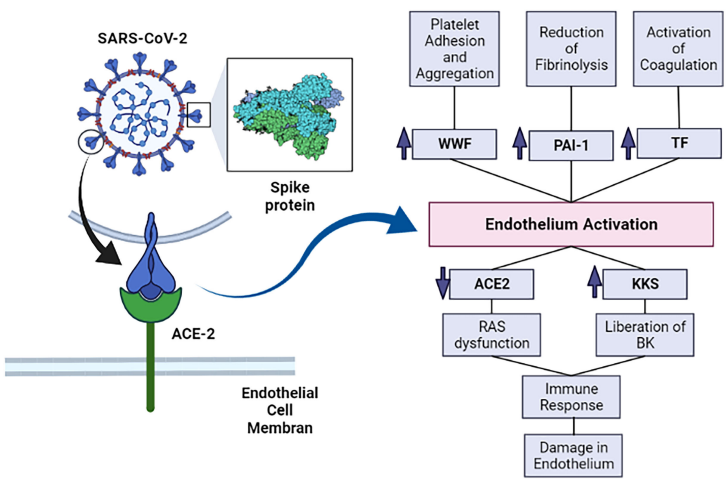

FIGURE 1 | The SARS-CoV-2's spike protein interacts with ACE-2 and allows SARS-CoV-2 infection. This infection causes activation of the endothelium and, subsequently, increases prothrombotic factors. The infection also enhances inflammation, which further damages the endothelium. ACE-2, angiotensin converting enzyme 2; KKS, Kallikrein-kinin system; RAS, renin-angiotensin system; BK, bradykinin; vWF, von Willebrand factor; PAI-1, plasminogen activator inhibitor–1; TF, Tissue factor. Image created in: biorender.com.

proteinase 3 (PR3), neutrophil elastase (NE) and cathepsin G (CG) (Qi et al., 2017). Long-term exposure of the endothelium to these enzymes can lead to disruption of the endothelial barrier and cell apoptosis, exposing the subendothelium to platelets and leukocytes (Caillon et al., 2021).

Autopsy studies have shown important endothelial damage of the lung microvasculature, including loss of "tight junctions", separation of the endothelium from its basal membrane and apoptosis of endothelial cells (O'Sullivan et al., 2020; Zhang et al., 2020). These apoptotic cells express the ACE-2 receptor, and analysis by electronic microscope found the presence of SARS-CoV-2 virions in these cells (Carsana et al., 2020).

ALTERATIONS IN THE NUMBER AND FUNCTION OF PLATELETS

Platelets are anucleate cell fragments derived from the bone marrow and lung megakaryocytes. When vascular lesion occurs, platelets quickly adhere to the exposed subendothelium. In conditions of high shear tension, which is present in arterial vessels, adhesion is mainly due to the binding of the vWF to glycoprotein Ib (GPIb) present on the platelet's surface. On the other hand, in conditions of low shear stress, which occur in the venous part of the circulatory system, platelet adhesion mainly happens through the interaction of collagen with the glycoprotein VI (GPVI) or the integrin alpha(2) beta(1) (Ruggeri et al., 2006). As a consequence of this adhesion, platelets become activated, there is a change in the organization of their cytoskeleton which changes its shape, from discoidal to irregular, with generation of filopodia. Besides, there is exocytosis of granules, which mainly contain agonists, like ADP and serotonin. These molecules interact with specific receptors on the platelet surface, and as a result activate more platelets. Platelet activation favors the binding of fibrinogen with integrin alpha (IIb)beta(3) and this binding is essential, as it allows a connection between adjacent platelets and platelet aggregation (Peter et al., 1998; Jurk and Kehrel, 2005).

Platelet's morphological and biochemical changes are relevant to COVID-19 pathophysiology. There is evidence that many pathways of platelet activation are intensified after infection with SARS-CoV-2, either by an indirect path through the action of inflammatory cytokines and endothelial damage or directly through viral infection. Moreover, it has been demonstrated that SARS-CoV-2 is capable to infect and replicate in megakaryocytes in the bone marrow and in the lung. Whether these megakaryocytes produce platelets carrying virions is still not known (Barrett et al., 2021). Overall, cytokine storm, thrombin generation, endothelium dysfunction, activation of (C3a) complement, increase in viscosity and hypoxia are considered the main reasons for platelet activation and aggregation caused by SARS-CoV-2.

Generally speaking, thrombocytopenia is frequent in severely ill patients, being associated with bad clinical prognosis and, also, death. Many COVID-19 patients, mainly those in intensive care, display thrombocytopenia, associated with the worst clinical outcomes. A meta-analysis of 31 studies with 7163 participants observed thrombocytopenia on stern cases, and this was associated with a 3-fold risk of developing severe COVID-19 (Jiang et al., 2020). Some mechanisms proposed as the main pathways leading to thrombocytopenia in COVID-19 are: impaired platelet production, immune depletion and trapping within growing thrombus and peripheral embolization (Zhang et al., 2020).

Some markers of platelet activity, such as the maturity and size of the platelets are significantly associated with severe COVID-19 cases and its lethality (Lyons and Ginsburg, 1994). Besides this, it has been shown that there is a difference in the transcriptome of platelets isolated from COVID-19 patients in comparison to non-infected platelets. The platelet phenotype is more immature, and changes occur on metabolic paths, including oxidative phosphorylation and glycolysis (Grove et al., 2009). Platelets do not act alone, as they amplify extracellular vesicle emission and tissue factor expression in monocytes through the interaction of P-selectin with P-selectin glycoprotein ligand-1 which is exposed on the surface of monocytes and neutrophils (Zhang et al., 2020). Communication with dysfunctional endothelium and neutrophils are key points for neutrophil and platelet activation (Hottz et al., 2020). In fact, it has been recently shown that alterations in circulating neutrophils rather than in the endothelium, are major contributors to the increased thrombotic diathesis in the hearts of COVID-19 patients (Johnson et al., 2022).

Other important playmakers in this process include extracellular vesicles (EV), released normally by activated leukocytes, platelets and endothelium. They carry and signal several physiological phenomena, such as inflammation, coagulation, and are related to thrombosis in some cardiovascular diseases (Ridger et al., 2017). They are important to coagulation, since they promote thrombin formation by exposing tissue factor and negatively charged phospholipids. Additionally, they promote thromboinflammation indirectly, stimulating the release of pro-inflammatory endothelial cytokines, inteleukin-8 (L-8), IL-6, and monocyte chemotactic protein 1 (MCP-1), inducing endothelial activation, expression of cyto-adhesins, and diapedesis. Some previous papers showed increased circulating EV secreted by platelets and leukocytes in patients with COVID-19 (Zaid et al., 2020; Krishnamachary et al., 2021). This is a topic that has not been fully explored and needs further studies to improve our scientific understanding.

Knowledge gathered until now has shown that some platelet activation mechanisms contribute to the thrombotic effects of COVID-19, hence platelet changes are relevant to the development and symptoms of this illness.

ALTERATIONS IN COAGULATION

The coagulation cascade is made up of a series of reactions that culminate in the formation of a fibrin clot, which contributes to prevent bleeding in a vascular lesion. The formation of fibrin depends on the action of thrombin, that cleaves fibrinogen, releasing A and B fibrinopeptides, so as to form the fibrin monomers that polymerize, forming an insoluble net of fibrin. Besides this, thrombin activates FXIII, which then connects the

fibrin fibrils through lysine residues, contributing to a greater stability of the clot (Siebenlist et al., 2001). Thrombin is generated from its inactive precursor – prothrombin - through the action of FXa.

It is possible to didactically divide the coagulation cascade into two distinct pathways that lead to the activation of FX: the extrinsic and intrinsic pathways. The extrinsic pathway starts when the lesion of the blood vessel exposes the tissue factor, which is made up of cells such as fibroblasts, and this contact with the intravascular medium, together with the FVIIa, activates FX. Through the intrinsic pathway, however, the contact of blood with the negative surfaces leads to the activation of FXII (contact activation) which starts a cascade that leads to the activation of FX (Macfarlane, 1964).

Activation of FXII to FXIIa by contact with negatively charged surfaces also starts the contact system. The contact system is part of the innate immune system and inflammatory response mechanism against pathogens. Factor XII, prekallikrein (PK) and high-molecular weight kininogen (HK) participate in the coagulation cascade as well as the contact system, having pivotal roles in the latter. This system can be activated by DNA, RNA, PAMPs, DAMPs, neutrophil extracellular traps and even activated platelets (Ito, 2014). In addition, both eukaryotic and prokaryotic RNA serve as activators of FXII and FXI, thus leading to activation of the contact system and inducing immunothrombosis (Kannemeier et al., 2007).

The kallikrein-kinin system (KSS) is also entangled in the mechanisms that maintain hemostasis. Although the contact system and the kallikrein-kinin system overlap, the activation of either has different implications. Activation of the KKS leads to the liberation of bradykinin (BK), a vasoactive peptide that plays a pivotal role in inflammation. After binding to bradykinin receptor 2 (B2R), BK activates a signaling pathway resulting in pain, fever, edema, hypotension, vasodilatation and increased vascular permeability (Oehmcke-Hecht and Köhler, 2018). It's important to mention that BK also stimulates the production of IL-1, TNF-alpha and reactive oxygen substances, which, in turn, cause endothelial disruption (Tiffany and Burch, 1989).

SARS-CoV-2 infection induces alteration in coagulation and, in severe cases, can trigger disseminated intravascular coagulation (DIC) and thrombotic events, especially in the pulmonary microvasculature, which contributes to the evolution of dysfunction in this organ (Kannemeier et al., 2007). The mechanisms that lead to this clinical manifestation are not fully understood, but it is likely that the intense release of pro-inflammatory cytokines contributes to trigger the activation of the coagulation cascade. In this sense, there is a large release of IL-1 and IL-6 and TNF-alpha during the cytokine storm induced by SARS-CoV-2 infection (Han et al., 2020). IL-6 has an especially well described role in helping to activate coagulation by promoting the synthesis of fibrinogen, FVIII and tissue factor (TF) (Stouthard et al., 1996). Additionally, SARS-CoV-2 infection reduces the amount of ACE-2, which results in increased levels of angiotensin II. Elevated levels of angiotensin II favor the activation of coagulation and inhibition of the fibrinolytic system, which favors the prothrombotic state in COVID-19 (**Figure 2**) (Lazzaroni et al., 2021; Salabei et al., 2021).

It is observed that coagulation tests such as activated partial thromboplastin time (aPTT) and prothrombin time (PT) tend to be higher in symptomatic COVID-19 patients than in healthy individuals (Zhu et al., 2021; Luo et al., 2021). Although several studies indicate that aPTT, and especially PT, are also considerably higher in patients who died than in people who had less severe cases of COVID-19, a meta-analysis indicated that the results described in the literature are very heterogeneous, requiring caution and more data to establish a clear relationship between the severity of COVID-19 and PT and aPTT values (Lin et al., 2021).

In patients with COVID-19, especially those with greater severity and who died, they presented increased levels of

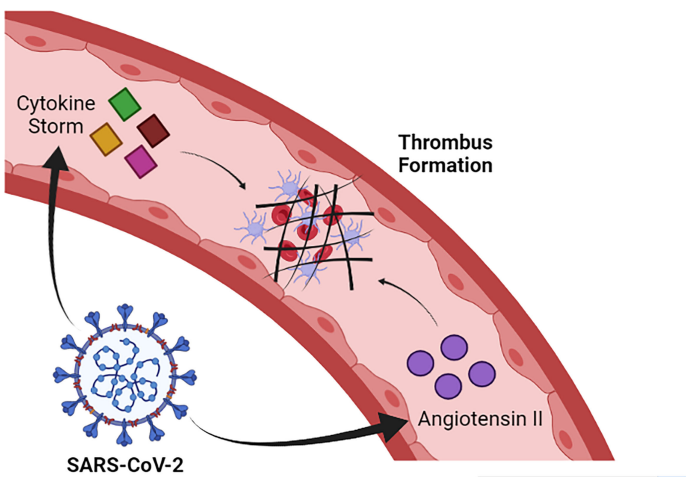

FIGURE 2 | SARS-CoV-2 induces cytokine storm formation and increased levels of angiotensin II. Such alterations contribute to the activation of the coagulation cascade and, consequently, to thrombus formation. Image created in: Biorender.com.

fibrinogen concentration. This finding is quite different from what is normally observed in cases of consumptive coagulopathy associated with sepsis, in which a fall in fibrinogen levels is associated with mortality (van Vught et al., 2021). Furthermore, sepsis-induced coagulopathy usually has a much more marked prolongation of global clotting times than in COVID-19 cases (Lin et al., 2021). Thus, changes in the coagulation cascade caused by COVID-19 seem to be quite distinct of this disease.

Another alteration typically observed in COVID-19 patients is an increase in the activity and amount of vWF. The vWF is a circulating adhesive glycoprotein that promotes platelet aggregation, contributes to blood coagulation forming a complex with factor VIII, regulates angiogenesis, and vascular permeability. vWF levels are elevated in inflammation, aging, diabetes and other diseases associated with endothelial dysfunction (Amraei and Rahimi, 2020). Besides this, in patients with severe cases, there is a downregulation in the activity of ADAMTS-13 through different mechanisms, with a small reduction of these activities, and an increase on the level of their inhibitors. The consumption of the vWF high molecular weight multimers (HMWM—vWF) is common in patients that require intensive therapy (Philippe et al., 2021). In contrast with other types of sepsis, an increase in the vWF/ADAMTS-13 ratio was observed, and a significant inverse correlation between vWF : Ag levels and ADAMTS-13 activity (Ward et al., 2021). This unbalance between substrate and enzyme in a tangential stress condition is probably even more noticeable in the lung microvasculature, the site where endothelial damage becomes more evident with greater formation of micro-thrombus. Moreover, it is known that the plasmatic distribution of the vWF multimers in these patients is similar to those found in acute thrombotic thrombocytopenic purpura patients (Ward et al., 2021).

ALTERATIONS IN THE FIBRINOLYTIC SYSTEM AND ANTICOAGULATION

The fibrinolytic system is an important defense against intravascular thrombosis, and there is substantial evidence that the imbalance of this system is involved in the pathophysiology of cardiovascular ischemic events and endothelial dysfunction. The imbalance is driven, at least in part, by inappropriate activity of the renin–angiotensin system, which interacts with the fibrinolytic system at the level of the endothelium (Chapin and Hajjar, 2015).

Although the formation of the fibrin network is essential to prevent blood leakage, a system is needed to prevent its unrestrained formation, which can obstruct the vessels. This function is mainly performed by the fibrinolytic system, whose main component is plasmin, a serine protease that degrades fibrin, generating soluble fibrin degradation products (FDP).

Plasmin is generated from its inactive precursor, plasminogen, which can be activated by tissue tPA or by urokinase plasminogen activator (uPA). Once initiated, fibrinolysis is accelerated by a positive feedback mechanism. These activators can be inhibited by PAI-1, whereas plasmin can be directly inhibited by alpha2-antiplasmin (Mutch et al., 2007). Endothelial cells and vascular smooth muscle cells are the main source of tPA and PAI-1, controlling fibrinolysis locally.

The coagulation cascade can still be inhibited in order to avoid its excessive activation. The most relevant coagulation inhibitors are tissue factor protease inhibitor (TFPI), protein S, thrombomodulin, protein C and antithrombin. The mechanisms of action of these inhibitors are varied. For example, antithrombin directly inhibits thrombin, which is facilitated by the presence of heparin or heparan sulfate, whereas TFPI, produced by endothelial cells, inhibits both the tissue factor/FVIIa complex and FXa. Also, the C1 esterase inhibitor (C1-INH), natural regulator of the complement, kallikrein-kinin, contact and fibrinolytic system, is being investigated for treatment of COVID-19, targeting multiple systems involved in the disease (Adesanya et al., 2021).

In critically ill COVID-19 patients, studies have demonstrated reduction of natural anticoagulant systems, with decreased serum concentration of antithrombin and protein C, which can contribute to the hypercoagulability state that characterizes SARS-CoV-2 pathophysiology. It is known that plasma natural coagulation is decreased in patients with sepsis or DIC, and is also associated with disease severity (Zhang et al., 2020). A hypofibrinolytic state, additionally, has been observed, reflecting changes in the fibrinolytic system, with increased TFPI concentration (Caciola et al., 2021). As a consequence, the thrombi formation becomes easier, mainly inside the pulmonary microvasculature. More studies are needed to evaluate other parameters of natural coagulation, in order to determine the importance of these changes on the whole picture of COVID-19 disease.

In COVID-19 it is also observed, especially in more severe cases, an increase in the concentration of D-dimers, molecules produced due to fibrin degradation. Markedly increased D-dimers were detected early on in patients with COVID-19 (Huang et al., 2020). Elevation in D-dimer levels was associated with poor disease prognosis, and its dosage was extensively performed globally as a laboratory test in patients' admission (Rostami and Hassan, 2020; Yu et al., 2020). Different papers try to suggest D-dimer cut-off levels as a prognostic indicator (Favaloro and Thachil, 2020; Zhou et al., 2020). Despite this, there is still controversy regarding the mechanism that causes the increase in the levels of D-dimers, and it is possible that this effect is a result only of the increase in the amount of fibrin formed in SARS-CoV-2 infection (Lazzaroni et al., 2021).

VASCULAR CHANGES IN THE LUNG

The pulmonary vasculature is responsible for the perfusion of these organs and is essential for proper hemostasis (Lammers et al., 2021). Histopathological studies demonstrating the structural and vascular changes in the lungs caused by COVID-19 are still limited. However, it has been reported that patients who died from COVID-19 often present hemorrhage, deposition of fibrin and, most importantly, formation of microthrombi in the pulmonary vasculature. In this sense, the

formation of microthrombi in pulmonary capillaries occurs with greater intensity in COVID-19 than in influenza and is a factor that reduces respiratory efficiency by contributing to increase the dead space in ventilation (Pannone et al., 2021).

Post-mortem analysis also suggests that severe SARS-CoV-2 infection increases angiogenesis in the lung more intensely than seen with other respiratory infections such as influenza. This effect can be explained, at least in part, by the infiltration of pro-inflammatory cells, mainly macrophages, which are also capable of releasing pro-angiogenic compounds. The excessive proliferation of blood vessels in severe cases of COVID-19 abnormally increases perfusion, and is thus a factor that reduces the ratio of ventilation to perfusion in the lungs, contributing to hypoxaemia (Osuchowski et al., 2021). The formation of pulmonary edema is also associated with severe COVID-19, which occurs as a result of increased permeability of alveolar blood vessels in response to the interaction between kinins and their receptors on endothelial cells (Pérez-Mies et al., 2021).

COVID-19, especially in severe cases, was still associated with bleeding higher risk of hemorrhage, deep vein thrombosis and, especially, pulmonary embolism than individuals without this disease. These effects of COVID-19 remained significant even when adjusting for correlations for comorbidities and other risk factors, such as the advanced age of patients. Furthermore, it was observed that these effects did not appear to be minimized in individuals undergoing chronic anticoagulant therapy (Katsoularis et al., 2022).

CONCLUSIONS

The clinical manifestations of COVID-19, especially in severe cases, are intrinsically related to hemostatic disorders caused directly or indirectly by SARS-CoV-2 infection. In general, COVID-19 promotes the occurrence of a prothrombotic state in the patient, which contributes to the obstruction of blood vessels. Thrombus formation in COVID-19 is mainly favored by the establishment of an inflammatory state that leads to endothelial activation, which, in turn, contributes to the excessive platelet aggregate formation, activation of the coagulation cascade and inhibition of the fibrinolytic system. In addition, the acquisition of ACE-2 influences the renin-angiotensin and kallikrein-kinin systems toward a prothrombotic state. The hemostatic changes resulting from COVID-19 are mainly manifested in the pulmonary microvasculature, being an important factor for the impairment of respiratory function observed in patients, especially those with more severe conditions.

FUTURE DIRECTIONS

The detailed investigation of the mechanisms related to these alterations can contribute not only to a better understanding of COVID-19 pathophysiological mechanisms but can also indicate new directions for possible treatments in the infection by SARS-CoV-2 and better monitoring of hospitalized patients. Therefore, this review aims to further improve the understanding of the pathophysiology of COVID-19 by providing a detailed description of the molecular mechanisms involved in human hemostasis alterations after SARS-CoV-2 infection. We believe that better understanding of the CS, KKS, RAS and/or the Coagulation/Fibrinolysis systems, as well as how the interactions occur between them, and their consequences in the hemostasis, can contribute to a better understanding of the thrombotic state, observed in COVID-19. The knowledge of these mechanisms is crucial for the better disease understanding and could lead to therapies that modulate the human hemostasis, attenuating or inhibiting vessel obstruction, especially of the pulmonary microvasculature, due to the formation of thrombi.

AUTHOR CONTRIBUTIONS

SA, DS, AT, ME, RC, CL, MS, and AC-T conceived the manuscript, reviewed the literature, and wrote the manuscript. All authors contributed to the article and approved the submitted version.

FUNDING

Financial support: CNPq, CAPES, FAPESP and Fundação Butantan.

ACKNOWLEDGMENTS

We are grateful to the Instituto Butantan, CAPES, FAPESP and CNPq for supporting us in writing this article.

REFERENCES

Adesanya, T. M. A., Campbell, C. M., Cheng, L., Ogbogu, P. U., and Kahwash, R. (2021). C1 Esterase Inhibition: Targeting Multiple Systems in COVID-19. *J. Clin. Immunol.*, 41(14), 729–732. doi: 10.1007/s10875-021-00972-1

Amraei, R., and Rahimi, N. (2020). COVID-19, Renin-Angiotensin System and Endothelial Dysfunction. *Cells* 9 (7), 1652. doi: 10.3390/cells9071652

Asakura, H., and Ogawa, H. (2021). COVID-19-Associated Coagulopathy and Disseminated Intravascular Coagulation. *Int. J. Hematol.* 113 (1), 45–57. doi: 10.1007/s12185-020-03029-y

Barrett, T. J., Bilaloglu, S., Cornwell, M., Burgess, H. M., Virginio, V. W., Drenkova, K., et al. (2021). Platelets Contribute to Disease Severity in COVID-19. *J. Thromb. Haemostasis* 19 (12), 3139–3153. doi: 10.1111/jth.15534

Caciola, R., Gentilini Cacciola, E., Vecchio, V., and Cacciola, E.. (2021). Cellular and Molecular Mechanisms in COVID-19 Coagulopathy: Role of Inflammation and Endotheliopathy. *J. Thromb. Thrombolysis.* 53(2), 282–290. doi: 10.1007/s11239-021-02583-4c

Caillon, A., Trimaille, A., Favre, J., Jesel, L., Morel, O., and Kauffenstein, G. (2021). Role of Neutrophils, Platelets, and Extracellular Vesicles and Their Interactions in COVID-19-Associated Thrombopathy. *J. ThrombHaemost.* 00, 1–15. doi: 10.1111/jth.15566

Carsana, L., Sonzogni, A., Nasr, A., Rossi, R. S., Pellegrinelli, A., Zerbi, P., et al. (2020). Pulmonary Post-Mortem Findings in a Series of COVID-19 Cases From Northern Italy: A Two-Centre Descriptive Study. *Lancet Infect. Dis.* 20 (10), 1135–1140. doi: 10.1016/S1473-3099(20)30434-5

Chapin, J. C., and Hajjar, K. A. (2015). Fibrinolysis and the Control of Blood Coagulation. *Blood Rev.* 29 (1), 17–24. doi: 10.1016/j.blre.2014.09.003

Dong, E., Du, H., and Gardner, L. (2020). An Interactive Web-Based Dashboard to Track COVID-19 in Real Time. *Lancet Infect. Dis.* 20 (5), 533–534. doi: 10.1016/S1473-3099(20)30120-1

Favaloro, E. J., and Thachil, J. (2020). Reporting of D-Dimer Data in COVID-19: Some Confusion and Potential for Misinformation. *Clin. Chem. Lab. Med.* 58 (8), 1191–1199. doi: 10.1515/cclm-2020-0573

Grove, E. L., Hvas, A.-M., and Kristensen, S. D. (2009). Immature Platelets in Patients With Acute Coronary Syndromes. *Thromb. Haemostasis* 101 (01), 151–153. doi: 10.1160/TH08-03-0186

Hamming, I., Timens, W., Bulthuis, M. L. C., Lely, A. T., Navis, G. J., and van Goor, H. (2004). Tissue Distribution of ACE2 Protein, the Functional Receptor for SARS Coronavirus. A First Step in Understanding SARS Pathogenesis. *J. Pathol.* 203 (2), 631–637. doi: 10.1002/path.1570

Han, H., Ma, Q., Li, C., Liu, R., Zhao, L., Wang, W., et al. (2020). Profiling Serum Cytokines in COVID-19 Patients Reveals IL-6 and IL-10 are Disease Severity Predictors. *Emerging Microbes Infections* 9 (1), 1123–1130. doi: 10.1080/22221751.2020.1770129

Heurich, A., Hofmann-Winkler, H., Gierer, S., Liepold, T., Jahn, O., and Pöhlmann, S. (2014). TMPRSS2 and ADAM17 Cleave ACE2 Differentially and Only Proteolysis by TMPRSS2 Augments Entry Driven by the Severe Acute Respiratory Syndrome Coronavirus Spike Protein. *J. Virol.* 88 (2), 1293–1307. doi: 10.1128/JVI.02202-13

Hoffmann, M., Kleine-Weber, H., Schroeder, S., Krüger, N., Herrler, T., Erichsen, S., et al. (2020). SARS-CoV-2 Cell Entry Depends on ACE2 and TMPRSS2 and Is Blocked by a Clinically Proven Protease Inhibitor. *Cell* 181 (2), 271–280.e8. doi: 10.1016/j.cell.2020.02.052

Hottz, E. D., Azevedo-Quintanilha, I. G., Palhinha, L., Teixeira, L., Barreto, E. A., Pão, C. R. R., et al. (2020). Platelet Activation and Platelet-Monocyte Aggregate Formation Trigger Tissue Factor Expression in Patients With Severe COVID-19. *Blood* 136 (11), 1330–1341. doi: 10.1182/blood.2020007252

Huang, C., Wang, Y., Li, X., Ren, L., Zhao, J., Hu, Y., et al. (2020). Clinical Features of Patients Infected With 2019 Novel Coronavirus in Wuhan, China. *Lancet.* 395 (10223), 497–506. doi: 10.1016/S0140-6736(20)30183-5

Ito, T. (2014). PAMPs and DAMPs as Triggers for DIC. *J. Intensive Care* 2 (1), 67. doi: 10.1186/s40560-014-0065-0

Jackson, C. B., Farzan, M., Chen, B., and Choe, H. (2021). Mechanisms of SARS-CoV-2 Entry Into Cells. *Nat. Rev. Mol. Cell Biol.*. 23(1), 3–20. doi: 10.1038/s41580-021-00418-x

Jiang, S. Q., Huang, Q. F., Xie, W. M., Lv, C., and Quan, X. Q. (2020). The Association Between Severe COVID-19 and Low Platelet Count: Evidence From 31 Observational Studies Involving 7613 Participants. *Br. J. haematol* 190 (1), e29–e33. doi: 10.1111/bjh.16817

Johansson, M. A., Quandelacy, T. M., Kada, S., Prasad, P. V., Steele, M., Brooks, J. T., et al. (2021). SARS-CoV-2 Transmission From People Without COVID-19 Symptoms. *JAMA Network Open* 4 (1), e2035057. doi: 10.1001/jamanetworkopen.2020.35057

Johnson, J. E., McGuone, D., Xu, M. L., Jane-Wit, D., Mitchell, R. N., Libby, P., et al. (2022). Coronavirus Disease 2019 (COVID-19) Coronary Vascular Thrombosis. *Am. J. Pathol.* 192 (1), 112–120. doi: 10.1016/j.ajpath.2021.09.004

Jurk, K., and Kehrel, B. E. (2005). Platelets: Physiology and Biochemistry. *Semin. Thromb. Hemostasis* 31 (04), 381–392. doi: 10.1055/s-2005-916671

Kannemeier, C., Shibamiya, A., Nakazawa, F., Trusheim, H., Ruppert, C., Markart, P., et al. (2007). Extracellular RNA Constitutes a Natural Procoagulant Cofactor in Blood Coagulation. *Proc. Natl. Acad. Sci. United States America* 104 (15), 6388–6393. doi: 10.1073/pnas.0608647104

Katsoularis, I., Fonseca-Rodríguez, O., Farrington, P., Jerndal, H., Lundevaller, E. H., Sund, M., et al. (2022). Risks of Deep Vein Thrombosis, Pulmonary Embolism, and Bleeding After Covid-19: Nationwide Self-Controlled Cases Series and Matched Cohort Study. *BMJ (Clinical Res. ed.)* 377, e069590. doi: 10.1136/bmj-2021-069590

Keidar, S., Kaplan, M., and Gamliellazarovich, A. (2007). ACE2 of the Heart: From Angiotensin I to Angiotensin (1–7). *Cardiovasc. Res.* 73 (3), 463–469. doi: 10.1016/j.cardiores.2006.09.006

Krishnamachary, B., Cook, C., Kumar, A., Spikes, L., Chalise, P., and Dhillon, N. K. (2021). Extracellular Vesicle-Mediated Endothelial Apoptosis and EV-Associated Proteins Correlate With COVID-19 Disease Severity. *J. Extracellular Vesicles* 10 (9), e12117. doi: 10.1002/jev2.12117

Lammers, S., Scott, D., Hunter, K., Tan, W., Shandas, R., and Stenmark, K. R. (2021). Mechanics and Function of the Pulmonary Vasculature: Implications for Pulmonary Vascular Disease and Right Ventricular Function. *Compr. Physiol.* 2 (1), 295–319. doi: 10.1002/cphy.c100070

Lazzaroni, M. G., Piantoni, S., Masneri, S., Garrafa, E., Martini, G., Tincani, A., et al. (2021). Coagulation Dysfunction in COVID-19: The Interplay Between Inflammation, Viral Infection and the Coagulation System. *Blood Rev.* 46, 100745. doi: 10.1016/j.blre.2020.100745

Leentjens, J., Haaps, T. F., Van, Wessels, P. F., Schutgens, R. E. G., and Middeldorp, S. (2021). COVID-19-Associated Coagulopathy and Antithrombotic Agents—Lessons After 1 Year. *Lancet Haematol* 8 (7), e524–e533. doi: 10.1016/S2352-3026(21)00105-8

Libby, P., and Lüscher, T. (2020). COVID-19 is, in the End, an Endothelial Disease. *Eur. Heart J.* 41 (32), 3038–3044. doi: 10.1093/eurheartj/ehaa623

Lin, J., Yan, H., Chen, H., He, C., Lin, C., He, H., et al. (2021). COVID-19 and Coagulation Dysfunction in Adults: A Systematic Review and Meta-Analysis. *J. Med. Virol.* 93 (2), 934–944. doi: 10.1002/jmv.26346

Luo, H. C., You, C. Y., Lu, S. W., and Fu, Y. Q. (2021). Characteristics of Coagulation Alteration in Patients With COVID-19. *Ann. Hematol.* 100 (1), 45–52. doi: 10.1007/s00277-020-04305-x

Lyons, S. E., and Ginsburg, D. (1994). Molecular and Cellular Biology of Von Willebrand Factor. *Trends Cardiovasc. Med.* 4 (1), 34–39. doi: 10.1016/1050-1738(94)90023-X

Macfarlane, R. G. (1964). An Enzyme Cascade in the Blood Clottig Mechanism, and its Function as a Biochemical Amplifier. *Nature* 202, 498–499. doi: 10.1038/202498a0

Maffei, F. H. A., Yoshida, W. B., Rollo, H. A., Moura, R.., Sobreira, M. L., Giannini, M., et al. (2015). *Peripheral Vascular Diseases. 5ª. Ed* (Rio de Janeiro: Guanabara).

Monteil, V., Kwon, H., Prado, P., Hagelkrüys, A., Wimmer, R. A., Stahl, M., et al. (2020). Inhibition of SARS-CoV-2 Infections in Engineered Human Tissues Using Clinical-Grade Soluble Human Ace2. *Cell* 181 (4), 905–913.e7. doi: 10.1016/j.cell.2020.04.004

Mutch, N. J., Thomas, L., Moore, N. R., Lisiak, K. M., and Booth, N. A. (2007). TAFIa, PAI-1 and ? 2 -Antiplasmin: Complementary Roles in Regulating Lysis of Thrombi and Plasma Clots. *J. Thromb. Haemostasis* 5 (4), 812–817. doi: 10.1111/j.1538-7836.2007.02430.x

O'Sullivan, J. M., Gonagle, D. M., Ward, S. E., Preston, R., and O'Donnell, J. S. (2020). Endothelial Cells Orchestrate COVID-19 Coagulopathy. *Lancet Haematol* 7 (8), e553–e555. doi: 10.1016/S2352-3026(20)30215-5

Oehmcke-Hecht, S., and Köhler, J. (2018). Interaction of the Human Contact System With Pathogens—An Update. *Front. Immunol.* 9. doi: 10.3389/fimmu.2018.00312

Osuchowski, M. F., Winkler, M. S., Skirecki, T., Cajander, S., Shankar-Hari, M., Lachmann, G., et al. (2021). The COVID-19 Puzzle: Deciphering Pathophysiology and Phenotypes of a New Disease Entity. *TheLancet. Respir. Med.* 9 (6), 622–642. doi: 10.1016/S2213-2600(21)00218-6

Pannone, G., Caponio, V., De Stefano, I. S., Ramunno, M. A., Meccariello, M., Agostinone, A., et al. (2021). Lung Histopathological Findings in COVID-19 Disease - A Systematic Review. *Infect. Agents Cancer* 16 (1), 34. doi: 10.1186/s13027-021-00369-0

Pérez-Mies, B., Gómez-Rojo, M., Carretero-Barrio, I., Bardi, T., Benito, A., García-Cosío, M., et al. (2021). Pulmonary Vascular Proliferation in Patientswithsevere COVID-19: Anautopsystudy. *Thorax* 76 (10), 1044–1046. doi: 10.1136/thoraxjnl-2020-216714

Peter, K., Schwarz, M., Ylänne, J., Kohler, B., Moser, M., Nordt, T., et al. (1998). Induction of Fibrinogen Binding and Platelet Aggregation as a Potential Intrinsic Property of Various Glycoprotein IIb/IIIa (αIibβ3) Inhibitors. *Blood* 92 (9), 3240–3249. doi: 10.1182/blood.V92.9.3240

Philippe, A., Chocron, R., Gendron, N., Bory, O., Beauvais, A., Peron, N., et al. (2021). Circulating Von Willebrand Factor and High Molecular Weight Multimers as Markers of Endothelial Injury Predict COVID-19 in-Hospital Mortality. *Angiogenesis*, 1–13. doi: 10.1007/s10456-020-09762-6

Qi, H., Yang, S., and Zhang, L. (2017). Neutrophil Extracellular Traps and Endothelial Dysfunction in Atherosclerosis and Thrombosis. *Front. Immunol.* 8. doi: 10.3389/fimmu.2017.00928

Ridger, V. C., Boulanger, C. M., Angelillo-Scherrer, A., Badimon, L., Blanc-Brude, O., Bochaton-Piallat, M.-L., et al. (2017). Microvesicles in Vascular

Homeostasis and Diseases. Position Paper of the European Society of Cardiology (ESC) Working Group on Atherosclerosis and Vascular Biology. *Thromb. Haemostasis* 117 (7), 1296–1316. doi: 10.1160/TH16-12-0943

Rostami, M., and Hassan, M. (2020). D-Dimer Level in COVID-19 Infection: A Systematic Review. *Expert Rev. Hematol.* 13 (11), 1265–1275. doi: 10.1080/17474086.2020.1831383

Ruggeri, Z. M., Orje, J. N., Habermann, R., Federici, A. B., and Reininger, A. J. (2006). Activation-Independent Platelet Adhesion and Aggregation Under Elevated Shear Stress. *Blood* 108 (6), 1903–1910. doi: 10.1182/blood-2006-04-011551

Salabei, J. K., Fishman, T. J., Asnake, Z. T., Ali, A., and Iyer, U. G. (2021). COVID-19 Coagulopathy: Current Knowledge and Guidelines on Anticoagulation. *Heart &lung J. Crit. Care* 50 (2), 357–360. doi: 10.1016/j.hrtlng.2021.01.011

Siebenlist, K., Meh, D., and Mosesson, M. (2001). Protransglutaminase (Factor XIII) Mediated Crosslinking of Fibrinogen and Fibrin*. *Thromb. Haemostasis* 86 (11), 1221–1228. doi: 10.1055/s-0037-1616055

Solinski, H. J., Gudermann, T., and Breit, A. (2014). Pharmacology and Signaling of MAS-Related G Protein–Coupled Receptors. *Pharmacol. Rev.* 66 (3), 570–597. doi: 10.1124/pr.113.008425

Stouthard, J. M. L., Levi, M., Hack, C. E., Veenhof, C. H. N., Romijn, H. A., Sauerwein, H. P., et al. (1996). Interleukin-6 Stimulates Coagulation, Not Fibrinolysis, in Humans. *Thromb. Haemostasis* 76 (05), 738–742. doi: 10.1055/s-0038-1650653

Tang, N. (2020). Response to "Lupus Anticoagulant is Frequent in Patients With Covid-19" (JTH-2020-00483). *J. Thromb. Haemostasis: JTH* 18 (8), 2065–2066. doi: 10.1111/jth.14890

Tiffany, C. W., and Burch, R. M. (1989). Bradykinin Stimulates Tumor Necrosis Factor and Interleukin-1 Release From Macrophages. *FEBS Lett.* 247 (2), 189–192. doi: 10.1016/0014-5793(89)81331-6

Turk, C., Turk, S., Malkan, U. Y., and Haznedaroglu, I. C. (2020). Three Critical Clinicobiological Phases of the Human SARS-Associated Coronavirus Infections. *Eur. Rev. Med. Pharmacol. Sci.* 24 (16), 8606–8620. doi: 10.26355/eurrev_202008_22660

van Vught, L. A., Uhel, F., Ding, C., Van't Veer, C., Scicluna, B. P., Peters-Sengers, H., et al. (2021). Consumptive Coagulopathy Is Associated With a Disturbed Host Response in Patients With Sepsis. *J. Thromb. Haemostasis: JTH* 19 (4), 1049–1063. doi: 10.1111/jth.15246

Varga, Z., Flammer, A. J., Steiger, P., Haberecker, M., Andermatt, R., Zinkernagel, A. S., et al. (2020). Endothelial Cell Infection and Endotheliitis in COVID-19. *Lancet* 395 (10234), 1417–1418. doi: 10.1016/S0140-6736(20)30937-5

Verdecchia, P., Cavallini, C., Spanevello, A., and Angeli, F. (2020). The Pivotal Link Between ACE2 Deficiency and SARS-CoV-2 Infection. *Eur. J. Internal Med.* 76, 14–20. doi: 10.1016/j.ejim.2020.04.037

Vickers, C., Hales, P., Kaushik, V., Dick, L., Gavin, J., Tang, J., et al. (2002). Hydrolysis of Biological Peptides by Human Angiotensin-Converting Enzyme-Related Carboxypeptidase. *J. Biol. Chem.* 277 (17), 14838–14843. doi: 10.1074/jbc.M200581200

Ward, S. E., Fogarty, H., Karampini, E., Lavin, M., Schneppenheim, S., Dittmer, R., et al The Irish COVID-19 Vasculopathy Study (iCVS) investigators (2021). ADAMTS13 Regulation of VWF Multimer Distribution in Severe COVID-19. *J. ThrombHaemost.* 19, 1914–1921. doi: 10.1111/jth.15409

WHO Coronavirus (COVID-19) Dashboard (2021) *World Health Organization* (Accessed December 2021).

Wichmann, D., Sperhake, J.-P., Lütgehetmann, M., Steurer, S., Edler, C., Heinemann, A., et al. (2020). Autopsy Findings and Venous Thromboembolism in Patients With COVID-19. *Ann. Internal Med.* 173 (4), 268–277. doi: 10.7326/M20-2003

Wiersinga, W. J., Rhodes, A., Cheng, A. C., Peacock, S. J., and Prescott, H. C. (2020). Pathophysiology, Transmission, Diagnosis, and Treatment of Coronavirus Disease 2019 (COVID-19): A Review. *JAMA* 324 (8), 782–793. doi: 10.1001/jama.2020.12839

Wu, K. K. (1992). Endothelial Cells in Hemostasis, Thrombosis, and Inflammation. *Hosp. Pract. (Office ed.)* 27 (4), 145–166.

Wu, M. A., Lopez, G., Nebuloni, M., Ottolina, D., Montomoli, J., Carsana, L., et al. (2021). Lung Histopathologic Clusters in Severe COVID-19: A Link Between Clinical Picture and Tissue Damage. *Crit. Care* 25, 423. doi: 10.1186/s13054-021-03846-5

Wu, K. K., and Thiagarajan, P. (1996). Role of Endothelium in Thrombosis and Hemostasis. *Annu. Rev. Med.* 47, 315–331. doi: 10.1146/annurev.med.47.1.315

Yang, J., Zheng, Y., Gou, X., Pu, K., Chen, Z., Guo, Q., et al. (2020). Prevalence of Comorbidities and Its Effects in Patients Infected With SARS-CoV-2: A Systematic Review and Meta-Analysis. *Int. J. Infect. Dis.* 94, 91–95. doi: 10.1016/j.ijid.2020.03.017

Yau, J. W., Teoh, H., and Verma, S. (2015). Endothelial Cell Control of Thrombosis. *BMC Cardiovasc. Disord.* 15 (1), 130. doi: 10.1186/s12872-015-0124-z

Yu, H. H., Qin, C., Chen, M., Wang, W., and Tian, D. S. (2020). D-Dimer Level is Associated With the Severity of COVID-19. *Thromb. Res.* 195, 219–225. doi: 10.1016/j.thromres.2020.07.047

Zaid, Y., Puhm, F., Allaeys, I., Naya, A., Oudghiri, M., Khalki, L., et al. (2020). Platelets Can Associate With SARS-CoV-2 RNA and Are Hyperactivated in COVID-19. *Circ. Res.* 127 (11), 1404–1418. doi: 10.1161/CIRCRESAHA.120.317703

Zhang, Y., Cao, W., Jiang, W., Xiao, M., Li, Y., Tang, N., et al. (2020). Profile of Natural Anticoagulant, Coagulant Factor and Anti-Phospholipid Antibody in Critically Ill COVID-19 Patients. *J. Thromb. thrombolysis* 50 (3), 580–586. doi: 10.1007/s11239-020-02182-9

Zhang, J., Tecson, K. M., and McCullough, P. A. (2020). Endothelial Dysfunction Contributes to COVID-19-Associated Vascular Inflammation and Coagulopathy. *Rev. Cardiovasc. Med.* 21 (3), 315–319. doi: 10.31083/j.rcm.2020.03.126

Zhang, Y., Zeng, X., Jiao, Y., Li, Z., Liu, Q., Ye, J., et al. (2020). Mechanisms Involved in the Development of Thrombocytopenia in Patients With COVID-19. *Thromb. Res.* 193, 110–115. doi: 10.1016/j.thromres.2020.06.008

Zhang, H., Zhou, P., Wei, Y., Yue, H., Wang, Y., Hu, M., et al. (2020). Histopathologic Changes and SARS-CoV-2 Immunostaining in the Lung of a Patient With COVID-19. *Ann. Internal Med.* 172 (9), 629–632. doi: 10.7326/M20-0533

Zhou, F., Yu, T., Du, R., Fan, G., Liu, Y., Liu, Z., et al. (2020). Clinical Course and Risk Factors for Mortality of Adult Inpatients With COVID-19 in Wuhan, China: A Retrospective Cohort Study. *Lancet (London England)* 395 (10229), 1054–1062. doi: 10.1016/S0140-6736(20)30566-3

Zhu, J., Pang, J., Ji, P., Zhong, Z., Li, H., Li, B., et al. (2021). Coagulation Dysfunction is Associated With Severity of COVID-19: A Meta-Analysis. *J. Med. Virol.* 93 (2), 962–972. doi: 10.1002/jmv.26336

Conflict of Interest: The authors declare that the research was conducted in the absence of any commercial or financial relationships that could be construed as a potential conflict of interest.

Publisher's Note: All claims expressed in this article are solely those of the authors and do not necessarily represent those of their affiliated organizations, or those of the publisher, the editors and the reviewers. Any product that may be evaluated in this article, or claim that may be made by its manufacturer, is not guaranteed or endorsed by the publisher.

Citation: *Andrade SA, de Souza DA, Torres AL, de Lima CFG, Ebram MC, Celano RMG, Schattner M and Chudzinski-Tavassi AM (2022) Pathophysiology of COVID-19: Critical Role of Hemostasis.*
Front. Cell. Infect. Microbiol. 12:896972. doi: 10.3389/fcimb.2022.896972

frontiers | Frontiers in Cellular and Infection Microbiology

ORIGINAL RESEARCH
published: 30 June 2022
doi: 10.3389/fcimb.2022.922422

Cytokine Profiles Associated With Acute COVID-19 and Long COVID-19 Syndrome

Maria Alice Freitas Queiroz[1†], Pablo Fabiano Moura das Neves[2†], Sandra Souza Lima[1], Jeferson da Costa Lopes[1,3], Maria Karoliny da Silva Torres[1,3], Izaura Maria Vieira Cayres Vallinoto[1,3], Carlos David Araújo Bichara[1,3], Erika Ferreira dos Santos[3,4], Mioni Thieli Figueiredo Magalhães de Brito[4], Andréa Luciana Soares da Silva[4], Mauro de Meira Leite[3,4], Flávia Póvoa da Costa[3,4], Maria de Nazaré do Socorro de Almeida Viana[3,4], Fabíola Brasil Barbosa Rodrigues[3,4], Kevin Matheus Lima de Sarges[3,4], Marcos Henrique Damasceno Cantanhede[3,4], Rosilene da Silva[3,4], Clea Nazaré Carneiro Bichara[2], Ana Virgínia Soares van den Berg[2], Adriana de Oliveira Lameira Veríssimo[5], Mayara da Silva Carvalho[5], Daniele Freitas Henriques[6], Carla Pinheiro dos Santos[6], Juliana Abreu Lima Nunes[7], Iran Barros Costa[7], Giselle Maria Rachid Viana[8], Francisca Regina Oliveira Carneiro[2], Vera Regina da Cunha Menezes Palacios[2], Juarez Antonio Simões Quaresma[2‡], Igor Brasil-Costa[7‡], Eduardo José Melo dos Santos[3‡], Luiz Fábio Magno Falcão[2‡] and Antonio Carlos Rosário Vallinoto[1‡]*

[1] Laboratório de Virologia, Instituto de Ciências Biológicas, Universidade Federal do Pará, Belém, Brazil, [2] Instituto de Ciências Biológicas e da Saúde, Universidade do Estado do Pará, Belém, Brazil, [3] Programa de Pós-Graduação em Biologia de Agentes Infecciosos e Parasitários, Universidade Federal do Pará, Belém, Brazil, [4] Laboratório de Genética de Doenças Complexas, Instituto de Ciências Biológicas, Universidade Federal do Pará, Belém, Brazil, [5] Hospital Adventista de Belém, Belém, Brazil, [6] Seção de Arbovirologia e Febres Hemorrágicas, Instituto Evandro Chagas, Secretária de Vigilância em Saúde, Ministério da Saúde do Brasil, Ananindeua, Brazil, [7] Laboratório de Imunologia, Seção de Virologia, Instituto Evandro Chagas, Secretária de Vigilância em Saúde, Ministério da Saúde do Brasil, Ananindeua, Brazil, [8] Laboratório de Pesquisas Básicas em Malária em Malária, Seção de Parasitologia, Instituto Evandro Chagas, Secretária de Vigilância em Saúde, Ministério da Saúde do Brasil, Ananindeua, Brazil

The duration and severity of COVID-19 are related to age, comorbidities, and cytokine synthesis. This study evaluated the impact of these factors on patients with clinical presentations of COVID-19 in a Brazilian cohort. A total of 317 patients diagnosed with COVID-19 were included; cases were distributed according to clinical status as severe (n=91), moderate (n=56) and mild (n=170). Of these patients, 92 had acute COVID-19 at sample collection, 90 had already recovered from COVID-19 without sequelae, and 135 had sequelae (long COVID syndrome). In the acute COVID-19 group, patients with the severe form had higher IL-6 levels (p=0.0260). In the post-COVID-19 group, there was no significant difference in cytokine levels between groups with different clinical conditions. In the acute COVID-19 group, younger patients had higher levels of TNF-α, and patients without comorbidities had higher levels of TNF-α, IL-4 and IL-2 (p<0.05). In contrast, patients over age 60 with comorbidities had higher levels of IL-6. In the post-COVID-19 group, subjects with long COVID-19 had higher levels of IL-17 and IL-2 (p<0.05), and subjects without sequelae had higher levels of IL-10, IL-6 and IL- 4 (p<0.05). Our results suggest that advanced age, comorbidities and elevated serum IL-6 levels are associated

OPEN ACCESS

Edited by:
Viviane Fongaro Botosso, Butantan Institute, Brazil

Reviewed by:
Jinyong Choi, The Catholic University of Korea, South Korea
Esra'a Keewan, Harvard Medical School, United States
Edecio Cunha-Neto, University of São Paulo, Brazil

***Correspondence:**
Antonio Carlos Rosário Vallinoto vallinoto@ufpa.br

[†]These authors have contributed equally to this work

[‡]These authors share senior authorship

Specialty section:
This article was submitted to Virus and Host, a section of the journal Frontiers in Cellular and Infection Microbiology

Received: *17 April 2022*
Accepted: *10 June 2022*
Published: *30 June 2022*

Citation:
Queiroz MAF, Neves PFMd, Lima SS, Lopes JdC, Torres MKdS, Vallinoto IMVC, Bichara CDA, Santos EFd, de Brito MTFM, da Silva ALS, Leite MdM, da Costa FP, Viana MdNdSdA, Rodrigues FBB, de Sarges KML, Cantanhede MHD, da Silva R, Bichara CNC, Berg AVSvd, Veríssimo AdOL, Carvalho MdS, Henriques DF, Santos CPd, Nunes JAL, Costa IB, Viana GMR, Carneiro FRO, Palacios VRdCM, Quaresma JAS, Brasil-Costa I, Santos EJMd, Falcão LFM and Vallinoto ACR (2022) Cytokine Profiles Associated With Acute COVID-19 and Long COVID-19 Syndrome. Front. Cell. Infect. Microbiol. 12:922422. doi: 10.3389/fcimb.2022.922422

with severe COVID-19 and are good markers to differentiate severe from mild cases. Furthermore, high serum levels of IL-17 and IL-2 and low levels of IL-4 and IL-10 appear to constitute a cytokine profile of long COVID-19, and these markers are potential targets for COVID-19 treatment and prevention strategies.

Keywords: SARS-CoV-2, COVID-19, long COVID-19, risk factor, cytokines

INTRODUCTION

Coronavirus disease 2019 (COVID-19) has had a great impact on people's lives worldwide. The disease and its consequences have been the cause of death for more than 5 million individuals in the past two years (WHO, 2022). Infection caused by severe acute respiratory syndrome coronavirus 2 (SARS-CoV-2) is responsible for COVID-19, which is characterized by symptoms ranging from fever to the development of severe acute respiratory syndrome (SARS) (Wang et al., 2020). The presence of different signs and symptoms determines the different clinical conditions of the disease, which can be asymptomatic, mild, moderate, severe or critical (WHO, 2021).

In most patients, SARS-CoV-2 infection is asymptomatic, especially in children (approximately 80%), but 20% of patients require admission to the intensive care unit (ICU); the mortality rate of these patients is 25%, with most deaths attributed to severe inflammation and thromboembolic complications (Buszko et al., 2020).

The duration and severity of COVID-19 is related to several factors, including viral (mutations) (Nagy et al., 2021) and host (age, sex, comorbidities and immunological) factors (Wang et al., 2021; Chang et al., 2021). SARS-CoV-2 infection begins with its binding to the ACE2 protein of alveolar epithelial cells, which induces activation of the innate and adaptive immune responses through the production and interaction of chemokines, colony-stimulating factors, interferons, interleukins, and tumor necrosis factor-α (TNF-α). These factors increase vascular permeability, determining COVID-19 development (Kaur et al., 2021; Torres et al., 2022).

As immunity is the essential component that determines the type of interaction between the pathogen and the host in any infectious disease; when the immune response is dysregulated, it contributes to disease pathogenesis, as in the case of a "cytokine storm" (Chen et al., 2021).

The term "cytokine storm" was coined to describe intense production of cytokines in infectious processes responsible for triggering immunopathological reactions (Teijaro, 2017). Among the inflammatory mediators released by immune cells, the cytokines IFN-α, IFN-γ, IL-1β, IL-6, IL-12, IL-18, IL-33, TNF-α and TGF-β are highlighted, and altered levels are associated with different clinical features of COVID-19 (Huang et al., 2021a; Chang et al., 2021). Indeed, cytokine storms correlate with the severity and progression of COVID-19 and can result in serious complications such as acute respiratory distress syndrome (ARDS) and multiple organ failure, which are the leading causes of death from the disease (Kunnumakkara et al., 2021).

Another complexity of COVID-19 is the emergence of new symptoms after the acute infection or illness. Patients infected with SARS-CoV-2 may continue to experience a variety of symptoms after the established period of COVID-19, which are not explained by other causes. These symptoms include fatigue, shortness of breath, "brain fog", sleep disturbances, fevers, gastrointestinal symptoms, anxiety and depression and can persist for months and range from mild to disabling (Collins, 2021; Parums, 2021).

The immune response is a critical factor in the evolution of COVID-19, and assessment of this response in different populations can provide a better understanding of how the host response influences the severity of the disease in some individuals, even though the majority of those infected with SARS-CoV-2 are asymptomatic or develop mild symptoms (Mortaz et al., 2020). Accordingly, we evaluated the levels of IL-17, IFN-γ, TNF-α, IL-10, IL-6, IL-4 and IL-2 in patients with clinical COVID-19 and long COVID-19, with cases classified as mild, moderate and severe, and associations with risk factors for sex, age and presence of comorbidities.

MATERIALS AND METHODS

Study Population and Sample Collection

The present study involved blood samples from 317 patients diagnosed with COVID-19 and classified according to the criteria established by the World Health Organization (WHO, 2021). The assessment included individuals of both sexes aged 18 years and over, who had not been vaccinated against SARS-CoV-2, and who were attended at the post-COVID-19 outpatient clinic at Universidade do Estado do Pará, Hospital Adventista de Belém or Instituto Evandro Chagas from July 2020 to May 2021. The group of post-COVID-19 patients included those who sought the long COVID-19 outpatient clinic at least 30 days after the recovery from acute COVID-19.

A total of 317 patients (n=317) were enrolled in our study aiming to access the cytokine profiles according to the symptoms severe (n=91), moderate (n=53) and mild (n=173), presented in the moment of acute disease. Aiming to analyze the cytokine profile among recovered patients of COVID-19 (n=225) that looked attending the long COVID-19 outpatient clinic at the Universidade do Estado do Pará, we divided the individuals into two groups: post-COVID-19 with (n=135) and without (n=90) sequelae (long COVID-19).

A 10-mL blood sample was collected by intravenous puncture using a vacuum collection system containing ethylenediaminetetraacetic acid (EDTA) as an anticoagulant.

The samples were transported to the Virology Laboratory of the Federal University of Pará, where they were processed to separate plasma and leukocytes; the former was used to determine cytokine levels.

Serum Cytokine Levels

Quantification of serum cytokine levels was performed using the flow cytometry technique and Cytometric Bead Array Kit (CBA) Human Th1/Th2/Th17 (BD Biosciences, San Diego, CA, USA) with BD FACS Canto II equipment. All procedures followed the manufacturer's guidelines. The methodology used is based on beads conjugated with a capture antibody: six populations of beads with different fluorescence intensities conjugated to a specific capture antibody for each cytokine are mixed to form the CBA, and results are determined using the FL-3 channel of a flow cytometer. The bead populations were observed according to their respective fluorescence intensities: from least bright to brightest (IL-17< IFN-γ < TNF-α < IL-10 < IL-6 < IL-4 < IL-2).

Statistical Analysis

The information obtained was entered into a database in Microsoft Office Excel 2013 software. Normality of the distribution of cytokine levels was analyzed using the Shapiro–Wilk test. Based on the results of the normality test, the evaluation of variations in the plasma levels of these markers between groups was performed using the nonparametric Mann–Whitney test. RStudio 4.0.2 software was used to assess the correlation (Pearson correlation) between IL-6 levels and age in the acute COVID-19 group. The frequency of epidemiological variables was estimated using direct counting, and the significance of differences between the groups was calculated using Fisher's exact test and the chi-square test. All tests were performed using the GraphPad Prism 5.0 program, and results with a p value < 0.05 were considered significant.

RESULTS

Table 1 shows the median cytokine levels of patients with severe and mild/moderate acute COVID-19 (acute SARS-CoV-2 infection) and individuals who recovered from the disease (with and without sequelae).

Assessment of cytokine levels among patients with acute COVID-19 and individuals in the post-COVID-19 period showed significantly higher levels of IL-17 (p=0.0002; **Figure 1A**), TNF-α (p<0.0001; **Figure 1C**) and IL-2 (p<0.0001; **Figure 1G**) in the post-COVID-19 group and higher levels of IL-6 (p<0.0001; **Figure 1E**) in the acute COVID-19 group. The cytokines levels IFN-γ (**Figure 1B**), IL-10 (**Figure 1D**) and IL-4 (**Figure 1F**) did not show significant differences between the groups.

Comparison of cytokine levels showed that patients with severe acute COVID-19 had significantly higher levels of IL-6 (p=0.0260; **Figure 2E**) as compared to mild/moderate group. Conversely, in the group of post-COVID-19 subjects, no significant differences in cytokine level among those with severe clinical forms compared to mild/moderate forms were observed (**Figures 2A–G**).

Some variables, such as sex, age and comorbidities (diabetes mellitus, hypertension, chronic kidney disease, obesity and immunosuppression), which can influence the immune response, were evaluated in relation to the clinical manifestations of patients with COVID-19 and levels of cytokines. When comparing the frequencies of the variables between the groups of patients with COVID-19, all variables showed significant differences (**Table 2**). The severe group had a higher frequency of males (p=0.0027), patients aged over 60 years (p<0.0001) and comorbidities (p<0.0001).

In the group with acute COVID-19, cytokine levels were evaluated in relation to epidemiological variables (**Table 3**). Patients aged 21-40 years had higher levels of TNF-α (p= 0.0257), and those over age 60 had higher levels of IL-6, with a p value close to statistical significance (p=0.0636). Patients without comorbidities had higher levels of TNF-α (p=0.0030), IL-4 (p=0.0020) and IL-2 (p=0.0021); IL-6 levels were higher in patients with comorbidities, but without statistical significance (p=0.0891). Analysis of IL-6 levels with the age in those with acute COVID-19 showed a slightly positive correlation (r= 0.218; p= 0.0381), but there was no correlation between the variables when the evaluation was performed according to the different clinical forms of the disease (**Figure 3**). IL-6 levels were higher in hospitalized patients admitted to the ICU (median= 15.41) than in those who did not require intensive care (median= 12.59), but the difference was not significant (p= 0.3353).

The post-COVID-19 group was divided into individuals who were undergoing medical follow-up for sequelae (long COVID) and those who had recovered and had no sequelae. Assessment of cytokine levels between these groups showed that individuals

TABLE 1 | - Median cytokine levels evaluated among patients with different clinical COVID-19 and post-COVID-19 conditions.

Clinical condition	IL-17Median (IQR)	IFN-γMedian (IQR)	TNF-αMedian (IQR)	IL-10Median (IQR)	IL-6Median (IQR)	IL-4Median (IQR)	IL-2Median (IQR)
COVID-19	15.45 (15.90)	8.13 (3.15)	6.20 (3.25)	9.50 (3.21)	12.22 (8.31)	8.83 (15.90)	6.88 (7.57)
Post-COVID-19	20.46 (15.59)	8.54 (2.51)	7.92 (4.65)	9.64 (3.19)	8.58 (4.47)	8.73 (89.48)	8.44 (2.72)
COVID-19							
Severe	15.80 (16.24)	8.42 (2.94)	6.17 (3.66)	9.46 (3.22)	13.53 (11.35)	8.04 (5.72)	6.81 (2.46)
Mild/Moderate	15.16 (15.28)	7.32 (3.58)	6.30 (3.19)	9.50 (4.14)	10.98 (5.01)	9.31 (5.72)	8.18 (2.60)
Post-COVID-19							
Severe	20.41 (13.09)	8.34 (3.76)	6.85 (6.76)	8.78 (2.95)	8.22 (4.6)	7.59 (7.61)	7.60 (3.26)
Mild/Moderate	20.50 (15.85)	8.57 (2.26)	8.23 (4.2)	9.75 (3.24)	8.67 (4.47)	8.83 (7.89)	8.60 (2.66)

IIQ, interquartile range.

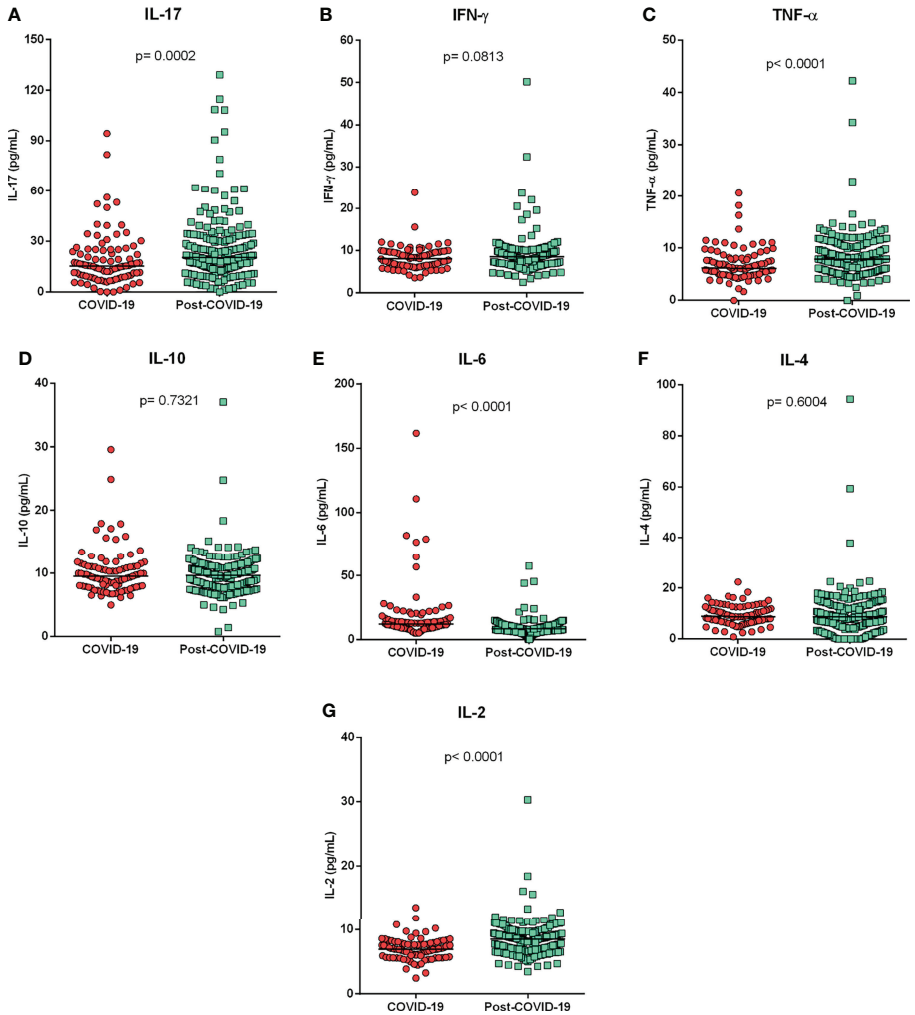

FIGURE 1 | Cytokine levels according to different clinical manifestations of COVID-19. Comparison of cytokine levels **(A)** IL-17, **(B)** IFN-y, **(C)** TNF-a, **(D)** IL-10, **(E)** IL-6, **(F)** IL-4 and **(G)** IL-2, between patients with acute COVID-19 and individuals in the post-COVID-19 period. Mann-Whitney test.

with long COVID (sequelae) had higher levels of IL-17 (p=0.0035; **Figure 4A**) and IL-2 (p=0.0219; **Figure 4G**) and that individuals without sequelae had higher levels of IL-10 (p=0.0406; **Figure 4D**) and IL-4 (p<0.0001; **Figure 4F**). A correlogram of cytokine levels in long COVID-19 patients revealed a positive correlation for most cytokines (**Figure 5**). The cytokines levels IFN-y (**Figure 4B**), TNF-a (**Figure 4C**) and IL-6 (**Figure 4E**) did not show significant differences between the groups.

DISCUSSION

The main risk factors for severe and long COVID-19 include age, male sex, smoking, presence of comorbidities (obesity, diabetes, hypertension, heart disease) and variations in the immune response of the host (Zhou et al., 2020; Ejaz et al., 2020; Wang et al., 2021; Chang et al., 2021). Evidence suggests that age is the most significant risk factor for the severe form of COVID-19 and related complications (Chen et al., 2021). In the present study, subjects in the post-COVID-19 group had higher levels of IL-17, TNF-α and IL-2 as compared to the acute COVID-19 group. In contrast, patients in the acute COVID-19 group had higher levels of IL-6. Younger patients had higher levels of TNF-α, and patients without comorbidities had higher levels of TNF-α, IL-4 and IL-2. Patients over age 60, with comorbidities, had higher levels of IL-6. In the post-COVID-19 group, subjects with long COVID-19 had higher levels of IL-17 and IL-2 and subjects without sequelae had higher levels of IL-10, IL-6 and IL- 4.

The death rate from COVID-19 is directly related to age, whereby older age is associated with greater risk. The rate varies from 0.4 to 3.3% in patients aged 40 years or younger, from 1.3 to 4.85% in those aged 40-50 years, 3.6-6.4% in those aged 60-70, 8.0 to 12.6% in those aged 70-80, and 14.8%-25.9% in those older than 80 (Chen et al., 2021). Overall, rates of hospitalizations, ICU

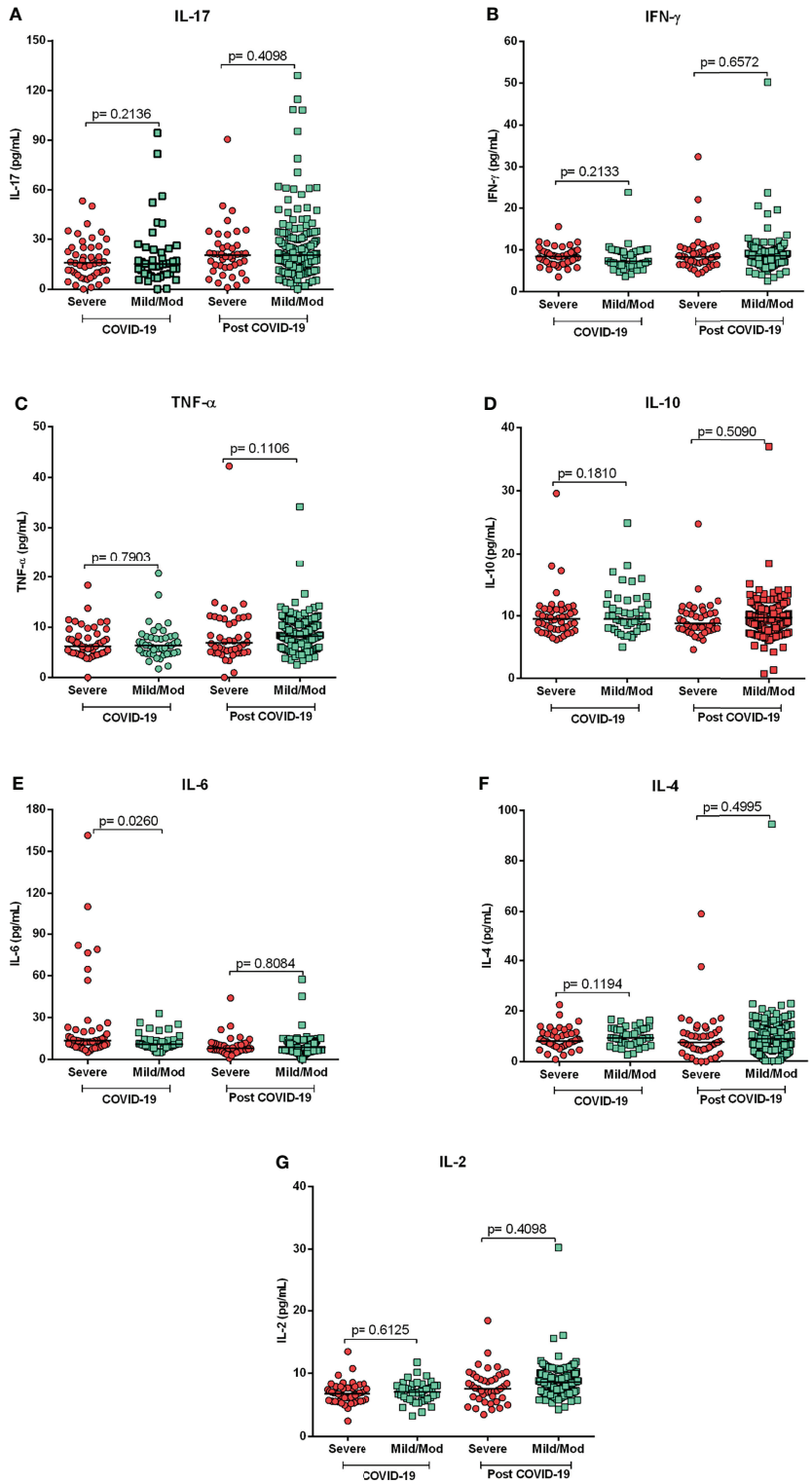

FIGURE 2 | Cytokine profiles in acute and post-COVID-19 syndrome. Comparison of cytokine levels of patients with severe and mild/moderate COVID-19 and post-COVID-19. Mild/Mod: mild/moderate. Mann-Whitney Test. **(A)** IL-17, **(B)** IFN-y, **(C)** TNF-a, **(D)** IL-10, **(E)** IL-6, **(F)** IL-4 and **(G)** IL-2.

TABLE 2 | Distribution of frequencies of epidemiological variables between groups with different clinical conditions of COVID-19.

Variables	Severe N = 91N (%)	Mild/Moderate N = 226N (%)	p
Sex			
Female	40 (43.96)	131 (58.00)	0.0027*
Male	51 (56.04)	95 (42.00)	
Age (years)			
21-40	22 (24.18)	106 (46.90)	<0.0001**
41-60	45 (49.45)	105 (46.46)	
>60	24 (26.37)	15 (6.64)	
Comorbidities			
Yes	49 (53.85)	61 (26.99)	<0.0001*
No	42 (46.15)	165 (73.01)	

*N, number of individuals/samples; * Fisher's exact test; ** Chi-square test.*

admissions, and death from COVID-19 increase with age (CDC COVID-19 Response Team, 2020), which occurs because of immune system remodeling or immunosenescence, rendering individuals more susceptible to infections, with more severe disease symptoms and lower response to vaccination (Pawelec, 2018; Bichara et al., 2021a; Bichara et al., 2021b). IL-6 levels showed a slight correlation with advanced age in acute COVID-19. However, there was no correlation of cytokine level with age according to the different clinical forms, which suggests that age may contribute to the increase in IL-6 levels but that these two factors are not sufficient to define the severity of the disease. Although IL-6 levels were higher in older patients with acute COVID-19, cytokine levels showed no statistically significant difference between age groups in this group, possibly due to the small sample size, which is a limitation of the study.

In our study, patients with the severe form of acute COVID-19 had higher levels of IL-6 and had some type of comorbidity (diabetes mellitus, hypertension, obesity, and immunosuppression). In the evaluation of patients with acute COVID-19, regardless of disease severity, individuals with comorbidities had higher levels of IL-6 (but without statistical significance). Comorbidities can contribute to the development of COVID-19 and are associated with worse prognosis due to the establishment of complex inflammatory symptoms (Ejaz et al., 2020; Fang et al., 2020).

The IL-6 contributes to inflammation in all insulin target tissues, including fat, the liver, and muscle, indicating the role of IL-6 in driving obesity and in the pathogenesis of systemic insulin resistance (Rocha and Folco, 2011; El-Kadre and Tinoco, 2013). In addition to IL-6, variations in the levels of different cytokines are involved in the development of different comorbidities (Mirhafez et al., 2014; Donath et al., 2019; Moghbeli et al., 2021). Although the cytokines TNF-α, IL-4 and IL-2 were not associated with severe COVID-19 in the present study, lower levels of these cytokines were observed in patients with comorbidities who had acute COVID-19.

The main risk factors associated with COVID-19, related to advanced age and the presence of comorbidities, are conditions characterized by constant low-grade activation of the inflammatory response (Geerlings and Hoepelman, 1999; Maggio et al., 2006; Franceschi and Campisi, 2014; Rodríguez-Iturbe et al., 2014), which promote impairment of the general immune response to infection. This suggests that although the clinical profile of severe COVID-19 is induced by an increase in cytokine production, it may be that this increase occurs in a moderate way and is sufficient to intensify inflammatory processes already existing in patients with the aforementioned risk factors and deregulate homeostasis. Furthermore, corticosteroid use in critically ill patients may also be

TABLE 3 | Comparison of cytokine levels in relation to epidemiological variables among patients with acute COVID-19.

Variables	IL-17 (pg/mL) Median (IIQ)	IFN-γ (pg/mL) Median (IIQ)	TNF-α (pg/mL) Median (IIQ)	IL-10 (pg/mL) Median (IIQ)	IL-6 (pg/mL) Median (IIQ)	IL-4 (pg/mL) Median (IIQ)	IL-2 (pg/mL) Median (IIQ)
Sex*							
Female	15.44 (17.66)	8.21 (3.71)	6.00 (3.50)	8.96 (3.82)	12.56 (8.84)	9.43 (7.02)	6.76 (2.03)
Male	15.45 (11.58)	8.24 (3.67)	6.25 (3.28)	9.95 (3.25)	11.70 (7.90)	8.09 (4.75)	6.96 (1.80)
p	0.9735	0.7270	0.7688	0.1618	0.8733	0.2121	0.3360
Age (years)**							
21-40	15.80 (9.30)	8.37 (3.09)	7.67 (3.94)	8.56 (2.32)	11.39 (4.27)	10.34 (4.82)	7.44 (2.10)
41-60	15.31 (16.76)	8.35 (3.29)	6.78 (2.94)	9.59 (3.50)	12.71 (9.24)	8.46 (5.26)	6.88 (1.95)
>60	11.74 (16.76)	8.05 (3.05)	5.95 (3.14)	10.43 (2.80)	14.51 (11.97)	7.86 (5.17)	5.52 (1.77)
p	0.6310	0.9853	0.0257	0.1674	0.0636	0.2700	0.1263
Comorbidities *							
Yes	16.40 (17.03)	7.70 (2.87)	5.69 (2.33)	9.63 (4.67)	13.13 (11.68)	7.27 (4.88)	6.61 (1.73)
No	15.45 (9.30)	8.65 (3.02)	7.05 (3.59)	9.39 (3.08)	11.35 (4.96)	10.19 (4.84)	7.49 (1.68)
p	0.9922	0.2527	0.0030	0.9893	0.0891	0.0020	0.0021

*IIQ, interquartile range; * Mann–Whitney test; ** Kruskal–Wallis test.*

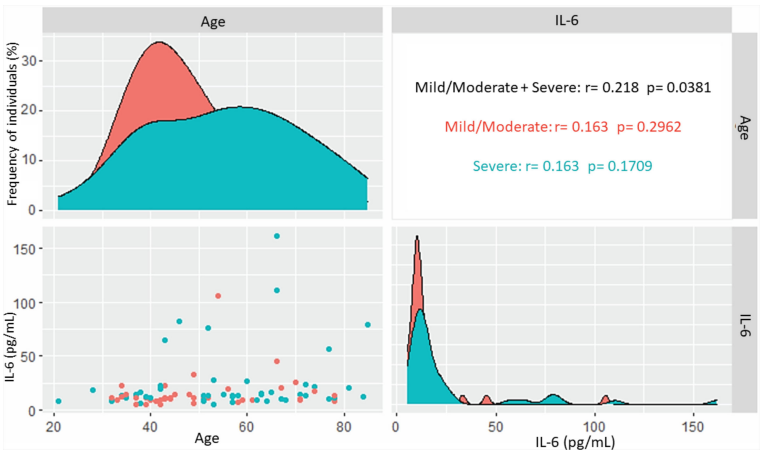

FIGURE 3 | Correlation of IL-6 levels and age in acute COVID-19. Correlation of all patients and patients with mild/moderate and severe forms of the disease.

associated with lower levels of cytokines compared to those with less aggressive forms of the disease.

IL-6 also contributes to increase vascular permeability and cause interstitial edema and tissue damage (Marin et al., 2001; Riedemann et al., 2003; Lowe et al., 2004). An increase in these events is related to the severity of COVID-19 and is responsible for many deaths (Klok et al., 2020; Helms et al., 2020; Wool and Miller, 2021).

Although the severity of COVID-19 is related to risk factors such as advanced age and comorbidities, Del Valle et al. (2020) noted that elevated serum levels of IL-6, IL-8, and TNF-α in COVID-19 patients at the time of hospitalization were strong and independent predictors of patient survival. IL-6 was one of the most robust prognostic markers of survival (surpassing CRP, D-dimer and ferritin), and elevated IL-6 levels were associated with severity and predictive of poor outcome. In our study, among the cytokines evaluated, only high levels of IL-6 were associated with the severity of COVID-19, confirming the relevance of this cytokine in the outcome of the disease. In this sense, maintenance of high levels of IL-6 in patients with the severe form of COVID-19 might be mainly related to the consequence of the inflammatory process resulting from the main risk factors for the disease, the presence of different comorbidities and advanced age and will contribute to intensifying the inflammatory process and the development of severe clotting events.

Some studies have evaluated symptoms related to long COVID-19 (Fernández-de-Las-Peñas et al., 2021; Abdallah et al., 2021; Huang et al., 2021a; Huang et al., 2021b; Logue et al., 2021; Augustin et al., 2021; Shuwa et al., 2021). However, most of these studies evaluated the long COVID-19 symptoms among patients who were hospitalized, i.e., only from patients who had severe COVID-19. Augustin et al. (2021) evaluated post-COVID syndrome in outpatients, but in order to correlate clinical symptoms with IgG antibodies, they did not evaluate molecular markers of inflammation. Cytokine IL-6 has been proposed as a potential mediator of neuropsychiatric symptoms of long COVID-19, possibly related to its persistence (Kappelmann et al., 2021). This relationship was not observed in our study, since individuals in the post-COVID-19 group had lower levels of IL-6, compared to patients with acute COVID-19. Furthermore, in the post-COVID group there was no significant difference in IL-6 levels between individuals with and without sequelae in the COVID-19 group. The relationship of IL-6 levels with the development of symptoms in long COVID-10, including neuropsychiatric symptoms, needs to be better investigated.

Shuwa et al. (2021) identified a likely risk of developing prolonged symptoms of COVID-19 in hospitalized patients, noting that convalescent patients had a lower frequency of IL-10^+ $CD4^+$ T cells, IL-17^+ $CD4^+$ T cells, and IL-6^+ B cells, compared to individuals with acute COVID-19. Although in our study we identified lower levels of IL-10 in the long COVID-19 group compared to subjects without sequelae in the post-COVID-19 group, IL-17 levels were higher in those subjects with long COVID-19. Furthermore, no difference was observed in IL-6 levels between the groups. The difference between the results presented here and those observed by Shuwa et al. (2021) may be due to the clinical moment at which the patients were analyzed. In our study, evaluated individuals in the post-COVID-19 period, including individuals with and without sequelae, as well as individuals who had acute COVID-19 with different clinical manifestations (mild, moderate and severe), showing that the development of long COVID-19 may not be related only with the severity of acute COVID-19. In addition, it was possible to identify immuno-inflammatory molecular patterns, through the characterization of the cytokine profile, which may be related to long COVID-19.

In relation to individuals in the post-COVID-19 group, higher levels of IL-10 and IL-4 were observed in the group that did not present sequelae after the disease. This suggests better control of the inflammatory process due to increased levels of anti-inflammatory cytokines in these individuals. Furthermore,

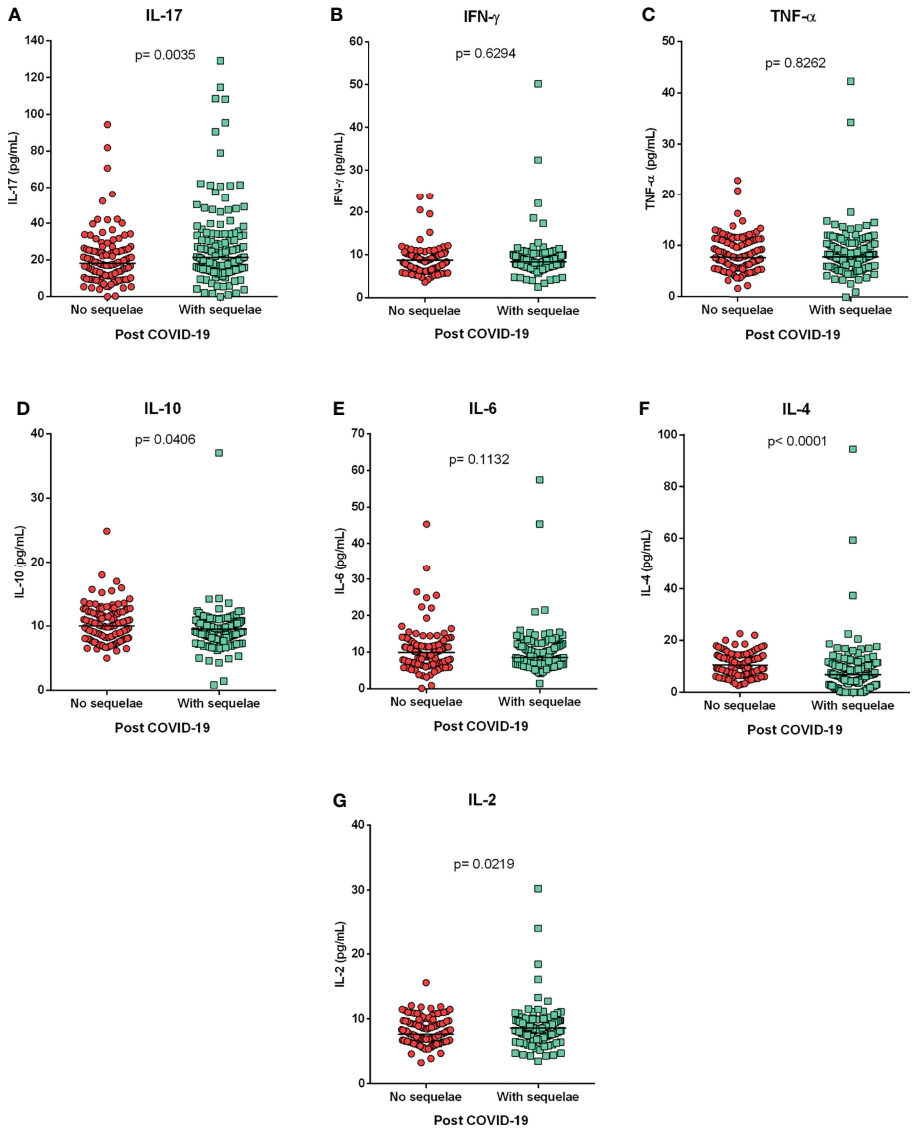

FIGURE 4 | Cytokine profile in the long COVID-19. Comparison of cytokine levels **(A)** IL-17, **(B)** IFN-y, **(C)** TNF-a, **(D)** IL-10, **(E)** IL-6, **(F)** IL-4 and **(G)** IL-2, between individuals with and without post-COVID-19 symptoms (sequelae). Mann-Whitney test.

individuals who continued to experience sequelae after infection (long COVID) had significantly higher levels of IL-17 and IL-2 and lower levels of Il-4 and IL-10, suggesting a possible "molecular signature" for long COVID characterized by a Th17 inflammatory profile with a reduced anti-inflammatory response mediated by IL-4 and IL-10, that must be confirmed by other studies enrolling a largest sample size.

The correlation of cytokine levels in the long COVID-19 group was positive among most of the cytokines evaluated. Hence, although the disease is associated with variations in levels of certain cytokines, it appears to induce an increase in levels of cytokines related to different types of inflammatory response. Post-COVID syndrome (long COVID) has been associated with residual inflammation, organ damage, preexisting health conditions or nonspecific effects due to hospitalization or prolonged ventilation (Moreno-Pérez et al., 2021), conditions easily related to the severe form of the disease. Nonetheless, it is important to emphasize that SARS-CoV-2 shows tropism for the nervous system, and neurological manifestations can be observed in patients with different clinical forms of the disease (mild, moderate and severe), ranging from anosmia, ageusia, headache, stroke, Guillain–Barré syndrome, seizure and encephalopathy (Camargo-Martínez et al., 2021). Thus, it is possible that microvascular

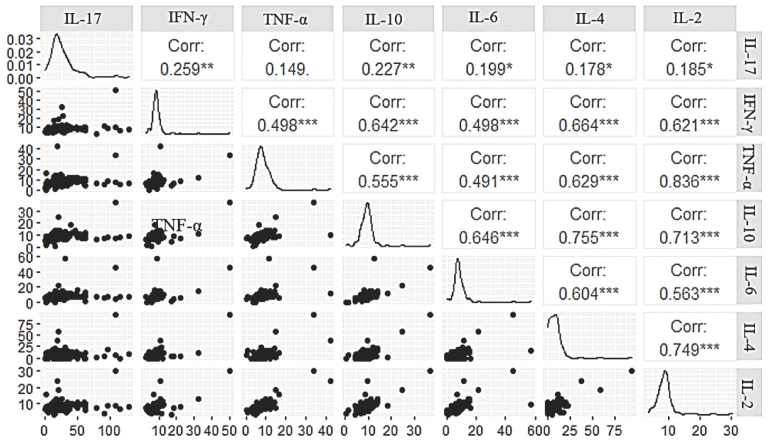

FIGURE 5 | Correlogram of cytokine levels evaluated in long COVID-19. *p<0.01; **p<0.001 and ***p<0.0001

inflammation in cells of the nervous system during infection may trigger mild symptoms of the disease (Lechner-Scott et al., 2021), which may persist even after the infection has resolved.

The consequences of the long COVID-19 are impacting health care resources, as up to 30% of the associated health burden may be due to prolonged disability induced by COVID-19 rather than mortality (Parums, 2021). Therefore, understanding the biological basis of long COVID-19 will allow us to identify factors that predispose to the development of long-term complications and guide effective therapies. In this sense, several studies have been developed, such as the REACT-GE study (in partnership with Genomics England) that aims to look for biological signatures that may be linked to the development of long COVID-19 and whether genes affect the severity of the COVID-19 and its long-term progression (Post-COVID-19 syndrome: in it for the long haul, 2021)

Some studies have evaluated the molecular signature of acute COVID-19 cytokines by different methodologies (Bergamaschi et al., 2021; Freire et al., 2021; Szabo et al., 2021; Schimke et al., 2022). In our study, IL-6 levels were associated with the severe form of acute COVID-19. Bergamaschi et al. (2021) also identified IL-6 persistence in severe disease, along with the TNF-α. In contrast, other studies have shown that disease severity was related to elevated levels of myeloid chemoattractants and neutrophil activation (Freire et al., 2021; Szabo et al., 2021; Schimke et al., 2022). Possible differences in results (molecular profiles) observed between different studies may be due to differences in methods used for investigation, different times of sample collection during infection, or even due to differences in the immunogenetic background of the investigated population. Therefore, identification of a molecular profile in relation to long COVID-19 still needs to be further investigated. Even though several studies have evaluated the main symptoms of long COVID-19 (Abdallah et al., 2021; Augustin et al., 2021; Darley et al., 2021; Fernández-de-Las-Peñas et al., 2021; Logue et al., 2021; Wu et al., 2021; Huang et al., 2021a; Huang et al., 2021b), none of them investigated the association of clinical manifestations with the immunoinflammatory profile of cytokines. Our study showed, for the first time, evidence for the existence of a long COVID-19-associated cytokine profile in a cohort of the Brazilian Amazon region. Further evaluated in studies conducted with larger cohorts from distinct geographic areas is needed.

Our results are important because it was possible to identify differences in cytokine synthesis and identify characteristic profiles in acute COVID-19 (higher levels of IL-6) and long COVID-19 (high levels of IL-2 and IL- 17).

In conclusion, the present study shows that advanced age, the presence of comorbidities and elevated serum IL-6 levels are associated with the severity of COVID-19 and represent good markers to differentiate severe COVID-19 from mild clinical forms. Furthermore, high serum levels of IL-17 and IL-2, as well as low levels of IL-4 and IL-10, appear to constitute a long COVID-19 cytokine profile (molecular signature), and identification of these markers as a potential target may establish more adequate treatment and prevention strategies for specific groups.

DATA AVAILABILITY STATEMENT

The original contributions presented in the study are included in the article/supplementary material. Further inquiries can be directed to the corresponding author.

ETHICS STATEMENT

The studies involving human participants were reviewed and approved by National Research Ethics Committee (CAEE:

33470020.1001.0018). The patients/participants provided their written informed consent to participate in this study.

AUTHOR CONTRIBUTIONS

AVa, LF, IV and ES conceived of the project. AQ, AVa, IB-C, JQ and ES wrote and reviewed the manuscript. SL and MQ performed the statistical analyses. AS, JL, MT, MB, CB, MC, IB-C, JN, ES, ML, FC, MV, FR, KS, RS, CB, AB, AVe, MC, DV, CO, GV, FC, VP, PN, and IB-C collected the biological samples and performed the laboratory analyses. All authors reviewed and approved the article.

FUNDING

The study was supported by the National Council for Scientific and Technological Development (CNPQ #401235/2020-3); Fundação Amazônia de Amparo a Estudos e Pesquisa do Pará (FAPESPA #005/2020 and #006/2020) and Secretaria de Estado de Ciência, Tecnologia e Educação Profissional e Tecnológica (#09/2021).

ACKNOWLEDGMENTS

The authors thank all patients who agreed to voluntarily participate in this study.

REFERENCES

Post-COVID-19 syndrome: in it for the long haul. (2021). *EBioMedicine* 67, 103424. doi: 10.1016/j.ebiom.2021.103424

Abdallah, S. J., Voduc, N., Corrales-Medina, V. F., McGuinty, M., Pratt, A., Chopra, A., et al. (2021). Symptoms, Pulmonary Function, and Functional Capacity Four Months After COVID-19. *Ann. Am. Thorac. Soc* 18, 1912–1917. doi: 10.1513/AnnalsATS.202012-1489RL

Augustin, M., Schommers, P., Stecher, M., Dewald, F., Gieselmann, L., Gruell, H., et al. (2021). Post-COVID Syndrome in non-Hospitalised Patients With COVID-19: A Longitudinal Prospective Cohort Study. *Lancet Reg. Health Eur.* 6, 100122. doi: 10.1016/j.lanepe.2021.100122

Bergamaschi, L., Mescia, F., Turner, L., Hanson, A. L., Kotagiri, P., Dunmore, B. J., et al. (2021). Longitudinal Analysis Reveals That Delayed Bystander CD8+ T Cell Activation and Early Immune Pathology Distinguish Severe COVID-19 From Mild Disease. *Immunity* 54, 1257–1275. doi: 10.1016/j.immuni.2021.05.010

Bichara, C. D. A., da Silva Graça Amoras, E., Vaz, G. L., da Silva Torres, M. K., Queiroz, M. A. F., do Amaral, I. P. C., et al. (2021b). Dynamics of Anti-SARS-CoV-2 IgG Antibodies Post-COVID-19 in a Brazilian Amazon Population. *BMC Infect. Dis.* 21, 443. doi: 10.1186/s12879-021-06156-x

Bichara, C. D. A., Queiroz, M. A. F., da Silva Graça Amoras, E., Vaz, G. L., Vallinoto, I. M. V. C., Bichara, C. N. C., et al. (2021a). Assessment of Anti-SARS-CoV-2 Antibodies Post-Coronavac Vaccination in the Amazon Region of Brazil. *Vaccines (Basel)* 9, 1169. doi: 10.3390/vaccines9101169

Buszko, M., Park, J. H., Verthelyi, D., Sen, R., Young, H. A., and Rosenberg, A. S. (2020). The Dynamic Changes in Cytokine Responses in COVID-19: A Snapshot of the Current State of Knowledge. *Nat. Immunol.* 21, 1146–1151. doi: 10.1038/s41590-020-0779-1

Camargo-Martínez, W., Lozada-Martínez, I., Escobar-Collazos, A., Navarro-Coronado, A., Moscote-Salazar, L., Pacheco-Hernández, A., et al. (2021). Post-COVID 19 Neurological Syndrome: Implications for Sequelae's Treatment. *J. Clin. Neurosci.* 88, 219–225. doi: 10.1016/j.jocn.2021.04.001

CDC COVID-19 Response Team. (2020). Severe Outcomes Among Patients With Coronavirus Disease 2019 (COVID-19) - United States, February 12-March 16, 2020. *MMWR Morb. Mortal. Wkly. Rep.* 69, 343–346. doi: 10.15585/mmwr.mm6912e2

Chang, S. H., Minn, D., Kim, S. W., and Kim, Y. K. (2021). Inflammatory Markers and Cytokines in Moderate and Critical Cases of COVID-19. *Clin. Lab.* 67 (9). doi: 10.7754/Clin.Lab.2021.210142

Chen, Y., Klein, S. L., Garibaldi, B. T., Li, H., Wu, C., Osevala, N. M., et al. (2021). Aging in COVID-19: Vulnerability, Immunity and Intervention. *Ageing Res. Rev.* 65, 101205. doi: 10.1016/j.arr.2020.101205

Collins, F. S. (2021) *NIH Launches New Initiative to Study "Long COVID"* (Bethesda, MD, USA: National Institutes of Health). Available at: https://www.nih.gov/about-nih/who-we-are/nih-director/statements/nih-launches-new-initiative-study-long-covid (Accessed 27/05/2022).

Darley, D. R., Dore, G. J., Byrne, A. L., Plit, M. L., Brew, B. J., Kelleher, A., et al. (2021). Limited Recovery From Post-Acute Sequelae of SARS-CoV-2 at 8 Months in a Prospective Cohort. *ERJ Open Res.* 7, 00384–02021. doi: 10.1183/23120541.00384-2021

Del Valle, D. M., Kim-Schulze, S., Huang, H. H., Beckmann, N. D., Nirenberg, S., Wang, B., et al. (2020). An Inflammatory Cytokine Signature Predicts COVID-19 Severity and Survival. *Nat. Med.* 6, 1636–1643. doi: 10.1038/s41591-020-1051-9

Donath, M. Y., Dinarello, C. A., and Mandrup-Poulsen, T. (2019). Targeting Innate Immune Mediators in Type 1 and Type 2 Diabetes. *Nat. Rev. Immunol.* 19, 734–746. doi: 10.1038/s41577-019-0213-9

Ejaz, H., Alsrhani, A., Zafar, A., Javed, H., Junaid, K., Abdalla, A. E., et al. (2020). COVID-19 and Comorbidities: Deleterious Impact on Infected Patients. *J. Infect. Public Health* 13, 1833–1839. doi: 10.1016/j.jiph.2020.07.014

El-Kadre, L. J., and Tinoco, A. C. (2013). Interleukin-6 and Obesity: The Crosstalk Between Intestine, Pancreas and Liver. *Curr. Opin. Clin. Nutr. Metab. Care* 16, 564–568. doi: 10.1097/MCO.0b013e32836410e6

Fang, X., Li, S., Yu, H., Wang, P., Zhang, Y., Chen, Z., et al. (2020). Epidemiological, Comorbidity Factors With Severity and Prognosis of COVID-19: A Systematic Review and Meta-Analysis. *Aging (Albany NY)* 12, 12493–12503. doi: 10.18632/aging.103579

Fernández-de-Las-Peñas, C., Palacios-Ceña, D., Gómez-Mayordomo, V., Rodríuez-Jiménez, J., Palacios-Ceña, M., Velasco-Arribas, M., et al. (2021). Long-Term Post-COVID Symptoms and Associated Risk Factors in Previously Hospitalized Patients: A Multicenter Study. *J. Infect.* 83, 237–279. doi: 10.1016/j.jinf.2021.04.036

Franceschi, C., and Campisi, J. (2014). Chronic Inflammation (Inflammaging) and its Potential Contribution to Age-Associated Diseases. *J. Gerontol A Biol. Sci. Med. Sci.* 69, S4–S9. doi: 10.1093/gerona/glu057

Freire, P. P., Marques, A. H., Baiocchi, G. C., Schimke, L. F., Fonseca, D. L., Salgado, R. C., et al. (2021). The Relationship Between Cytokine and Neutrophil Gene Network Distinguishes SARS-CoV-2-Infected Patients by Sex and Age. *JCI Insight* 6, e147535. doi: 10.1172/jci.insight.147535

Geerlings, S. E., and Hoepelman, A. I. (1999). Immune Dysfunction in Patients With Diabetes Mellitus (DM). *FEMS Immunol. Med. Microbiol.* 26, 259–265. doi: 10.1111/j.1574-695X.1999.tb01397.x

Helms, J., Tacquard, C., Severac, F., Leonard-Lorant, I., Ohana, M., Delabranche, X., et al. (2020). High Risk of Thrombosis in Patients With Severe SARS-CoV-2 Infection: A Multicenter Prospective Cohort Study. *Intensive Care Med.* 46, 1089–1098. doi: 10.1007/s00134-020-06062-x

Huang, C., Huang, L., Wang, Y., Li, X., Ren, L., Gu, X., et al. (2021b). 6-Month Consequences of COVID-19 in Patients Discharged From Hospital: A Cohort Study. *Lancet* 397, 220–232. doi: 10.1016/S0140-6736(20)32656-8

Huang, C., Wang, Y., Li, X., Ren, L., Zhao, J., Hu, Y., et al. (2021a). Clinical Features of Patients Infected With 2019 Novel Coronavirus in Wuhan, China. *Lancet* 395, 497–506. doi: 10.1016/S0140-6736(20)30183-5

Kappelmann, N., Dantzer, R., and Khandaker, G. M. (2021). Interleukin-6 as Potential Mediator of Long-Term Neuropsychiatric Symptoms of COVID-19. *Psychoneuroendocrinology* 131, 105295. doi: 10.1016/j.psyneuen.2021.105295

Kaur, S., Bansal, R., Kollimuttathuillam, S., Gowda, A. M., Singh, B., Mehta, D., et al. (2021). The Looming Storm: Blood and Cytokines in COVID-19. *Blood Rev.* 46, 100743. doi: 10.1016/j.blre.2020.100743

Klok, F. A., Kruip, M. J. H. A., van der Meer, N. J. M., Arbous, M. S., Gommers, D. A. M. P. J., Kant, K. M., et al. (2020). Incidence of Thrombotic Complications in Critically Ill ICU Patients With COVID-19. *Thromb. Res.* 191, 145–147. doi: 10.1016/j.thromres.2020.04.013

Kunnumakkara, A. B., Rana, V., Parama, D., Banik, K., Girisa, S., Henamayee, S., et al. (2021). COVID-19, Cytokines, Inflammation, and Spices: How are They Related? *Life Sci.* 284, 119201. doi: 10.1016/j.lfs.2021.119201

Lechner-Scott, J., Levy, M., Hawkes, C., Yeh, A., and Giovannoni, G. (2021). Long COVID or Post COVID-19 Syndrome. *Mult. Scler. Relat. Disord.* 55, 103268. doi: 10.1016/j.msard.2021.103268

Logue, J. K., Franko, N. M., McCulloch, D. J., McDonald, D., Magedson, A., Wolf, C. R., et al. (2021). Sequelae in Adults at 6 Months After COVID-19 Infection. *JAMA Netw. Open* 4, e210830. doi: 10.1001/jamanetworkopen.2021.0830

Lowe, G. D., Rumley, A., McMahon, A. D., Ford, I., O'Reilly, D. S., Packard, C. J., et al. (2004). Interleukin-6, Fibrin D-Dimer, and Coagulation Factors VII and XIIa in Prediction of Coronary Heart Disease. *Arterioscler. Thromb. Vasc. Biol.* 24, 1529–1534. doi: 10.1161/01.ATV.0000135995.39488.6c

Maggio, M., Guralnik, J. M., Longo, D. L., and Ferrucci, L. (2006). Interleukin-6 in Aging and Chronic Disease: A Magnificent Pathway. *J. Gerontol A Biol. Sci. Med. Sci.* 61, 575–584. doi: 10.1093/gerona/61.6.575

Marin, V., Montero-Julian, F. A., Grès, S., Boulay, V., Bongrand, P., Farnarier, C., et al. (2001). The IL-6-Soluble IL-6Ralpha Autocrine Loop of Endothelial Activation as an Intermediate Between Acute and Chronic Inflammation: An Experimental Model Involving Thrombin. *J. Immunol.* 167, 3435–4342. doi: 10.4049/jimmunol.167.6.3435

Mirhafez, S. R., Mohebati, M., Feiz Disfani, M., Saberi Karimian, M., Ebrahimi, M., Avan, A., et al. (2014). An Imbalance in Serum Concentrations of Inflammatory and Anti-Inflammatory Cytokines in Hypertension. *J. Am. Soc. Hypertens.* 8, 614–623. doi: 10.1016/j.jash.2014.05.007

Moghbeli, M., Khedmatgozar, H., Yadegari, M., Avan, A., Ferns, G. A., and Ghayour Mobarhan, M. (2021). Cytokines and the Immune Response in Obesity-Related Disorders. *Adv. Clin. Chem.* 101, 135–168. doi: 10.1016/bs.acc.2020.06.004

Moreno-Pérez, O., Merino, E., Leon-Ramirez, J. M., Andres, M., Ramos, J. M., Arenas-Jiménez, J., et al. (2021). Post-Acute COVID-19 Syndrome. Incidence and Risk Factors: A Mediterranean Cohort Study. *J. Infect.* 82, 378–383. doi: 10.1016/j.jinf.2021.01.004

Mortaz, E., Tabarsi, P., Varahram, M., Folkerts, G., and Adcock, I. M. (2020). The Immune Response and Immunopathology of COVID-19. *Front. Immunol.* 11. doi: 10.3389/fimmu.2020.02037

Nagy, Á., Pongor, S., and Győrffy, B. (2021). Different Mutations in SARS-CoV-2 Associate With Severe and Mild Outcome. *Int. J. Antimicrob. Agents* 57, 106272. doi: 10.1016/j.ijantimicag.2020

Parums, D. V. (2021). Editorial: Long COVID, or Post-COVID Syndrome, and the Global Impact on Health Care. *Med. Sci. Monit.* 27, e933446. doi: 10.12659/MSM.933446

Pawelec, G. (2018). Age and Immunity: What Is "Immunosenescence"? *Exp. Gerontol.* 105, 4–9. doi: 10.1016/j.exger.2017.10.024

Riedemann, N. C., Neff, T. A., Guo, R. F., Bernacki, K. D., Laudes, I. J., Sarma, J. V., et al. (2003). Protective Effects of IL-6 Blockade in Sepsis are Linked to Reduced C5a Receptor Expression. *J. Immunol.* 170, 503–507. doi: 10.4049/jimmunol.170.1.503

Rocha, V. Z., and Folco, E. J. (2011). Inflammatory Concepts of Obesity. *Int. J. Inflam.* 2011, 529061. doi: 10.4061/2011/529061

Rodríguez-Iturbe, B., Pons, H., Quiroz, Y., and Johnson, R. J. (2014). The Immunological Basis of Hypertension. *Am. J. Hypertens.* 27, 1327–1337. doi: 10.1093/ajh/hpu142

Schimke, L. F., Marques, A. H. C., Baiocchi, G. C., de Souza Prado, C. A., Fonseca, D. L. M., et al. (2022). Severe COVID-19 Shares a Common Neutrophil Activation Signature With Other Acute Inflammatory States. *Cells* 11, 847. doi: 10.3390/cells11050847

Shuwa, H. A., Shaw, T. N., Knight, S. B., Wemyss, K., McClure, F. A., Pearmain, L., et al. (2021). Alterations in T and B Cell Function Persist in Convalescent COVID-19 Patients. *Med. (N Y)* 2, 720–735.e4. doi: 10.1016/j.medj.2021.03.013

Szabo, P. A., Dogra, P., Gray, J. I., Wells, S. B., Connors, T. J., Weisberg, S. P., et al. (2021). Longitudinal Profiling of Respiratory and Systemic Immune Responses Reveals Myeloid Cell-Driven Lung Inflammation in Severe COVID-19. *Immunity* 54, 797–814. doi: 10.1016/j.immuni.2021.03.005

Teijaro, J. R. (2017). Cytokine Storms in Infectious Diseases. *Semin. Immunopathol.* 39, 501–503. doi: 10.1007/s00281-017-0640-2

Torres, M. K. S., Bichara, C. D. A., Almeida, M. N. S., Vallinoto, M. C., Queiroz, M. A. F., Vallinoto, I. M. V. C., et al. (2022). The Complexity of SARS-CoV-2 Infection and the COVID-19 Pandemic. *Front. Microbiol.* 13. doi: 10.3389/fmicb.2022.789882

Wang, F., Cao, J., Yu, Y., Ding, J., Eshak, E. S., Liu, K., et al. (2020). Epidemiological Characteristics of Patients With Severe COVID-19 Infection in Wuhan, China: Evidence From a Retrospective Observational Study. *Int. J. Epidemiol.* 49, 1940–1950. doi: 10.1093/ije/dyaa180

WHO (2021) *WHO Global Clinical Platform for the Clinical Characterization of COVID-19: Statistical Analysis Plan*. Available at: https://www.who.int/publications/i/item/WHO-2019-nCoV-Clinical-Analytic-plan-2021.1 (Accessed 15/02/2022).

WHO (2022) *WHO Coronavirus (COVID-19) Dashboard*. Available at: https://covid19.who.int/ (Accessed 08/02/2022).

Wool, G. D., and Miller, J. L. (2021). The Impact of COVID-19 Disease on Platelets and Coagulation. *Pathobiology* 88, 15–27. doi: 10.1159/000512007

Wu, L., Wu, Y., Xiong, H., Mei, B., and You, T. (2021). Persistence of Symptoms After Discharge of Patients Hospitalized Due to COVID-19. *Front. Med. (Lausanne)* 8. doi: 10.3389/fmed.2021.761314

Zhou, F., Yu, T., Du, R., Fan, G., Liu, Y., Liu, Z., et al. (2020). Clinical Course and Risk Factors for Mortality of Adult Inpatients With COVID-19 in Wuhan, China: A Retrospective Cohort Study. *Lancet* 395, 1054–1062. doi: 10.1016/S0140-6736(20)30566-3

Conflict of Interest: The authors declare that the research was conducted in the absence of any commercial or financial relationships that could be construed as a potential conflict of interest.

Publisher's Note: All claims expressed in this article are solely those of the authors and do not necessarily represent those of their affiliated organizations, or those of the publisher, the editors and the reviewers. Any product that may be evaluated in this article, or claim that may be made by its manufacturer, is not guaranteed or endorsed by the publisher.

frontiers | Frontiers in Cellular and Infection Microbiology

TYPE Review
PUBLISHED 27 July 2022
DOI 10.3389/fcimb.2022.922511

OPEN ACCESS

EDITED BY
Viviane Fongaro Botosso,
Butantan Institute, Brazil

REVIEWED BY
Chao Zhang,
Fifth Medical Center of the PLA General Hospital, China
Yongfen Xu,
Institut Pasteur of Shanghai (CAS), China
Jorge Quarleri,
Consejo Nacional de Investigaciones Científicas y Técnicas (CONICET), Argentina
Ping Zhao,
Second Military Medical University, China

*CORRESPONDENCE
Yunqing Chen
yqing_c@qq.com

SPECIALTY SECTION
This article was submitted to Virus and Host, a section of the journal Frontiers in Cellular and Infection Microbiology

RECEIVED 18 April 2022
ACCEPTED 01 July 2022
PUBLISHED 27 July 2022

CITATION
Chen Y, Xu Y, Zhang K, Shen L and Deng M (2022) Ferroptosis in COVID-19-related liver injury: A potential mechanism and therapeutic target. *Front. Cell. Infect. Microbiol.* 12:922511. doi: 10.3389/fcimb.2022.922511

Ferroptosis in COVID-19-related liver injury: A potential mechanism and therapeutic target

Yunqing Chen[1]*, Yan Xu[1], Kan Zhang[1], Liang Shen[2] and Min Deng[1]

[1]Department of Infectious Diseases, Affiliated Hospital of Jiaxing University, Jiaxing, China, [2]Department of Cardiology, Affiliated Hospital of Jiaxing University, Jiaxing, China

The outbreak and worldwide spread of coronavirus disease 2019 (COVID-19), which is caused by severe acute respiratory syndrome coronavirus 2 (SARS-CoV-2), has been a threat to global public health. SARS-CoV-2 infection not only impacts the respiratory system but also causes hepatic injury. Ferroptosis, a distinct iron-dependent form of non-apoptotic cell death, has been investigated in various pathological conditions, such as cancer, ischemia/reperfusion injury, and liver diseases. However, whether ferroptosis takes part in the pathophysiological process of COVID-19-related liver injury has not been evaluated yet. This review highlights the pathological changes in COVID-19-related liver injury and presents ferroptosis as a potential mechanism in the pathological process. Ferroptosis, as a therapeutic target for COVID-19-related liver injury, is also discussed. Discoveries in these areas will improve our understanding of strategies to prevent and treat hepatic injuries caused by COVID-19.

KEYWORDS

COVID-19, ferroptosis, liver, SARS-CoV-2, hyperferritinemia

Introduction

Since it was first reported in December 2019, severe acute respiratory syndrome coronavirus 2 (SARS-CoV-2) has become a severe threat to public health. The World Health Organization (WHO) declared the SARS-CoV-2 infection epidemic an international public health emergency, naming it coronavirus disease 2019 (COVID-19) on 11 February 2020. According to the WHO COVID-19 dashboard, the number of confirmed cases of COVID-19 has exceeded 500 million, leading to more than six million deaths.

SARS-CoV-2 is an RNA virus and has a tropism for cells expressing angiotensin-converting enzyme 2 (ACE2) receptors (Wan et al., 2020). Respiratory symptoms, such as fever, pharyngalgia, and dry cough, are the most common complaints from patients with COVID-19. However, the lung is not the only organ affected by SARS-CoV-2; the virus can affect various systems and result in multiple organ failure (Zaim et al., 2020).

Ferroptosis is a relatively novel cell death type that was first termed by Dixon et al. in 2012 (Dixon et al., 2012). Ferroptosis is an iron-dependent regulated cell death (RCD) characterized by iron overload and lipid peroxidation. The main morphological features of ferroptosis are mitochondrial shrinkage accompanied by increased mitochondrial membrane density and degenerated mitochondrial crista without changes in the nucleus (Dixon et al., 2012). Ferroptosis is regulated by several metabolic pathways, including iron, lipid, and amino acid metabolisms (Yan et al., 2021). Once the balance of iron absorption, storage, and exportation is disrupted, excessive cytosolic Fe^{2+} catalyzes the Fenton reaction and activates iron-dependent metabolic enzymes, leading to the production of highly reactive hydroxyl radicals (·OH) and oxidized polyunsaturated fatty acids (PUFAs) and eventually promoting the accumulation of lipid reactive oxygen species (ROS) and ferroptosis (He et al., 2022). In contrast, the metabolism of amino acids, especially the system Xc^-glutathione–glutathione peroxidase 4 (system Xc^-/GSH/GPX4) axis, is central to eliminating lipid ROS, with GPX4 regarded as a key regulator of ferroptosis (Yang et al., 2014). During ferroptosis, GPX4 expression is downregulated, while iron absorption and PUFA oxidation are upregulated. Additionally, two GPX4-independent pathways, nicotinamide adenine dinucleotide phosphate–ferroptosis suppressor protein 1–Coenzyme Q10 (Bersuker et al., 2019; Doll et al., 2019) and guanosine triphosphate cyclohydrolase 1–tetrahydrobiopterin/dihydrobiopterin axis (Kraft et al., 2020), allegedly participate in the regulation of ferroptosis.

At present, ferroptosis can be induced by four classes of compounds collectively called ferroptosis-inducing agents (FINs). These include (i) FINs that inhibit system Xc^- and prevent cystine imports, like erastin, sorafenib, and sulfasalazine; (ii) FINs that directly inhibit GPX4, such as Ras-selective lethal small molecule 3 (RSL3), (1S,3R)-RSL3; (iii) FINs that degrade GPX4, for example, FIN56; and (iv) FINs that indirectly inhibit GPX4 (Li et al., 2020).

Researchers from many fields have meticulously investigated ferroptosis in the past decade and have proposed it as a novel therapeutic target for a variety of diseases, including cancer (Alvarez et al., 2017; Lee et al., 2020), ischemia/reperfusion injury (Friedmann Angeli et al., 2014; Fang et al., 2019), and neurodegenerative disorders (Do Van et al., 2016; Park et al., 2021). Recently, the role of ferroptosis in various types of liver diseases, for instance, hepatitis, non-alcoholic fatty liver disease (NAFLD), liver cirrhosis, and hepatocellular carcinoma, has been explored as well (Chen et al., 2022). Liver injury has been reported as a common feature in COVID-19 (Amin, 2021); however, to date, no investigation has elucidated the potential role of ferroptosis in COVID-19-related liver injury. Recent studies showed that hepatitis virus caused liver injury through ferroptosis (Komissarov et al., 2021; Liu et al., 2021). In addition, chrysophanol could attenuate hepatitis B virus-induced hepatic fibrosis by inhibiting ferroptosis (Kuo et al., 2020). Hence, ferroptosis might also participate in SARS-CoV-2 infection-associated liver injury.

In this review, we deliberate current evidence pointing to a potential pathogenic role for ferroptosis in COVID-19-related liver injury and discuss potential therapeutic options with ferroptosis as the target.

COVID-19 and liver injury

Although SARS-CoV-2 mostly affects the respiratory system, the virus also causes the dysfunction of other organs. A few studies have shown that liver injury occurs in patients with COVID-19 (Huang et al., 2020; Guan et al., 2020; Fan et al., 2020; Cai et al., 2020). COVID-19-related hepatic injury is characterized primarily by elevated levels of alanine aminotransferase and/or aspartate aminotransferase as well as macrovesicular and microvesicular steatosis, lobular and portal inflammation, ductular proliferation, and liver cell necrosis (Nardo et al., 2021). Additionally, decreased albumin and increased total bilirubin levels, along with alkaline phosphatase and gamma-glutamyl transferase, have been reported in COVID-19 patients (Wang et al., 2020; Yadav et al., 2021). However, not all SARS-CoV-2-infected patients have elevated transaminase. Patients with severe COVID-19 are more likely to have increased liver enzymes compared to non-severe COVID-19 patients (Guan et al., 2020). Furthermore, patients with viral hepatitis have a higher risk of severe COVID-19 (Hariyanto et al., 2022), and the risk could increase further in the presence of other comorbidities such as diabetes and cardiovascular diseases (Zhou et al., 2020; Gold et al., 2020). Moreover, NAFLD (Singh et al., 2021), cirrhosis (Choudhary et al., 2021; Qi et al., 2021), and hepatic carcinoma (Chagas et al., 2020) increase the risk of progression to severe COVID-19, which might be partly because the expression of ACE2 is significantly amplified in liver fibrotic/cirrhotic conditions (Paizis et al., 2005; Huang et al., 2009).

Recently, Sonzogni et al. found SARS-CoV-2 in liver samples from deceased COVID-19 patients (Sonzogni et al., 2020). In addition, Wanner *et al.* (Wanner et al., 2022) detected SARS-CoV-2 RNA in approximately 70% of autopsied liver specimens and isolated infectious SARS-CoV-2 from liver tissues postmortem. They also established that SARS-CoV-2 liver tropism is associated with the upregulation of interferon (IFN) responses, providing comprehensive evidence of the direct impact of SARS-CoV-2 on the liver.

A broad spectrum of potential mechanisms of COVID-19-associated hepatic dysfunctions has been proposed, including direct cytotoxicity due to the active viral replication of SARS-CoV-2 in hepatocytes and biliary epithelial cells, immune and cytokine-mediated liver destruction stemming from severe inflammatory responses, coagulopathy-driven vascular microthrombosis, endotheliopathy resulting from hypoxic and/or ischemic injury, congestion from right heart failure, and drug-induced liver injury (Amin, 2021; Nardo et al., 2021; Moreira et al., 2021).

The link between COVID-19 and ferroptosis

Nowadays, several studies have provided evidence of ferroptosis in COVID-19. The ferroptosis signature was first reported in a 48-year-old male COVID-19 patient with cardiogenic shock (Jacobs et al., 2020). In this case, the authors found that E06 staining, which reflects lipid peroxidation during ferroptosis, was positive in the patient's cardiomyocytes. Additionally, staining with E06 and 4-hydroxynonenal (a reactive breakdown product of lipid peroxides that carry out ferroptosis) was positive in renal proximal tubulin. However, it is unclear whether ferroptosis is directly induced by SARS-CoV-2 or if it is secondary to the pathological processes caused by COVID-19, such as ischemia/reperfusion injury. A Vero cell study found a significantly low mRNA expression of GPX4 after SARS-CoV-2 infection (Wang et al., 2021). In another investigation, the lung tissues of hamsters infected with SARS-CoV-2 exhibited increased apoptosis and ferroptosis (Bednash et al., 2022), indicating that SARS-CoV-2 possibly has a direct effect on ferroptosis. Most recently, Han et al. (Han et al., 2022) determined that SARS-CoV-2 infected human embryonic stem cell-derived SAN-like pacemaker cells and highlighted ferroptosis as a potential mechanism for cardiac arrhythmias in COVID-19 patients and deferoxamine (DFO, an iron chelator) as a drug candidate for blocking SARS-CoV-2 infection and subsequent ferroptosis.

In fact, many clues point to ferroptosis as participating in COVID-19. As the name implies, iron is pivotal to ferroptosis because erastin-induced cell death depends on iron rather than other metal ions (Dixon et al., 2012). Iron metabolism is one of the major pathways that trigger ferroptosis (Chen et al., 2020). As with human immunodeficiency virus, human cytomegalovirus, and hepatitis B virus, SARS-CoV-2 replication also requires iron; therefore, it is likely that more iron would be transferred into cells through transferrin receptor 1, activating the Fenton reaction and generating excessive lipid ROS. In addition, COVID-19 has recently been proposed as a part of the hyperferritinemic syndrome because of several similar clinical and laboratory characteristics, including high serum ferritin and cytokine storm (Perricone et al., 2020; Colafrancesco et al., 2020). The excess of ferritin could contribute to the accumulation of cellular iron through ferritinophagy, eventually resulting in ferroptosis (Mancias et al., 2014; Dowdle et al., 2014). Besides this, SARS-CoV-2 infection activates the hepcidin pathway, which, in turn, suppresses the exportation of Fe^{2+}, leading to the progression of ferroptosis (Banchini et al., 2020).

The involvement of the system Xc^-/GSH/GPX4 axis, another key pathway that regulates ferroptosis (Yang et al., 2014), has also been investigated. The expression of GPX4, a vital regulator of ferroptosis, is decreased, and the surface expression of system Xc^- in the hepatocytes of COVID-19 patients is lower than that in healthy individuals (Krishnan et al., 2021). Moreover, numerous investigations have demonstrated GSH deficiency in severe COVID-19 patients (Bartolini et al., 2021; Kumar et al., 2021). GSH supplementation has been proposed as adjunctive therapy for COVID-19 (Guloyan et al., 2020; Silvagno et al., 2020).

Like the iron and amino acid metabolic pathways, the lipid metabolic pathway also plays an essential role in the regulation of ferroptosis. During ferroptosis, PUFAs are first converted to PUFA–CoAs by acyl–CoA synthetase long-chain family member 4 (Kuch et al., 2014; Doll et al., 2017). The PUFA–CoAs are then esterified by lysophosphatidylcholine acyltransferase 3 to generate phospholipids containing polyunsaturated fatty acid chains (PUFA-PLs). Finally, lipoxygenases oxidized PUFA-PLs to generate excessive lipid ROS (Yang et al., 2016; Kagan et al., 2017). Some researchers have suggested that lipid peroxidation is a hallmark of poor outcomes in COVID-19 patients (Martin-Fernandez et al., 2021; Zarkovic et al., 2021).

Taken together, three major pathways of ferroptosis are involved in COVID-19, and along with the direct evidence of the SARS-CoV-2 infection-induced signature of ferroptosis, it is reasonable to deduce that there is an association between ferroptosis and COVID-19.

Next, we discuss the potential role of ferroptosis in SARS-CoV-2 infection-caused liver injury.

Ferroptosis possibly participates in COVID-19-associated liver injury

Although the molecular mechanisms by which ferroptosis causes liver diseases are largely unknown, mounting evidence indicates that ferroptosis is fundamental to the pathogenesis of numerous types of liver diseases (Chen et al., 2022)—for example, ferroptosis probably promotes the progression of NASH by activating inflammatory responses, oxidative stress, and cell damage (Tsurusaki et al., 2019). In addition, ferroptosis

is associated with the replication of hepatitis C virus (Yamane et al., 2021) and liver fibrosis (Yuan et al., 2022). Therefore, we hypothesize that ferroptosis might be involved in COVID-19-related liver injury as well (Figure 1).

Notably, the histopathological changes in the livers of patients with SARS-CoV-2 infection largely consist of hepatic steatosis, Kupffer cell activation, thrombosis, and inflammatory infiltration (Sonzogni et al., 2020; Diaz et al., 2020; Lagana et al., 2020; Zhao et al., 2021). Here we examine the potential links between ferroptosis and these pathological features.

Ferroptosis and hepatic steatosis

Hepatic steatosis is defined as increased lipid accumulation in hepatocytes of at least 5% of liver weight, usually caused by the disruption of hepatic lipid homeostasis (Manne et al., 2018). A postmortem study of 48 patients who died from COVID-19 in two main hospitals in northern Italy noted hepatic steatosis in 54% of the samples (Sonzogni et al., 2020). Besides this, a meta-analysis of autopsy data from five studies, including 116 COVID-19 patients, also observed that more than half of the patients infected with SARS-CoV-2 displayed hepatic steatosis (Diaz et al., 2020). In addition to autopsy studies, the computed tomography scans of SARS-CoV-2-positive patients have exhibited higher frequencies of hepatic steatosis as well (Medeiros et al., 2020).

In patients with NASH, hepatocytic ferroptosis is arguably the trigger for inflammation (Tsurusaki et al., 2019), and liproxstatin-1 could reverse the severity of hepatic steatosis in mice fed with a methionine/choline-deficient diet (Qi et al., 2020). Additionally, enoyl coenzyme A hydratase 1, a key component in mitochondrial fatty acid β-oxidation, alleviates hepatic steatosis by inhibiting ferroptosis (Liu et al., 2021). Hence, suppressing ferroptosis could be a therapeutic strategy for ameliorating COVID-19-caused hepatic steatosis.

Ferroptosis and thrombosis

There is evidence that SARS-CoV-2 stimulates thrombosis as a result of increased coagulation and decreased fibrinolysis (Sastry et al., 2022). The SARS-CoV-2 virus enters the endotheliocyte through the ACE2 receptor, leading to the accumulation of inflammatory cells and release of cytokines. As a result, endothelial cell death and vessel wall injury occur and finally contribute to the formation of thrombus (Shao et al., 2021). Nuclear factor erythroid 2-related factor 2 constitutes an imperative target for the suppression of ferroptosis and associated endothelial cell inflammation and thrombosis (Shao

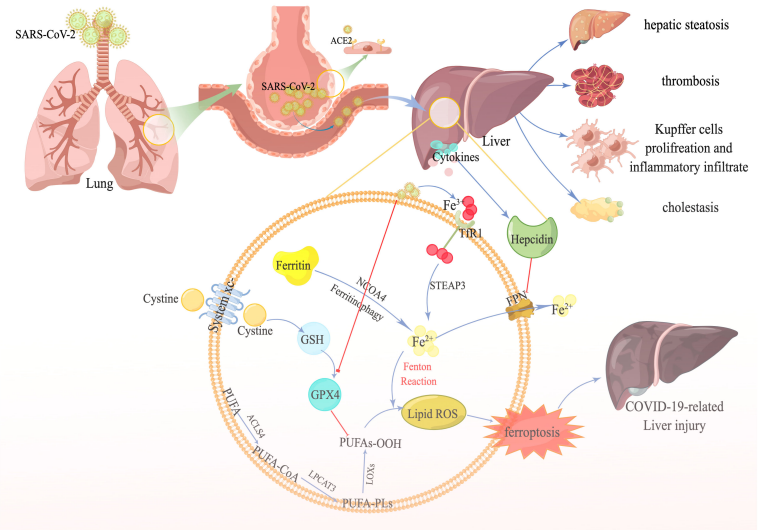

FIGURE 1
The potential link between ferroptosis and COVID-19-related liver injury. SARS-CoV-2 recognizes the angiotensin-converting enzyme 2 receptor in the alveoli, especially type II alveolar cells. SARS-CoV-2 subsequently reaches the blood circulation through the damaged blood–air barrier. Next, SARS-CoV-2 further infects the liver. After the infection, a plethora of transferrins carrying Fe^{3+} is transferred into the cell through transferrin receptor1. Eventually, Fe^{3+} is transformed to Fe^{2+} by STEAP family member 3, in addition to the Fe^{2+} degraded from excessive ferritin by nuclear receptor coactivator 4—contributing to the accumulation of ferrous iron in the cell. Numerous cytokines are also released during the infection, stimulating hepcidin expression, suppressing ferroportin, and aggravating the accumulation of iron even more. On the other hand, SARS-CoV-2 decreases the expression of GPX4, facilitating the iron overload-induced Fenton reaction, accompanied by polyunsaturated fatty acids, and producing massive amounts of lipid reactive oxygen species. Ultimately, ferroptosis occurs and causes liver injury.

et al., 2021). Furthermore, ferroptosis and platelet activation are interconnected, accompanied by proteasome and inflammasome activations, leading to thromboembolism (NaveenKumar et al., 2019).

Ferroptosis and inflammatory infiltration

Intense inflammatory reactions have been recorded in the portal and lobular regions during a SARS-CoV-2 infection. Meanwhile, Kupffer cells, an indispensable component of the liver, have also been shown to be activated and to participate in the inflammatory process (Nardo et al., 2021). In fact, ferroptosis and inflammatory infiltration in COVID-19 might be of reciprocal causation, forming a vicious circle. In the course of COVID-19, plenty of cytokines are released, among which interleukin-6 (IL-6) is the precise factor that stimulates hepcidin and ferritin syntheses (Moore and June, 2020). Eventually, the increments in hepcidin and ferritin contribute to iron overload, Kupffer cell activation (Li et al., 2022), and ferroptosis. Once the ferroptosis of hepatocytes occurs, damage-associated molecular patterns, inflammatory cytokines, and chemokines are released (Martin-Sanchez et al., 2017), which, in turn, enhance the infiltration of inflammatory cells and further aggravate COVID-19-associated liver injury.

Taken together, despite no direct evidence yet demonstrating the role of ferroptosis in SARS-CoV-2 infection-related liver injury, we believe that ferroptosis participates in the process of COVID-19-related liver injury in the following ways: (1) ferroptosis is closely associated with hepatic steatosis, which is one of the main characteristics of COVID-19-related liver injury; (2) SARS-CoV-2 stimulates the release of hepcidin, a peptide hormone produced by hepatocytes, leading to iron overload in the liver and triggering ferroptosis; and (3) SARS-CoV-2 infection disrupts the metabolism of lipids, potentially promoting lipid peroxidation in the context of iron overload. Moreover, ferroptosis-related liver injury in the course of a COVID-19 infection may share some similar mechanisms with other liver diseases, including but not limited to inflammatory reactions, immune responses, oxidative stress, and cell damage. Naturally, because direct cytotoxicity resulting from viral replication is considered the main mechanism of SARS-CoV-2-induced hepatic injury, the impact of ferroptosis on the replication of the virus could be the major difference in ferroptosis-induced liver injury between COVID-19 and other non-viral liver diseases.

Therapeutic opportunities

The discussion up to this point suggests a close link between ferroptosis and COVID-19-associated liver injury. Hence, targeting ferroptosis could be a promising therapeutic option. So far, ferroptosis can be suppressed mainly by iron chelators and lipophilic antioxidants. Iron chelators, like DFO, deferasirox, and deferiprone, chelate iron and prevent lipid peroxidation by regulating the Fenton reaction. Lipophilic antioxidants, including ferrostatin-1 (Fer-1), liproxstatin-1 (Lip-1), and α-tocopherol, scavenge lipid peroxides and block ferroptosis.

Deferoxamine has been shown to inhibit the replication of human immunodeficiency virus type-1 (Georgiou et al., 2000) and enhance hepatitis B virus infection response to IFN-α treatment (Bayraktar et al., 1996). In addition, deferoxamine decreases the levels of IL-6, the central inflammatory cytokine released during COVID-19, indicating that deferoxamine could be a potential drug treatment for COVID-19-induced liver injury. However, others have argued that deferoxamine is probably harmful to COVID-19 since iron chelators aggravate anemia from inflammation, weakening the ability of the host innate immunity to be counterproductive (Garrick and Ghio, 2021).

Fer-1 and Lip-1 are well-known ferroptosis inhibitors. Numerous studies have demonstrated that these inhibitors prevent the progression of liver steatosis and fibrosis (Qi et al., 2020; Liu et al., 2021; Zhu et al., 2021); however, no investigation has yet assessed the impact of their efficiency in the treatment of COVID-19. α-Tocopherol is a type of vitamin E reported to have the ability to suppress the SARS-CoV-2-RNA-dependent RNA polymerase (Pacl et al., 2021) and inhibit the main protease (Linani et al., 2022). Selenium, n-acetylcysteine, and polyphenols are all antioxidants and are regarded as ferroptosis suppressors; however, the administration of n-acetylcysteine yielded no benefit to severe COVID-19 sufferers, and the effects of selenium and polyphenols on COVID-19 are yet to be determined in larger clinical trials (Iddir et al., 2020; de Alencar et al., 2021; Balboni et al., 2022).

Notably, SARS-CoV-2 infection-induced tissue injury-related cell death is not limited to ferroptosis. Several other types of regulated cell deaths have also been linked to COVID-19 (Yapasert et al., 2021; Paolini et al., 2021). Therefore, simultaneously inhibiting different cell death types could alleviate SARS-CoV-2-induced injuries. Necrostatin-1, a widely used inhibitor of necroptosis, suppresses ferroptosis as well (Tonnus et al., 2021). It has been shown to protect against acetaminophen-induced hepatotoxicity (Takemoto et al., 2014; Saleh et al., 2021), which possibly participates in drug-generated liver injury during COVID-19.

Furthermore, inflammatory cytokine storms are thought to be critical factors in the causation of multiple organ failure syndrome in severe COVID-19 patients. Combining anti-inflammatory cytokines and interfering with ferric ion metabolism to improve the patients' resilience would be promising and should be investigated in future studies.

Conclusion and perspectives

Liver injury is common in patients infected with SARS-CoV-2, but the mechanism of COVID-19-related liver injury is largely unknown. Given the potential association between ferroptosis and liver histopathological changes in patients with COVID-19, we hypothesize that ferroptosis participates in SARS-CoV-2 infection-related liver injury. Targeting ferroptosis could be a promising strategy to reduce COVID-19-related hepatic injury.

However, to the best of our knowledge, there is no evidence of ferroptosis signature in the liver tissues of COVID-19 patients, let alone clinical trials evaluating inhibitors of ferroptosis in COVID-19-related liver injury. Although much progress has been made in our understanding of the pathological role of ferroptosis in liver diseases, we still have no idea of the precise role of ferroptosis, if any, in SARS-CoV-2-impaired liver and how ferroptosis drives the initiation of inflammation contributing to liver injury. By extension, we even have no idea whether ferroptosis during COVID-19 is the result of SARS-CoV-2 infection or if it is a compensatory mechanism to facilitate the replication and toxicity of SARS-CoV-2. Generally, several mechanisms are involved in ferroptosis, and we have described the link between three major ferroptosis pathways and COVID-19. However, we have no idea whether all these elements play significant roles in COVID-19-related hepatic injury.

Recent studies have identified apoptosis (Wang et al., 2020; Shirazi Tehrani et al., 2022) and autophagy (Shirazi Tehrani et al., 2022), the two most widely known RCD types, in the hepatic tissues of patients with COVID-19 as well. Moreover, pyroptosis, another form of RCD, is also said to contribute to COVID-19 pathogenesis (Junqueira et al., 2022). Therefore, it is rather difficult to decipher which RCD type is dominant in COVID-19-related liver injury. Studies using different antagonists to target corresponding cell death types in SARS-CoV-2-caused liver injury models could provide a better understanding of the matter.

Furthermore, even if ferroptosis can be considered a therapeutic target for COVID-19-related hepatic injury, other questions must still be answered: which sensitive biomarkers of ferroptosis can be identified, when should therapy start, and how can ferroptosis be inhibited without affecting healthy cells? What is more, the use of iron chelators could impact the hepatic iron metabolism, which, in turn, would disrupt iron-related cellular processes, such as energy production, oxygen transport, and DNA synthesis (Sheftel et al., 2012; Dev and Babitt, 2017) as well as impair immune response to the pathogen (Girelli et al., 2021). All these questions must be resolved to provide a complete and convincing argument for the clinical application of ferroptosis inhibitors.

Cell death is the termination of various pathophysiological processes and the basis of tissue injury. As a novel but important cell death type, ferroptosis might be a new and effective target for preventing and treating hepatic damage after a SARS-CoV-2 infection. Investigations are needed to establish the occurrence of ferroptosis in COVID-19 and elucidate its exact mechanism as well as its association with COVID-19-related liver injury.

Author contributions

LS and YX drafted the manuscript, KZ and MD edited the manuscript, and YC designed the study and revised the manuscript. All authors contributed to the article and approved the submitted version.

Funding

This research was funded by the Special Anti-epidemic Project by hospitals directly affiliated with universities—A Project Supported by the Scientific Research Fund of Zhejiang Provincial Education Department (grant no. Y202043882), Jiaxing Key Laboratory of Virus-Mediated Infectious Diseases (grant no. 2021-bdzdsys), Jiaxing Research Institute of Hepatology (grant no. jxsgbyjs), Jiaxing Key Supporting Discipline of Medicine (grant no. 2019-zc-02), and Program of the First Hospital of Jiaxing (grant no. 2021-YA-001).

Acknowledgments

We thank Figdraw (www.figdraw.com) for helping us produce the figures.

Conflict of interest

The authors declare that the research was conducted in the absence of any commercial or financial relationships that could be construed as a potential conflict of interest.

Publisher's note

References

Alvarez, S. W., Sviderskiy, V. O., Terzi, E. M., Papagiannakopoulos, T., Moreira, A. L., Adams, S., et al. (2017). NFS1 undergoes positive selection in lung tumours and protects cells from ferroptosis. *Nature* 551, 639–643. doi: 10.1038/nature24637

Amin, M. (2021). COVID-19 and the liver: overview. *Eur. J. Gastroenterol. Hepatol.* 33, 309–311. doi: 10.1097/MEG.0000000000001808

Balboni, E., Zagnoli, F., Filippini, T., Fairweather-Tait, S. J., and Vinceti, M. (2022). Zinc and selenium supplementation in COVID-19 prevention and treatment: a systematic review of the experimental studies. *J. Trace Elem. Med. Biol.* 71, 126956. doi: 10.1016/j.jtemb.2022.126956

Banchini, F., Vallisa, D., and Maniscalco P and Capelli, P. (2020). Iron overload and hepcidin overexpression could play a key role in COVID infection, and may explain vulnerability in elderly, diabetics, and obese patients. *Acta Biomed.* 91, e2020013. doi: 10.23750/abm.v91i3.9826

Bartolini, D., Stabile, A. M., Bastianelli, S., Giustarini, D., Pierucci, S., Busti, C., et al. (2021). SARS-CoV2 infection impairs the metabolism and redox function of cellular glutathione. *Redox Biol.* 45, 102041. doi: 10.1016/j.redox.2021.102041

Bayraktar, Y., Koseoglu, T., Somner, C., Kayhan, B., Temizer, A., Uzunalimoglu, B., et al. (1996). The use of deferoxamine infusions to enhance the response rate to interferon-alpha treatment of chronic viral hepatitis b. *J. Viral Hepat.* 3, 129–135. doi: 10.1111/j.1365-2893.1996.tb00003.x

Bednash, J. S., Kagan, V. E., Englert, J. A., Farkas, D., Tyurina, Y. Y., Tyurin, V. A., et al. (2022). Syrian Hamsters as a model of lung injury with SARS-CoV-2 infection: Pathologic, physiologic, and detailed molecular profiling. *Transl. Res.* 240, 1–16. doi: 10.1016/j.trsl.2021.10.007

Bersuker, K., Hendricks, J. M., Li, Z., Magtanong, L., Ford, B., Tang, P. H., et al. (2019). The CoQ oxidoreductase FSP1 acts parallel to GPX4 to inhibit ferroptosis. *Nature* 575, 688–692. doi: 10.1038/s41586-019-1705-2

Cai, Q., Huang, D., Yu, H., Zhu, Z., Xia, Z., Su, Y., et al. (2020). COVID-19: Abnormal liver function tests. *J. Hepatol.* 73, 566–574. doi: 10.1016/j.jhep.2020.04.006

Chagas, A. L., Fonseca, L. G. D., Coelho, F. F., Saud, L., Abdala, E., Andraus, W., et al. (2020). Management of hepatocellular carcinoma during the COVID-19 pandemic - sao paulo clinicas liver cancer group multidisciplinary consensus statement. *Clinics (Sao Paulo).* 75, e2192. doi: 10.6061/clinics/2020/e2192

Chen, J., Li, X., Ge, C., and Min J and Wang, F. (2022). The multifaceted role of ferroptosis in liver disease. *Cell Death Differ.* 29, 467–480. doi: 10.1038/s41418-022-00941-0

Chen, X., Yu, C., and Kang R and Tang, D. (2020). Iron metabolism in ferroptosis. *Front. Cell Dev. Biol.* 8, 590226. doi: 10.3389/fcell.2020.590226

Choudhary, N. S., Dhampalwar, S., and Saraf N and Soin, A. S. (2021). Outcomes of COVID-19 in patients with cirrhosis or liver transplantation. *J. Clin. Exp. Hepatol.* 11, 713–719. doi: 10.1016/j.jceh.2021.05.003

Colafrancesco, S., Alessandri, C., and Conti F and Priori, R. (2020). COVID-19 gone bad: A new character in the spectrum of the hyperferritinemic syndrome? *Autoimmun. Rev.* 19, 102573. doi: 10.1016/j.autrev.2020.102573

de Alencar, J. C. G., Moreira, C. L., Muller, A. D., Chaves, C. E., Fukuhara, M. A., da Silva, E. A., et al. (2021). Double-blind, randomized, placebo-controlled trial with n-acetylcysteine for treatment of severe acute respiratory syndrome caused by coronavirus disease 2019 (COVID-19). *Clin. Infect. Dis.* 72, e736–e741. doi: 10.1093/cid/ciaa1443

Dev, S., and Babitt, J. L. (2017). Overview of iron metabolism in health and disease. *Hemodial. Int.* 21 Suppl 1, S6–S20. doi: 10.1111/hdi.12542

Diaz, L. A., Idalsoaga, F., Cannistra, M., Candia, R., Cabrera, D., Barrera, F., et al. (2020). High prevalence of hepatic steatosis and vascular thrombosis in COVID-19: A systematic review and meta-analysis of autopsy data. *World J. Gastroenterol.* 26, 7693–7706. doi: 10.3748/wjg.v26.i48.7693

Dixon, S. J., Lemberg, K. M., Lamprecht, M. R., Skouta, R., Zaitsev, E. M., Gleason, C. E., et al. (2012). Ferroptosis: an iron-dependent form of nonapoptotic cell death. *Cell* 149, 1060–1072. doi: 10.1016/j.cell.2012.03.042

Doll, S., Freitas, F. P., Shah, R., Aldrovandi, M., da Silva, M. C., Ingold, I., et al. (2019). FSP1 is a glutathione-independent ferroptosis suppressor. *Nature* 575, 693–698. doi: 10.1038/s41586-019-1707-0

Doll, S., Proneth, B., Tyurina, Y. Y., Panzilius, E., Kobayashi, S., Ingold, I., et al. (2017). ACSL4 dictates ferroptosis sensitivity by shaping cellular lipid composition. *Nat. Chem. Biol.* 13, 91–98. doi: 10.1038/nchembio.2239

Do Van, B., Gouel, F., Jonneaux, A., Timmerman, K., Gele, P., Petrault, M., et al. (2016). Ferroptosis, a newly characterized form of cell death in parkinson's disease that is regulated by PKC. *Neurobiol. Dis.* 94, 169–178. doi: 10.1016/j.nbd.2016.05.011

Dowdle, W. E., Nyfeler, B., Nagel, J., Elling, R. A., Liu, S., Triantafellow, E., et al. (2014). Selective VPS34 inhibitor blocks autophagy and uncovers a role for NCOA4 in ferritin degradation and iron homeostasis *in vivo*. *Nat. Cell Biol.* 16, 1069–1079. doi: 10.1038/ncb3053

Fan, Z., Chen, L., Li, J., Cheng, X., Yang, J., Tian, C., et al. (2020). Clinical features of COVID-19-related liver functional abnormality. *Clin. Gastroenterol. Hepatol.* 18, 1561–1566. doi: 10.1016/j.cgh.2020.04.002

Fang, X., Wang, H., Han, D., Xie, E., Yang, X., Wei, J., et al. (2019). Ferroptosis as a target for protection against cardiomyopathy. *Proc. Natl. Acad. Sci. U. S. A.* 116, 2672–2680. doi: 10.1073/pnas.1821022116

Friedmann Angeli, J. P., Schneider, M., Proneth, B., Tyurina, Y. Y., Tyurin, V. A., Hammond, V. J., et al. (2014). Inactivation of the ferroptosis regulator Gpx4 triggers acute renal failure in mice. *Nat. Cell Biol.* 16, 1180–1191. doi: 10.1038/ncb3064

Garrick, M. D., and Ghio, A. J. (2021). Iron chelation may harm patients with COVID-19. *Eur. J. Clin. Pharmacol.* 77, 265–266. doi: 10.1007/s00228-020-02987-w

Georgiou, N. A., van der Bruggen, T., Oudshoorn, M., Nottet, H. S., Marx, J. J., and van Asbeck, B. S. (2000). Inhibition of human immunodeficiency virus type 1 replication in human mononuclear blood cells by the iron chelators deferoxamine, deferiprone, and bleomycin. *J. Infect. Dis.* 181, 484–490. doi: 10.1086/315223

Girelli, D., Marchi, G., and Busti F and Vianello, A. (2021). Iron metabolism in infections: Focus on COVID-19. *Semin. Hematol.* 58, 182–187. doi: 10.1053/j.seminhematol.2021.07.001

Gold, M. S., Sehayek, D., Gabrielli, S., Zhang, X., McCusker, C., and Ben-Shoshan, M. (2020). COVID-19 and comorbidities: a systematic review and meta-analysis. *Postgrad. Med.* 132, 749–755. doi: 10.1080/00325481.2020.1786964

Guan, W. J., Ni, Z. Y., Hu, Y., Liang, W. H., Ou, C. Q., He, J. X., et al. (2020). Clinical characteristics of coronavirus disease 2019 in China. *N. Engl. J. Med.* 382, 1708–1720. doi: 10.1056/NEJMoa2002032

Guloyan, V., Oganesian, B., Baghdasaryan, N., Yeh, C., Singh, M., Guilford, F., et al. (2020). Glutathione supplementation as an adjunctive therapy in COVID-19. *Antioxid. (Basel)* 9, 914–935. doi: 10.3390/antiox9100914

Han, Y., Zhu, J., Yang, L., Nilsson-Payant, B. E., Hurtado, R., Lacko, L. A., et al. (2022). SARS-CoV-2 infection induces ferroptosis of sinoatrial node pacemaker cells. *Circ. Res.* 130, 963–977. doi: 10.1161/CIRCRESAHA.121.320518

Hariyanto, T. I., Jodhinata, C., and Halim DA and Kurniawan, A. (2022). Association between viral hepatitis and increased risk of severe coronavirus disease 2019 (COVID-19) outcome: a systematic review and meta-analysis. *Gastroenterol. Hepatol. Bed Bench.* 15, 9–14.

He, J., Li, Z., Xia, P., Shi, A., FuChen, X., and Zhang J and Yu, P. (2022). Ferroptosis and ferritinophagy in diabetes complications. *Mol. Metab.* 60, 101470. doi: 10.1016/j.molmet.2022.101470

Huang, C., Wang, Y., Li, X., Ren, L., Zhao, J., Hu, Y., et al. (2020). Clinical features of patients infected with 2019 novel coronavirus in wuhan, China. *Lancet* 395, 497–506. doi: 10.1016/S0140-6736(20)30183-5

Huang, Q., Xie, Q., Shi, C. C., Xiang, X. G., Lin, L. Y., Gong, B. D., et al. (2009). Expression of angiotensin-converting enzyme 2 in CCL4-induced rat liver fibrosis. *Int. J. Mol. Med.* 23, 717–723. doi: 10.3892/ijmm_00000185

Iddir, M., Brito, A., Dingeo, G., Fernandez Del Campo, S. S., Samouda, H., and La Frano MR and Bohn, T. (2020). Strengthening the immune system and reducing inflammation and oxidative stress through diet and nutrition: Considerations during the COVID-19 crisis. *Nutrients* 12, 1562–1600. doi: 10.3390/nu12061562

Jacobs, W., Lammens, M., Kerckhofs, A., Voets, E., Van San, E., Van Coillie, S., et al. (2020). Vanden berghe T and jorens PG. fatal lymphocytic cardiac damage in coronavirus disease 2019 (COVID-19): autopsy reveals a ferroptosis signature. *ESC Heart Fail* 7(6), 3372–3781. doi: 10.1002/ehf2.12958

Junqueira, C., Crespo, A., Ranjbar, S., de Lacerda, L. B., Lewandrowski, M., Ingber, J., et al. (2022). FcgammaR-mediated SARS-CoV-2 infection of monocytes activates inflammation. *Nature* 606(7914), 576–584. doi: 10.1038/s41586-022-04702-4

Kagan, V. E., Mao, G., Qu, F., Angeli, J. P., Doll, S., Croix, C. S., et al. (2017). Oxidized arachidonic and adrenic PEs navigate cells to ferroptosis. *Nat. Chem. Biol.* 13, 81–90. doi: 10.1038/nchembio.2238

Komissarov, A. A., Karaseva, M. A., Roschina, M. P., Shubin, A. V., Lunina, N. A., and Kostrov SV and Demidyuk, I. V. (2021). Individual expression of hepatitis a virus 3c protease induces ferroptosis in human cells *in vitro*. *Int. J. Mol. Sci.* 22, 7906–7919. doi: 10.3390/ijms22157906

Kraft, V. A. N., Bezjian, C. T., Pfeiffer, S., Ringelstetter, L., Muller, C., Zandkarimi, F., et al. (2020). GTP cyclohydrolase 1/tetrahydrobiopterin counteract ferroptosis through lipid remodeling. *ACS Cent. Sci.* 6, 41–53. doi: 10.1021/acscentsci.9b01063

Krishnan, S., Nordqvist, H., Ambikan, A. T., Gupta, S., Sperk, M., Svensson-Akusjarvi, S., et al. (2021). Metabolic perturbation associated with COVID-19

disease severity and SARS-CoV-2 replication. *Mol. Cell Proteomics* 20, 100159. doi: 10.1016/j.mcpro.2021.100159

Kuch, E. M., Vellaramkalayil, R., Zhang, I., Lehnen, D., Brugger, B., Sreemmel, W., et al. (2014). Differentially localized acyl-CoA synthetase 4 isoenzymes mediate the metabolic channeling of fatty acids towards phosphatidylinositol. *Biochim. Biophys. Acta* 1841, 227–239. doi: 10.1016/j.bbalip.2013.10.018

Kumar, P., Osahon, O., Vides, D. B., Hanania, N., and Minard CG and Sekhar, R. V. (2021). Severe glutathione deficiency, oxidative stress and oxidant damage in adults hospitalized with COVID-19: implications for GlyNAC (Glycine and n-acetylcysteine) supplementation. *Antioxid. (Basel)* 11, 50–62. doi: 10.3390/antiox11010050

Kuo, C. Y., Chiu, V., Hsieh, P. C., Huang, C. Y., Huang, S. J., Tzeng, I. S., et al. (2020). Chrysophanol attenuates hepatitis b virus X protein-induced hepatic stellate cell fibrosis by regulating endoplasmic reticulum stress and ferroptosis. *J. Pharmacol. Sci.* 144, 172–182. doi: 10.1016/j.jphs.2020.07.014

Lagana, S. M., Kudose, S., Iuga, A. C., Lee, M. J., Fazlollahi, L., Remotti, H. E., et al. (2020). Hepatic pathology in patients dying of COVID-19: a series of 40 cases including clinical, histologic, and virologic data. *Mod. Pathol.* 33, 2147–2155. doi: 10.1038/s41379-020-00649-x

Lee, J. Y., Nam, M., Son, H. Y., Hyun, K., Jang, S. Y., Kim, J. W., et al. (2020). Polyunsaturated fatty acid biosynthesis pathway determines ferroptosis sensitivity in gastric cancer. *Proc. Natl. Acad. Sci. U. S. A.* 117, 32433–32442. doi: 10.1073/pnas.2006828117

Li, J., Cao, F., Yin, H. L., Huang, Z. J., Lin, Z. T., Mao, N., et al. (2020). Ferroptosis: past, present and future. *Cell Death Dis.* 11, 88. doi: 10.1038/s41419-020-2298-2

Li, L. X., Guo, F. F., and Liu H and Zeng, T. (2022). Iron overload in alcoholic liver disease: underlying mechanisms, detrimental effects, and potential therapeutic targets. *Cell Mol. Life Sci.* 79, 201. doi: 10.1007/s00018-022-04239-9

Linani, A., Benarous, K., Bou-Salah, L., and Yousfi M and Goumri-Said, S. (2022). Exploring structural mechanism of COVID-19 treatment with glutathione as a potential peptide inhibitor to the main protease: molecular dynamics simulation and mm/pbsa free energy calculations study. *Int. J. Pept. Res. Ther.* 28, 55. doi: 10.1007/s10989-022-10365-6

Liu, G. Z., Xu, X. W., Tao, S. H., and Gao MJ and Hou, Z. H. (2021). HBx facilitates ferroptosis in acute liver failure *via* EZH2 mediated SLC7A11 suppression. *J. BioMed. Sci.* 28, 67. doi: 10.1186/s12929-021-00762-2

Liu, B., Yi, W., Mao, X., and Yang L and Rao, C. (2021). Enoyl coenzyme a hydratase 1 alleviates nonalcoholic steatohepatitis in mice by suppressing hepatic ferroptosis. *Am. J. Physiol. Endocrinol. Metab.* 320, E925–E937. doi: 10.1152/ajpendo.00614.2020

Mancias, J. D., Wang, X., Gygi, S. P., and Harper JW and Kimmelman, A. C. (2014). Quantitative proteomics identifies NCOA4 as the cargo receptor mediating ferritinophagy. *Nature* 509, 105–109. doi: 10.1038/nature13148

Manne, V., Handa, P., and Kowdley, K. V. (2018). Pathophysiology of nonalcoholic fatty liver disease/nonalcoholic steatohepatitis. *Clin. Liver Dis.* 22, 23–37. doi: 10.1016/j.cld.2017.08.007

Martin-Fernandez, M., Aller, R., Heredia-Rodriguez, M., Gomez-Sanchez, E., Martinez-Paz, P., Gonzalo-Benito, H., et al. (2021). Lipid peroxidation as a hallmark of severity in COVID-19 patients. *Redox Biol.* 48, 102181. doi: 10.1016/j.redox.2021.102181

Martin-Sanchez, D., Ruiz-Andres, O., Poveda, J., Carrasco, S., Cannata-Ortiz, P., Sanchez-Nino, M. D., et al. (2017). Ferroptosis, but not necroptosis, is important in nephrotoxic folic acid-induced AKI. *J. Am. Soc. Nephrol.* 28, 218–229. doi: 10.1681/ASN.2015121376

Medeiros, A. K., Barbisan, C. C., Cruz, I. R., de Araujo, E. M., Libanio, B. B., Albuquerque, K. S., et al. (2020). Higher frequency of hepatic steatosis at CT among COVID-19-positive patients. *Abdom. Radiol. (NY).* 45, 2748–2754. doi: 10.1007/s00261-020-02648-7

Moore, J. B., and June, C. H. (2020). Cytokine release syndrome in severe COVID-19. *Science* 368, 473–474. doi: 10.1126/science.abb8925

Moreira, J. L. S., Barbosa, S. M. B., and Goncalves Junior, J. (2021). Pathophysiology and molecular mechanisms of liver injury in severe forms of COVID-19: An integrative review. *Clin. Res. Hepatol. Gastroenterol.* 45, 101752. doi: 10.1016/j.clinre.2021.101752

Nardo, A. D., Schneeweiss-Gleixner, M., Bakail, M., Dixon, E. D., and Lax SF and Trauner, M. (2021). Pathophysiological mechanisms of liver injury in COVID-19. *Liver Int.* 41, 20–32. doi: 10.1111/liv.14730

NaveenKumar, S. K., Hemshekhar, M., and Kemparaju K and Girish, K. S. (2019). Hemin-induced platelet activation and ferroptosis is mediated through ROS-driven proteasomal activity and inflammasome activation: Protection by melatonin. *Biochim. Biophys. Acta Mol. Basis Dis.* 1865, 2303–2316. doi: 10.1016/j.bbadis.2019.05.009

Pacl, H. T., Tipper, J. L., Sevalkar, R. R., Crouse, A., Crowder, C., Institute, UABPM, et al. (2021). Water-soluble tocopherol derivatives inhibit SARS-CoV-2 RNA-dependent RNA polymerase. *bioRxiv*. doi: 10.1101/2021.07.13.449251

Paizis, G., Tikellis, C., Cooper, M. E., Schembri, J. M., Lew, R. A., Smith, A. I., et al. (2005). Chronic liver injury in rats and humans upregulates the novel enzyme angiotensin converting enzyme 2. *Gut* 54, 1790–1796. doi: 10.1136/gut.2004.062398

Paolini, A., Borella, R., De Biasi, S., Neroni, A., Mattioli, M., Lo Tartaro, D., et al. (2021). Cell death in coronavirus infections: Uncovering its role during COVID-19. *Cells* 10 1585–1605. doi: 10.3390/cells10071585

Park, M. W., Cha, H. W., Kim, J., Kim, J. H., Yang, H., Yoon, S., et al. (2021). NOX4 promotes ferroptosis of astrocytes by oxidative stress-induced lipid peroxidation *via* the impairment of mitochondrial metabolism in alzheimer's diseases. *Redox Biol.* 41, 101947. doi: 10.1016/j.redox.2021.101947

Perricone, C., Bartoloni, E., Bursi, R., Cafaro, G., Guidelli, G. M., and Shoenfeld Y and Gerli, R. (2020). COVID-19 as part of the hyperferritinemic syndromes: the role of iron depletion therapy. *Immunol. Res.* 68, 213–224. doi: 10.1007/s12026-020-09145-5

Qi, J., Kim, J. W., Zhou, Z., and Lim CW and Kim, B. (2020). Ferroptosis affects the progression of nonalcoholic steatohepatitis *via* the modulation of lipid peroxidation-mediated cell death in mice. *Am. J. Pathol.* 190, 68–81. doi: 10.1016/j.ajpath.2019.09.011

Qi, X., Liu, Y., Wang, J., Fallowfield, J. A., Wang, J., Li, X., et al. (2021). Clinical course and risk factors for mortality of COVID-19 patients with pre-existing cirrhosis: a multicentre cohort study. *Gut* 70, 433–436. doi: 10.1136/gutjnl-2020-321666

Saleh, N. E. H., Saad, A. H., Elbassuoni, E. A., El-Tahawy, N. F., and Abdel-Hakeem, E. A. (2021). Potential benefits of using hydrogen sulfide, vitamin e and necrostatin-1 to counteract acetaminopheninduced hepatotoxicity in rats. *Bratisl. Lek. Listy.* 122, 732–738. doi: 10.4149/BLL_2021_117

Sastry, S., Cuomo, F., and Muthusamy, J. (2022). COVID-19 and thrombosis: The role of hemodynamics. *Thromb. Res.* 212, 51–57. doi: 10.1016/j.thromres.2022.02.016

Shao, Y., Saredy, J., Xu, K., Sun, Y., Saaoud, F., Ct, D., et al. (2021). Endothelial immunity trained by coronavirus infections, DAMP stimulations and regulated by anti-oxidant NRF2 may contribute to inflammations, myelopoiesis, COVID-19 cytokine storms and thromboembolism. *Front. Immunol.* 12, 653110. doi: 10.3389/fimmu.2021.653110

Sheftel, A. D., Mason, A. B., and Ponka, P. (2012). The long history of iron in the universe and in health and disease. *Biochim. Biophys. Acta* 1820, 161–187. doi: 10.1016/j.bbagen.2011.08.002

Shirazi Tehrani, A., Tabatabaei Mirakabad, F. S., Abdollahifar, M. A., Mollazadehghomi, S., Darabi, S., Forozesh, M., et al. (2022). Severe acute respiratory syndrome coronavirus 2 induces hepatocyte cell death, active autophagosome formation and caspase 3 up-regulation in postmortem cases: stereological and molecular study. *Tohoku J. Exp. Med.* 256, 309–319. doi: 10.1620/tjem.2022.J007

Silvagno, F., Vernone, A., and Pescarmona, G. P. (2020). The role of glutathione in protecting against the severe inflammatory response triggered by COVID-19. *Antioxid. (Basel)* 9, 624–639. doi: 10.3390/antiox9070624

Singh, A., Hussain, S., and Antony, B. (2021). Non-alcoholic fatty liver disease and clinical outcomes in patients with COVID-19: A comprehensive systematic review and meta-analysis. *Diabetes Metab. Syndr.* 15, 813–822. doi: 10.1016/j.dsx.2021.03.019

Sonzogni, A., Previtali, G., Seghezzi, M., Grazia Alessio, M., Gianatti, A., Licini, L., et al. (2020). Liver histopathology in severe COVID 19 respiratory failure is suggestive of vascular alterations. *Liver Int.* 40, 2110–2116. doi: 10.1111/liv.14601

Takemoto, K., Hatano, E., Iwaisako, K., Takeiri, M., Noma, N., Ohmae, S., et al. (2014). Necrostatin-1 protects against reactive oxygen species (ROS)-induced hepatotoxicity in acetaminophen-induced acute liver failure. *FEBS Open Bio.* 4, 777–787. doi: 10.1016/j.fob.2014.08.007

Tonnus, W., Meyer, C., Steinebach, C., Belavgeni, A., von Massenhausen, A., Gonzalez, N. Z., et al. (2021). Dysfunction of the key ferroptosis-surveilling systems hypersensitizes mice to tubular necrosis during acute kidney injury. *Nat. Commun.* 12, 4402. doi: 10.1038/s41467-021-24712-6

Tsurusaki, S., Tsuchiya, Y., Koumura, T., Nakasone, M., Sakamoto, T., Matsuoka, M., et al. (2019). Hepatic ferroptosis plays an important role as the trigger for initiating inflammation in nonalcoholic steatohepatitis. *Cell Death Dis.* 10, 449. doi: 10.1038/s41419-019-1678-y

Wang, Y., Huang, J., Sun, Y., Stubbs, D., He, J., Li, W., et al. (2021). SARS-CoV-2 suppresses mRNA expression of selenoproteins associated with ferroptosis, endoplasmic reticulum stress and DNA synthesis. *Food Chem. Toxicol.* 153, 112286. doi: 10.1016/j.fct.2021.112286

Wang, Y., Liu, S., Liu, H., Li, W., Lin, F., Jiang, L., et al. (2020). SARS-CoV-2 infection of the liver directly contributes to hepatic impairment in patients with COVID-19. *J. Hepatol.* 73, 807–816. doi: 10.1016/j.jhep.2020.05.002

Wanner, N., Andrieux, G., Badia, I. M. P., Edler, C., Pfefferle, S., Lindenmeyer, M. T., et al. (2022). Molecular consequences of SARS-CoV-2 liver tropism. *Nat. Metab.* 4, 310–319. doi: 10.1038/s42255-022-00552-6

Wan, Y., Shang, J., Graham, R., and Baric RS and Li, F. (2020). Receptor recognition by the novel coronavirus from wuhan: an analysis based on decade-

long structural studies of SARS coronavirus. *J. Virol.* 94, e00127–20. doi: 10.1128/JVI.00127-20

Yadav, D. K., Singh, A., Zhang, Q., Bai, X., Zhang, W., Yadav, R. K., et al. (2021). Involvement of liver in COVID-19: systematic review and meta-analysis. *Gut* 70, 807–809. doi: 10.1136/gutjnl-2020-322072

Yamane, D., Hayashi, Y., Matsumoto, M., Nakanishi, H., Imagawa, H., Kohara, M., et al. (2021). FADS2-dependent fatty acid desaturation dictates cellular sensitivity to ferroptosis and permissiveness for hepatitis c virus replication. *Cell Chem. Biol* 29(5)799–810. doi: 10.1016/j.chembiol.2021.07.022

Yang, W. S., Kim, K. J., Gaschler, M. M., Patel, M., Shchepinov, M. S., and Stockwell, B. R. (2016). Peroxidation of polyunsaturated fatty acids by lipoxygenases drives ferroptosis. *Proc. Natl. Acad. Sci. U. S. A.* 113, E4966–E4975. doi: 10.1073/pnas.1603244113

Yang, W. S., SriRamaratnam, R., Welsch, M. E., Shimada, K., Skouta, R., Viswanathan, V. S., et al. (2014). Regulation of ferroptotic cancer cell death by GPX4. *Cell* 156, 317–331. doi: 10.1016/j.cell.2013.12.010

Yan, H. F., Zou, T., Tuo, Q. Z., Xu, S., Li, H., and Belaidi AA and Lei, P. (2021). Ferroptosis: mechanisms and links with diseases. *Signal Transduct. Target Ther.* 6, 49. doi: 10.1038/s41392-020-00428-9

Yapasert, R., Khaw-On, P., and Banjerdpongchai, R. (2021). Coronavirus infection-associated cell death signaling and potential therapeutic targets. *Molecules* 26, 7459–7485. doi: 10.3390/molecules26247459

Yuan, S., Wei, C., Liu, G., Zhang, L., Li, J., Li, L., et al. (2022). Sorafenib attenuates liver fibrosis by triggering hepatic stellate cell ferroptosis *via* HIF-1alpha/SLC7A11 pathway. *Cell Prolif.* 55, e13158. doi: 10.1111/cpr.13158

Zaim, S., Chong, J. H., Sankaranarayanan, V., and Harky, A. (2020). COVID-19 and multiorgan response. *Curr. Probl. Cardiol.* 45, 100618. doi: 10.1016/j.cpcardiol.2020.100618

Zarkovic, N., Orehovec, B., Milkovic, L., Barsic, B., Tatzber, F., Wonisch, W., et al. (2021). Preliminary findings on the association of the lipid peroxidation product 4-hydroxynonenal with the lethal outcome of aggressive COVID-19. *Antioxid. (Basel)* 10, 1341–1350. doi: 10.3390/antiox10091341

Zhao, C. L., Rapkiewicz, A., Maghsoodi-Deerwester, M., Gupta, M., Cao, W., Palaia, T., et al. (2021). Pathological findings in the postmortem liver of patients with coronavirus disease 2019 (COVID-19). *Hum. Pathol.* 109, 59–68. doi: 10.1016/j.humpath.2020.11.015

Zhou, F., Yu, T., Du, R., Fan, G., Liu, Y., Liu, Z., et al. (2020). Clinical course and risk factors for mortality of adult inpatients with COVID-19 in wuhan, China: a retrospective cohort study. *Lancet* 395, 1054–1062. doi: 10.1016/S0140-6736(20)30566-3

Zhu, Z., Zhang, Y., Huang, X., Can, L., Zhao, X., Wang, Y., et al. (2021). Thymosin beta 4 alleviates non-alcoholic fatty liver by inhibiting ferroptosis *via* up-regulation of GPX4. *Eur. J. Pharmacol.* 908, 174351. doi: 10.1016/j.ejphar.2021.174351

frontiers | Frontiers in Cellular and Infection Microbiology

TYPE Original Research
PUBLISHED 16 September 2022
DOI 10.3389/fcimb.2022.932563

OPEN ACCESS

EDITED BY
Viviane Fongaro Botosso,
Butantan Institute, Brazil

REVIEWED BY
Jessica Snowden,
University of Arkansas for Medical Sciences, United States
Adriana Malheiro,
Federal University of Amazonas, Brazil

*CORRESPONDENCE
Antonio Carlos R. Vallinoto
vallinoto@ufpa.br

SPECIALTY SECTION
This article was submitted to Clinical Microbiology, a section of the journal Frontiers in Cellular and Infection Microbiology

RECEIVED 29 April 2022
ACCEPTED 29 August 2022
PUBLISHED 16 September 2022

CITATION
da Silva Torres MK, Lopes FT, de Lima ACR, Cordeiro Lima CN, dos Santos Brito WR, Gonçalves JSS, dos Santos Oliveira O, de Oliveira Freitas V, dos Santos BC, Santos de Sousa R, Carvalho Gomes JL, Sarmento Botelho BJ, Alves Correa AC, Machado LFA, Martins Feitosa RN, Lima SS, Cayres Vallinoto IMV and Vallinoto ACR (2022) Changes in the seroprevalence and risk factors between the first and second waves of COVID-19 in a metropolis in the Brazilian Amazon. *Front. Cell. Infect. Microbiol.* 12:932563. doi: 10.3389/fcimb.2022.932563

Changes in the seroprevalence and risk factors between the first and second waves of COVID-19 in a metropolis in the Brazilian Amazon

Maria Karoliny da Silva Torres[1,2], Felipe Teixeira Lopes[1,2], Aline Cecy Rocha de Lima[1,2], Carlos Neandro Cordeiro Lima[1,2], Wandrey Roberto dos Santos Brito[1,2], Janete Silvana S. Gonçalves[1,2], Onayane dos Santos Oliveira[1,2], Vanessa de Oliveira Freitas[1], Bernardo Cintra dos Santos[1], Renata Santos de Sousa[1,2], Jayanne Lilian Carvalho Gomes[1], Bruno José Sarmento Botelho[1], Ana Carolina Alves Correa[1], Luiz Fernando A. Machado[1,2], Rosimar Neris Martins Feitosa[1,2], Sandra Souza Lima[1,2], Izaura Maria Vieira Cayres Vallinoto[1,2] and Antonio Carlos R. Vallinoto[1,2]*

[1]Laboratory of Virology, Institute of Biological Sciences, Federal University of Pará, Belém, Brazil, [2]Graduate Program in Biology of Infectious and Parasitic Agents, Federal University of Pará, Belém, Brazil

In Brazil, the coronavirus disease 2019 (COVID-19) epidemic spread rapidly in a heterogeneous way, mainly due to the different socioeconomic and behavioral characteristics of different regional populations and different evaluation periods. We performed a cross-sectional study including 1,337 individuals (first wave = 736/second wave = 601) after the first two waves of COVID-19 in the city of Belém, the capital of the state of Pará. The detection of IgG anti-SARS-CoV-2 antibodies was performed using an enzyme-linked immunosorbent assay test followed by statistical analysis using the RStudio program. Our results showed an increase in the seroprevalence (first wave= 39.1%/second wave= 50.1%) of anti-severe acute respiratory syndrome coronavirus 2 (SARS-CoV-2) IgG antibodies in the population of Belém from the first to the second pandemic wave. Advanced age, primary or secondary education level, lack of social isolation, and a low frequency of protective mask use were considered risk factors for SARS-CoV-2 infection during the first wave compared to the second wave. This study is one of the firsts to provide important information about the dynamics of virus circulation and the groups vulnerable to exposure in the two major periods. Our data emphasize the socioeconomic characteristics of the affected population and that nonpharmacological prevention measures are crucial for combating the pandemic.

KEYWORDS

SARS-CoV-2, COVID-19, seroepidemiology, Belém, Amazon, Brazil

Introduction

As of March 19, 2022, Brazil had reported approximately 29,882,397 confirmed cases of severe acute respiratory syndrome coronavirus 2 (SARS-CoV-2) infection and approximately 659,241 deaths due to coronavirus disease 2019 (COVID-19) (Brasil, 2022a). In the state of Pará, northern Brazil, the number of cases and deaths, respectively, was higher at the peak of the first wave (from May 2020 to February 2021) of COVID-19 than at the peak of the second wave (in March 2021). The city of Belém, the capital of the state, thus far has reported 135,542 confirmed cases and approximately 5,294 deaths, with a case fatality rate (3.91%) that is higher than that observed for the state of Pará (2.42%) (SESPA, 2022). Incidence, prevalence, and mortality rates have varied throughout the country, depending on the region and the strategies adopted to control viral spread, which have been inconsistent among states of the federation over time (Ribeiro et al., 2020).

At the population level, the incidence of infection during each period, the factors associated with symptomatic or asymptomatic disease, and the duration of the antibody response against infection remain unclear. Seroprevalence studies allow a better understanding of the course of the disease in the general population and the identification of population groups less protected by public health measures, generating important information that stimulates the formulation of more efficient prevention strategies for future epidemic waves.

Therefore, our study sought to assess the seroprevalence of IgG anti-SARS-CoV-2 antibodies in the population of the city of Belém at two key moments in the COVID-19 pandemic, after the first and second wave of the pandemic, respectively. In addition, we sought to identify and compare the socioeconomic and behavioral profiles and risk factors for exposure to SARS-CoV-2 infection in the two periods to contribute to a better description and understanding of the impact of this pandemic in the city of Belém.

Materials and methods

Ethical aspects

The project was submitted to and approved by the National Research Ethics Committee (CONEP) and the Ethics Committee in Research with Human Beings of the Institute of Health Sciences of the Federal University of Pará (CAAE: 31800720.1.0000.0018) in compliance with the guidelines and standards of regulatory agencies for research involving human subjects. The participants were recruited from public calls published in different locations in the city of Belém (schools, churches, community centers, condominiums, and university) where health actions were carried out. Only voluntary individuals were included in the survey. Individuals already vaccinated with one or two doses against SARS-CoV-2, those who did not respond to the epidemiological questionnaire, those who did not sign the informed consent form, and those under 7 years of age were excluded from the research. There was no overlap of the individuals analyzed in the two study periods.

After signing the free and informed consent form, the individuals were interviewed using a structured questionnaire that included questions about clinical, demographic, and behavioral characteristics related to possible risk factors for SARS-CoV-2 infection. We obtained signed informed consent forms from individuals aged 18 years or older. Children aged 7–11 years and adolescents aged 12–17 years signed a free and informed assent term, and their respective parents or guardians signed an informed consent form.

Collection, processing, and storage of samples

After completing the questionnaire and signing the informed consent form, blood samples (10 ml) were collected *via* venipuncture in a vacuum tube containing EDTA. Subsequently, the samples were processed anonymously in the virology laboratory, separating plasma and leukocytes, which were stored at -70°C.

Study design and sampling

This cross-sectional study included 1,337 volunteer individuals residing in the city of Belém during two major periods: after the first wave of COVID-19 (October 2020 to February 2021, 736 individuals) and after the second wave of COVID-19 (March 2021 to December 2021, 601 individuals).

The following information was collected by self-declaration from each participant: (i) sociodemographic data (age, sex, income based on minimum wage, skin color), (ii) presence of comorbidities, and (iii) behavioral information about prevention measures, such as mask use, travel, hand hygiene, social distancing, and having had contact with people infected with SARS-COV-2. Considering that the current population of the city of Belém was composed of a mixture of three ethnicities (white European, indigenous, and black African) and that the three ethnic components are completely integrated in the current population, we classified the volunteers of the present study based on self-identification in relation to skin color, using the same criteria used by the IBGE (Brazilian Institute of Geography and Statistics— https://www.ibge.gov.br) to carry out the Brazilian census. Participant data were recorded using EPI Info software version TM 7.2.4 (CDC, 2021) and stored on

the local server of the Virus Laboratory of the Federal University of Pará.

Detection of anti-SARS-CoV-2 IgG antibodies

The detection of anti-SARS-CoV-2 IgG antibodies was performed using an enzyme-linked immunosorbent assay (Euroimmun, Lübeck, Germany) that utilized the recombinant structural peptide S1 (RBD domain) of the spike protein as an antigen. The protocol followed the manufacturer's recommendations. The samples were classified as non-reagent (ratio <0.8), indeterminate (0.8 ≤ ratio ≤ 1.1) or reagent (ratio >1.1) for IgG, as suggested by the manufacturer. The assay has a clinical sensitivity of 75–93.8% (>10–20 days to ≥21 days after disease onset) and a specificity of 99.6% for IgG antibodies, according to the manufacturer's guidelines.

Statistical analysis

All analyses were performed in R Studio version 4.1.1 using the R packages. Associations between the presence of anti-SARS-CoV-2 IgG antibodies and the study variables were estimated using univariate analyses and chi-square test or G test. A *P*-value less than or equal to 0.05 was considered statistically significant. Uni- and multivariate logistic regression analyses were performed to explore the associations between risk factors (social, economic, and behavioral characteristics and symptoms) and the presence of anti-SARS-CoV-2 antibodies as well as the relationships between symptomatic and asymptomatic disease and the presence of these antibodies. To classify symptomatic individuals, the definitions established by the Brazilian Ministry of Health (Brasil, 2020) were used. Cases that did not meet these criteria or individuals who did not present any symptoms were classified as asymptomatic. The graphs presented herein were created in GraphPad Prism 8.0 and R Studio version 4.1.1.

Results

Seroprevalence

After the first wave of COVID-19, 736 individuals were invited and agreed to participate in the study. According to the serology results, 275 (37.3%) individuals were classified as reagent with regard to anti-SARS-CoV-2 IgG antibodies, 429 (58.2%) were classified as non-reagent, and 32 (4.3%) had indeterminate results. After the second wave, 601 individuals participated in the study; 284 (47.2%) were classified as reagent regarding IgG anti-SARS-CoV-2 antibodies, 274 (45.6%) were classified as non-reagent, and 43 (7.2%) had indeterminate results.

In total, only 704 individuals (95.6%) after the first wave and 558 (92.8%) after the second wave with confirmed laboratory diagnoses were selected for statistical analysis because they had accurate confirmation of the diagnosis (reagents or non-reagents). Individuals with indeterminate results, that is, with inconclusive laboratory results, were excluded from the statistical analyzes. In both periods, the seroprevalence of anti-SARS-CoV-2 IgG antibodies was higher in female individuals (first wave: $F = 65.1\%$/second wave: $F = 64.4\%$; $p = 0.8009$) than in male individuals (Table 1).

In the first wave, the seroprevalence was highest in individuals with advanced age [≥70 years (47.6%)], which was different from the second wave, in which younger individuals were the most affected (19–29 years: 96.6%) (Figure 1A). Individuals with primary and secondary education levels had the highest seroprevalence rates in the first wave, while those with higher education (35.9%) levels were more affected in the second wave (Figure 1B). Self-declared brown skin color (first wave = 62.0%/second wave = 53.9%; $p = 0.0385$) (Figure 1C) and a family income ≤2 times the minimum wage (first wave = 41.9%/second wave = 42.3%; $p = 0.2953$) (Figure 1D) were associated with the highest antibody rates in the two periods. The most frequent comorbidities in both periods were hypertension (first wave = 24.7%/second wave = 11.3%; $p < 0.0001$) and asthma (first wave = 9.1%/second wave = 8.10%; $p = 0.6756$). There was no correlation between seropositivity for anti-SARS-CoV-2 IgG antibody and the presence of comorbidities (Table 1).

Seroprevalence associated with behavioral characteristics

During the second wave, there were increases in the number of people with a travel history (OR = 0.69; 95% CI = 0.49–0.9; $p = 0.0346$) and with contact with infected people (OR = 0.65; 95% CI = 0.44–0.95; $p = 0.0290$), resulting in higher seroprevalence compared to that in the first wave (Table 2). In addition, in the same period, we observed reductions in the number of people who reported wearing masks (OR = 2.89; 95% CI = 1.12–7.40; $p = 0.0270$), washing their hands (OR = 1.15; 95% CI = 0.78–2.91; $p = 0.2169$), and practicing social isolation (OR = 1.99; 95% CI = 1.13–3.48; $p = 0.0157$) (Figure 2).

Risk factors associated with SARS-CoV-2 infection

Individuals aged between 60 and 69 years (OR = 6.41; 95% CI = 2.12–19.3; $p = 0.0009$) and ≥70 years (OR = 3.41; 95% CI = 1.26–10.6; $p = 0.0166$), with an elementary school (OR = 3.55; 95% CI = 1.56–10.6; $p < 0.0001$) or high school education level (OR = 3.44; 95% CI = 1.98–5.93; $p < 0.0001$), who did not use a mask frequently (OR = 3.38; 95% CI = 1.24–9.18; $p = 0.0168$), and who

10.3389/fcimb.2022.932563

TABLE 1 Socioeconomic characteristics, prevalence of comorbidities, and risk of SARS-CoV-2 infection.

Variables	First Wave (%)	95% IC	Second wave (%)	95% IC	Univariate analysisOR (95% IC)	*P*	Multivariate analysisOR (95% IC)	*P*
Total	275 (39.1)	–	284 (50.1)	–	–			
Sex								
Female	179 (65.1)	59–70	183 (64.4)	58–70	(Ref)			
Male	96 (34.9)	29–40	101 (35.6)	30–41	0.96 (0.67–1.35)	0.8009		
Age								
≤18	18 (26.9)	3–9	20 (50.0)	4–10	(Ref)		(Ref)	
19–29	55 (47.4)	15–24	86 (96.6)	24–35	0.72 (0.35–1.48)	0.3784		
30–39	29 (31.9)	6–14	58 (33.7)	15–25	0.55 (0.2–1.20)	0.1383		
40–49	48 (38.4)	13–21	44 (42.7)	11–19	1.21 (0.5–2.58)	0.6183		
50–59	55 (44.7)	15–24	45 (60.8)	16–20	1.38 (0.65–2.92)	0.3958		
60–69	37 (37.0)	9–17	10 (21.7)	1–5	4.11 (1.50–10.5)	**0.0033**	6.41 (2.12–19.3)	**0.0009**
≥70	30 (47.6)	7–14	9 (75.0)	1–5	3.58 (1.34–9.56)	**0.0109**	3.68 (1.26–10.6)	**0.0166**
NI	3 (15.8)	–	12 (54.5)	–				
Education								
Illiterate	–	–	02 (0.70)	–	–	*		
Elementary school	38 (13.8)	9–17	23 (8.10)	4–11	4.80 (2.53–9.11)	**<0.0001**	3.55 (1.56–8.03)	**<0.0001**
High school	110 (40.0)	34–45	68 (23.9)	19–28	4.58 (2.82–7.44)	**<0.0001**	3.44 (1.98–5.93)	**<0.0001**
Undergraduate school	89 (32.4)	36–37	102 (35.9)	30–41	3.04 (1.87–4.91)	**<0.0001**		
Graduate school	38 (13.8)	9–17	84 (29.6)	24–34	(Ref)		(Ref)	
NI	0	–	05 (1.76)	–	–			
Skin color								
Yellow	3 (1.1)	–	07 (2.46)	0–4	0.40 (0.10–1.65)	0.2089		
White	62 (22.5)	17–27	60 (21.1)	16–25	(Ref)			
Black	36 (13.1)	9–17	58 (20.4)	15–25	0.59 (0.34–1.02)	**0.0590**		
Brown	173 (62.1)	57–68	153 (53.9)	48–59	0.70 (1.62–0.74)	0.7473		
NI	1 (0.4)	–	06 (2.11)	–				
Income								
≤ 1 or 2	135 (49.1)	43–55	120 (42.3)	36–48	1.22 (0.82–1.80)	0.3216		
3 or 4	53 (19.3)	14–23	66 (23.2)	18–28	0.86 (0.53–1.39)	0.5490		
≥5	79 (28.7)	23–34	84 (29.6)	24–34	(Ref)			
NI	8 (2.9)	–	14 (4.93)	–				
Comorbidity								
Diabetes	22 (8.0)	4–11	20 (7.04)	4–10	1.15 (0.61–2.15)	0.6678		
Asthma	25 (9.1)	5–12	23 (8.10)	4–11	1.13 (0.62–2.05)	0.6756		
Autoimmune disease	5 (1.8)	–	05 (1.76)	–	1.03 (0.29–3.60)	0.9590		
Cardiovascular disease	11 (4.0)	1–6	07 (2.46)	0–4	1.81 (0.70–4.65)	0.2215		
Hypertension	68 (24.7)	19–29	32 (11.3)	7–14	2.64 (1.66–4.16)	**<0.0001**		
Obesity	13 (4.7)	2–7	10 (3.52)	1–5	1.47 (0.64–3.87)	0.3626		
Tuberculosis	1 (0.4)	–	0 (0.0)	–	–			
None	157 (57.1)	–	176 (62.0)	–	(Ref)			

OR, odds ratio; NI, not informed; *, not significant.
Bold means the values are statiscally significant.

10.3389/fcimb.2022.932563

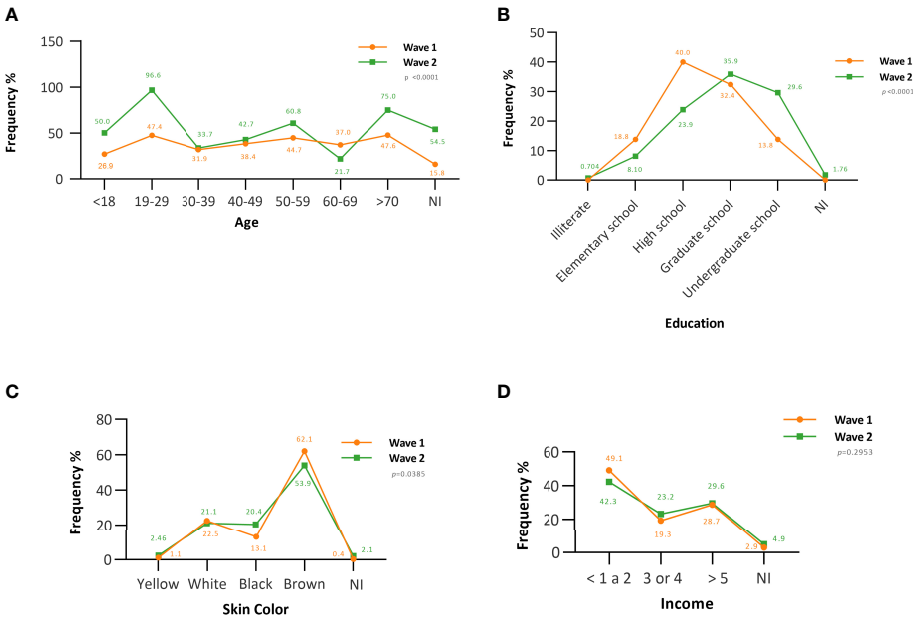

FIGURE 1
The frequency of anti-SARS-CoV-2 IgG antibodies according to socioeconomic characteristics. **(A)** Age-associated seroprevalence. **(B)** Seroprevalence associated with education level. **(C)** Seroprevalence associated with skin color. **(D)** Seroprevalence associated with family income. NI, not informed.

TABLE 2 Seropositivity associated with behavioral characteristics after the first and second waves of COVID-19.

Variables	First wave (%)	95% IC	Second wave (%)	95% IC	Univariate analysisOR (95% IC)	*P*	Multivariate analysisOR (95% IC)	*P*
Total	275 (39.1)		284 (50.1)					
Contact with an infected person								
Yes	82 (29.8)	24–35	212 (74.6)	69–79	0.65 (0.44–0.95)	**0.0290**		
No	189 (68.7)	36–74	61 (21.5)	16–26	(Ref)			
NI	4 (1.5)		11 (3.87)					
Social isolation								
Yes	234 (85.1)	80–89	251 (88.4)	84–92	(Ref)		(Ref)	
No	39 (14.2)	10–18	21 (7.39)	4–10	1.99 (1.13–3.48)	**0.0157**	2.12 (1.13–3.94)	**0.0184**
NI	2 9 (0.7)		12 (4.23)					
Handwashing								
Rarely	24 (8.7)	5–12	16 (5.63)	3–8	1.15 (0.78–2.91)	0.2169		
Many times a day	250 (90.9)	87–94	252 (88.7)	85–92	(Ref)			
NI	1 (0.4)		17 (5.63)					
Use of mask								
Sometimes	18 (6.5)	3–9	8 (3.7)	0–4	2.89 (1.12–7.40)	**0.0270**	3.38 (1.24–9.18)	**0.0168**
Always	245 (89.1)	85–92	236 (83.1)	78–87	(Ref)		(Ref)	
NI	12 (4.4)		40 (14.1)					
Travel history								
Yes	106 (38.5)	32–43	129 (45.4)	39–41	0.69 (0.49–0.97)	**0.0346**		
No	167 (60.7)	55–66	147 (51.8)	45–57	(Ref)			
NI	2 (0.8)		8 (2.8)					

OR, odds ratio; NI, not informed.
Bold means the values are statiscally significant.

10.3389/fcimb.2022.932563

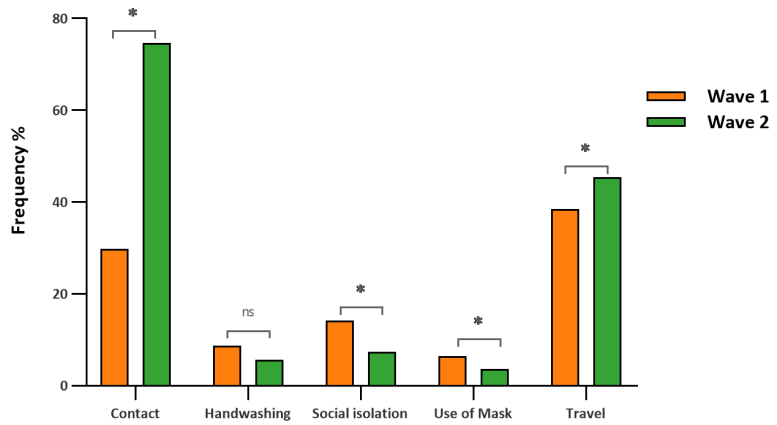

FIGURE 2
Behavioral characteristics associated with seropositivity after the first and second waves of COVID-19. *, significant values ($p < 0.05$); ns, nonsignificant values ($p > 0.05$).

did not practice social isolation (OR = 2.12; 95% CI = 1.13–3.94; $p = 0.0184$) had a higher risk of SARS-CoV-2 infection in the first wave of the disease than in the second (Figure 3).

Prevalence of symptoms after the first and second waves of COVID-19

Among the anti-SARS-CoV-2 IgG seropositive participants, 62.5 and 63.4% were symptomatic and 37.5 and 36.6% were asymptomatic during the first and second waves, respectively. There was no significant difference between the groups regarding seropositivity (Figure 4A). We found a substantial difference in symptoms between the two periods studied. Symptoms including fever (first wave = 48.7%/second wave = 30.6%; $p = 0.0039$), abdominal pain (first wave = 26.5%/second wave = 16.9%; $p = 0.0339$), loss of smell (first wave = 50.5%/second wave = 29.9%; $p = 0.0021$), and loss of taste (first wave = 48.4%/second wave = 31.3%; $p = 0.0100$) were more prevalent in the first wave than in the second wave (Figure 4B; Table 3).

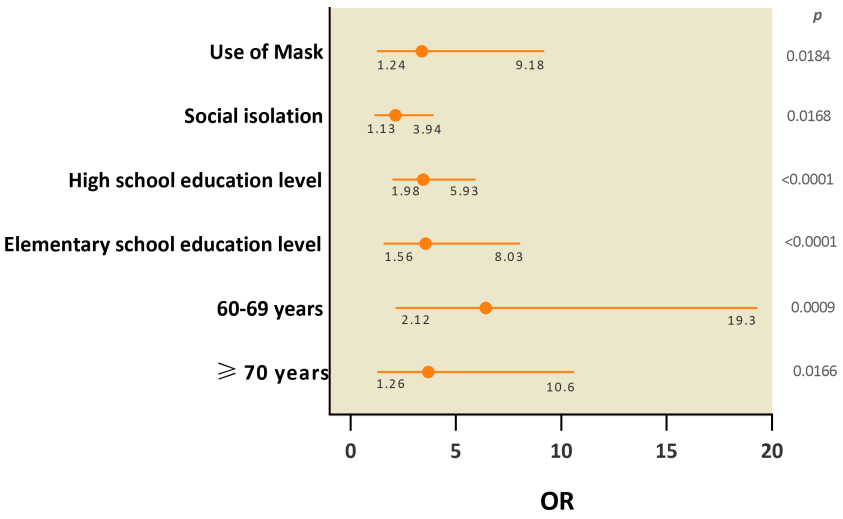

FIGURE 3
Socioeconomic and behavioral variables associated with the risk of SARS-CoV-2 infection after the first two waves of COVID-19 in the city of Belém.

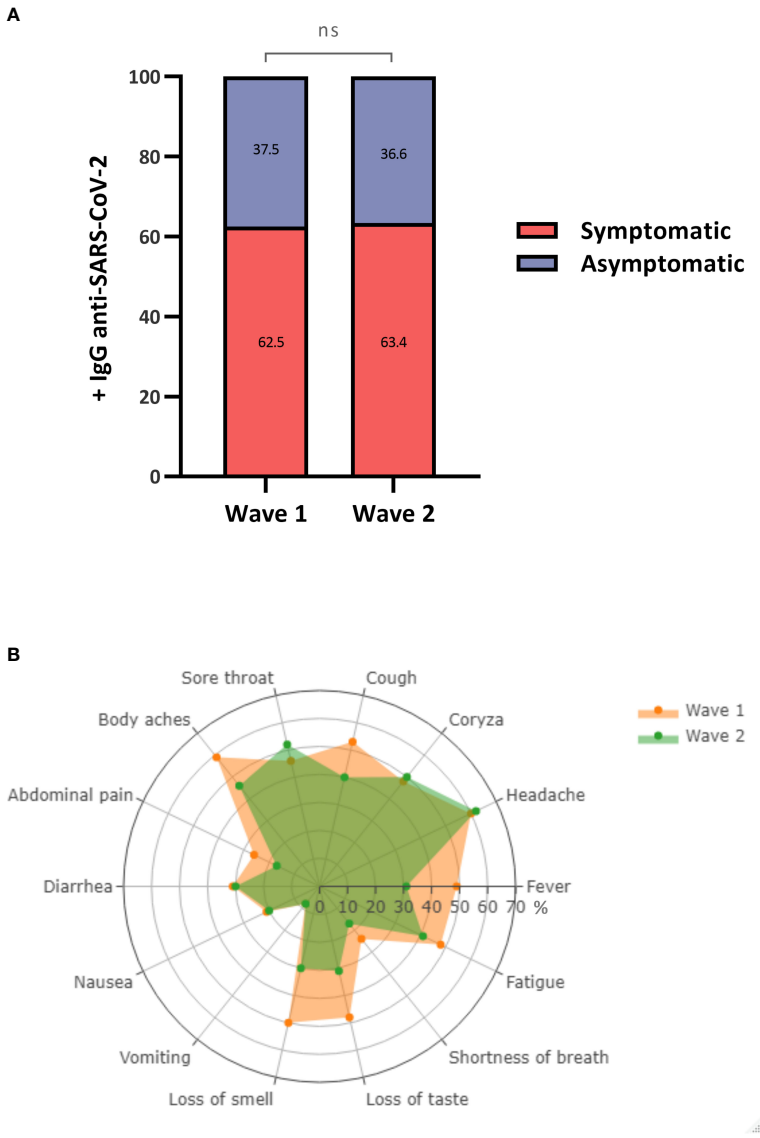

FIGURE 4
Prevalence and frequency of antibodies and symptoms among symptomatic and asymptomatic individuals. **(A)** Percentage of +/- anti-SARS-CoV-2 IgG antibodies between symptomatic and asymptomatic individuals. **(B)** Frequency of symptoms characteristic of COVID-19. ns, not significant.

Discussion

In the present study, we performed a comparative analysis of the prevalence of anti-SARS-CoV-2 IgG antibodies against the S1 subunit of the spike glycoprotein and the factors potentially associated with infection after the first and second waves of COVID-19 in the city of Belém, the capital of the state of Pará, the largest metropolis in the Brazilian Amazon. To date, this is one of the first seroepidemiological and comparative studies that highlight changes in the affected population profile between two major periods of the pandemic. Our findings indicate an increase in seroprevalence in individuals between the first and second waves of COVID-19 in the city of Belém; moreover, the seroprevalence was higher than that observed in Manaus (first and second waves = 6.61%/first wave = 27.7%/second wave = 34.3%), which is considered one of the regions most affected by the pandemic in Brazil (Lalwani et al., 2021).

Seropositivity in young adults aged 19 to 29 years was higher in the second wave than in the first wave, during which elderly individuals had the highest rate of infection. This result is not surprising, as vaccination in individuals over 70 years of age soon after the first viral wave provided protection in this group during the second wave. Age disparities between the two outbreak periods, similar to that observed in our study, were

TABLE 3 Prevalence of symptom characteristics of COVID-19 in IgG+ individuals.

Symptoms	First wave (%)	95% IC	Second wave 2 (%)	95% IC	*p*
Total	275 (31.9)	–	284 (50.1)	–	–
Fever	134 (48.7)	42–54	87 (30.6)	25–36	**0.0039**
Headache	164 (60.0)	53–65	176 (61.9)	56–67	0.8334
Coryza	130 (47.6)	41–53	143 (50.3)	44–56	0.7240
Cough	145 (53.5)	46–58	114 (40.1)	34–45	0.0833
Sore throat	125 (46.2)	39–51	148 (52.1)	46–57	0.9842
Body aches	161 (58.9)	52–64	132 (46.4)	40–52	0.1276
Abdominal pain	73 (26.5)	21–31	48 (16.9)	12–21	**0.0339**
Diarrhea	86 (31.3)	26–36	85 (29.9)	24–36	0.8699
Nausea	59 (21.5)	16–26	57 (20.0)	15–24	0.8222
Vomiting	23 (8.0)	0–4	24 (8.4)	5–11	0.9062
Loss of smell	137 (50.5)	43–55	85 (29.9)	24–35	**0.0021**
Loss of taste	132 (48.4)	42–53	89 (31.3)	25–36	**0.0100**
Shortness of breath	65 (24.0)	18–28	48 (16.9)	12–21	0.1306
Fatigue	130 (48.0)	41–53	118 (41.5)	35–47	0.4419

Bold means the values are statiscally significant.

also observed in other parts of the world (Capai et al., 2021; Visscher et al., 2022). Notably, during the second wave, high seroprevalence rates were observed in individuals with higher education levels and with high family incomes; this was most likely attributed to the gradual opening of institutions during the second period (schools, bars, workplaces, and restaurants).

Our analyses showed that behavioral characteristics, including the frequency of travel, the frequency of mask use, hand hygiene, social isolation, and contact with infected people, were related to a higher seroprevalence (Leung et al., 2020; Howarda et al., 2021). It is likely that the relaxation of prevention measures, "pandemic fatigue," and the increasing availability of diagnostic tests influenced this pattern.

Individuals aged 60 years or older, those had been in elementary or high school education level, those who rarely used protective face masks, and those who did not practice social isolation had a higher risk of infection during the first wave of the disease than their counterparts. We attribute this increased risk to (i) the lack of vaccination of elderly individuals at the beginning of the pandemic, (ii) socioeconomic discrepancies, which are most evident in the population with low education and/or income, among the most vulnerable populations due to the lack of social isolation as a result of the need to guarantee their subsistence, and (iii) the lack of information about the proper use of masks.

The proportion of asymptomatic individuals in the seropositive population was relatively high during both periods (first wave = 37.5%/second wave = 36.6%) and was proportional to those described in other regions of Brazil (Silva et al., 2020; Borges et al., 2020; Vale et al., 2022). This finding highlights the importance of continuous monitoring and disease prevention measures, as the identification of asymptomatic individuals is still one of the main challenges and these individuals are an important source of transmission of the virus. Among the symptomatic population, symptoms such as fever, cough, abdominal pain, and loss of smell and taste were the most frequent in the first wave of the pandemic. Changes in the most frequent symptoms occurred with the circulation of different viral variants at different times; these variants showed differences in not only their genomic characteristics but also their transmissibility and pathogenesis. During the first wave, the variants circulating in Brazil were Gamma and Alpha, and during the second wave, the Delta variant predominated (Brasil, 2022b).

The main limitations of the present study, which could bias the results, were as follows: (i) the inability to investigate acute infections at the time of sample collection and to determine the circulating molecular variant, (ii) grouping of individuals based on self-reported skin color, and (iii) random sampling based on the voluntary adherence of participants. In addition, we found it difficult to obtain additional samples due to government lockdown decrees. On the other hand, our analyses provide detailed data on the socioeconomic and behavioral characteristics of the infected population (including asymptomatic and recovered patients); these data provide more accurate estimates of the prevalence of SARS-CoV-2 infection in the population of Belém in the Brazilian Amazon during the two main periods of the pandemic. This is the first epidemiological study to evaluate and compare the risk factors for SARS-CoV-2 infection shortly after the first two waves of COVID-19 in the capital of the state of Pará and to show that the pandemic waves had distinct epidemiological characteristics that need to be understood to guide the formulation of public policies that will help prevent the further spread of the infection.

In conclusion, our results showed high seroprevalence rates after the two initial periods of the pandemic in the city of Belém. These findings highlight the importance of serosurveillance, especially after the easing of prevention measures, to estimate the real impact of the COVID-19 pandemic and identify vulnerable populations and ongoing transmission. This information can guide the planning of adequate public health measures and nonpharmacological interventions in areas with few financial resources and high viral transmission rates.

Data availability statement

The raw data supporting the conclusions of this article will be made available by the authors, without undue reservation.

Ethics statement

This study was reviewed and approved by Ethics Committee in Research with Human Beings of the Institute of Health Sciences of the Federal University of Pará (CAAE: 31800720.1.0000.0018). The patients/participants provided their written informed consent to participate in this study.

Author contributions

AV and MT conceptualized the study and wrote the article. Sample collection and experimental analyses were performed by MT, FL, OO, CL, AL, WB, JSG, VF, BS, BB, AC, LM and RF. The epidemiological database was compiled by RS and JLG. The statistical analyses were performed by SL and MT. Study coordination was performed by IV and AV. All authors contributed to the article and approved the submitted version.

Funding

The study received financial support from the National Council for Scientific and Technological Development (CNPq, #302935/2021-5, and #401235/2020-3), Fundação Amazônia Pará de Amparo à Pesquisa (FAPESPA—005/2020), Coordination of Improvement of Higher Education Personnel (CAPES), and the Dean of Research and Graduate Studies at the Federal University of Pará (PROPESP/UFPA).

Acknowledgment

The authors thank all patients who agreed to voluntarily participate in this study.

Conflict of interest

The authors declare that the research was conducted in the absence of any commercial or financial relationships that could be construed as a potential conflict of interest.

Publisher's note

References

Borges, L. P., Martins, A. F., Melo, M. S., Oliveira, M. G. B., Neto, J. M. R., Dósea, M. B., et al. (2020). Seroprevalence of SARS-CoV-2 IgM and IgG antibodies in an asymptomatic population in sergipe, Brazil. *Rev. Panam Salud Publica* 44, 1–7. doi: 10.26633/RPSP.2020.108

Brasil (2020). *Ministério da saúde. protocolo de manejo clínico para o Novo coronavírus, (2019-nCoV)*, Vol. 2020.

Brasil (2022a)Ministério da saúde. painel de casos de doença pelo coronavírus 2019 (COVID-19) no brasil. Available at: https://covid.saude.gov.br/ (Accessed 19/03/2022).

Brasil (2022b)Ministério da saúde. filodinâmica do SARS-CoV-2 no brasil. Available at: http://www.genomahcov.fiocruz.br/gisaid/ (Accessed 28/03/2022).

Capai, L., Masse, S., Fourié, T., Decarreaux, D., Canarelli, J., Simeoni, M., et al. (2021). Impact of the second epidemic wave of SARS-CoV-2: Increased exposure of young people. *Front. Public Health* 9. doi: 10.3389/fpubh.2021.715192

CDC (2021)EPI InfoTM. version 7.2.4. Atlanta: Centers for disease control and prevention. Available at: http://www.cdc.gov/epiinfo (Accessed 20/01/2021).

Howarda, J., Huangc, A., Lid, Z., Tufekci, Z., Zdimalf, V., Westhuizeng, H. V., et al. (2021). An evidence review of face masks against COVID-19. *PNAS* 118, e2014564118. doi: 10.1073/pnas.2014564118

Lalwani, P., Araujo-Castillo, R. V., Ganoza, C. A., Salgado, B. B., Pereira Filho, I. V., Silva, D. S. S., et al. (2021). High anti-SARS-CoV-2 antibody seroconversion rates before the second wave in manaus, Brazil, and the protective effect of social behaviour measures: results from the prospective DETECTCoV-19 cohort. *Lancet* 9, e1508-e1516. doi: 10.1016/S2214-109X(21)00355-7

Leung, N. H. L., Chu, D. K. W., Shiu, E. Y. C., Chan, K. H., McDevitt, J. J., Hau, B. J. P., et al. (2020). Respiratory virus shedding in exhaled breath and efficacy of face masks. *Nat. Med.* 26, 676–680. doi: 10.1038/s41591-020-0843-2

Ribeiro, H. V., Sunahara, A. S., Sutton, J., Perc, M., and Hanley, Q. S. (2020). City size and the spreading of COVID-19 in Brazil. *PloS One* 15, e0239699. doi: 10.1371/journal.pone.0239699

Secretaria de Saúde Pública do estado do Pará (SESPA). Available at: http://contratoemergencial.belem.pa.gov.br/painel-covid-19/ (Accessed 25/01/2022).

Silva, A. A. M. D., Lima-Neto, L. G., Azevedo, C.M.P.E.S., Costa, L. M. M. D., Bragança, M. L. B. M., Barros Filho, A. K. D., et al. (2020). Population-based seroprevalence of SARS-CoV-2 and the herd immunity threshold in maranhão. *Rev. Saude Publica* 14, 54:131. doi: 10.11606/s1518-8787.2020054003278

Vale, N. M. R., Latinia, F. R. M., Arnonia, C. P., Parreira, R. M., gIRÃO, M. J. B. C., Cortez, A. J. P., et al. (2022). Increasing rate of anti-SARS-CoV-2 antibodies between the first and second waves of COVID-19 in são paulo, Brazil: A cross-sectional blood donors-based study. *Clinics* 77, 100016. doi: 10.1016/j.clinsp.2022.100016

Visscher, N., Holemans, X., Gillain, A., Kornreich, A., Lagasse, R., Piette, P., et al. (2022). SARS-CoV-2 seroprevalence among health care workers after the first and second pandemic wave. *medRxiv* 14 (7), 1535. doi: 10.1101/2022.03.03.22271855

frontiers | Frontiers in Cellular and Infection Microbiology

TYPE Original Research
PUBLISHED 04 October 2022
DOI 10.3389/fcimb.2022.960938

OPEN ACCESS

EDITED BY
Edmarcia Elisa De Souza,
University of São Paulo, Brazil

REVIEWED BY
Santosh Verma,
Sanjay Gandhi Post Graduate Institute of Medical Sciences (SGPGI), India
António Machado,
Universidad San Francisco de Quito, Ecuador

*CORRESPONDENCE
Dakang Hu
18111220048@fudan.edu.cn
Bin Ma
B.Ma@murdoch.edu.au

SPECIALTY SECTION
This article was submitted to Clinical Microbiology, a section of the journal Frontiers in Cellular and Infection Microbiology

RECEIVED 03 June 2022
ACCEPTED 20 September 2022
PUBLISHED 04 October 2022

CITATION
Hu D, Wang T, Uddin J, Greene WK, Hu D and Ma B (2022) Development of a high-sensitivity and short-duration fluorescence *in situ* hybridization method for viral mRNA detection in HEK 293T cells.
Front. Cell. Infect. Microbiol. 12:960938.
doi: 10.3389/fcimb.2022.960938

Development of a high-sensitivity and short-duration fluorescence *in situ* hybridization method for viral mRNA detection in HEK 293T cells

Dailun Hu[1], Tao Wang[2,3], Jasim Uddin[4], Wayne K. Greene[5], Dakang Hu[6]* and Bin Ma[5]*

[1]Clinical College, Hebei Medical University, Shijiazhuang, China, [2]Telethon Kids Institute, Perth Children's Hospital, Nedlands, WA, Australia, [3]Medical School, University of Western Australia, Nedlands, WA, Australia, [4]School of Veterinary Medicine, Murdoch University, Murdoch, WA, Australia, [5]Medical, Molecular and Forensic Sciences, Murdoch University, Murdoch, WA, Australia, [6]Department of Laboratory Medicine, Taizhou Municipal Hospital, Taizhou, China

Coronavirus disease 2019 (COVID-19) is an extremely contagious illness caused by severe acute respiratory syndrome coronavirus 2 (SARS-CoV-2). Early disease recognition of COVID-19 is crucial not only for prompt diagnosis and treatment of the patients, but also for effective public health surveillance and response. The reverse transcription-polymerase chain reaction (RT-PCR) is the most common method for the detection of SARS-CoV-2 viral mRNA and is regarded as the gold standard test for COVID-19. However, this test and those for antibodies (IgM and IgG) and antigens have certain limitations (e.g., by yielding false-negative and false-positive results). We have developed an RNA fluorescence *in situ* hybridization (FISH) method for high-sensitivity detection of SARS-CoV-2 mRNAs in HEK 293T cell cultures as a model. After transfection of HEK 293T cells with plasmids, Spike (S)/envelope (E) proteins and their mRNAs were clearly detected inside the cells. In addition, hybridization time could be reduced to 2 hours for faster detection when probe concentration was increased. Our approach might thus significantly improve the sensitivity and specificity of SARS-CoV-2 detection and be widely applied for the high-sensitivity single-molecular detection of other RNA viruses (e.g., Middle East respiratory syndrome coronavirus (MERS-CoV), Hepatitis A virus, all influenza viruses, and human immunodeficiency virus (HIV)) in various types of samples including tissue, body fluid, blood, and water. RNA FISH can also be utilized for the detection of DNA viruses (e.g., Monkeypox virus, human papillomavirus (HPV), and cytomegalovirus (CMV)) by detection of their mRNAs inside cells or body fluid.

KEYWORDS

SARS-CoV-2, fluorescence *in situ* hybridization, mRNA, HEK 293T cell, RNA virus

Introduction

Coronavirus disease 2019 (COVID-19) is an extremely contagious illness caused by severe acute respiratory syndrome coronavirus 2 (SARS-CoV-2; Borges do Nascimento et al., 2021; Aimrane et al., 2022; Al-Awwal et al., 2022). Recent evidence indicates over 430 million cases and 5.92 million deaths worldwide (Al-Awwal et al., 2022). The early disease recognition of COVID-19 is crucial not only for the prompt diagnosis and treatment of patients, but also for effective public health surveillance, containment, and response (Borges do Nascimento et al., 2021; Aimrane et al., 2022; Al-Awwal et al., 2022).

Coronaviruses, which include SARS-CoV-2, severe acute respiratory syndrome coronavirus 1 (SARS-CoV-1), and Middle East respiratory syndrome coronavirus (MERS-CoV), are a group of RNA viruses that can infect many different types of animals (including mammals and birds) and cause mild to severe respiratory infections (V'kovski et al., 2021; da Silva Torres et al., 2022). They are spherical enveloped viruses with a positive-sense single-stranded RNA genome (ranging from 26.4 to 31.7 kilobases) and a helically symmetrical nucleocapsid (N; V'kovski et al., 2021). At the 5′ end, the genomic RNA contains two large open reading frames (ORF; ORF1a and ORF1b) encoding 16 non-structural proteins. At the 3' end, the genome encodes four structural proteins [spike (S), envelope (E), membrane (M), and N], and nine accessory proteins (ORF3a, 3b, 6, 7a, 7b, 8, 9a, 9b, and 10; V'kovski et al., 2021).

The polymerase chain reaction (PCR)-based method (including the reverse transcription-polymerase chain reaction (RT-PCR)) is the most commonly used for the detection of SARS-CoV-2 viral RNA in both symptomatic and asymptomatic patients and is considered the gold standard test for COVID-19 (Lin et al., 2015; Mardian et al., 2021; Rabaan et al., 2021; Yoo et al., 2021). The three main SARS-CoV-2-specific, highly conserved, and abundantly expressed genes targeted by RT-PCR are the ORF1ab, N, and E genes (Chu et al., 2020; Corman et al., 2020). However, RT-PCR has several limitations for SARS-CoV-2 detection. The first is the possibility that a false-negative result arises because of several factors ranging from sample collection to data interpretation (Mardian et al., 2021). False negatives have been reported in ~30% (range 10–40%) of patients with COVID-19 (Weissleder et al., 2020). Missed detection caused by false negatives therefore has severe consequences because a super-spreader might remain or be released into the community without further quarantine and/or treatment. Some patients only produce a positive result after a few negative results, significantly affecting and delaying follow-up treatments. The second limitation of RT-PCR is the possibility of a false-positive result attributable to technical errors (particularly contamination during sample collection and manual RT-PCR processing; Keaney et al., 2021; Mardian et al., 2021). The third is that the requirements for setting up an RT-PCR laboratory are usually high. An RT-PCR laboratory needs instruments capable of nucleic acid extraction and of carrying out quantitative fluorescence PCR; such instruments might only be available in some clinical laboratories (Hong et al., 2020). In addition, a level P2 laboratory as a minimum (plus P3 protection) is needed to avoid viral cross-contamination and infection of medical health professionals.

The COVID-19 Antibody (IgG and IgM) Test is a blood test that determines whether an individual has previously had a SARS-CoV-2 infection by the detection of antibodies against specific viral proteins (Lindsay et al., 2021; Ravi et al., 2021). As the first antibody to appear during infection, IgM is often utilized as a marker of acute infection. With the development of infection, the level of IgG increases, and the concentration of IgM gradually decreases, possibly disappearing after a certain time. Compared with the RT-PCR, the antibody test is more straightforward, faster, and more efficient (often showing strong sensitivity and specificity; Ravi et al., 2021). However, this test also has certain limitations. The first is the possibility of a false-negative result. For example, if the test is performed too early following an infection, a negative result may be obtained (Ravi et al., 2021). The second limitation is that specific IgM and IgG tests also suffer from false positives arising (Lindsay et al., 2021). For example, some weak positive results near the positive judgment value (cut-off value) are likely to be false positives. In addition, the presence of endogenous or exogenous interfering substances can lead to false positives. Furthermore, cross-reactivity is a significant challenge, since six other coronaviruses can also infect humans (Chia et al., 2020).

The COVID-19 Rapid Antigen Test (RAT) is an immunoassay for the qualitative detection of SARS-CoV-2 N antigen in nasal swabs and saliva (Wang et al., 2021; Gans et al., 2022; Khalid et al., 2022). These tests have moderate sensitivity and specificity for the detection of SARS-CoV-2. However, false-positive results are reported to be as high as 40% under certain conditions (Gans et al., 2022). Therefore, the sensitivity and specificity of the antigen assay are still inferior to those of the RT-PCR assay and might not match the requirements for clinical diagnosis and the screening of COVID-19 infections.

RNA fluorescence *in situ* hybridization (FISH; Ma et al., 2010; Ma and Tanese, 2013) has been applied to detect several RNA viruses including the influenza virus (Lakdawala et al., 2014). Since SARS-CoV-2 is a positive-sense single-stranded RNA coronavirus, our intention has been to develop a highly sensitive and reliable RNA-FISH method for the early accurate detection and screening of SARS-CoV-2 by using HEK 293T cell culture as a model system.

Materials and methods

Cell culture and transfection

Glass coverslips (round, 13mm diameter; ProSciTech, Kirwan, QLD, Australia) were briefly rinsed with 70% ethanol and then treated with 0.1 mg/L poly-D-lysine (PDL; Sigma, Bayswater, VIC, Australia) for 10 min. After being washed three times with distilled water, the coverslips were ready for the culture of HEK 293T cells (Sigma).

10,000-15,000 HEK293T cells [in 1.0 ml Dulbecco's modified Eagle's medium (DMEM; Sigma) with 10% fetal bovine serum (FBS; Thermo Fisher Scientific, Malaga, WA, Australia) and Penicillin (100 units/ml)-Streptomycin (100 µg/ml; Sigma)] were seeded on the PDL-coated glass coverslips in 24-well culture plates and cultivated in a humidified SANYO MCO-5AC incubator (SANYO, Osaka, Japan) at 37°C, supplemented with 5% CO_2.

After reaching 70-80% confluency, cells were transfected by using the Lipofectamine™ 3000 Transfection Reagent (Thermo Fisher Scientific) according to the instructions of the manufacturer. In Tube 1, 0.75 µl Lipofectamine 3000 reagent was diluted in 25 µl Opti-MEM™ I Reduced Serum Medium (Thermo Fisher Scientific) for each well in a 24-well culture plate. In Tube 2, 200 ng pUNO1-SARS2-S (D614G) plasmid (*In vivo*Gen, San Diego, California, US), 200 ng pUNO1-SARS2-E plasmid (*In vivo*Gen), and 0.5 µl P3000™ reagent were added to 25 µl Opti-MEM™ I Reduced Serum Medium for each well. We used 400 ng plasmid for single transfection. The solution in Tube 2 solution was added to that in Tube 1. After being mixed well, the mixture was incubated for 10 min at room temperature and then added to the cell culture wells (50 µl/well). At various time points after transfection (e.g., 2 h, 4 h, 8 h, 16 h, and 24 h), cells were fixed and processed for further analysis.

FISH

The steps for cell culture/transfection and FISH are shown in Supplementary Figure 1. Diethyl pyrocarbonate (DEPC)-treated water (ribonuclease-free water) was used for the preparation of phosphate-buffered saline (PBS) and other reagents (Ma and Tanese, 2013). Cells on glass coverslips were rinsed briefly in PBS, fixed with 4% paraformaldehyde (PFA; Electron Microscopy Sciences, Hatfield, PA, USA) for 10 min, and then washed three times with PBS. The cells were subsequently permeabilized with 0.25% Triton X-100 (Sigma) in PBS for 5 min.

After a 5-min rinse with 1× sodium chloride/sodium citrate (1 × SSC), coverslips (upside down on a paraffin film in a humidified box) were incubated in 40 µl hybridization buffer [25% dextran sulfate (Sigma), 40% formamide (Sigma), 30 µg/ml single-stranded salmon sperm DNA (Sigma), 30 µg/ml yeast tRNA (Sigma), 0.4% bovine serum albumin (BSA; Sigma), 20 mM ribonucleoside vanadyl complex (Sigma), 0.01 M sodium phosphate buffer (pH 7.0), 2 × SSC] in an Extron HI 2001 hybridization oven (Bartelt Instruments, Heidelberg West, Victoria, Australia) for 1 h at 37°C for pre-hybridization. The cells were then hybridized with probes (single probe: 400 ng; mixed probes: 200 ng Probe 1 + 200 ng Probe 2) diluted in 40 µl hybridization buffer in the hybridization oven for 4 h at 37°C. The sequences and sources of digoxin (DIG)-labeled probes are shown in Table 1. For experiments with a 2-h hybridization time, we utilized 800 ng probe (400 ng Probe 1 + 400 ng Probe 2) in 40 µl hybridization buffer. As a positive control for our FISH method, an Oligo dT probe (targeting the poly-A tail of all mRNAs) was used to detect the total mRNAs in the HEK 293T cells.

After hybridization, cells were washed with 40% formamide/1 × SSC for 30 min at 37°C with gentle shaking (in the hybridization oven), followed by washes for 3 × 10 min in 1 × SSC with gentle shaking on an orbital shaker at room temperature.

Antibodies

The specificities and sources of antibodies are described in Table 2.

Detection of DIG-labeled probes and immunofluorescence staining

Coverslips with cells were rinsed briefly with PBS. All washes (3×5 min) between steps were performed with PBS at room

TABLE 1 Sequences and sources of probes used for FISH.

Probe	Sequences	Company
BME-001	CACTAGCCATCCTTACTGCGCTTCGATTGTGTGCGTACTGCTGC/3DiG_N/	Integrated DNA Technologies(Coralville, Iowa, United States)
BME-002	GCCATCCTTACTGCGCTTCGATTGTGTGCGTACTGCTGCA/3DiG_N/	Integrated DNA Technologies
BMS-001	TGGCCATGGTACATTTGGCTAGGTTTTATAGCTGGCTTGATTGCCATAGT/3DiG_N/	Integrated DNA Technologies
BMS-002	GCACACGCCTATTAATTTAGTGCGTGATCTCCCTCAGGGT/3DiG_N/	Integrated DNA Technologies
Oligo dT	Single-stranded sequence of deoxythymine (dT), 24mer-DIG	Life Technologies, Grand Island, NY

TABLE 2 Specificities and sources of primary and secondary antibodies.

Target	Conjugate	Species and isotype	Company
Digoxin(CDIG-65A)		Chick IgY, polyclonal	Immunology Consultants Laboratory (Portland, OR, USA)
SARS-CoV-2 1/2 Spike protein(2B3E5)		Mouse IgG, monoclonal	Cell Signaling Technology (Danvers, MA, United States)
SARS-CoV-2 E protein		Rabbit IgG, polyclonal	Abcam Australia (Melbourne, Australia)
Chick IgG	Alexa Fluor® 488	Goat polyclonal	Abcam Australia
Chick IgG	Alexa Fluor® 555	Goat polyclonal	Abcam Australia
Rabbit IgG H&L	Alexa Fluor® 488	Goat polyclonal	Abcam Australia
Rabbit IgG H&L	Alexa Fluor® 555	Goat polyclonal	Abcam Australia
Mouse IgG	Alexa Fluor® 647	Goat polyclonal	Abcam Australia

temperature. Cells were then incubated with antibody dilution buffer [2% goat serum (Sigma) in PBS] for 20 min at room temperature to block any potential non-specific binding sites to the antibodies. The cells of the experimental group were incubated with primary antibodies for 1 h at room temperature. Primary antibodies were omitted in negative controls.

Cells were then incubated with secondary antibodies for 45 min at room temperature. Finally, coverslips (upside down) were mounted on microscope slides (25mm× 75mm; ProSciTech) by means of Fluorescence Mounting Medium (DAKO, North Sydney, Australia).

Confocal microscopy and image processing

Confocal microscopy was carried out on a Nikon C2 Plus Confocal Microscope (Nikon Instruments, Melville, NY, USA) with three lasers (488 nm, 561 nm, and 633 nm). A Plan Apo λ 60x/1.40 oil immersion objective lens was utilized for all imaging. The operation program for the confocal microscope was NIS-Elements AR. Maximal intensity projection of a Z-stack was performed by using the "Maximal intensity projection" of the NIS-Elements AR program. 3D reconstruction was performed by using the "Volume rendering" in the NIS-Elements AR program. The images were then saved as bitmap (BMP) image files and further edited (cropping and labeling) by using Corel PaintShop Pro 2020 (Corel, Ottawa, Canada).

Results

Co-detection of SARS-CoV-2 E/S and their mRNAs

At first, we tested our mRNA FISH by using a single DNA probe for SARS-CoV-2 E mRNA. HEK 293T cells were transfected with SARS-CoV-2 E plasmids. At 24 h after transfection, SARS-CoV-2 E mRNA and protein were detected using FISH and immunofluorescent staining, respectively. The results are shown in Figure 1. Abundant E mRNAs (demonstrated by solid granular staining) were observed inside the HEK 293T cells. Furthermore, colocalization of E protein and mRNA (appearing yellow in the merged image) indicated the E protein being translated (Figure 1). We also utilized optic sectioning and 3D reconstruction for a better demonstration of E mRNA and protein inside the HEK 293T cells (Figure 1B-D and Supplementary Video 1).

We then tested our mRNA FISH by using two DNA probes for SARS-CoV-2 E mRNA. HEK 293T cells were transfected with SARS-CoV-2 E and S plasmids, and 24 h after transfection, SARS-CoV-2 E mRNAs and E/S proteins were detected by using FISH and immunofluorescent staining, respectively. The results are shown in Figure 2A. We also observed abundant SARS-CoV-2 E mRNA (solid granular staining) together with SARS-CoV-2 E/S protein (solid granular staining) inside the cells. As a positive control for our FISH method, an Oligo dT probe (targeting the poly-A tail of all mRNAs) was used to detect the total mRNAs in the HEK 293T cells, and the results are shown in Figure 2B. In negative controls, no fluorescent signals were observed when only secondary antibodies were applied (Figure 2C).

We also tested our mRNA FISH approach by using two DNA probes for SARS-CoV-2 S mRNA. HEK 293T cells were transfected with SARS-CoV-2 S and E plasmids. At 24 h after transfection, SARS-CoV-2 S mRNAs and S/E proteins were detected by using FISH and immunofluorescent staining, respectively. The results are shown in Figure 3A. We observed abundant SARS-CoV-2 S mRNA (solid granular staining) together with SARS-CoV-2 E/S protein (solid granular staining) inside the cells. In negative controls for secondary antibodies, no fluorescent signals were observed when primary antibodies were omitted (Figure 3B).

FISH of SARS-CoV-2 S mRNAs at various time points after transfection

We then checked whether, after transfection, mRNAs could be detected at various time points mimicking viral replication in the human body. HEK 293T cells were transfected with SARS-

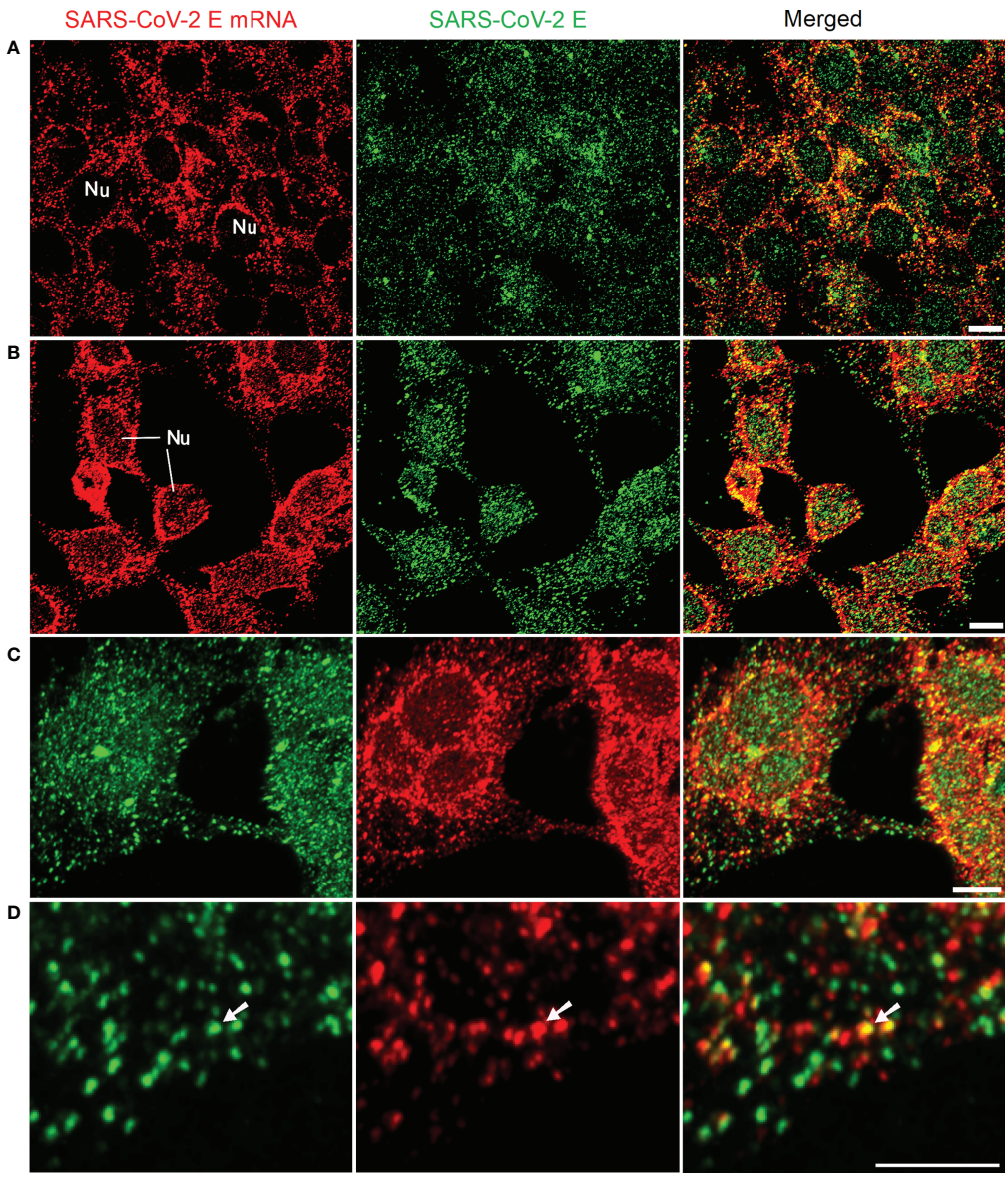

FIGURE 1
Detection of SARS-CoV-2 E mRNA (with single probe-BME001; red) and SARS-CoV-2 E protein (green) in HEK 293T cells at 24 h after transfection with SARS-CoV-2 E plasmids. The yellow color in merged images shows the colocalization of SARS-CoV-2 E and its mRNA **(A)** 2D images for E mRNA and E protein. **(B)** Images are maximal intensity projections of a Z-Stack. Optical slice interval: 0.50 μm; Stack size: 6.0 μm. **(C)** 3D projection by using the Z-stack in (B; cropped). **(D)** High-resolution view of images in (C; cropped). The white arrows indicate the colocalization of E mRNA and E protein inside the cells. Objective lens: 60×; Scale bar: 10 μm; Nu, nucleus.

CoV-2 S plasmids. At 2 h, 4 h, 8 h, and 24 h after transfection, SARS-CoV-2 S mRNA and protein were detected using FISH and immunofluorescent staining, respectively. The results are shown in Figure 4. SARS-CoV-2 S mRNA was clearly demonstrated by the solid granular staining inside HEK 293T cells at all time points. In addition, the S protein demonstrated by granular staining was also observed inside HEK 293T cells at all time points. Therefore, SARS-CoV-2 mRNA and protein could be observed as early as 2 h after transfection with S plasmid.

FISH of SARS-CoV-2 mRNAs with reduced hybridization time

We then checked whether the time for pre-hybridization and hybridization could be reduced to achieve faster detection of viral mRNAs. At 2 h, 4 h, and 16 h after transfection with SARS-CoV-2 S plasmid, HEK 293T cells were pre-hybridized for 30 min and then hybridized with an increased amount of probes (800 ng in total) for 2 h. The results are shown in Figure 5. We observed solid

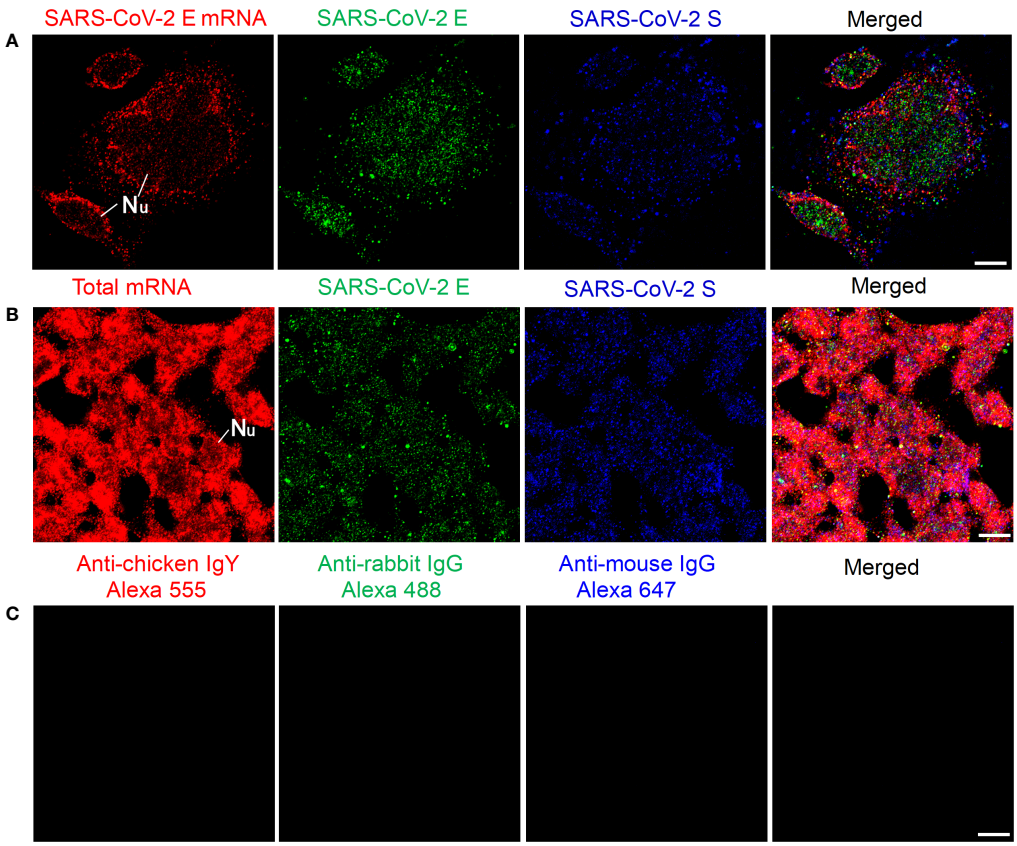

FIGURE 2
Detection of SARS-CoV-2 E mRNA and E/S protein in HEK 293T cells at 24 h after transfection with SARS-CoV-2 E and S plasmids. **(A)** SARS-CoV-2 E mRNA (with mixed probes containing BME001 and BME002), SARS-CoV-2 E, and SARS-CoV-2 S are shown in red, green, and blue, respectively. **(B)** Total mRNAs (detected by Oligo dT probes), SARS-CoV-2 E, and SARS-CoV-2 S are shown in red, green, and blue, respectively. **(C)** Negative controls by using secondary antibodies. Objective lens: 60×; Scale bar: 10 μm; Nu, nucleus.

granular FISH signals for SARS-CoV-2 S at all time points, together with granular staining signals for SARS-CoV-2 S protein.

We also applied the same FISH protocol (with reduced pre-hybridization and hybridization times) for SARS-CoV-2 E mRNA, and the results are shown in Figure 6. SARS-CoV-2 E mRNA was detectable inside HEK 293T cells at all time points (similar to the SARS-CoV-2 S mRNA) after transfection. Although S mRNA and E mRNA were readily detectable with reduced pre-hybridization and hybridization times, the resulting images (shown in Figures 5-6) were not as sharp as those shown in Figures 1-3.

Discussion

We have developed an RNA FISH approach as a high-sensitivity single-molecular (particle) detection method for viral mRNAs (including S and E) inside HEK 293T cells. Short DNA probes (about 40-50 nt) have been utilized for the detection of mRNAs, and this method enables us to conduct qualitative, quantitative, and cellular localization/analysis of RNAs by using fluorescent or confocal microscopy. Although our method can detect single-molecule mRNA (or mRNA fragments) inside the cells, the observed granular staining might contain a few mRNAs, since SARS-CoV-2 viral RNA replicates within double-membrane vesicles (DMVs; Gómez et al., 2021) in the cytoplasm of HEK 293T cells. These DMVs are similar to the mRNA granules that we have described in previous studies, since both of them might contain a few mRNA molecules (Ma et al., 2010; Ma et al., 2012; Lakdawala et al., 2014; Gómez et al., 2021). We have established this method by using cell culture on coverslips, similar to the smears made from nasopharyngeal or oropharyngeal swabs.

RNA FISH might improve sensitivity and reduce false negatives

In our previous studies, we have compared RT-PCR and mRNA FISH in the detection of mRNA/RNAs (Ma et al., 2012).

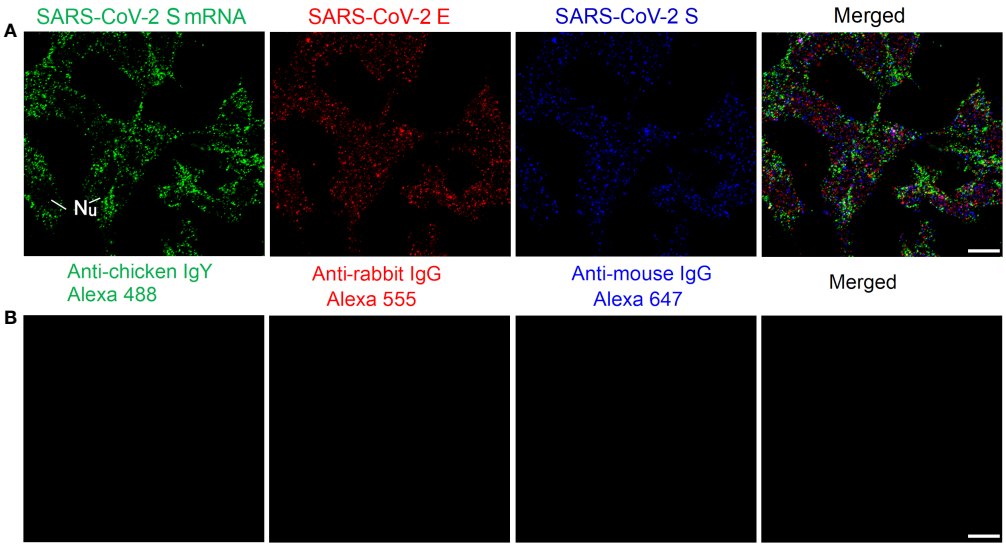

FIGURE 3
Detection of SARS-CoV-2 S mRNA and S/E proteins in HEK 293T cells at 24 h after transfection with SARS-CoV-2 S and E plasmids. **(A)** SARS-CoV-2 S mRNA (with mixed probes containing BMS001 and BMS002), SARS-CoV-2 E, and SARS-CoV-2 S are shown in green, red, and blue, respectively. **(B)** Negative controls by using secondary antibodies. Objective lens: 60×; Scale bar: 10 μm; Nu, nucleus.

PCR is an extremely sensitive detection method since it can amplify a specific region of DNA sequence 10^6 times *in vitro*. To detect fluorescent signals, a threshold must be set to distinguish signal from noise (Mardian et al., 2021; Rabaan et al., 2021). Although RT-PCR is extremely sensitive, The Centers for Disease Control and Prevention (CDC) assays present detection limits ranging from 85 to 499 copies/ml, depending on the extraction method and the thermocycler used (Fung et al., 2020).

In RNA FISH, there are no requirements for RNA extraction, reverse transcription, or DNA amplification. FISH enhances the hybridization signal and improves the sensitivity through multiple immunochemical reactions, and its sensitivity is comparable with that of radioactive probes (Ma et al., 2012). Thus, RNA FISH enables high-sensitivity single-molecular (particle) detection of virus/viral RNA/RNA granules. The sensitivity of viral detection is therefore improved leading to a more accurate diagnosis.

In RT-PCR, the cycle threshold (Ct) value is the cycle number at which the fluorescence generated within a reaction crosses the fluorescence threshold, i.e., the fluorescent signal is significantly above that of the background fluorescence. It is inversely proportional to the original relative expression level of the gene of interest. However, Ct values might be affected by pre-analytic, analytic, and post-analytic variables (such as collection technique, specimen type, sampling time, viral kinetics, transport/storage conditions, nucleic acid extraction, viral RNA load, primer designing, real-time PCR efficiency, thermocycler used, and Ct value determination method; Mardian et al., 2021; Rabaan et al., 2021). In addition, Ct threshold values can demonstrate wide variation across differing populations and over time (Walker et al., 2021). For data interpretation, a Ct value smaller than 40 for all target genes is normally defined as a positive test (Mardian et al., 2021). Therefore, extra care should be taken when interpreting the results, especially when the Ct value is near the cut-off value. In RNA FISH, no cut-off value similar to the Ct is needed to distinguish between positive and negative results. Nevertheless, a threshold for differentiating fluorescent signal from noise (similar to RT-PCR) is needed. This type of threshold can be set up by the use of appropriate negative controls in the FISH. In our study, we performed these controls and obtained a clear background (low noise level).

RAT typically targets the SARS-CoV-2 N gene, which is not a mutation hotspot. A false-negative result might occur if the N antigen level is below the detection limit of the test. Moreover, RAT has been reported only to have high sensitivity when the viral load is high (e.g., 90% when $20 \leq Ct \leq 25$). For example, detection of the viral antigen might be difficult during early infection or during the incubation period. When Ct is larger than 25, the sensitivity of RAT might only be 10% (Barrera-Avalos et al., 2022). In addition, RAT sensitivity might be much lower in asymptomatic or child patients (Brümmer et al., 2021; Fujita-Rohwerder et al., 2022). Therefore, RAT might have some limitations in the clinical diagnosis of SARS-CoV-2, although it is much faster and more convenient than RT-PCR or RNA FISH.

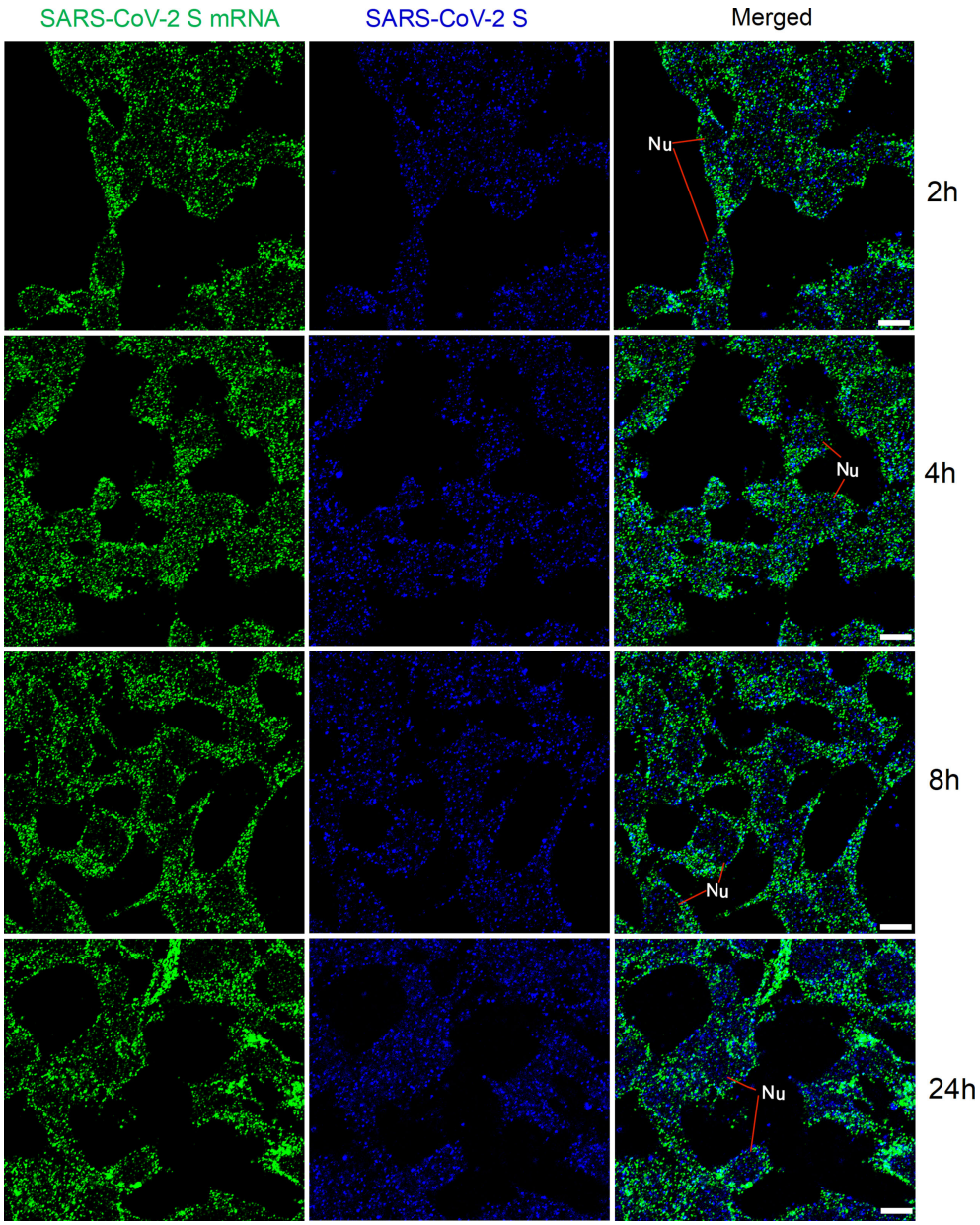

FIGURE 4
Detection of SARS-CoV-2 S mRNA (with mixed probes containing BMS001 and BMS002; green) and SARS-CoV-2 S (blue) in HEK 293T cells after transfection (2 h, 4 h, 8 h, and 24 h) with SARS-CoV-2 S plasmids. Objective lens: 60×; Scale bar: 10 μm; Nu, nucleus.

Our RNA FISH might overcome these problems and detect viral mRNA at each period/stage of infection/disease.

RNA FISH might improve specificity and reduce false positives

SARS-CoV-2 RT-PCR testing is associated with a small number of false-positive results that are normally caused by cross-contamination or/and non-specificity of primers (Keaney et al., 2021; Layfield et al., 2021; Mardian et al., 2021). Since RT-PCR can amplify a DNA sequence 10^6 times, even a few virus/viral mRNAs can cause false-positive results. Cross-contamination might occur during sample collection (e.g., large-scale nucleic acid test) or sample preparation (e.g., negative samples are contaminated by strongly positive samples nearby or a healthy person inhales a few viruses floating in the air at the testing site; Layfield et al., 2021). In

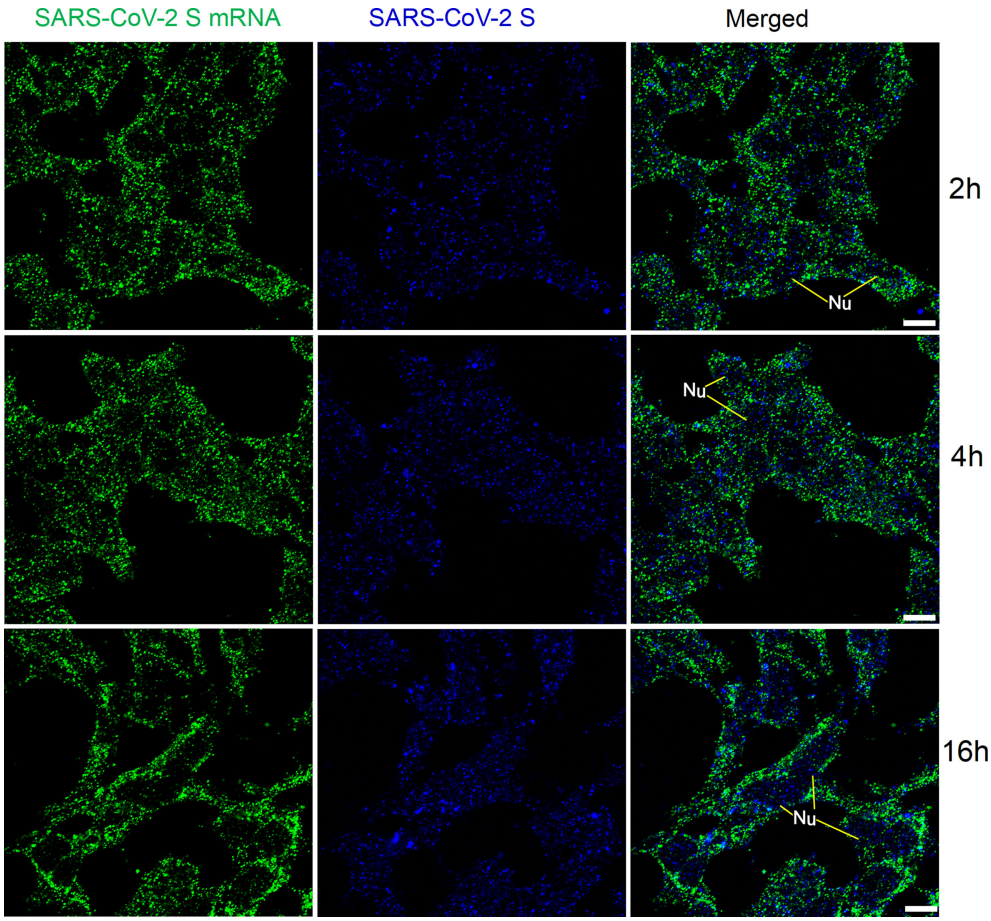

FIGURE 5
Detection of SARS-CoV-2 S mRNA (with mixed probes containing BMS001 and BMS002; with 2 h hybridization time; green) and SARS-CoV-2 S (blue) in HEK 293T cells after transfection (2 h, 4 h, and 16 h) with SARS-CoV-2 S plasmids. Objective lens: 60×; Scale bar: 10 μm; Nu, nucleus.

RNA FISH, viral RNA/genome from cross-contamination cannot be amplified, since there is no nucleic acid amplification step. In addition, smears made from nasopharyngeal or oropharyngeal swabs can be used for RNA FISH, and it is improbable that the virus/viral mRNAs from contamination will appear inside the cells.

The non-specificity of primers in RT-PCR is usually attributable to the quality of the manufacturer's reagent (Westhaus et al., 2021). This problem might also be present in RNA FISH. However, the lengths of the probes that we have used in RNA FISH are about 40-50 nt, which is longer than those of regular RT-PCR primers (about 20 nt). Longer probes will have better specificity than shorter probes, although the hybridization/reaction time might be longer.

False positives might also be a problem in RAT in some circumstances. RAT can be more reliably applied in areas with community prevalence (e.g., the positive rate is higher than or equal to 5%). In low-endemic or non-endemic areas, false-positive results (up to 60%) are more likely to occur if RT-PCR is used as a "gold standard" (Gans et al., 2022).

RNA FISH allows subcellular localization and analysis

PFA fixation of infectious samples can improve both biosafety and the speed of detection, while preserving the ultrastructure of biological material without interfering significantly with the preparation (i.e., negative staining) and the detection of viruses. Fixed samples can be kept for a long time (e.g., for retrospective analysis), and the infection risk of medical professionals is minimalized.

Subcellular localization and the analysis of RNA/mRNA in cells/tissues are not possible with RT-PCR. Our RNA FISH method can detect the uncoated RNA genome, replicating mRNA/RNA (by detecting the negative-strand mRNAs), and

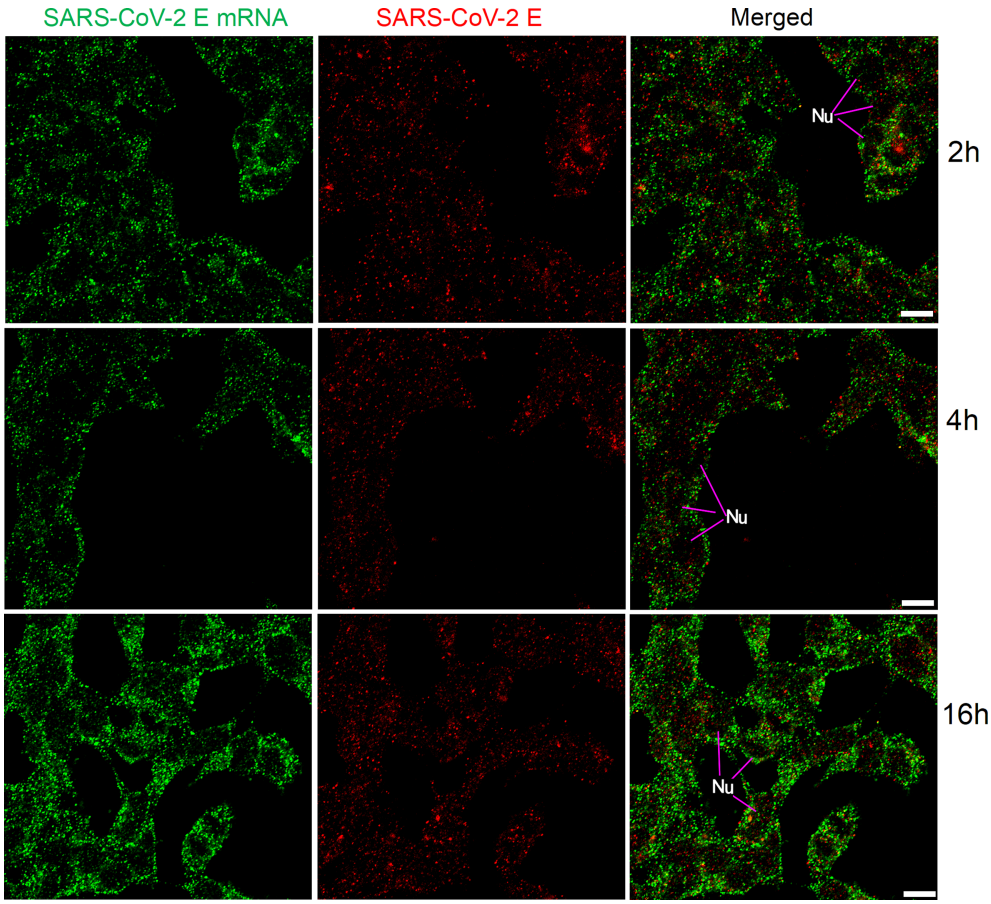

FIGURE 6
Detection of SARS-CoV-2 E mRNA (with mixed probes containing BME001 and BME002; with 2 h hybridization time; green) and SARS-CoV-2 E protein (red) in HEK 293T cells after transfection (2 h, 4 h, and 16 h) with SARS-CoV-2 E plasmids. Objective lens: 60×; Scale bar: 10 μm; Nu, nucleus.

RNAs in viral particles inside cells and tissue fluid (e.g., sputum and saliva). Therefore, RNA FISH enables the detection of viral replication and of active infection. In addition, the cellular localization of mRNA/RNA can exclude some false positives since virus/viral RNA from cross-contamination is unlikely to be localized inside the cells.

The Ct values of RT-PCR can be correlated with viral load and disease severity in COVID-19 (Rabaan et al., 2021). However, no quantitative analysis can be performed by RT-PCR for RNA inside the samples. Our RNA FISH can localize mRNA/RNA inside the cells on smears so that both qualitative and quantitative analyses are possible (Ma et al., 2012). Quantitative analysis can be performed by examining the fluorescent intensity or the number of granules/DMVs containing RNA inside the cells on the smears (Rabaan et al., 2021). In addition, for smears without cells (e.g., smears prepared from saliva or wastewater), absolute quantitative analysis can be performed in order to obtain the number or concentration of viruses.

The determination of RT-PCR results is automatic, whereas result determination in RNA FISH is manually performed by pathologists. Nevertheless, we can also use artificial intelligence technology and digital pathology for automatic FISH and image analysis/result determination (van der Logt et al., 2015).

FISH might be cost-effective and convenient

The cost of RNA FISH is much lower than that of RT-PCR. RNA FISH does not require a large amount of primers and enzymes for amplification, and so the cost might be lower than that of RT-PCR. In addition, RNA FISH does not need expensive instruments such as automated DNA/RNA purification systems,

thermocyclers, and RT-PCR Detection Systems. A wide-field fluorescent microscope is sufficient for the final examination of slides enabling laboratory tests to be carried out in a regular laboratory with no sophisticated facilities and instruments [e.g., in small clinics/hospitals, in rural/remote/undeveloped regions (i.e., Australian Quarantine Centre at Christmas Island), or in some military bases].

The time required for RNA FISH is a little longer than that for RT-PCR because of the multiple steps involved including fixation, FISH, and immunodetection. However, we can use a few approaches to reduce the time needed. For example, in this study, we have reduced the hybridization time to 2 h and have still obtained excellent results. In addition, we can use directly fluorescent dye-labeled probes for direct hybridization, possibly reducing the time further. Furthermore, both RNA FISH and result determination can be automatized to reduce test time and labor (van der Logt et al., 2015).

Another limitation of mRNA FISH might be unspecific staining or background attributable to either non-specific antibody binding to endogenous Fc receptors (FcRs) or a combination of ionic and hydrophobic interactions (Buchwalow et al., 2011). If a primary antibody (e.g., anti-DIG) binds epitopes other than its target, it can generate unspecific signals that can be further amplified by dye-conjugated secondary antibodies. However, several approaches [e.g., use of highly specific antibodies, optimization of the antibody dilutions, use of negative controls for secondary antibodies, employment of $F(ab')_2$ fragments of antibodies only, and use of high-quality goat serum or BSA for blocking before immunostaining] can be utilized to minimize this effect (Ma and Tanese, 2013).

In summary, our approach might significantly improve the accuracy and sensitivity of SARS-CoV-2 detection. In the present work, we have only compared our method with other methods from methodological viewpoints. We have applied our mRNA FISH on several clinical samples (smears made from nasopharyngeal or oropharyngeal swabs) successfully. However, we have not tested its sensitivity and specificity for clinical diagnosis, because of biosafety/ethical issues.

Our RNA FISH can be performed on smears containing cells (e.g., from nasopharyngeal swabs) or smears without cells (e.g., from sputum, saliva, and wastewater). It can also be widely used for the high-sensitivity single-molecular detection of other RNA viruses [e.g., SARS-CoV-1, MERS-CoV, Hepatitis A virus, all influenza viruses, and human immunodeficiency virus (HIV)] in various type of samples (including tissue, body fluid, blood, and water). In addition, our RNA FISH can also be utilized for the detection of DNA viruses [e.g., Monkeypox virus, human papillomavirus (HPV), and cytomegalovirus (CMV)] *via* the detection of their mRNAs inside cells. We believe that our RNA FISH approach will increasingly find applications for more accurate diagnosis and more effective public health surveillance of viral infectious diseases.

Data availability statement

The original contributions presented in the study are included in the article/Supplementary Material. Further inquiries can be directed to the corresponding authors.

Author contributions

WG, DakH, and BM conceived the study and designed the experiments. DakH and BM wrote the paper. DaiH, TW, JU, and BM performed experiments and analyzed the data. All authors contributed to the article and approved the submitted version.

Conflict of interest

The authors declare that the research was conducted in the absence of any commercial or financial relationships that could be construed as a potential conflict of interest.

Publisher's note

Supplementary material

The Supplementary Material for this article can be found online at: https://www.frontiersin.org/articles/10.3389/fcimb.2022.960938/full#supplementary-material

SUPPLEMENTARY FIGURE 1
Flowchart of experimental design. Washing steps are not shown. PFA; paraformaldehyde; DIG; digoxin.

SUPPLEMENTARY VIDEO 1
Detection of SARS-CoV-2 E mRNA (with probe-BME001; red) and SARS-CoV-2 E (green) in HEK 293T cells at 24 h after transfection with SARS-CoV-2 E plasmids. The video was generated by volume rendering of a Z-Stack (as shown in Figure 1B; cropped). Optical slice interval: 0.50 µm; Stack size: 6.0 µm. Objective lens: 60×.

References

Aimrane, A., Laaradia, M. A., Sereno, D., Perrin, P., Draoui, A., Bougadir, B., et al. (2022). Insight into COVID-19's epidemiology, pathology, and treatment. *Heliyon* 8, e08799. doi: 10.1016/j.heliyon.2022.e08799

Al-Awwal, N., Dweik, F., Mahdi, S., El-Dweik, M., and Anderson, S. H. (2022). A review of SARS-CoV-2 disease (COVID-19): Pandemic in our time. *Pathogens* 11, 368. doi: 10.3390/pathogens11030368

Barrera-Avalos, C., Luraschi, R., Vallejos-Vidal, E., Mella-Torres, A., Hernández, F., Figueroa, M., et al. (2022). The rapid antigen detection test for SARS-CoV-2 underestimates the identification of COVID-19 positive cases and compromises the diagnosis of the SARS-CoV-2 (K417N/T, E484K, and N501Y) variants. *Front. Public Health* 9. doi: 10.3389/fpubh.2021.780801

Borges do Nascimento, I. J., O'Mathúna, D. P., von Groote, T. C., Abdulazeem, H. M., Weerasekara, I., Marusic, A., et al. (2021). Coronavirus disease (COVID-19) pandemic: An overview of systematic reviews. *BMC Infect. Dis.* 21, 525. doi: 10.1186/s12879-021-06214-4

Brümmer, L. E., Katzenschlager, S., Gaeddert, M., Erdmann, C., Schmitz, S., Bota, M., et al. (2021). Accuracy of novel antigen rapid diagnostics for SARS-CoV-2: A living systematic review and meta-analysis. *PloS Med.* 18, e1003735. doi: 10.1371/journal.pmed.1003735

Buchwalow, I., Samoilova, V., Boecker, W., and Tiemann, M. (2011). Non-specific binding of antibodies in immunohistochemistry: Fallacies and facts. *Sci. Rep.* 1, 28. doi: 10.1038/srep00028

Chia, W. N., Tan, C. W., Foo, R., Kang, A. E. Z., Peng, Y., Sivalingam, V., et al. (2020). Serological differentiation between COVID-19 and SARS infections. *Emerg. Microbes Infect.* 9, 1497–1505. doi: 10.1080/22221751.2020.1780951

Chu, D. K. W., Pan, Y., Cheng, S. M. S., Hui, K. P. Y., Krishnan, P., Liu, Y., et al. (2020). Molecular diagnosis of a novel coronavirus, (2019-nCoV) causing an outbreak of pneumonia. *Clin. Chem.* 66, 549–555. doi: 10.1093/clinchem/hvaa029

Corman, V. M., Landt, O., Kaiser, M., Molenkamp, R., Meijer, A., Chu, D. K., et al. (2020). Detection of 2019 novel coronaviru -nCoV) by real-time RT-PCR. *Euro. Surveill.* 25, 2000045. doi: 10.2807/1560-7917.ES.2020.25.3.2000045

da Silva Torres, M. K., Bichara, C. D. A., de Almeida, M. N. D. S., Vallinoto, M. C., Queiroz, M. A. F., Vallinoto, I. M. V. C., et al. (2022). The complexity of SARS-CoV-2 infection and the COVID-19 pandemic. *Front. Microbiol.* 13. doi: 10.3389/fmicb.2022.789882

Fujita-Rohwerder, N., Beckmann, L., Zens, Y., and Verma, A. (2022). Diagnostic accuracy of rapid point-of-care tests for diagnosis of current SARS-CoV-2 infections in children: A systematic review and meta-analysis. *BMJ Evid. Based Med.* 27, 274–287. doi: 10.1136/bmjebm-2021-111828

Fung, B., Gopez, A., Servellita, V., Arevalo, S., Ho, C., Deucher, A., et al. (2020). Direct comparison of SARS-CoV-2 analytical limits of detection across seven molecular assays. *J. Clin. Microbiol.* 58, e01535–e01520. doi: 10.1128/JCM.01535-20

Gans, J. S., Goldfarb, A., Agrawal, A. K., Sennik, S., Stein, J., and Rosella, L. (2022). False-positive results in rapid antigen tests for SARS-CoV-2. *JAMA* 327, 485–486. doi: 10.1001/jama.2021.24355

Gómez, S. A., Rojas-Valencia, N., Gómez, S., Egidi, F., Cappelli, C., and Restrepo, A. (2021). Binding of SARS-CoV-2 to cell receptors: A tale of molecular evolution. *Chembiochem.* 22, 724–732. doi: 10.1002/cbic.202000618

Hong, K. H., Lee, S. W., Kim, T. S., Huh, H. J., Lee, J., Kim, S. Y., et al. (2020). Guidelines for laboratory diagnosis of coronavirus disease 2019 (COVID-19) in Korea. *Ann. Lab. Med.* 40, 351–360. doi: 10.3343/alm.2020.40.5.351

Keaney, D., Whelan, S., Finn, K., and Lucey, B. (2021). Misdiagnosis of SARS-CoV-2: A critical review of the influence of sampling and clinical detection methods. *Med. Sci. (Basel)* 9, 36. doi: 10.3390/medsci9020036

Khalid, M. F., Selvam, K., Jeffry, A. J. N., Salmi, M. F., Najib, M. A., Norhayati, M. N., et al. (2022). Performance of rapid antigen tests for COVID-19 diagnosis: A systematic review and meta-analysis. *Diagnostics (Basel)* 12, 110. doi: 10.3390/diagnostics12010110

Lakdawala, S. S., Wu, Y., Wawrzusin, P., Kabat, J., Broadbent, A. J., Lamirande, E. W., et al. (2014). Influenza a virus assembly intermediates fuse in the cytoplasm. *PloS Pathog.* 10, e1003971. doi: 10.1371/journal.ppat.1003971

Layfield, L. J., Camp, S., Bowers, K., and Miller, D. C. (2021). SARS-CoV-2 detection by reverse transcriptase polymerase chain reaction testing: Analysis of false positive results and recommendations for quality control measures. *Pathol. Res. Pract.* 225, 153579. doi: 10.1016/j.prp.2021.153579

Lindsay, L., Secrest, M. H., Rizzo, S., Keebler, D. S., Yang, F., and Tsai, L. (2021). Factors associated with COVID-19 viral and antibody test positivity and assessment of test concordance: A retrospective cohort study using electronic health records from the USA. *BMJ Open* 11, e051707. doi: 10.1136/bmjopen-2021-051707

Lin, C., Ye, R., and Xia, Y. (2015). A meta-analysis to evaluate the effectiveness of real-time PCR for diagnosing novel coronavirus infections. *Genet. Mol. Res.* 14, 15634–15641. doi: 10.4238/2015.December.1.15

Ma, B., Baj, G., Tongiorgi, E., Chao, M. V., and Tanese, N. (2010). Localization of BDNF mRNA with the huntington's disease protein in rat brain. *Mol. Neurodegener.* 5, 22. doi: 10.1186/1750-1326-5-22

Mardian, Y., Kosasih, H., Karyana, M., Neal, A., and Lau, C. Y. (2021). Review of current COVID-19 diagnostics and opportunities for further development. *Front. Med. (Lausanne)* 8. doi: 10.3389/fmed.2021.615099

Ma, B., Savas, J. N., Chao, M. V., and Tanese, N. (2012). Quantitative analysis of BDNF/TrkB protein and mRNA in cortical and striatal neurons using α-tubulin as a normalization factor. *Cytometry A* 81, 704–717. doi: 10.1002/cyto.a.22073

Ma, B., and Tanese, N. (2013). Combined FISH and immunofluorescent staining methods to colocalize proteins and mRNA in neurons and brain tissue. *Methods Mol. Biol.* 1010, 123–138. doi: 10.1007/978-1-62703-411-1_9

Rabaan, A. A., Tirupathi, R., Sule, A. A., Aldali, J., Mutair, A. A., Alhumaid, S., et al. (2021). Viral dynamics and real-time RT-PCR ct values correlation with disease severity in COVID-19. *Diagnostics (Basel)* 11, 1091. doi: 10.3390/diagnostics11061091

Ravi, A. B., Singh, V. P. P., Chandran, R., Venugopal, K., Haridas, K., and Kavitha, R. (2021). COVID-19 antibody tests: An overview. *J. Pharm. Bioallied Sci.* 13, S48–S51. doi: 10.4103/jpbs.JPBS_786_20

van der Logt, E. M., Kuperus, D. A., van Setten, J. W., van den Heuvel, M. C., Boers, J. E., Schuuring, E., et al. (2015). Fully automated fluorescent *in situ* hybridization (FISH) staining and digital analysis of HER2 in breast cancer: A validation study. *PloS One* 10, e0123201. doi: 10.1371/journal.pone.0123201

V'kovski, P., Kratzel, A., Steiner, S., Stalder, H., and Thiel, V. (2021). Coronavirus biology and replication: Implications for SARS-CoV-2. *Nat. Rev. Microbiol.* 19, 155–170. doi: 10.1038/s41579-020-00468-6

Walker, A. S., Pritchard, E., House, T., Robotham, J. V., Birrell, P. J., Bell, I., et al. (2021). Ct threshold values, a proxy for viral load in community SARS-CoV-2 cases, demonstrate wide variation across populations and over time. *Elife* 10, e64683. doi: 10.7554/eLife.64683

Wang, Y. H., Wu, C. C., Bai, C. H., Lu, S. C., Yang, Y. P., Lin, Y. Y., et al. (2021). Evaluation of the diagnostic accuracy of COVID-19 antigen tests: A systematic review and meta-analysis. *J. Chin. Med. Assoc.* 84, 1028–1037. doi: 10.1097/JCMA.0000000000000626

Weissleder, R., Lee, H., Ko, J., and Pittet, M. J. (2020). COVID-19 diagnostics in context. *Sci. Transl. Med.* 12, eabc1931. doi: 10.1126/scitranslmed.abc1931

Westhaus, S., Weber, F. A., Schiwy, S., Linnemann, V., Brinkmann, M., Widera, M., et al. (2021). Detection of SARS-CoV-2 in raw and treated wastewater in Germany - suitability for COVID-19 surveillance and potential transmission risks. *Sci. Total Environ.* 751, 141750. doi: 10.1016/j.scitotenv.2020.141750

Yoo, H. M., Kim, I. H., and Kim, S. (2021). Nucleic acid testing of SARS-CoV-2. *Int. J. Mol. Sci.* 22, 6150. doi: 10.3390/ijms22116150

frontiers | Frontiers in Cellular and Infection Microbiology

TYPE Original Research
PUBLISHED 27 October 2022
DOI 10.3389/fcimb.2022.1010683

OPEN ACCESS

EDITED BY
Viviane Fongaro Botosso,
Butantan Institute, Brazil

REVIEWED BY
Wei Zhang,
Zhejiang Provincial People's Hospital, China
Chenghao Zhanghuang,
Kunming Children's Hospital, China
Yuyong Jiang,
Capital Medical University, China

*CORRESPONDENCE
Jixun Xu
2068187@qq.com
Bo Hu
hubo@mail.sysu.edu.cn

†These authors have contributed equally to this work

SPECIALTY SECTION
This article was submitted to Virus and Host, a section of the journal Frontiers in Cellular and Infection Microbiology

RECEIVED 03 August 2022
ACCEPTED 11 October 2022
PUBLISHED 27 October 2022

CITATION
Chen Y, Gong J, He G, Jie Y, Chen J, Wu Y, Hu S, Xu J and Hu B (2022) An early novel prognostic model for predicting 80-day survival of patients with COVID-19.
Front. Cell. Infect. Microbiol. 12:1010683.
doi: 10.3389/fcimb.2022.1010683

An early novel prognostic model for predicting 80-day survival of patients with COVID-19

Yaqiong Chen[1†], Jiao Gong[1†], Guowei He[1], Yusheng Jie[2], Jiahao Chen[1], Yuankai Wu[2], Shixiong Hu[3], Jixun Xu[3*] and Bo Hu[1*]

[1]Department of Laboratory Medicine, Third Affiliated Hospital of Sun Yat-sen University, Guangzhou, Guangdong, China, [2]Department of Infectious Diseases, Key Laboratory of Liver Disease of Guangdong Province, Third Affiliated Hospital of Sun Yat-sen University, Guangzhou, Guangdong, China, [3]Department of Laboratory Medicine, Huangshi Hospital of Traditional Chinese Medicine (TCM) (Infectious Disease Hospital), Huangshi, Hubei, China

The outbreak of the novel coronavirus disease 2019 (COVID-19) has had an unprecedented impact worldwide, and it is of great significance to predict the prognosis of patients for guiding clinical management. This study aimed to construct a nomogram to predict the prognosis of COVID-19 patients. Clinical records and laboratory results were retrospectively reviewed for 331 patients with laboratory-confirmed COVID-19 from Huangshi Hospital of Traditional Chinese Medicine (TCM) (Infectious Disease Hospital) and Third Affiliated Hospital of Sun Yat-sen University. All COVID-19 patients were followed up for 80 days, and the primary outcome was defined as patient death. Cases were randomly divided into training (n=199) and validation (n=132) groups. Based on baseline data, we used statistically significant prognostic factors to construct a nomogram and assessed its performance. The patients were divided into Death (n=23) and Survival (n=308) groups. Analysis of clinical characteristics showed that these patients presented with fever (n=271, 81.9%), diarrhea (n=20, 6.0%) and had comorbidities (n=89, 26.9.0%). Multivariate Cox regression analysis showed that age, UREA and LDH were independent risk factors for predicting 80-day survival of COVID-19 patients. We constructed a qualitative nomogram with high C-indexes (0.933 and 0.894 in the training and validation groups, respectively). The calibration curve for 80-day survival showed optimal agreement between the predicted and actual outcomes. Decision curve analysis revealed the high clinical net benefit of the nomogram. Overall, our nomogram could effectively predict the 80-day survival of COVID-19 patients and hence assist in providing optimal treatment and decreasing mortality rates.

KEYWORDS

COVID-19, nomogram, prognosis, predict, survival

Introduction

As of July 24, 2022, just under 567 million confirmed cases of COVID-19 and a global death toll exceeding 6.3 million deaths had been reported globally (https://www.who.int) (2022). Severe Acute Respiratory Syndrome coronavirus 2 (SARS-CoV-2) is the cause of the serious life-threatening disease known as COVID-19 (Liu et al., 2020a). COVID-19 mortality is intricately linked to the lack of access to specific therapeutic agents or vaccines (Cascella et al., 2020), given that the global health system is significantly burdened by this pandemic (Momtazmanesh et al., 2020).

Most patients have mild or common symptoms and can be discharged after symptomatic treatment. However, some patients may require further hospitalization with disease progression, presenting critical symptoms or complications, such as dyspnea, hypoxemia and acute respiratory distress syndrome (Huang et al., 2020; Zhu et al., 2020). Owing to the rapid spread of COVID-19, medical resources in many countries, especially the intensive care unit (ICU), are being over-requisitioned and almost exhausted (Wu et al., 2020b). Therefore, decreasing COVID-19-related deaths and alleviating the burden on overloaded medical facilities emphasize the need for a model for early prediction of severe disease progression and death. Many risk factors associated with severe COVID-19 disease progression have been identified, including comorbidity, older age, lower lymphocyte and higher lactate dehydrogenase (LDH), viral load and so on (Gong et al., 2020; Ji et al., 2020; Pujadas et al., 2020). Subsequently, these risk factors were harnessed to construct prediction models (Li et al., 2020a; Wu et al., 2020a; Zhou et al., 2020), such as CALL score and Patient Information Based Algorithm (PIBA) (Ji et al., 2020; Wang et al., 2020b; Schiaffino et al., 2021).

A nomogram is a graphical representation of predictive statistical models for individual patients and also an alternative method for various types of diseases (Gong et al., 2020; Li et al., 2020b; Liu et al., 2020b; Xu et al., 2020). However, few nomograms have hitherto been developed to predict the prognosis of COVID-19 patients. In this retrospective study, we analyzed the laboratory tests of COVID-19 patients and constructed a nomogram to predict the prognosis more accurately based on baseline data from two clinical centers. Importantly, our nomogram could guide clinicians in predicting the death risk of COVID-19 patients, providing early intervention, prioritizing medical resources and reducing mortality.

Materials and methods

Data collection

Clinical records and laboratory results were retrospectively reviewed for 331 patients with COVID-19 from Huangshi Hospital of Traditional Chinese Medicine (Infectious Disease Hospital) and Third Affiliated Hospital of Sun Yat-sen University between January 20, 2020 and May 20, 2020. Patients younger than 14 years of age were excluded from the study. Two patient between 14 to 15 years old was included in this study. Demographic data, including age, sex, clinical signs and symptoms such as fever and diarrhea, presence of comorbidities and clinical laboratory test results, were all collected upon admission. All included COVID-19 patients were followed up for 80 days on admission by phone to determine whether they survived (Survival group) or not (Death group).

The study was approved by the Ethics Committee of Third Affiliated Hospital of Sun Yat-sen University and the Ethics Commission of Huangshi Infectious Disease Hospital and exempted from informed consent given the retrospective nature of this study.

Patients diagnosed with COVID-19 were included in the study. The diagnosis of SARS-CoV-2 infection has been described previously (Gong et al., 2020). A confirmed case was defined as an individual with laboratory-confirmed SARS-CoV-2, which required positive results of SARS-CoV-2 RNA, regardless of clinical symptoms and signs.

Laboratory methods

The clinical laboratory examination results of patients for white blood cell (WBC), red blood cell (RBC), hemoglobin (HGB), blood platelet (PLT), neutrophils, lymphocyte, neutrophil-lymphocyte ratio (NLR), monocyte, international normalized ratio (INR), albumin (ALB), C-reactive protein (CRP), direct bilirubin (DBIL), UREA, lactate dehydrogenase (LDH), glucose (GLU) were collected. All biochemical parameters were obtained through standard automated laboratory methods and commercial kits in accordance with the instrument operating procedures.

Statistical analysis

Categorical variables were expressed as frequency and percentage; continuous variables as mean (standard deviation [SD]) or median (interquartile spacing [IQR]), as appropriate. The Fisher exact test was used to analyze the significance of Categorical variables. The Student's t-test was used to compare continuous variables with a normal distribution. The Mann-Whitney U test was used for continuous variables with a non-parametric distribution. SPSS 22.0 statistical software package (SPSS, Inc., Chicago, IL, USA) was used for the above statistical analysis. To determine the relative importance of each feature, the Least Absolute Shrinkage and Selection Operator (LASSO) was used for feature selection, and the logistic regression was used to establish the regression prediction model.

To minimize bias of the regression coefficient, predictors with a missing rate of more than 5% were excluded. As

previously described (Gong et al., 2020), the missing values were imputed by the expectation-maximization (EM) method using SPSS statistical software. The nomogram was established with the rms package, and the performance of the nomogram was evaluated by discrimination (Harrell's concordance index) and calibration (calibration plots and Hosmer-Lemeshow calibration test) analyses in R. R software (version 3.6.2) was used for all statistical analysis except SPSS analysis. The optimal cut-off value of total points of the nomogram was determined by the R package survminer, which uses the maximally selected rank statistics from the 'maxstat' R package. Survival curves were depicted by the Kaplan-Meier analysis and compared by the log-rank test. A P-value < 0.05 was statistically significant.

Results

Demographics and characteristics of COVID-19 patients

A total of 331 patients with COVID-19 were included from the Third Affiliated Hospital of Sun Yat-sen University (n=18) and Huangshi Hospital of Traditional Chinese Medicine (Infectious Disease Hospital) (n=313). All patients were followed-up and then divided into death (n=23) and survival (n=308) groups (Figure 1). The median age of the Death and Survival groups was significantly different (69 years and 51 years, respectively, P<0.01). Analysis of clinical characteristics showed that these patients presented with fever (n=271, 81.9%), diarrhea (n=20, 6.0%) and had comorbidities (n=89, 26.9.0%). Moreover, the number of patients with older age and comorbidities in the Death group was significantly greater than in the Survival group (P<0.05) (Table 1). There were no significant differences in sex, clinical symptoms such as fever and diarrhea and laboratory markers WBC, HGB, and monocyte between both groups. However, the neutrophil count, NLR, INR, CRP, DBIL, UREA, LDH and GLU were significantly higher in the Death group than in the Survival group (P<0.01), while RBC, PLT, lymphocyte count and ALB levels were significantly lower in the Death group than in the Survival group (P<0.01) (Table 1).

Multivariate Cox regression analysis for 80-day survival of patients with COVID-19

All patients were randomly divided into training (n=199) and validation (n=132) groups. There were no significant differences in age and sex between the training and validation groups (Supplementary Table 1). A total of 21 features were collected from each patient. After removing irrelevant and redundant features, 14 features were retained for LASSO regression analysis (Figures 2A, B). The LASSO regression analysis showed that age, DBIL, UREA and LDH were predictive prognostic factors for the 80-day survival of COVID-19 patients in the training group. All these 4 features were incorporated in the multivariate Cox regression analysis. The multivariate Cox regression analysis demonstrated that age, UREA and LDH were independent prognostic factors for the 80-day survival of patients with COVID-19 (Figure 2C).

Prognostic nomogram for 80-day survival of patients with COVID-19

To predict 80-day survival of patients with COVID-19, a prognostic nomogram was constructed based on the above-mentioned statistically significant independent prognostic factors (Figure 3A). The bootstrap-corrected concordance

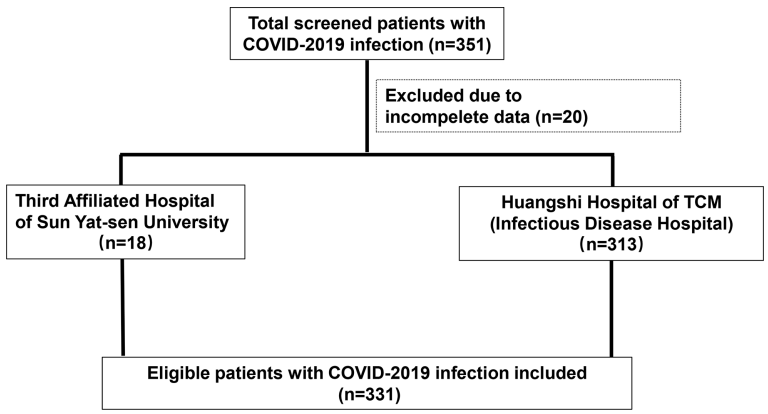

FIGURE 1
Flow chart of enrolled patients with COVID-19.

TABLE 1 Baseline demographic and clinical characteristics of COVID-19 patients in Survival and Death groups.

Variable	Survival (n=308)	Death (n=23)	*p*-value
Age (years)	51.00 (39.00, 62.00)	69.00 (60.00, 84.00)	<0.01
Sex			0.83
Female	158 (51.3%)	11 (47.8%)	
Male	150 (48.7%)	12 (52.2%)	
Fever			1.00
No	56 (18.2%)	4 (17.4%)	
Yes	252 (81.8%)	19 (82.6%)	
Diarrhea			0.15
No	291 (94.5%)	20 (87.0%)	
Yes	17 (5.5%)	3 (13.0%)	
Comorbidities			0.03
No	230 (74.7%)	12 (52.2%)	
Yes	78 (25.3%)	11 (47.8%)	
WBC ($\times10^9$/L)	4.51 (3.58, 5.54)	5.55 (3.75, 7.35)	0.05
RBC ($\times10^{12}$/L)	4.48 (0.61)	4.08 (0.81)	<0.01
HGB (g/L)	132.04 (16.80)	125.17 (17.97)	0.06
PLT ($\times10^9$/L)	159.00 (130.00, 197.50)	123.00 (90.00, 176.00)	<0.01
Neutrophils ($\times10^9$/L)	2.82 (2.06, 3.71)	4.27 (2.71, 6.41)	<0.01
Lymphocyte ($\times10^9$/L)	1.13 (0.81, 1.48)	0.66 (0.46, 0.77)	<0.01
NLR	2.27 (1.54, 3.56)	7.22 (3.86, 15.93)	<0.01
Monocyte ($\times10^9$/L)	0.45 (0.31, 0.58)	0.36 (0.21, 0.53)	0.08
INR	0.91 (0.87, 0.95) (n=279)	0.96 (0.90, 1.04) (n=22)	<0.01
ALB (g/L)	40.60 (36.80, 43.40) (n=303)	35.60 (30.00, 38.40)	<0.01
CRP (mg/L)	20.18 (6.71, 47.74) (n=300)	53.05 (37.05, 91.13)	<0.01
DBIL (umol/L)	6.30 (4.80, 7.70) (n=303)	8.90 (6.50, 12.00)	<0.01
UREA (mmol/L)	3.71 (3.00, 4.71)	5.49 (4.50, 9.67)	<0.01
LDH (U/L)	241.00 (195.00, 312.00) (n=294)	391.00 (316.00, 574.00) (n=22)	<0.01
GLU (mmol/L)	5.71 (5.21, 6.45)	6.94 (5.80, 9.93)	<0.01

All variables with missing values are labeled with a specific number of samples.
WBC, white blood cell; RBC, red blood cell; HGB, hemoglobin; PLT, blood platelet; NLR, neutrophil-to-lymphocyte ratio; INR, international normalized ratio; ALB, albumin; CRP, C-reactive protein; DBIL, direct bilirubin; LDH, lactate dehydrogenase; GLU, glucose.

index (C-index) was 0.933 (0.879-0.987) and 0.894 (0.819-0.969) for the training and validation groups, respectively. The calibration plot for the probability of 80-day survival showed optimal agreement between the prediction and actual outcomes in training (Figure 3B) and validation (Figure 3C) groups. Furthermore, a total score was obtained by the sum of scores of the associated predictors and referred to as the probability of 80-day survival in the bottom axis. We divided these patients in the training group into high and low-score groups according to the optimal cut-off score value (86.72142), determined by the R package survminer. COVID-19 patients in the high-score group had a poor prognosis compared to the low-score group (Figure 3D). Similar results were observed in the validation group (Figure 3E). To evaluate the clinical applicability of our prognostic nomogram, we conducted a decision curve analysis (DCA). DCA substantiated the net clinical benefit of the prognostic nomogram in the training group (Figure 4).

Moreover, we compared the performance of our nomogram in predicting the survival probability of COVID-19 with other models reported in the literature (Cai's model: age, D-dimer, CRP; Cheng's model: UREA, age, D-dimer) (Cheng et al., 2020a; Cai et al., 2021). The parameters age, D-dimer, CRP, UREA, and LDH were available for 170 patients in the training group. Although there was no significant difference during calibration curve analysis between the 3 models (Supplementary Figure 1), the C-index of our model was relatively higher (0.930, 95%CI: 0.875-0.985) than that of Cai's (0.882, 95%CI: 0.799-0.965) and Cheng's nomogram (0.888, 95%CI:.805-0.971).

Discussion

In this study, age, UREA and LDH were identified as independent prognostic factors for COVID-19 patients and used

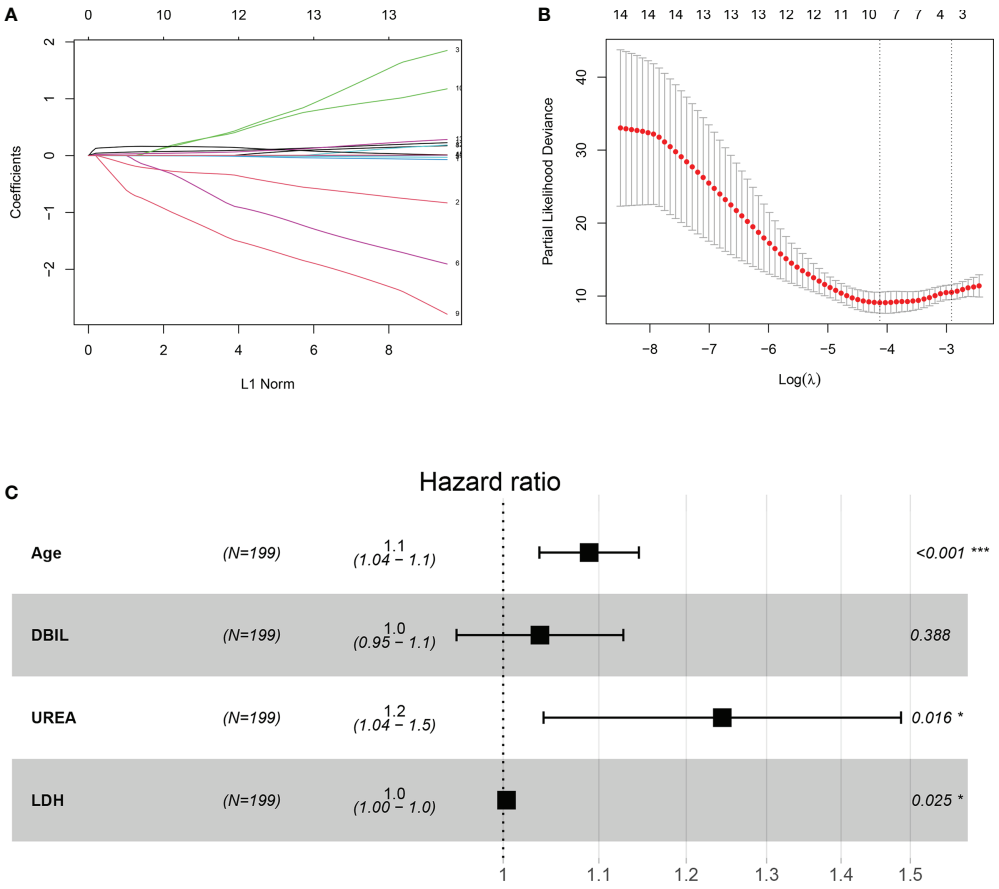

FIGURE 2
Construction of the integrated prognostic features of patients with COVID-19. **(A)** LASSO coefficient profiles of the 21 prognostic features. **(B)** Selection of the tuning parameter (lambda) in the LASSO model by fivefold cross-validation based on minimum criteria for prognosis; the lower X-axis shows log (lambda), and the upper X-axis shows the average number of prognostic features. The Y-axis indicates the partial likelihood deviance error. Red dots represent average partial likelihood deviances for every model with a given lambda, and vertical bars indicate the upper and lower values of the partial likelihood deviance errors. The vertical gray dotted lines define the optimal values of lambda, which provides the best fit. **(C)** Forest plots of multivariate Cox regression analysis for 80-day survival of patients with COVID-19. DBIL, direct bilirubin; LDH, lactate dehydrogenase.

to construct a quantitative nomogram to predict 80-day mortality, which yielded a high C-index in the training and validation groups. The nomogram yielded a high optimal agreement between predicted and actual outcomes for predicting the risk of death by calibration curve analysis and a high clinical net benefit by decision curve analysis. We also found that our model yielded a higher C-index than previously established models reported in the literature.

An increasing body of evidence suggests that risk factors for COVID-19-related mortality include older age, higher severity of illness scores, higher C-reactive protein level, lower lymphocyte counts, secondary infection and comorbidities such as diabetes (Chen et al., 2020; Wang et al., 2020a; Zhang et al., 2020). In a previous study, we found that high LDH and UREA were associated with the risk of severe COVID-19 (Gong et al., 2020). Interestingly, in the present study, we found that both markers were also associated with mortality. The serum LDH and UREA levels were significantly higher in the Death group than in the Survival group; after adjusting for DBIL, they remained independent prognostic risk factors for COVID-19. SARS-CoV-2 infection can induce an inflammatory response and subsequent kidney damage, leading to elevated LDH and UREA. LDH is a biomarker for tissue damage and systemic inflammatory response (Kishaba et al., 2014; Ferrari et al., 2020; Kermali et al., 2020) that is often significantly elevated in COVID-19 patients and is an independent risk factor for COVID-19-associated mortality. UREA is a biomarker for kidney damage (Cheng et al., 2020b) that has also been reported as an independent risk factor for in-hospital death of COVID-19 patients. The above findings were in line with the results of the present study.

Cheng et al. established a nomogram consisting of BUN, D-dimer and age to predict the survival probability of COVID-19.

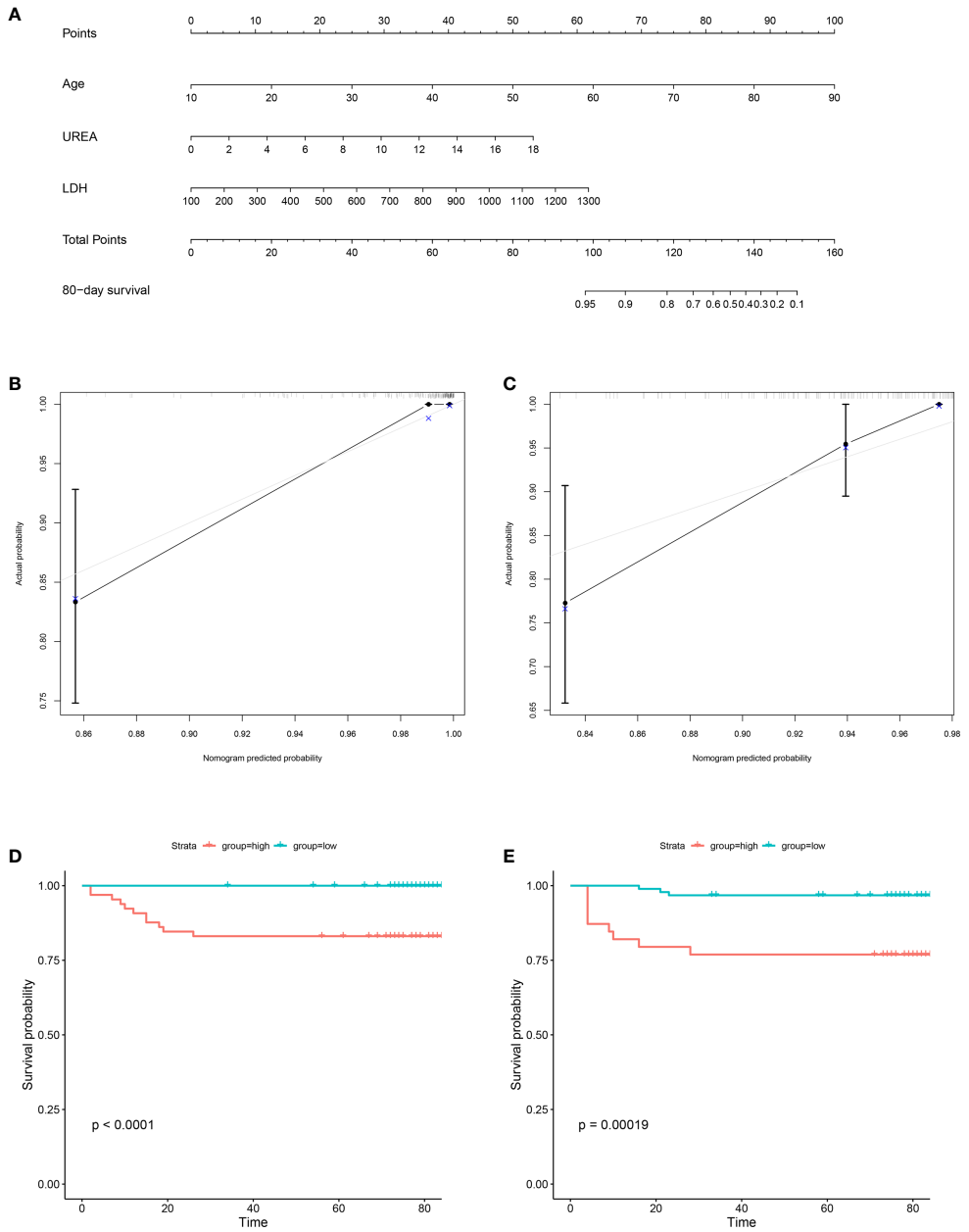

FIGURE 3
Construction of prognostic nomogram for 80-day survival of patients with COVID-19. The prognostic nomogram composed of age, UREA and LDH was developed. **(A)** Nomogram predicting 80-day survival probability in patients with COVID-19 was plotted. To use this nomogram during clinical practice, each variable axis has a separate parameter, and a line is drawn up to calculate the number of points corresponding to each parameter. The sum of these scores is located on the total point axis, and a line is drawn down along the line to get the 80-day survival probability of patients with COVID-19. **(B, C)** Calibration plot of the prognostic nomogram. The nomogram was calibrated for the probability of 80-day survival in patients with COVID-19 in the training group **(B)** and validation group **(C)**. The predicted probability of 80-day survival is plotted on the x-axis; the actual probability of 80-day survival is plotted on the y-axis (bootstrap 1,000 repetitions). **(D, E)** Kaplan-Meier Analysis for the patients with COVID-19 in the training group **(D)** and validation group **(E)**. Blue line: total points < 86.72142 (low group); red line: total points ≥86.72142 (high group).

Moreover, Li Cai et al.'s model included age, D-dimer and CRP. Interestingly, D-dimer was found to be an important prognostic factor and included in both models (Cheng et al., 2020a; Cai et al., 2021). In our research, D-dimer had more than a 5% missing rate and was hence excluded from further analysis. The parameters age, D-dimer, CRP, UREA, and LDH were available for 170 patients in the training group. Importantly, the C-index of our model was higher than that of Cheng's and Cai's,

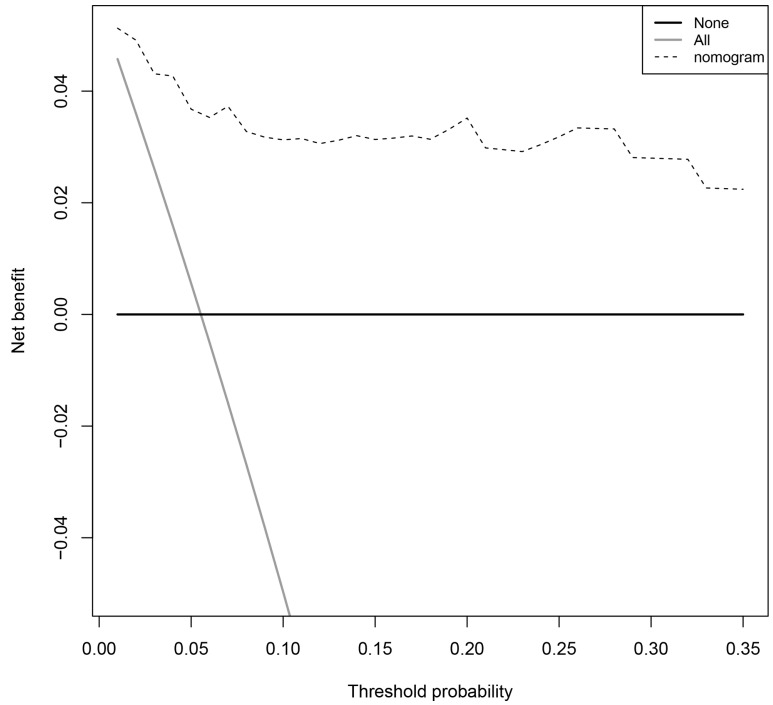

FIGURE 4
Decision curves for predicting the net benefit of the prognostic nomogram. A perfect prediction model (grey line), screen none (horizontal solid black line), and screen based on the nomogram (black dotted line).

suggesting its robust predictive ability for mortality. Although a high CRP was observed in the death group compared with the survival group, LDH was selected by LASSO regression as an important feature instead of CRP. It is widely thought that the LDH concentration is a useful marker in evaluating the prognosis of different types of pneumonia, such as pneumocystis jiroveci pneumonia and community-acquired pneumonia, and a significant correlation between LDH and CRP in COVID-19 has been documented (Ashraf et al., 2022). We also observed a moderate correlation between LDH and CRP (r=0.562), which might explain why the lasso model did not recognize CRP as an important feature.

Strengths of our nomogram include its accuracy, objectivity, and simplicity. Although a high Sequential Organ Failure Assessment (SOFA) score helps identify COVID-19 patients with poor prognosis at an early stage (Moreno et al., 1999; Zhou et al., 2020), it comprises 7 factors, and one of these is a non-objective indicator—the Glasgow Coma Scale Score (GCS) (Li et al., 2019). The predictors in our proposed nomogram are relatively inexpensive and easy to obtain in clinical practice, which makes the nomogram highly practical and easily implementable. Indeed, it is highly likely that clinicians working in community hospitals can easily judge a COVID-19-infected patient's condition by using our nomogram. Moreover, our nomogram yielded good performance in predicting survival, and its predictive accuracy (C-index) exceeded 0.9 (95%CI, 0.879-0.987) during COX regression analysis.

Importantly, we developed a practical quantitative prediction tool consisting of 3 commonly used, relatively cheap, easy-to-obtain indicators. The median follow-up time was 80 days. It was worth noting that all COVID-19 patients in the Death group experienced death within 30 days, suggesting that most people who get COVID-19 recover within a few weeks, and the same results would be obtained for predicting the 30-day mortality. In addition, our nomogram exhibited a net clinical benefit highlighting that it has huge prospects for application in clinical practice. There were some limitations in the study. First, given its retrospective nature, only 331 COVID-19 patients from two centers were included. Moreover, our nomogram was not externally validated. Therefore, more studies with larger patient cohorts are warranted to further validate our findings.

Conclusion

This study developed an accurate prognostic nomogram to early predict mortality of COVID-19 patients. This new nomogram could help clinicians in the early screening of patients with poor prognoses and optimizing the use of

available medical resources to decrease the burden on healthcare facilities.

Data availability statement

The raw data supporting the conclusions of this article will be made available from the corresponding author by request, without undue reservation.

Ethics statement

The studies involving human participants were reviewed and approved by Ethics Committee of Third Affiliated Hospital of Sun Yat-sen University and the Ethics Commission of Huangshi Hospital of Traditional Chinese Medicine (Infectious Disease Hospital). Written informed consent from the participants' legal guardian/next of kin was not required to participate in this study in accordance with the national legislation and the institutional requirements.

Author contributions

BH and JX conceived and designed this study. GH, YJ, JC, YW and SH collected the data. YC and JG drafted and critically revised the manuscript. All authors have read and approved the final manuscript. All authors contributed to the article and approved the submitted version.

Funding

This work was supported by grants from the Science and Technology Program of Guangzhou, China [201903010039]; Guangdong Key R&D Plan of China [2020B1111160003]; Guangdong Key R&D Plan of China [2019B020231001].

Conflict of interest

The authors declare that the research was conducted in the absence of any commercial or financial relationships that could be construed as a potential conflict of interest.

Publisher's note

All claims expressed in this article are solely those of the authors and do not necessarily represent those of their affiliated organizations, or those of the publisher, the editors and the reviewers. Any product that may be evaluated in this article, or claim that may be made by its manufacturer, is not guaranteed or endorsed by the publisher.

Supplementary material

The Supplementary Material for this article can be found online at: https://www.frontiersin.org/articles/10.3389/fcimb.2022.1010683/full#supplementary-material

References

Ashraf, A., Liaquat, A., Shabbir, S., Bokhari, S. A., Tariq, Z., Furrukh, Z., et al. (2022). High level of lactate dehydrogenase and ischaemia-reperfusion injury regulate the multiple organ dysfunction in patients with COVID-19. *Postgrad. Med. J.* doi: 10.1136/postgradmedj-2022-141573

Cai, L., Zhou, X., Wang, M., Mei, H., Ai, L., Mu, S., et al. (2021). Predictive nomogram for severe COVID-19 and identification of mortality-related immune features. *J. Allergy Clin. Immunol. Pract.* 9, 177–184.e173. doi: 10.1016/j.jaip.2020.10.043

Cascella, M., Rajnik, M., Cuomo, A., Dulebohn, S. C., and Di Napoli, R. (2020). Features, evaluation and treatment coronavirus (COVID-19) In: *StatPearls [Internet]*. Treasure Island (FL): StatPearls Publishing.

Cheng, A., Hu, L., Wang, Y., Huang, L., Zhao, L., Zhang, C., et al. (2020a). Diagnostic performance of initial blood urea nitrogen combined with d-dimer levels for predicting in-hospital mortality in COVID-19 patients. *Int. J. Antimicrob. Agents* 56, 106110. doi: 10.1016/j.ijantimicag.2020.106110

Cheng, Y., Luo, R., Wang, K., Zhang, M., Wang, Z., Dong, L., et al. (2020b). Kidney disease is associated with in-hospital death of patients with COVID-19. *Kidney Int.* 97, 829–838. doi: 10.1016/j.kint.2020.03.005

Chen, N., Zhou, M., Dong, X., Qu, J., Gong, F., Han, Y., et al. (2020). Epidemiological and clinical characteristics of 99 cases of 2019 novel coronavirus pneumonia in wuhan, China: a descriptive study. *Lancet* 395, 507–513. doi: 10.1016/S0140-6736(20)30211-7

Ferrari, D., Motta, A., Strollo, M., Banfi, G., and Locatelli, M. (2020). Routine blood tests as a potential diagnostic tool for COVID-19. *Clin. Chem. Lab. Med.* 58 (7), 1095–1099. doi: 10.1515/cclm-2020-0398

Gong, J., Ou, J., Qiu, X., Jie, Y., Chen, Y., Yuan, L., et al. (2020). A tool to early predict severe corona virus disease 2019 (COVID-19) : A multicenter study using the risk nomogram in wuhan and guangdong, China. *Clin. Infect. Dis.* 71 (15), 833–840. doi: 10.1093/cid/ciaa443

Huang, C., Wang, Y., Li, X., Ren, L., Zhao, J., Hu, Y., et al. (2020). Clinical features of patients infected with 2019 novel coronavirus in wuhan, China. *Lancet* 395, 497–506. doi: 10.1016/S0140-6736(20)30183-5

Ji, D., Zhang, D., Xu, J., Chen, Z., Yang, T., Zhao, P., et al. (2020). Prediction for progression risk in patients with COVID-19 pneumonia: The CALL score. *Clin. Infect. Dis.* 71, 1393–1399. doi: 10.1093/cid/ciaa414

Kermali, M., Khalsa, R. K., Pillai, K., Ismail, Z., and Harky, A. (2020). The role of biomarkers in diagnosis of COVID-19 - a systematic review. *Life Sci.* 254, 117788. doi: 10.1016/j.lfs.2020.117788

Kishaba, T., Tamaki, H., Shimaoka, Y., Fukuyama, H., and Yamashiro, S. (2014). Staging of acute exacerbation in patients with idiopathic pulmonary fibrosis. *Lung* 192, 141–149. doi: 10.1007/s00408-013-9530-0

Li, Y., Lu, S., Lan, M., Peng, X., Zhang, Z., and Lang, J. (2020b). A prognostic nomogram integrating novel biomarkers identified by machine learning for cervical squamous cell carcinoma. *J. Transl. Med.* 18, 223. doi: 10.1186/s12967-020-02387-9

Liu, J., Liu, Y., Xiang, P., Pu, L., Xiong, H., Li, C., et al. (2020a). Neutrophil-to-lymphocyte ratio predicts critical illness patients with 2019 coronavirus disease in the early stage. *J. Transl. Med.* 18, 206. doi: 10.1186/s12967-020-02374-0

Liu, M., Song, C., Zhang, P., Fang, Y., Han, X., Li, J., et al. (2020b). A nomogram for predicting cancer-specific survival of patients with gastrointestinal stromal tumors. *Med. Sci. Monit.* 26, e922378. doi: 10.12659/MSM.922378

Li, X., Xu, S., Yu, M., Wang, K., Tao, Y., Zhou, Y., et al. (2020a). Risk factors for severity and mortality in adult COVID-19 inpatients in Wuhan. *J. Allergy Clin. Immunol.* 146 (1), 110–118. doi: 10.1016/j.jaci.2020.04.006

Li, Q. X., Zhao, X. J., Fan, H. Y., Li, X. N., Wang, D. L., Wang, X. J., et al. (2019). Application values of six scoring systems in the prognosis of stroke patients. *Front. Neurol.* 10, 1416. doi: 10.3389/fneur.2019.01416

Momtazmanesh, S., Ochs, H. D., Uddin, L. Q., Perc, M., Routes, J. M., Vieira, D. N., et al. (2020). All together to fight COVID-19. *Am. J. Trop. Med. Hyg.* 102, 1181–1183. doi: 10.4269/ajtmh.20-0281

Moreno, R., Vincent, J. L., Matos, R., Mendonça, A., Cantraine, F., Thijs, L., et al. (1999). The use of maximum SOFA score to quantify organ dysfunction/failure in intensive care. results of a prospective, multicentre study. working group on sepsis related problems of the ESICM. *Intensive Care Med.* 25, 686–696. doi: 10.1007/s001340050931

Pujadas, E., Chaudhry, F., Mcbride, R., Richter, F., Zhao, S., Wajnberg, A., et al. (2020). SARS-CoV-2 viral load predicts COVID-19 mortality. *Lancet Respir. Med.* 8, e70. doi: 10.1016/S2213-2600(20)30354-4

Schiaffino, S., Codari, M., Cozzi, A., Albano, D., Ali, M., Arioli, R., et al. (2021). Machine learning to predict in-hospital mortality in COVID-19 patients using computed tomography-derived pulmonary and vascular features. *J. Of Personalized Med.* 11 (6), 501. doi: 10.3390/jpm11060501

Wang, D., Hu, B., Hu, C., Zhu, F., Liu, X., Zhang, J., et al. (2020a). Clinical characteristics of 138 hospitalized patients with 2019 novel coronavirus-infected pneumonia in wuhan, China. *Jama* 323, 1061–1069. doi: 10.1001/jama.2020.1585

Wang, L., Li, J., Guo, S., Xie, N., Yao, L., Cao, Y., et al. (2020b). Real-time estimation and prediction of mortality caused by COVID-19 with patient information based algorithm. *Sci. Total Environ.* 727, 138394. doi: 10.1016/j.scitotenv.2020.138394

World Health Organization (2022) *Weekly epidemiological update on COVID-19 - July 27 2022*. Available at: https://www.who.int/publications/m/item/weekly-epidemiological-update-on-covid-19 (Accessed 27-july-2022).

Wu, C., Chen, X., Cai, Y., Xia, J., Zhou, X., Xu, S., et al. (2020a). Risk factors associated with acute respiratory distress syndrome and death in patients with coronavirus disease 2019 pneumonia in wuhan, China. *JAMA Intern. Med.* 180 (7), 934–943. doi: 10.1001/jamainternmed.2020.0994

Wu, J., Huang, J., Zhu, G., Wang, Q., Lv, Q., Huang, Y., et al. (2020b). Elevation of blood glucose level predicts worse outcomes in hospitalized patients with COVID-19: A retrospective cohort study. *BMJ Open Diabetes Res. Care* 8 (1), e001476. doi: 10.1136/bmjdrc-2020-001476

Xu, C., Yuan, B., He, T., Ding, B., and Li, S. (2020). Prognostic values of YTHDF1 regulated negatively by mir-3436 in glioma. *J. Cell Mol. Med.* 24 (13), 7538–7549. doi: 10.1111/jcmm.15382

Zhang, Z. L., Hou, Y. L., Li, D. T., and Li, F. Z. (2020). Laboratory findings of COVID-19: a systematic review and meta-analysis. *Scand. J. Clin. Lab. Invest.* 80 (6), 441–447. doi: 10.1080/00365513.2020.1768587

Zhou, F., Yu, T., Du, R., Fan, G., Liu, Y., Liu, Z., et al. (2020). Clinical course and risk factors for mortality of adult inpatients with COVID-19 in wuhan, China: A retrospective cohort study. *Lancet* 395, 1054–1062. doi: 10.1016/s0140-6736(20)30566-3

Zhu, N., Zhang, D., Wang, W., Li, X., Yang, B., Song, J., et al. (2020). A novel coronavirus from patients with pneumonia in chin. *N. Engl. J. Med.* 382, 727–733. doi: 10.1056/NEJMoa2001017

frontiers | Frontiers in Cellular and Infection Microbiology

TYPE Original Research
PUBLISHED 09 December 2022
DOI 10.3389/fcimb.2022.921950

OPEN ACCESS

EDITED BY
Timothy Yong James,
University of Michigan, United States

REVIEWED BY
Kelly A. Speer,
Smithsonian Conservation Biology Institute (SI), United States
Jie Cui,
Chinese Academy of Sciences (CAS), China

*CORRESPONDENCE
Elizabeth H. Loh
eloh@transy.edu
Alessandra Nava
navaveterinaria@gmail.com

SPECIALTY SECTION
This article was submitted to Clinical Microbiology, a section of the journal Frontiers in Cellular and Infection Microbiology

RECEIVED 16 April 2022
ACCEPTED 28 October 2022
PUBLISHED 09 December 2022

CITATION
Loh EH, Nava A, Murray KA, Olival KJ, Guimarães M, Shimabukuro J, Zambrana-Torrelio C, Fonseca FR, de Oliveira DBL, Campos ACdA, Durigon EL, Ferreira F, Struebig MJ and Daszak P (2022) Prevalence of bat viruses associated with land-use change in the Atlantic Forest, Brazil. *Front. Cell. Infect. Microbiol.* 12:921950. doi: 10.3389/fcimb.2022.921950

Prevalence of bat viruses associated with land-use change in the Atlantic Forest, Brazil

Elizabeth H. Loh[1,2*], Alessandra Nava[3*], Kris A. Murray[4], Kevin J. Olival[5], Moisés Guimarães[6], Juliana Shimabukuro[7], Carlos Zambrana-Torrelio[8], Fernanda R. Fonseca[3], Daniele Bruna Leal de Oliveira[9], Angélica Cristine de Almeida Campos[9], Edison L. Durigon[9], Fernando Ferreira[7], Matthew J. Struebig[2] and Peter Daszak[5]

[1]Division of Natural Sciences and Mathematics, Transylvania University, Lexington, KY, United States, [2]Durrell Institute of Conservation and Ecology, School of Anthropology and Conservation, University of Kent, Canterbury, United Kingdom, [3]Instituto Leônidas e Maria Deane – Fiocruz Amazônia, Manaus, Amazonas, Brazil, [4]MRC Unit The Gambia at London School of Hygiene and Tropical Medicine, Fajara, Gambia, [5]EcoHealth Alliance, New York, NY, United States, [6]Departamento de Recursos Naturais, Faculdade de Ciências Agronomicas, Universidade Estadual Paulista, Botucatu, Brazil, [7]Departamento de Medicina Veterinária Preventiva e Saúde Animal da Faculdade de Medicina Veterinária e Zootecnia da Universidade de São Paulo, São Paulo, Brazil, [8]Department of Environmental Science and Policy, George Mason University, Fairfax VA, United States, [9]Departamento de Microbiologia, Instituto de Ciências Biomédicas-II, Universidade de São Paulo, São Paulo, Brazil

Introduction: Bats are critical to maintaining healthy ecosystems and many species are threatened primarily due to global habitat loss. Bats are also important hosts of a range of viruses, several of which have had significant impacts on global public health. The emergence of these viruses has been associated with land-use change and decreased host species richness. Yet, few studies have assessed how bat communities and the viruses they host alter with land-use change, particularly in highly biodiverse sites.

Methods: In this study, we investigate the effects of deforestation on bat host species richness and diversity, and viral prevalence and richness across five forested sites and three nearby deforested sites in the interior Atlantic Forest of southern Brazil. Nested-PCR and qPCR were used to amplify and detect viral genetic sequence from six viral families (corona-, adeno-, herpes-, hanta-, paramyxo-, and astro-viridae) in 944 blood, saliva and rectal samples collected from 335 bats.

Results: We found that deforested sites had a less diverse bat community than forested sites, but higher viral prevalence and richness after controlling for confounding factors. Viral detection was more likely in juvenile males located in deforested sites. Interestingly, we also found a significant effect of host bat species on viral prevalence indicating that viral taxa were detected more frequently in some species than others. In particular, viruses from the

Coronaviridae family were detected more frequently in generalist species compared to specialist species.

Discussion: Our findings suggest that deforestation may drive changes in the ecosystem which reduce bat host diversity while increasing the abundance of generalist species which host a wider range of viruses.

KEYWORDS

viral richness, diversity, bat host, deforestation, land-use change, viral prevalence

Introduction

Emerging viruses with wildlife origins are a significant threat to global health (e.g. Ebolaviruses, SARS and MERS coronaviruses) (Jones et al., 2008). Analyses of recent emerging infectious disease (EID) events show that anthropogenic changes including land-use change (e.g. habitat degradation, deforestation, forest fragmentation), intensification of food production, and global trade and travel are key factors in disease emergence (Loh et al., 2015; Allen et al., 2017; Rulli et al., 2017; Reaser et al., 2022). Further, nearly one-third of all EIDs, and a higher proportion of zoonoses, are associated with land-use change specifically (Loh et al., 2015). This suggests that increasing and/or novel interactions among hosts, vectors and pathogens following land-use change are significant contributors to disease emergence.

In tropical and subtropical environments, the pace of land-use change is unprecedented and continues to increase globally as demand for natural resources grows (Song et al., 2018). Bats are globally threatened, with 15% of bat species being listed as threatened or vulnerable, and habitat loss in the tropics is a major driver of population declines (Frick et al., 2020). Land-use change has also been associated with the emergence of many recent zoonotic diseases (Gibb et al., 2020). Yet, the relationship between land-use change and disease emergence is poorly understood. Recent studies have hypothesized that land-use change may increase the risk of disease emergence through more frequent human-animal interactions, or by influencing pathogen diversity, either directly by changing pathogen prevalence and/or diversity, or indirectly *via* impacts on host assemblages (Bradley et al., 2008; Vittor et al., 2009; Murray and Daszak, 2013; Rulli et al., 2017). However, mechanistic studies have tended to focus on how abundance and prevalence of specific pathogens, or their vectors and hosts, vary over the landscape (Ostfeld and Keesing, 2000; LoGiudice et al., 2003; Kilpatrick et al., 2006a; Kilpatrick et al., 2006b; Bradley et al., 2008; Vittor et al., 2009). Others have used meta-analyses to try to identify generality and mechanisms involved (Salkeld et al., 2013; Gottdenker et al., 2014; Civitello et al., 2015). Few empirical studies have taken a community approach to examine how viral assemblages in host communities vary with land-use change.

In this study, we investigate the effects of deforestation on bat host abundance and diversity, and viral prevalence and richness. We work with bats because they are diverse, abundant, and geographically widespread (Rex et al., 2008), comprising species from nearly every trophic level, with wide differences in their dispersal abilities (Kingston, 2010). Further, some of their life history traits and characteristics (e.g. diet, ability to fly, torpor and hibernations, and roosting behaviors) make them suitable hosts of viruses and other pathogens (Calisher et al., 2006) and many bat species are strongly impacted by land-use changes. Bats are important hosts of pathogens that have had significant impact on public health (e.g. Ebola, SARS, MERS, rabies). They also harbor the highest proportion of zoonotic viruses of any mammal order (Jones et al., 2008; Olival et al., 2017), as well as significant emerging diseases of people, livestock and wildlife. Finally, while no bat viruses have emerged from the Atlantic Forest to our knowledge, we chose this region as our study site because of the high biodiversity it contains and the large-scale deforestation it has undergone. Our study focuses on three questions: (1) Does bat abundance and diversity differ in forested versus non-forested areas? (2) Does viral prevalence differ between bat communities in forested versus deforested areas? (3) What biological and ecological factors determine the likelihood of viral detection?

Materials and methods

Ethical statement

This study was carried out with animal handling permits issued from the Brazilian Ministry of the Environment (#33078-4). Animal handling ethics approval was provided by the University of California, Davis (#16048). Bat handling

followed strict personal protection and biosafety requirements and short capture times to minimize stress on individual animals. All captured individuals were released at the point of capture.

Study site

Morro do Diabo State Park (municipality of Teodoro Sampaio, São Paulo state, Brazil, Figure 1) is located in the Pontal do Paranapanema region and contains the largest preserved area of interior Atlantic Forest in Sao Paulo State. The park covers an area of 33,845 ha (Durigan and Franco, 2006) and is comprised of mesophytic semideciduous forest and a small area of Cerrado (savanna-like vegetation). The climate is characterized as subtropical, with dry winters and wet summers. Mean annual temperature is 22°C, and annual rainfall ranges between 1100 and 1300 mm (de Faria and Pires, 2006). The matrix around the park is comprised of 63 small properties of agrarian reform settlements, as well as pasture (~60%) and agriculture (~15%), and forest fragments ranging from 2 to 2000 ha in area, most of which are privately owned (Uezu and Metzger, 2011). The forested study sites were chosen to control for similar characteristics including elevation, vegetation structure and rainfall. We sampled bats and viruses at five intact forested sites (>200ha) and three nearby deforested sites, located 3-5km away and defined as areas where more than 20% of forest cover has been removed and converted from the original forest to agrarian reform settlements.

Bat capture and sample collection

Bats were sampled during April to November of 2014. At each site we sampled a 100m x 100m grid using eight horizontal mist nets (9m x 3m), one canopy mist net (6m x 3m) and one harp trap (1.5m x 1.5m). At least 150 individuals were collected from deforested sites and from forested sites each. Additional sampling effort was required in the forested areas due to lower catch rates. Bats were captured for a period of five consecutive nights at each site, totaling 2040 m^2/270 hours capture effort across all sites. Mist nets were opened at sunset and remained open for six hours. Nets were checked at 30-minute intervals and bats processed immediately.

Samples were collected from bats with no clinical or neurological symptoms and in good body condition, defined as mass divided by forearm length which has been validated in temperate bats (Wilkinson and Brunet-Rossinni, 2009). All animals were released immediately following processing. Blood, saliva, and rectal swabs were collected from each captured animal, with feces and urine opportunistically collected. All samples were placed in cryovials containing 200 ml of Viral Transportation Media (VTM) and stored in liquid nitrogen in a dry shipper while in the field, then transferred to -80C freezers at the Institute of Biomedical Sciences at the University of Sao Paulo. External morphological measurements (including forearm/radius length, body length, head length) were collected by a bat taxonomist to assist in species identification. Several bat identification keys from the region were also used for reference (Reis et al., 2013; Reis et al., 2017). Sex and age were determined by the presence of scrotal

FIGURE 1
The study area, in and around Morro do Diabo State Park, located in the Pontal do Paranapanema region, Sao Paulo state. Bat surveys (yellow and red circles) were undertaken across forested (n=5) and deforested sites (n=3).

testes and well developed teats (Wilkinson and Brunet-Rossinni, 2009). Before release, each individual was marked with a non-toxic pen to determine the rate of within-trip recapture. This was used to ensure that the same bat was not re-sampled within sampling trips.

Viral detection

Total nucleic acid was extracted from all samples using the EasyMag (bioMérieux, Inc.) platform, and cDNA synthesis performed using SuperScript III first-strand synthesis supermix (Invitrogen), all according to the manufacturer's instructions. Viral discovery was performed using nested-PCR assays targeting coronaviruses (Quan et al., 2010), astroviruses (Atkins et al., 2009), paramyxoviruses (Tong et al., 2008), and herpesviruses (VanDevanter et al., 1996), while real-time PCR was used to target hantaviruses (Araujo et al., 2011) described below (Box 1). PCR results were visualized on a 2% agarose gel and Sanger sequencing was performed using ABI3100 (Applied Biosystems) equipment and BigDye Terminator v3.1 Cycle Sequencing Kit at the Institute of Biomedical Sciences II at the University of Sao Paulo. Sequences were analysed and edited

BOX 1. Primers used for viral screening in this study.

	Viral Family	Target	Amplicon size	Primer name	Primer sequence 5'- 3'	Reference
ConventionalPCR/Semi – Nested/Nested – PCR reaction	**Astroviridae**	RNA-Dependent RNA Polymerase (RdRp)	Round 1 431bp	Astr4380F	GAYTGGRCN CGNTWYGATGGNACIAT	Atkins et al., 2009
				Astr4811R	GGYTTNACCC ACATNCCAAA	
			Round 2 342bp	Astr4380F + Astr4722R	ARNCKRTCATCNCCATA	
	Coronaviridae	RNA-Dependent RNA Polymerase (RdRp)	Round 1 520bp	CoV-FWD1	CGTTGGIACWAAYBT VCCWYTICARBTRGG	Quan et al., 2010
				CoV-RVS1	GGTCATKATAGCRTCA VMASWWGCNACATG	
			Round 2 328pb	CoV-FWD2	GGCWCCWCCH GGNGARCAATT	
				CoV-RVS2	GGWAWCCCCA YTGYTGWAYRTC	
	Herpesviridae	Polymerase (Pol)	Round 1 variable	DFA	gAY TTY gCN AgY YTN TAY CC	
				ILK	TCC Tgg ACA AgC AgC ARN YSg CNM TNA A	Van Devanter et al., 1996
				KG1	gTC TTg CTC ACC AgN TCN ACN CCY TT	
			Round 2215-315	TGV	TgT AAC TCg gTg TAY ggN TTY ACN ggN gT	
				IYG	CAC AgA gTC CgT RTC NCC RTA DAT	
	Paramyxoviridae	Polymerase (Pol)	Round 1 639bp	PAR-F1	gAA ggI TAT TgT CAI AAR NTN Tgg AC	Tong et al., 2008
				PAR-R	gCT gAA gTT ACI ggI TCI CCD ATR TTN C	
			Round 2 561bp	PAR-R +PAR-F2	gTT gCT TCA ATg gTT CAR ggN gAY AA	
SYBRGreen	**Hantaviridae**	S segment	141bp	JAN-F	CCC TgT Tgg ATC AAC Tgg TTT Tg	Araujo et al., 2011
				JAN-R	TgT AAT gTg CTC TTg TTA ACg TCA TCT	

using Geneious (version 6.0.3). Sequences were aligned with ClustalW and MUSCLE, and phylogenetic trees (see Text S1) constructed with neighbor-joining (p-distance, pairwise deletion, 1,000 bootstraps), maximum-likelihood (1,000 bootstraps), and Bayesian (GTR+I - Mr Bayes) algorithms. In Mr. Bayes, we discarded the first 25% of trees as burn-in, and used the remaining trees to estimate the posterior probability value (PP) of 0.7. The chains ran for 2,000,000 cycles (mcmc ngen = 2,000,000). Trees were reconstructed with unconstrained branch lengths and unrooted. In MEGA 7 (macOS available in: https://www.megasoftware.net/) we used Maximum Likelihood with heuristic search and GTR+gamma+I algorithm. For the ML tree, we conducted 1,000 fast bootstrap ML replicates to assess the support values of internal nodes and visualized the trees in FigTree software version 1.4.4 with Midpoint Root (available in: http://tree.bio.ed.ac.uk/software/figtree/)(Supplementary Figures 1–5). Sequences were segregated into discrete viruses, defined as a viral species, based on distinct monophyletic clustering following Anthony et al. (2013).

Data analysis

Statistical analysis was performed using R 3.5.1, with ggplot2 for graphing. To compare estimated bat species diversity between forested and deforested sites, we calculated abundance-based diversity profiles with Hill numbers (effective number of species) using the iNEXT package based on the parameter q (Chao and Jost, 2015). This parameter controls the relative emphasis placed on rare or common species. In addition to providing information on species richness, this diversity profile estimator also accounts for species abundances to differing degrees. With increasing order q, the weight of dominant species increases in the calculation of species diversity. We used three widely used species diversity measures: Species richness (number of observed species; q=0), Shannon diversity (number of typical species; q=1) and Simpson diversity (number of most common species; q=2). We then applied a bootstrap method (1,000 bootstraps) using observed detections to obtain approximate variances of the proposed profiles and to construct the associated confidence intervals. These estimations take into account the effect of undetected species in samples. Estimated viral diversity could not be explored using these methods due to limited sample sizes. However we compared viral species richness and overall viral prevalence across treatments using a Fisher's Exact Test. To account for the uneven number of captures per bat species, we used Bartels rank test of randomness to determine whether viruses were randomly distributed among bat host species by examining whether viral prevalence significantly differed among species. Due to low detection rates in other viral families, our analysis was limited to the *coronaviridae* family.

We use a Generalized Linear model (GLM) of viral detection with a logit link function. We use "viral detection" as the response variable in our model based on the presence or absence of a viral detection for each individual bat. After testing for collinearity among the response variables, no variables were excluded based on their variance inflation factor (VIF) scores. Seven variables were selected for the final analysis. Definitions of the variables used are given in Table 1. In a "stepwise backwards-selection", factors were eliminated from the full model in an iterative process based on the Akaike information criterion (AIC) (Akaike, 1973) with the stepAIC function of the MASS package (Venables and Ripley, 2002) in the statistical software R 3.5.1.

Results

Bat diversity

We recorded 18 bat species from three families (*Phyllostomidae, Molossidae, and Vespertilionidae*) and five dietary guilds (frugivorous, insectivorous, nectarivorous, sanguivorous, omnivourous) from 335 mist-net captures. No bats were captured using the vertical canopy net or harp trap. After accounting for sampling effort, capture rates were similar between forested (n = 163 captures) and deforested (n = 172 captures) sites (Paired t-test, t = 1.883, p = 0.081). Bat species richness in the deforested sites (n=11 species) was slightly higher than the forested sites (n = 9 species); however, this difference was not significant as indicated by the empirical diversity profiles that show overlap between the 95% confidence intervals at q = 0 (Figure 2). In contrast, at q>1 (i.e. measures of diversity that incorporate abundance information) the forested sites were found to be more diverse than deforested sites. When correcting for the bias introduced by the non-detection of species in the samples, bat diversity was reduced in deforested sites; species richness was slightly higher in forested areas (n=15 species) compared to deforested areas (n = 11 species). However, for q > 1.25, this difference in community diversity was statistically significant, as reflected by the two non-overlapped confidence intervals.

TABLE 1 Description of predictor variables used in the generalized linear models.

Predictor variables	Definition
Treatment	Forested versus Deforested
Sex	Male versus Female
Pregnancy status	Yes or No
Age	Three categories including: juveniles, subadults and adults
Genus	12 unique genera
Species	18 unique species
Abundance	Total number of individuals captured per species

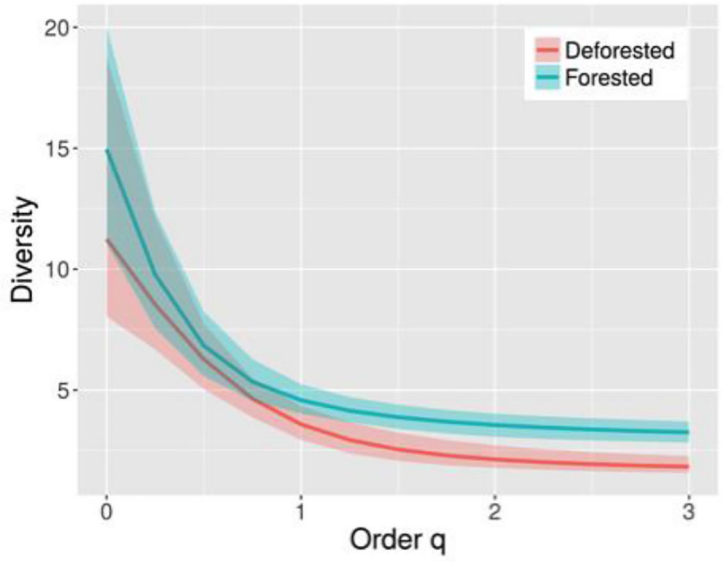

FIGURE 2
Estimated diversity profiles for bat species data in forested (green line) and deforested (red line) sites for q between 0 and 3 with 95% confidence interval (shaded areas based on a bootstrap method of 1000 replications). The numbers show the estimated diversities for q = 0, 1, 2 and 3.

Viral prevalence and richness

Overall, a total of 22 individual bats from three families (*Phyllostomidae, Molossidae, Vespertilionidae*) were positive for 13 viral species in the following viral families: *Astroviridae*, *Coronaviridae*, *Hantaviridae*, *Herpesviridae*, and *Paramyxoviridae*, with a combined viral prevalence of 6.6% (22/335) (Table 2). None of the samples were positive for adenoviruses, despite previous studies documenting their presence in other bat species (Jánoska et al., 2011; Van Vuren et al., 2018). Only one individual bat yielded more than one viral species - a coinfection by a coronavirus and herpesvirus was found in *Artibeus planirostris*. Viral species were not evenly distributed among bat species, with all detected viruses coming from just five of 18 sampled bat species (Figure 3). After accounting for the number of captures per bat species by looking at viral prevalence as opposed to number of positive detections, we found a significant effect of host bat species on viral prevalence indicating that viral taxa were detected more frequently in some species than others. In particular, viruses from the *Coronaviridae* family were detected more frequently in generalist species compared to specialist species ($P<0.01$, Bartel's Rank Test). Viral prevalence also differed among viral families; *Coronaviridae* had the highest prevalence of 3.6%, followed by *Astroviridae* (1.2%), *Paramyxoviridae* (0.6%), *Herpesviridae* (0.9%) and *Hantaviridae* (0.3%).

Treatment (forested vs. deforested), sex and age were the only significant predictors of overall viral detection (presence/absence) ($P < 0.05$, $df = 1$) (Table 3). This result was supported by the logistic regression model with the lowest AIC value (Table 4), which demonstrates that the odds of a positive viral detection decreases in forested habitat.

With all viral families combined, viral prevalence in deforested sites (9.3%) was significantly higher than in forested sites (3.68%) ($P<0.05$, Fisher's Exact Test). Deforested sites also had higher viral richness (n = 13 unique viral taxa) compared to forested sites (n = 2).

Discussion

In the Atlantic Forest of Brazil, higher bat host diversity is not associated with higher viral prevalence or richness. Despite lower bat host species richness in deforested areas, viral richness and prevalence is significantly higher. This result does not appear to be associated with the abundance of bat hosts, which was not significantly different (based on mist-net capture frequency) in deforested versus forested areas.

Bats are known to harbor a wide diversity of viruses, and have received growing attention due to their role in the emergence of several recent infectious disease outbreaks (e.g. Severe Acute Respiratory Syndrome (SARS), Middle East Respiratory Syndrome, Nipah virus) (Quan et al., 2010; Hu et al., 2015; Epstein et al., 2020). While studies exploring viral diversity in bat host species have increased, few studies have assessed how bat communities and the viruses they host alter with land-use change, particularly in highly biodiverse sites. Overall, this study identified 13 unique viral taxa from four viral families known to infect humans. We found that different viral families were not evenly distributed within different bat host species and between habitats (forested vs deforested).

TABLE 2 Total captures of bat species and total viral detections in forested and deforested habitat in the Interior Atlantic Forest.

FAMILY/Species	Captures	*Corona-*	*Herpes-*	*Hanta-*	*Astro-*	*Paramyxo-*
PHYLLOSTOMIDAE						
Artibeus lituratus	66	1	0	0	0	0
Artibeus fimbriatus	34	0	0	0	0	0
Artibeus planirostris	130	6	3	1	4	1
Carollia perspicillata	55	4	0	0	0	0
Desmodus rotundus	1	0	0	0	0	0
Diaemus youngi	2	0	0	0	0	0
Glossophaga soricina	1	0	0	0	0	0
Phyllostomus hastatus	3	0	0	0	0	1
Sturnira lilium	17	1	0	0	0	0
Vampyrodes caracciol	9	0	0	0	0	0
MOLOSSIDAE						
Molossus molossus	3	0	0	0	0	0
Eumops glaucinus	2	0	0	0	0	0
VESPERTILIONIDAE						
Lasiurus blossevillii	1	0	0	0	0	0
Myotis nigricans	1	0	0	0	0	0
Myotis albescens	3	0	0	0	0	0
Myotis riparius	3	0	0	0	0	0
Myotis unidentified A	1	0	0	0	0	0
Myotis unidentified B	3	0	0	0	0	0

Specifically, viruses from *Coronoviridae* were primarily found in species considered to be generalists, including *Artibeus planirostris*, *Carollia perspicillata*, *Artibeus literatus*, and *Sturnira lillium*. We suggest that such differences in virus prevalence could be related to viral ecology (i.e., their ability to infect host cells and to persist and replicate) and to the ecology and behavior of the bat hosts in a given habitat. Specifically, we found that viral detection is more likely in juvenile, male bats. Indeed, previous studies have shown that the behavior between many species of young male and female bats differ considerably, with young males immediately leaving the maternity roost once they are weaned, while females continue to forage with their mothers. This difference in behavior could result in younger males having a greater frequency of contacts with new host species or with shared food resources that increase their exposure to potential pathogens. For example, younger vampire bats appear to have higher exposure to pathogens such as rabies virus because younger male bats are more exploratory and are more likely to feed on novel hosts (Carter et al., 2018).

Previous studies of bats have demonstrated that even moderate forest disturbance can result in an increase of certain generalist species that can successfully adapt to human-modified landscapes (Delaval and Charles-Dominique, 2006; Meyer and Kalko, 2008). The strategies they employ such as greater dispersal ability, and the ability to exploit a variety of resources, allow these species to tolerate a wide range of habitats, leading to higher colonization rates throughout human-modified landscapes. In our study area, *A. planirostris and A. fimbriatus* were the two species most commonly captured in deforested sites. Both species are large-bodied frugivores, which feed heavily on figs in the canopy (Handley et al., 1991). In many tropical landscapes, figs are not regularly available throughout the year, thus *Artibeus* species are more likely to occupy disturbed landscapes which provide a variety of food resources (Gorresen and Willig, 2004). *Artibeus* spp. bats accounted for 73% (n=16/22) of all viruses detected, after accounting for the number of captures per bat species.

Here, we show that deforested sites support higher viral richness despite lower bat species richness. While we did not measure disease risk directly, we hypothesize that humans living close to forest edges disturbed by deforestation may be particularly exposed to zoonotic infections not only because of the higher likelihood for humans to be in contact with disease reservoirs, but also because of the higher viral richness found in deforested areas. Yet, previous studies examining the link between land-use change and disease in have been equivocal (Randolph and Dobson, 2012; Salkeld et al., 2013; Civitello et al., 2015; Rulli et al., 2017). Some studies of single-pathogens (e.g. West Nile virus, Hantavirus, the Lyme disease pathogen *Borellia burgdorferi*) in multi-host systems have found that higher pathogen prevalence is associated with decreased continuous forest area (LoGiudice et al., 2003; Suzán et al., 2008; Kilpatrick, 2011). Results from a recent meta-analysis from studies in Southeast Asia shows that people who live or work on agricultural land are more likely to be infected with zoonotic

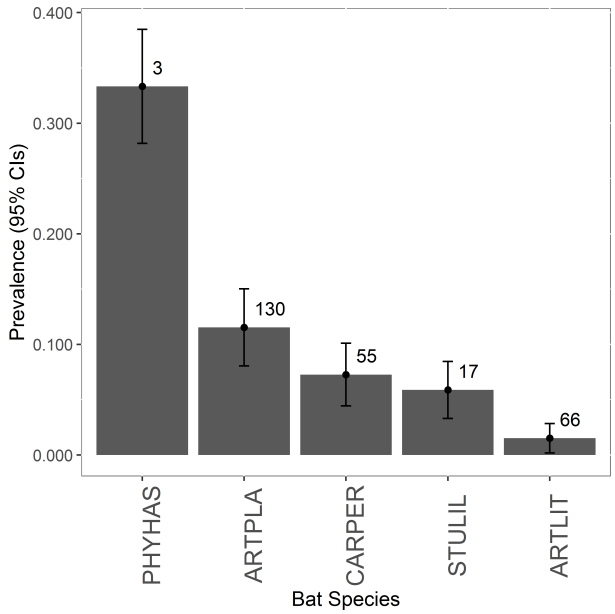

FIGURE 3
Overall viral prevalence by bat species with sample sizes. Error bars represent the 95% Clopper-Pearson binomial confidence intervals. Species codes: ARTLIT, *Artibeus lituratus*; ARTPLA, *Artibeus planirostris*; CARPER, *Carollia perspicillata*; PHYHAS, *Phyllostomus hastatus*; STULIL, *Sturnira lillium*.

diseases (Shah et al., 2019), and in West and Central Africa, previous research shows that the index cases of Ebola virus outbreaks (i.e. spillover cases from wildlife reservoirs) occurred mostly in areas of forest fragmentation and deforestation (Rulli et al., 2017). Further, urbanized and agricultural areas that have undergone deforestation have been associated with higher rates of disease transmission of West Nile Virus in the United States, increased risk of malaria in Peru (Vittor et al., 2009), Leishmaniasis in Costa Rica (Wijeyaratne et al., 1994) and hantavirus in Panama (Suzán et al., 2008), in part because of changes in host and vector abundance in human-modified areas.

Our study provides further evidence from a multi-pathogen, multi-host species system that deforestation can increase viral prevalence and richness in bat hosts. However, studies of *Plasmodium* infections in Australia (Laurance et al., 2013), Cameroon (Chasar et al., 2009), and Brazil (Ribeiro et al., 2005)

TABLE 3 Best model of viral detection with different categories of land-use change, sex and age.

	Estimate	SE	z	P value
Intercept	-3.272	0.492	-6.646	3e-11
Treatment (forested vs deforested)	-1.274	0.536	-2.378	0.017
Sex (male vs female)	1.502	0.534	2.812	0.005
Age (juvenile vs adult)	1.247	0.596	2.094	0.036
Age (subadult vs adult)	-0.564	1.067	-0.528	0.597

TABLE 4 Logistic regression model selection table comparing top four models based on lowest AICc.

Model description	AIC	ΔAIC	Null d.f	Residual deviance	Residual d.f.
~ treatment + sex + age	6.63	0	333	19.24	329
~ treatment + sex + age + abundance	6.92	0.29	333	19.15	328
~ treatment + sex + pregnancy + age + abundance	8.29	1.66	333	19.11	327
~ treatment + species + sex + pregnancy + age + abundance	31.8	25.1	333	18.52	310

found a positive correlation between continuous forest area and pathogen prevalence. In Sabah, Seltmann et al., 2017 found that reduced body mass in bats in logged forests was associated with chronic stress and impaired health status for some species of bats. Interestingly, this did not translate into an increase in coronavirus and astrovirus detection rates among more disturbed sites (Seltmann et al., 2017), perhaps due to the extent of disturbance. Unlike our system, which is more than 30 years post-fragmentation and fully converted, the Sabah study sites are still ongoing active deforestation and fragmentation, which may result in delays in species' responses.

Our study examines some of the complexities in the relationship among deforestation, viral prevalence and host and viral community assemblages by addressing how viral richness and prevalence in bat hosts varies with land-use change. Our findings suggest that deforestation can increase the abundance of generalist species that, in our case, host the majority of viruses detected. From a theoretical point of view, the dilution effect hypothesis explores how the decrease of biodiversity may increase the amplification of zoonotic diseases. It suggests that high species diversity in a community can reduce infectious disease risk, provided that hosts differ in competency for transmitting a pathogen (Schmidt and Ostfeld, 2001). While this study does not test the 'dilution effect' as laid out for Lyme disease and other single pathogen systems (LoGiudice et al., 2003; Kilpatrick et al., 2005), these findings provide further evidence that anthropogenic land use change can in some cases, lead to increased abundance of reservoirs that harbor a higher diversity and prevalence of potential pathogens. As pressures on the environment continue to grow, further research is needed on viral and host ecology and how they are structured across varying landscapes.

Data availability statement

The original contributions presented in the study are included in the article/Supplementary Material. Further inquiries can be directed to the corresponding author.

Ethics statement

This study was carried out with animal handling permits from the Brazilian Ministry of the Environment (#33078-4). Animal handling ethics approval was provided by the University of California, Davis (#16048) and by the Ethics Committee of the Faculty of Veterinary Medicine and Zootechnics at the University of Sao Paulo.

Author contributions

All authors contributed to the article and approved the submitted version.

Funding

This study was made possible by the United States Agency for International Development (USAID) Emerging Pandemic Threats PREDICT program (cooperative agreement no., GHN-A-OO-09-00010-00). The contents are the responsibility of the authors and do not necessarily reflect the views of USAID or the United States Government. This work was also supported by The American Association of University Women (Dissertation Fellowship) and by the International Development Research Centre (project no. 106150-001).

Conflict of interest

The authors declare that the research was conducted in the absence of any commercial or financial relationships that could be construed as a potential conflict of interest.

Publisher's note

Supplementary material

The Supplementary Material for this article can be found online at: https://www.frontiersin.org/articles/10.3389/fcimb.2022.921950/full#supplementary-material

SUPPLEMENTARY FIGURE 1
Paramyxovirus Maximum Likelihood Phylogenetic Tree. Genetic analysis of 558 nucleotide partial L gene. Tree reconstructed by MEGA7 with heuristic search, Neighbor-Joining "NJ" algorithm and Model GTR +gamma+I. The principal node values superior to 70% represent 1,000 *bootstrap* replicates.

SUPPLEMENTARY FIGURE 2
Coronavirus Maximum Likelihood Phylogenetic Tree. Genetic analysis of 394 nucleotide partial RdRp gene. Tree reconstructed by MEGA7 with heuristic search, Neighbor-Joining "NJ" algorithm and Model GTR +gamma+I. The principal node values superior to 70% represent 1,000 *bootstrap* replicates.

SUPPLEMENTARY FIGURE 3
Astrovirus Maximum Likelihood Phylogenetic Tree. Genetic analysis of 369 nucleotide partial RdRp gene. Tree reconstructed by MEGA7 with heuristic search, Neighbor-Joining "NJ" algorithm and Model GTR +gamma+I. The principal node values superior to 70% represent 1,000 *bootstrap* replicates.

SUPPLEMENTARY FIGURE 4
Herpesvirus Maximum Likelihood Phylogenetic Tree. Genetic analysis of 189 nucleotide partial Polymerase (pol) gene. Tree reconstructed by MEGA7 with heuristic search, Neighbor-Joining "NJ" algorithm and Model GTR+gamma+I. The principal node values superior to 70% represent 1,000 *bootstrap* replicates.

SUPPLEMENTARY FIGURE 5
Hantavirus Maximum Likelihood Phylogenetic Tree. Genetic analysis of 89 nucleotide partial S segment. Tree reconstructed by MEGA7 with heuristic search, Neighbor-Joining "NJ" algorithm and Model GTR+gamma+I. The principal node values superior to 70% represent 1,000 *bootstrap* replicates.

References

Akaike, H. (1973). *Information theory and an extension of the maximum likelihood principle* (Budapest, Hungary: Akadémiai Kiadó).

Allen, T., Murray, K. A., Zambrana-Torrelio, C., Morse, S. S., Rondinini, C., Di Marco, M., et al. (2017). Global hotspots and correlates of emerging zoonotic diseases. *Nat. Commun.* 8 (1), 1124. doi: 10.1038/s41467-017-00923-8

Anthony, S. J., Epstein, J. H., Murray, K. A., Navarrete-Macias, I., Zambrana-Torrelio, C. M., Solovyov, A., et al. (2013). A strategy to estimate unknown viral diversity in mammals. *Mbio* 4 (5):1028–1038 doi: 10.1128/mBio.00598-13

Araujo, J., Pereira, A., Nardi, M., Henriques, D., Lautenschalager, D., Dutra, L., et al. (2011). Detection of hantaviruses in Brazilian rodents by SYBR-green-based real-time RT-PCR. *Arch. virology.* 156 (7), 1269–1274. doi: 10.1007/s00705-011-0968-1

Atkins, A., Wellehan, J. F., Childress, A. L., Archer, L. L., Fraser, W. A., and Citino, S. B. (2009). Characterization of an outbreak of astroviral diarrhea in a group of cheetahs (Acinonyx jubatus). *Veterinary Microbiol.* 136 (1), 160–165. doi: 10.1016/j.vetmic.2008.10.035

Bradley, C. A., Gibbs, S. E., and Altizer, S. (2008). Urban land use predicts West Nile virus exposure in songbirds. *Ecol. Applications.* 18 (5), 1083–1092. doi: 10.1890/07-0822.1

Calisher, C. H., Childs, J. E., Field, H. E., Holmes, K. V., Schountz, T, et al (2006). Bats: important reservoir hosts of emerging viruses. *Clinical microbiology reviews* 19.3, 531–545.

Carter, G. G., Forss, S., Page, R. A., and Ratcliffe, J. M. (2018). Younger vampire bats (Desmodus rotundus) are more likely than adults to explore novel objects. *PloS One* 13 (5), e0196889. doi: 10.1371/journal.pone.0196889

Chao, A., and Jost, L. (2015). Estimating diversity and entropy profiles *via* discovery rates of new species. *Methods Ecol. Evolution.* 6 (8), 873–882. doi: 10.1111/2041-210X.12349

Chasar, A., Loiseau, C., Valkiūnas, G., Iezhova, T., Smith, T. B., and Sehgal, R. N. (2009). Prevalence and diversity patterns of avian blood parasites in degraded African rainforest habitats. *Mol. Ecology.* 18 (19), 4121–4133. doi: 10.1111/j.1365-294X.2009.04346.x

Civitello, D. J., Cohen, J., Fatima, H., Halstead, N. T., Liriano, J., McMahon, T. A., et al. (2015). Biodiversity inhibits parasites: broad evidence for the dilution effect. *Proc. Natl. Acad. Sci.* 112 (28), 8667–8671. doi: 10.1073/pnas.1506279112

de Faria, H. H., and Pires, A. (2006). *Parque estadual do morro do diabo: plano de manejo* (Santa Cruz do Rio Pardo: Editora Viena), 311.

Delaval, M., and Charles-Dominique, P. (2006). Edge effects on frugivorous and nectarivorous bat communities in a neotropical primary forest in French Guiana. *Revue d'Ecologie, Terre et Vie* 61.4, 343–352.

Durigan, G., and Franco, G. (2006). "Vegetação," in *Parque estadual do morro do diabo: plano de manejo* (Santa Cruz do Rio Pardo: Editora Viena), 111–118.

Epstein, J. H., Anthony, S. J., Islam, A., Kilpatrick, A. M., Ali Khan, S., Balkey, M. D., et al. (2020). Nipah virus dynamics in bats and implications for spillover to humans. *Proc. Natl. Acad. Sci.* 117 (46), 29190–29201. doi: 10.1073/pnas.2000429117

Frick, W. F., Kingston, T., and Flanders, J. (2020). A review of the major threats and challenges to global bat conservation. *Ann. New York Acad. Sci.* 1469 (1), 5–25. doi: 10.1111/nyas.14045

Gibb, R., Redding, D. W., Chin, K. Q., Donnelly, C. A., Blackburn, T. M., Newbold, T., et al. (2020). Zoonotic host diversity increases in human-dominated ecosystems. *Nature* 584 (7821), 398–402. doi: 10.1038/s41586-020-2562-8

Gorresen, P. M., and Willig, M. R. (2004). Landscape responses of bats to habitat fragmentation in Atlantic forest of Paraguay. *J. Mammalogy.* 85 (4), 688–697. doi: 10.1644/BWG-125

Gottdenker, N. L., Streicker, D. G., Faust, C. L., and Carroll, C. (2014). Anthropogenic land use change and infectious diseases: a review of the evidence. *Ecohealth* 11 (4), 619–632. doi: 10.1007/s10393-014-0941-z

Handley, C. O.Jr., Wilson, D. E., and Gardner, A. L. (1991). *Demography and natural history of the common fruit bat, artibeus jamaicensis, on barro Colorado island, Panama*. doi: 10.5479/si.00810282.511

Hu, B., Ge, X., Wang, L.-F., and Shi, Z. (2015). Bat origin of human coronaviruses. *Virol. J.* 12 (1), 1–10. doi: 10.1186/s12985-015-0422-1

Jánoska, M., Vidovszky, M., Molnár, V., Liptovszky, M., Harrach, B., and Benkő, M. (2011). Novel adenoviruses and herpesviruses detected in bats. *Veterinary J.* 189 (1), 118–121. doi: 10.1016/j.tvjl.2010.06.020

Jones, K. E., Patel, N., Levy, M., Storeygard, A., Balk, D., Gittleman, J. L., et al. (2008). Global trends in emerging infectious diseases. *Nature* 451, 990–993. doi: 10.1038/nature06536

Kilpatrick, A. M. (2011). Globalization, land use, and the invasion of West Nile virus. *Science* 334 (6054), 323–327. doi: 10.1126/science.1201010

Kilpatrick, A. M., Daszak, P., Jones, M. J., Marra, P. P., and Kramer, L. D. (2006a). Host heterogeneity dominates West Nile virus transmission. *Proc. R. Soc. London B: Biol. Sci.* 273 (1599), 2327–2333.

Kilpatrick, A. M., Daszak, P., Kramer, L., Marra, P. P., Dobson, A. P., Hudson, P. J., et al. (2006b). Predicting the transmission of West Nile virus. *Am. J. Trop. Med. Hygiene.* 75 (5), 139.

Kilpatrick, A. M., Jones, M., Kramer, L. D., Marra, P. P., and Daszak, P. (2005). West Nile Virus vector ecology across an urbanization gradient. *Am. J. Trop. Med. Hygiene.* 73 (6), 307–308. doi: 10.3201/eid1103.040364

Kingston, T. (2010). Research priorities for bat conservation in southeast Asia: a consensus approach. *Biodiversity Conserv.* 19 (2), 471–484. doi: 10.1007/s10531-008-9458-5

Laurance, S. G., Jones, D., Westcott, D., Mckeown, A., Harrington, G., and Hilbert, D. W. (2013). Habitat fragmentation and ecological traits influence the prevalence of avian blood parasites in a tropical rainforest landscape. *PloS One* 8 (10), e76227. doi: 10.1371/journal.pone.0076227

LoGiudice, K., Ostfeld, R. S., Schmidt, K. A., and Keesing, F. (2003). The ecology of infectious disease: effects of host diversity and community composition on Lyme disease risk. *Proc. Natl. Acad. Sci.* 100 (2), 567–571. doi: 10.1073/pnas.0233733100

Loh, E. H., Zambrana-Torrelio, C., Olival, K. J., Bogich, T. L., Johnson, C. K., Mazet, J. A., et al. (2015). Targeting transmission pathways for emerging zoonotic disease surveillance and control. *Vector-Borne Zoonotic Diseases.* 15 (7), 432–437. doi: 10.1089/vbz.2013.1563

Meyer, C. F., and Kalko, E. K. (2008). Assemblage-level responses of phyllostomid bats to tropical forest fragmentation: land-bridge islands as a model system. *J. Biogeography.* 35 (9), 1711–1726. doi: 10.1111/j.1365-2699.2008.01916.x

Murray, K. A., and Daszak, P. (2013). Human ecology in pathogenic landscapes: two hypotheses on how land use change drives viral emergence. *Curr. Opin. virology.* 3 (1), 79–83. doi: 10.1016/j.coviro.2013.01.006

Olival, K. J., Hosseini, P. R., Zambrana-Torrelio, C., Ross, N., Bogich, T. L., and Daszak, P. (2017). Host and viral traits predict zoonotic spillover from mammals. *Nature* 546, 646–650. doi: 10.1038/nature22975

Ostfeld, R. S., and Keesing, F. (2000). Biodiversity and disease risk: the case of Lyme disease. *Conserv. Biol.* 14 (3), 722–728. doi: 10.1046/j.1523-1739.2000.99014.x

Quan, P.-L., Firth, C., Street, C., Henriquez, J. A., Petrosov, A., Tashmukhamedova, A., et al. (2010). Identification of a severe acute respiratory syndrome coronavirus-like virus in a leaf-nosed bat in Nigeria. *MBio* 1 (4), e00208–e00210. doi: 10.1128/mBio.00208-10

Randolph, S. E., and Dobson, A. (2012). Pangloss revisited: a critique of the dilution effect and the biodiversity-buffers-disease paradigm. *Parasitology* 139 (7), 847–863. doi: 10.1017/S0031182012000200

Reaser, J. K., Hunt, B. E., Ruiz-Aravena, M., Tabor, G. M., Patz, J. A., Becker, D. J., et al. (2022). Fostering landscape immunity to protect human health: A science-based rationale for shifting conservation policy paradigms. *Conserv. Lett.*, e12869. doi: 10.1111/conl.12869

Reis, N. R., Fregonezi, M. N., Peracchi, A. L., and Shibatta, O. A. (2013). *Morcegos do brasil: guia de campo* (*1st edn*). (Rio de Janeiro: Technical Books Editora), 225 pp.

Reis, N. R., Peracchi, A. L., Batista, C. B., de Lima, I. P., and Pereira, A. D. (2017). *História natural dos morcegos brasileiros: chave de identificação de espécies* (Rio de Janeiro: Technical Books Editora), 416.

Rex, K., Kelm, D. H., Wiesner, K., Kunz, T. H., and Voigt, C. C. (2008). Species richness and structure of three Neotropical bat assemblages. *Biol. J. Linn. Society.* 94 (3), 617–629. doi: 10.1111/j.1095-8312.2008.01014.x

Ribeiro, S., Sebaio, F., Branquinho, F., Marini, M., Vago, A., and Braga, E. (2005). Avian malaria in Brazilian passerine birds: parasitism detected by nested PCR using DNA from stained blood smears. *Parasitology* 130 (03), 261–267. doi: 10.1017/S0031182004006596

Rulli, M. C., Santini, M., Hayman, D. T., and D'Odorico, P. (2017). The nexus between forest fragmentation in Africa and Ebola virus disease outbreaks. *Sci. Rep.* 7, 41613. doi: 10.1038/srep41613

Salkeld, D. J., Padgett, K. A., and Jones, J. H. (2013). A meta-analysis suggesting that the relationship between biodiversity and risk of zoonotic pathogen transmission is idiosyncratic. *Ecol. Letters.* 16 (5), 679–686. doi: 10.1111/ele.12101

Schmidt, K. A., and Ostfeld, R. S. (2001). Biodiversity and the dilution effect in disease ecology. *Ecology* 82 (3), 609–619. doi: 10.1890/0012-9658(2001)082[0609:BATDEI]2.0.CO;2

Seltmann, A., Czirják, GÁ, Courtiol, A., Bernard, H., Struebig, M. J., and Voigt, C. C. (2017). Habitat disturbance results in chronic stress and impaired health status in forest-dwelling paleotropical bats. *Conserv. Physiol.* 5 (1). doi: 10.1093/conphys/cox020

Shah, H. A., Huxley, P., Elmes, J., and Murray, K. A. (2019). Agricultural land-uses consistently exacerbate infectious disease risks in southeast Asia. *Nat. Commun.* 10 (1), 1–13. doi: 10.1038/s41467-019-12333-z

Song, X.-P., Hansen, M. C., Stehman, S. V., Potapov, P. V., Tyukavina, A., Vermote, E. F., et al. (2018). Global land change from 1982 to 2016. *Nature* 560 (7720), 639. doi: 10.1038/s41586-018-0411-9

Suzán, G., Marcé, E., Giermakowski, J. T., Armién, B., Pascale, J., Mills, J., et al. (2008). The effect of habitat fragmentation and species diversity loss on hantavirus prevalence in Panama. *Ann. New York Acad. Sci.* 1149 (1), 80–83. doi: 10.1196/annals.1428.063

Tong, S., Chern, S.-W. W., Li, Y., Pallansch, M. A., and Anderson, L. J. (2008). Sensitive and broadly reactive reverse transcription-PCR assays to detect novel paramyxoviruses. *J. Clin. Microbiol.* 46 (8), 2652–2658. doi: 10.1128/JCM.00192-08

Uezu, A., and Metzger, J. P. (2011). Vanishing bird species in the Atlantic forest: relative importance of landscape configuration, forest structure and species characteristics. *Biodiversity Conserv.* 20 (14), 3627–3643. doi: 10.1007/s10531-011-0154-5

VanDevanter, D. R., Warrener, P., Bennett, L., Schultz, E. R., Coulter, S., Garber, R. L., et al. (1996). Detection and analysis of diverse herpesviral species by consensus primer PCR. *J. Clin. Microbiol.* 34 (7), 1666–1671. doi: 10.1128/jcm.34.7.1666-1671.1996

Van Vuren, P. J., Allam, M., Wiley, M. R., Ismail, A., Storm, N., Birkhead, M., et al. (2018). A novel adenovirus isolated from the Egyptian fruit bat in south Africa is closely related to recent isolates from China. *Sci. Rep.* 8 (1), 9584. doi: 10.1038/s41598-018-27836-w

Venables, W., and Ripley, B. (2002). *Modern applied statistics with s. 4th Edition ed* (Berlin: Springer).

Vittor, A. Y., Pan, W., Gilman, R. H., Tielsch, J., Glass, G., Shields, T., et al. (2009). Linking deforestation to malaria in the Amazon: characterization of the breeding habitat of the principal malaria vector, anopheles darlingi. *Am. J. Trop. Med. Hyg.* 81 (1), 5.

Wijeyaratne, P., Arsenault, L. J., and Murphy, C. (1994). Endemic disease and development: the leishmaniases. *Acta Tropica.* 56 (4), 349–364. doi: 10.1016/0001-706X(94)90106-6

Wilkinson, G. S., and Brunet-Rossinni, A. (2009). "Methods for age estimation and the study of senescence in bats," in T. H. Kunz and S. Parsons eds *Ecological and behavioral methods for the study of bats* (Baltimore, Maryland, John Hopkins University Press), 315–325.

Frontiers in
Cellular and Infection Microbiology

Investigates how microorganisms interact with their hosts

Explores bacteria, fungi, parasites, viruses, endosymbionts, prions and all microbial pathogens as well as the microbiota and its effect on health and disease in various hosts.

Discover the latest Research Topics

See more →

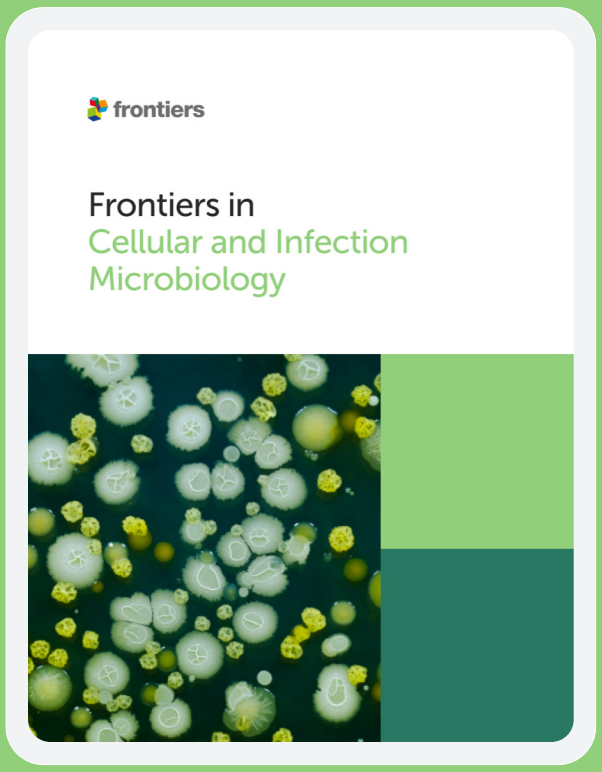

Frontiers

Avenue du Tribunal-Fédéral 34
1005 Lausanne, Switzerland
frontiersin.org

Contact us

+41 (0)21 510 17 00
frontiersin.org/about/contact